Master's thesis

NTNU
Norwegian University of Science and Technology
Faculty of Natural Sciences
Department of Chemistry

Edvard Solli Stenset

Selective functionalization of x-D-glucopyranosides in the synthesis towards sugar fatty acid esters

Master's thesis in chemistry
Supervisor: Nebojsa Simic
May 2019

NTNU
Norwegian University of
Science and Technology

NTNU – Trondheim
Norwegian University of
Science and Technology

Selective functionalization of α-D-glucopyranosides in the synthesis towards sugar fatty acid esters

Edvard Solli Stenset

May 2019

Department of Chemistry
Norwegian University of Science and Technology

Supervisor: Nebojsa Simic

Co-Supervisor: Sondre Nervik

Co-Supervisor: Odrun Arna Gederaas

Den lange, lange Sti over Myrene og ind i Skogene, hvem har traakket op den? Manden, Mennesket, den første som var her. Det var ingen Sti før ham.

— *Hamsun, Markens Grøde*

Declaration

I hereby declare that all work presented in this thesis has been done individually, in the time period from September 2017 to May 2019, and under the supervision of associate professor Nebojsa Simic, and my co-supervisors, Ph.D. candidate Sondre Nervik and associate professor Odrun Arna Gederaas.

This master thesis and all work I have conducted with this particular project, has been done in accordance with the guidelines for the two-year study program Master in Chemistry, as presented by the Department of Chemistry at the Norwegian University of Science and Technology, NTNU.

Trondheim, May 19, 2019

Edvard Solli Stenset

Preface

First of all I wish to thank my supervisor, associate professor Nebojsa Simic, for the opportunity to join this exiting research group. He has provided immense help over the last two years, especially with NMR analysis, where his expertise is hardly matched by any other at this department.

I would also like to thank my co-supervisor, Ph.D. candidate Sondre Nervik, for his indispensable help with all synthetic work. His presence in the laboratory was crucial for the great working environment, making these two years unforgettable.

My co-supervisor, associate professor Odrun Arna Gederaas, has helped with all bioactivity assessments, proving extremely valuable in a field outside of my expertise.

Other important contributors have been: Roger Aarvik for providing chemicals and materials, Susana Villa Gonzalez for mass spectrometry analysis, professor Bård Helge Hoff and associate professor Odd Reidar Gautun for help with synthetic strategies and providing excellent literature.

Lastly, I wish to thank my friends and family. Especially Henrik Haugom Solum, Ola Marius Løfgren Bjørnerud, Marcus de Bourg and Jonas Røe for proof reading parts of this thesis. Tobias Fløe Faukald and Sverre Hjelsvold have been my companions in "Studio Sokrates".

Abstract

As a part of a larger total synthesis endeavour, selected reactions pertaining to the overall synthetic strategy were explored. Regioselective protection of allylated α-D-glucopyranosides, esterification and subsequent deprotection have been the focal points of the synthetic work presented in this thesis. As a subordinate goal, the resulting sugar fatty acid ester products were subjected to biological evaluation by *in vitro* MTT assays.

The protective work started with Fischer glycosidation of the anomeric position employing allyl alcohol, followed by acetalization of positions 6 and 4, yielding anomerically pure α-D-glucopyranoside. Continued work on the synthetic strategy resulted in the synthesis of three intermediates with a single free hydroxyl in position 1, 4 and 6, respectively. Anomerization was observed in the synthesis towards the 1-*O* intermediate with α:β= 78:22. Sugar fatty acid esters were synthesized in low to medium yield (5 - 67 %). Using 1D and 2D NMR experiments, present C=C double bonds in unsaturated fatty acid esters were deemed stable. Migration of acyl groups was observed during deprotection of 4-*O*-esterified derivatives. From MTT assays, one sugar fatty acid ester synthesized herein were confirmed to possess anticancer biological activity, when applied to F98 glioma cell lines.

Graphical abstract

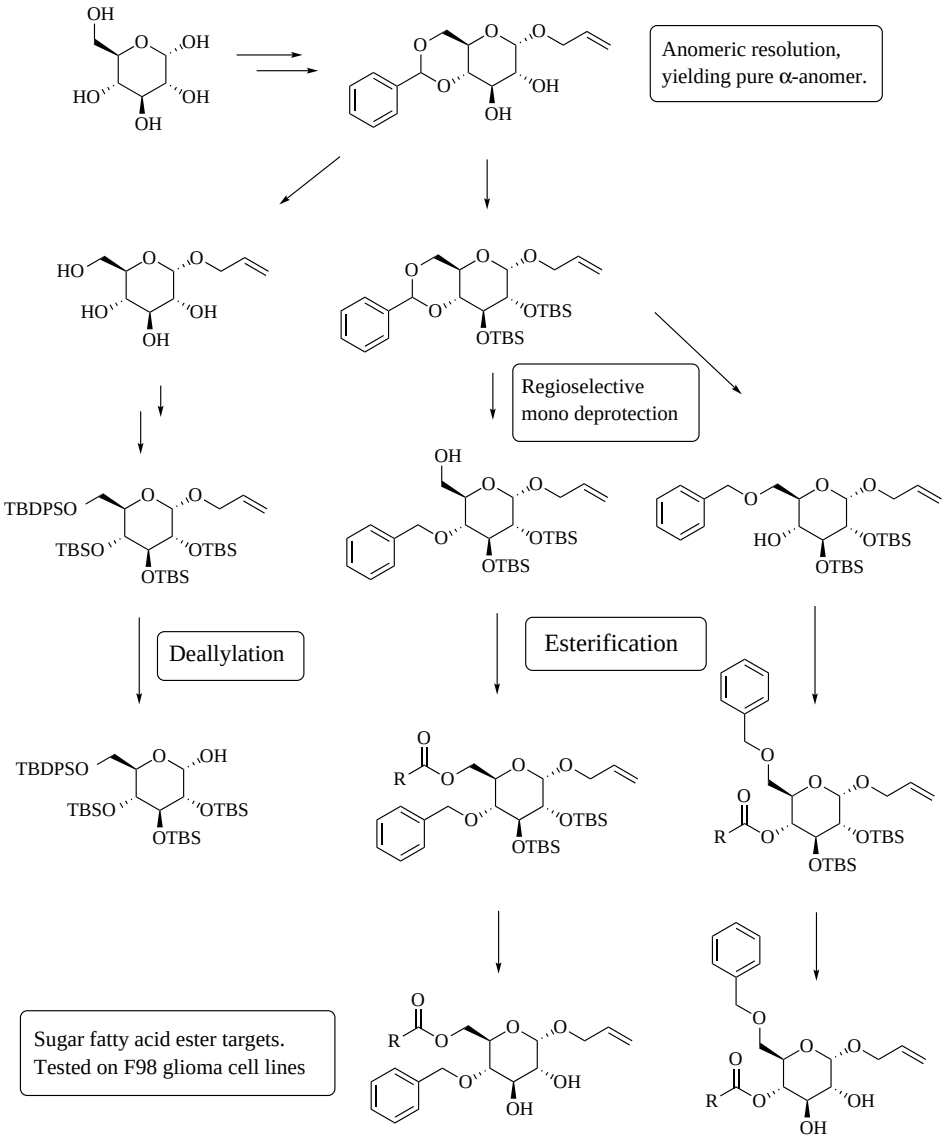

Sammendrag

Som en del av et større synteseprosjekt ble utvalgte reaksjoner, nyttige i den overordnede syntesestrategien, utforsket. Regioselektiv beskyttelse av allylerte α-D-glukopyranosider, esterifisering og videre avbeskyttelse har vært hovedpunktene i arbeidet presentert i denne avhandlingen. Som et underordnet mål ble de syntetiserte sukkerestere undersøkt for sin biologiske aktivitet ved å benytte *in vitro* MTT-eksperimenter.

Beskyttelsesstrategien ble initiert med Fischer glykosidering av anomerisk posisjon, fulgt av acetalisering på posisjonene 6 og 4 i syntesen mot et anomerisk rent α-D-glukopyranosid. Videre syntesearbeid gav tre beskyttede intermediater med én fri hydroksyl i posisjonene 1, 4 og 6. Anomerisering ble observert i syntesen av 1-*O* intermediatet med et anomerisk forhold på α:β= 78:22. Sukkerestere ble syntetisert i lavt til medium utbytte (5 - 67 %). Ved å bruke 1D og 2D NMR-eksperimenter, ble det observert at C=C dobelt bindinger var stabile under både forestring og avbeskyttelseforholdene. Migrasjon av estergruppene ble observert under avbeskyttelsesteget for noen av derivatene. Fra MTT testene ble det kartlagt en ester med biologisk aktivitet mot F98 glioma cellelinjer.

Grafisk sammendrag

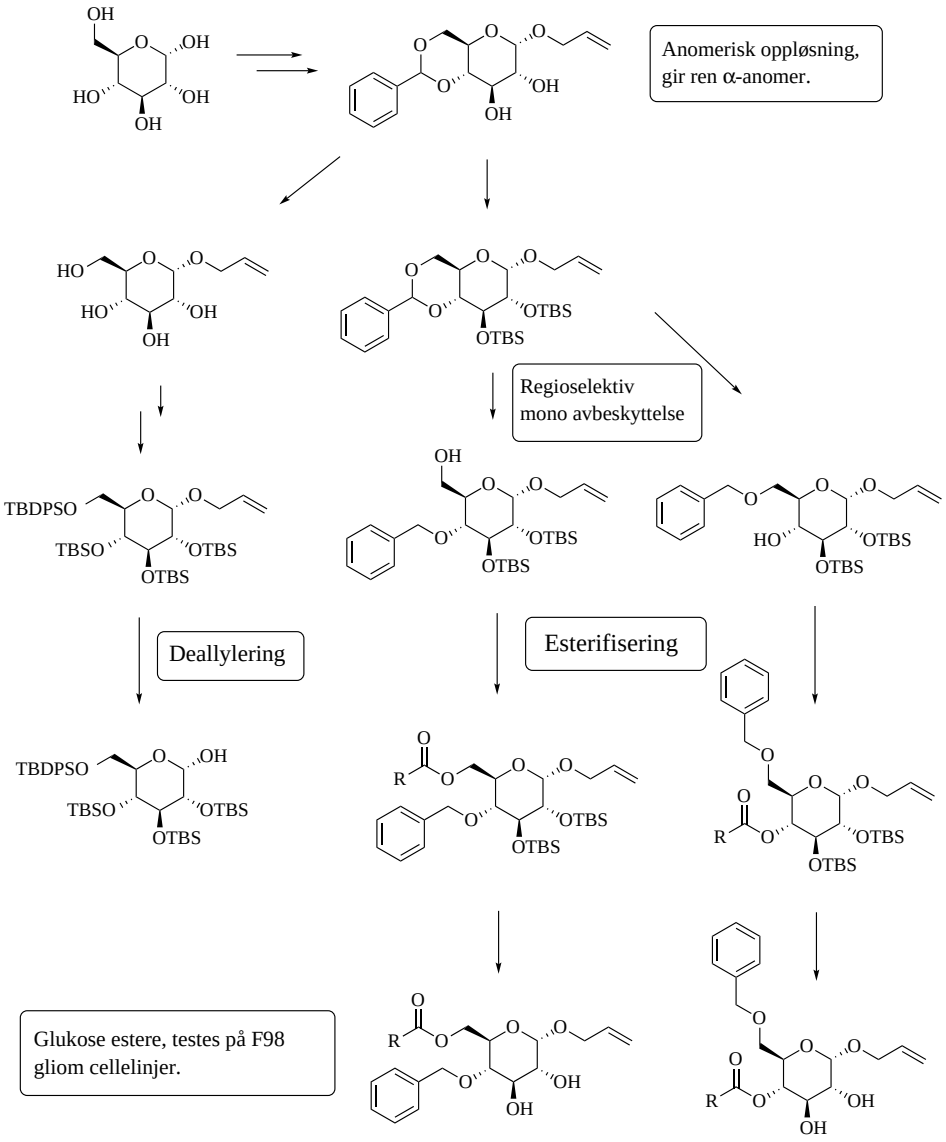

Contents

Numbered compounds

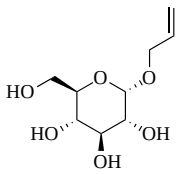

1

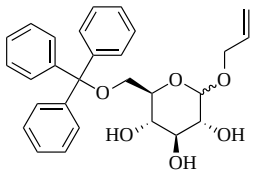

2

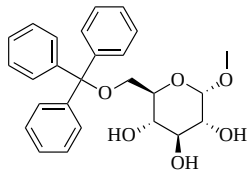

3

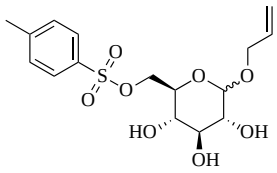

4

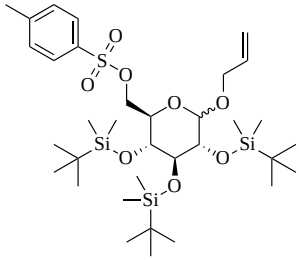

5

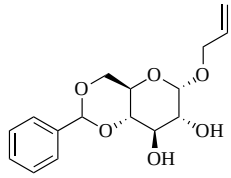

6

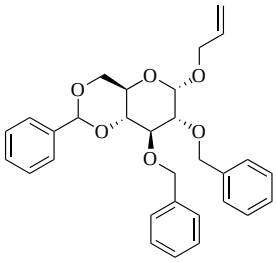

7

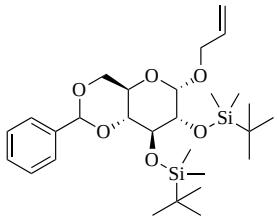

8

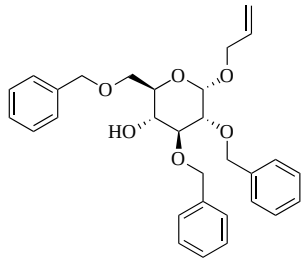

9

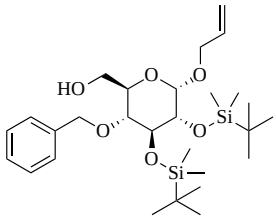

10

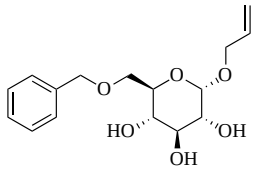

11

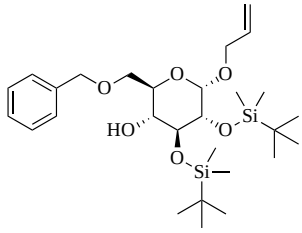

12

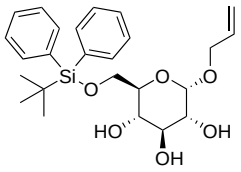

13

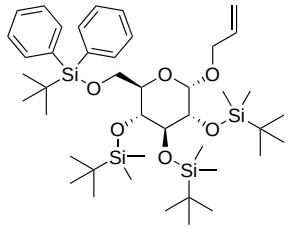

14

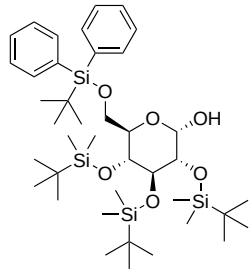

15

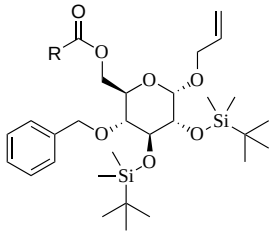

16: R = Stearate (18:0)
17: R = Elaidate (18:1)
18: R = α–linolenate (18:3)

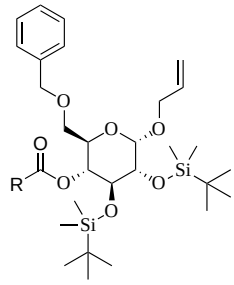

19: R = Stearate (18:0)
20: R = α–linolenate (18:3)

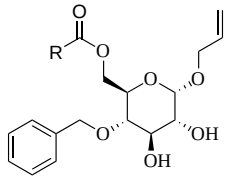

21: R = Stearate (18:0)
22: R = Elaidate (18:1)
23: R = α–linolenate (18:3)

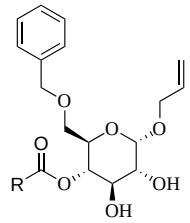

24: R = Stearate (18:0)
25: R= α–linolenate (18:3)

List of Abbreviations

Ac	Acetate
ACN	Acetonitrile
ALLA	α-linolenic acid
Bn	Benzyl-
COSY	Correlation spectroscopy
DCC	N,N'-Dicyclohexylcarbodiimide
DCM	Dichloromethane
DIBAL-H	Diisobutylaluminium hydride
DMF	N,N-Dimethylformamide
EDCI	1-Ethyl-3-(3-dimethylaminopropyl)carbodiimide
EA	Elaidic acid
HMBC	Heteronuclear multiple bond correlation spectroscopy

HSQC	Heteronuclear single quantum correlation spectroscopy
MTT	3-(4,5-dimethylthiazolyl-2)-2,5-diphenyltetrazolium bromide
MOM	Methoxymethyl
NOESY	Nuclear Overhauser effect spectroscopy
PL	Phospholipase
rt	Room temperature (20 - 25 °C)
SAR	Structure activity relationship
SD	Standard
SM	Starting material
SQAG	Sulfoquinovosyl diacyl glycerol
TBAF	Tetrabutylammonium fluoride
TBAI	Tetrabutylammonium iodide
TBDMS	*t*-Butyldimethylsilyl ether
TBDPS	*t*-Butyldiphenylsilyl ether
TCT	Cyanuric chloride
THP	Tetrahydropyran
TMS	Trimethylsilyl

Tr	Trityl / Triphenylmethyl
Ts	Tosyl / Toluensulfonyl

Chapter 1 - Introduction

The work presented in this master thesis is, together with several other masters projects, part of a natural product synthesis study at the Department of Chemistry under the Norwegian University of Science and Technology, NTNU. The main goal in this study is the total synthesis of 1-*O*-(3-*O*-linolenoyl-6-deoxy-6-sulfo-α-D-glucopyranosyl)glycerol (**1a**, Figure 1.1).

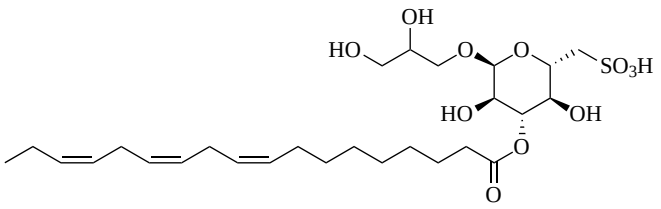

1a

Figure 1.1: 1-*O*-(3-*O*-linolenoyl-6-deoxy-6-sulfo-α-D-glucopyranosyl)glycerol) (**1a**) extracted from *Schlerochloa dura*.

The target compound (**1a**), structurally similar to sulfoquinovosyl diacyl glycerols (SQAGs), was previously extracted from *Schlerochloa dura*, a plant commonly used in traditional medicine in South-East Serbia [1, 2]. The target molecule (**1a**) also exhibit anti inflammatory properties, possibly mediated by the inhibition of the phospholipase A_2 (PLA_2) enzyme. The PLA_2 enzyme is responsible for the release of arachidonic acid in the inflammatory cascade [3].

The structure of this natural compound (**1a**) is based on the α-D-glucopyranose skeleton, with glycerol in position 1, linolenate (18:3) in position 3, and sulfonic acid in position 6. The proposed synthetic strategy for obtaining the target molecule (**1a**) starts from 1,2:5,6-di-*O*-isopropylidene-α-D-glucofuranose, due to the readily available hydroxyl function at C-3. A retrosynthetic analysis gives the reader an overview over the strategy towards the target molecule (**1a**, Scheme 1.1).

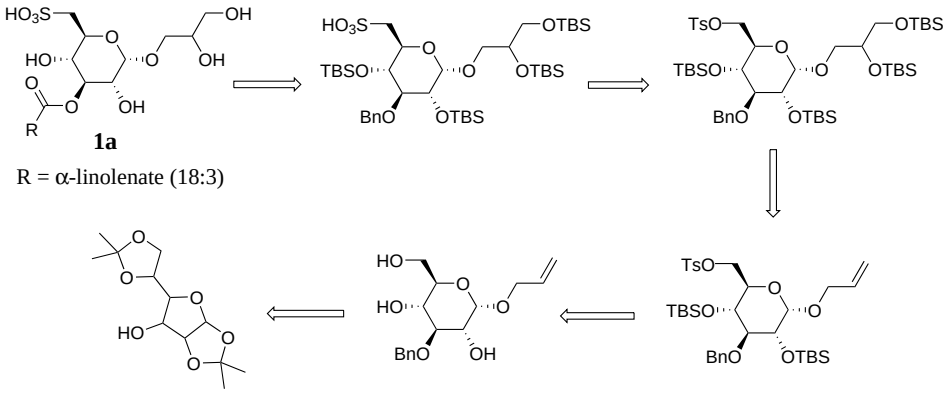

Scheme 1.1: Reterosynthetic analysis for the generation of **1a** from 1,2:5,6-Di-*O*-isopropylidene-α-D-glucofuranose.

Previous work on the project addressing the issues of regioselective protection, separation and isolation of anomers, and insertion of sulfonic acid on the glucose backbone, has been performed by other members of the research group.

This thesis primarily addresses challenges related to the synthesis of compound **1a**, by exploration of protective groups, selective deprotections, and development of suitable esterification conditions, useful in the total synthesis of the target compound (**1a**). Biological evaluation on some functionalized sugar fatty acid intermediates, using *in vitro* 3-(4,5-dimethylthiazolyl-2)-2,5-diphenyltetrazolium bromide (hereby abbreviated MTT) assays on F98 glioma cell lines, was established as a subordinate goal and conducted in collaboration with another member of the research group.

The motivation for this project was the necessity of efficient and mild esterification conditions, compatible with a range of fatty acids, as well as simple and non interfering de-protective techniques in the synthesis of target molecule (**1a**, Figure 1.1) [3]. In addition, the establishment of a library with esterified α-D-glucopyranose intermediates for biological evaluation is valuable, in terms of future structure-activity relationship studies.

1.1 Synthetic strategy

Underneath follows schematic representations towards the synthetic goals for this masters thesis. Scheme 1.2 illustrates the strategy used to obtain regioselective protected intermediates, suitable for selective esterification.

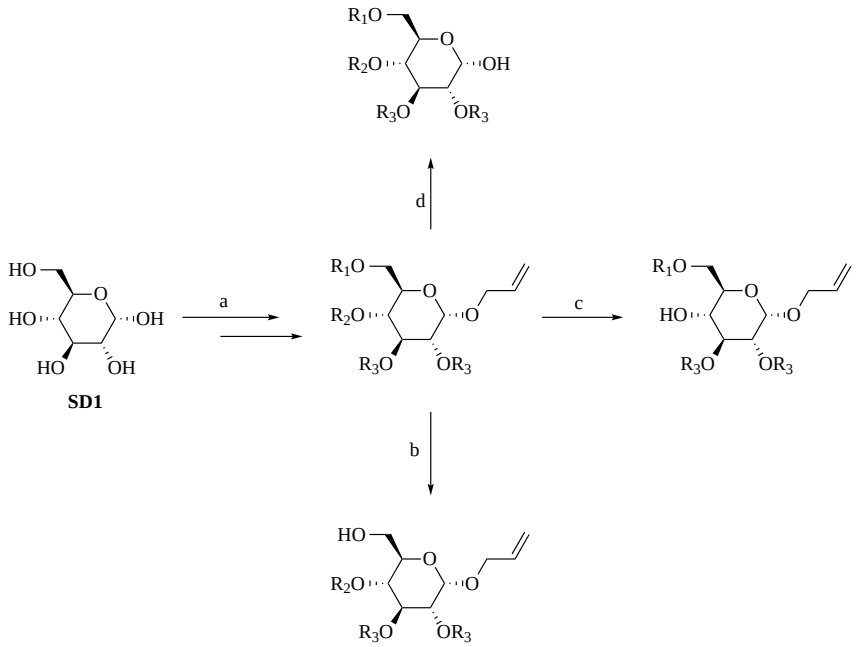

Scheme 1.2: Synthetic route to obtain regioselective protected glucopyranose intermediates with one free hydroxyl group. a: path towards a fully protected moiety, b: route to 6-*O* intermediate, c: route to 4-*O* intermediate, c: route to 1-*O* intermediate.

The strategy relies on reaching a fully protected moiety (a), which then is selectively deprotected (d, c, b) to yield three intermediates with one free hydroxyl in positions 1, 4 and 6, respectively. Deep investigation of each synthetic step is also carried out.

Scheme 1.3 shows the synthetic pathway to obtain sugar fatty acid esters from the intermediates presented in Scheme 1.2.

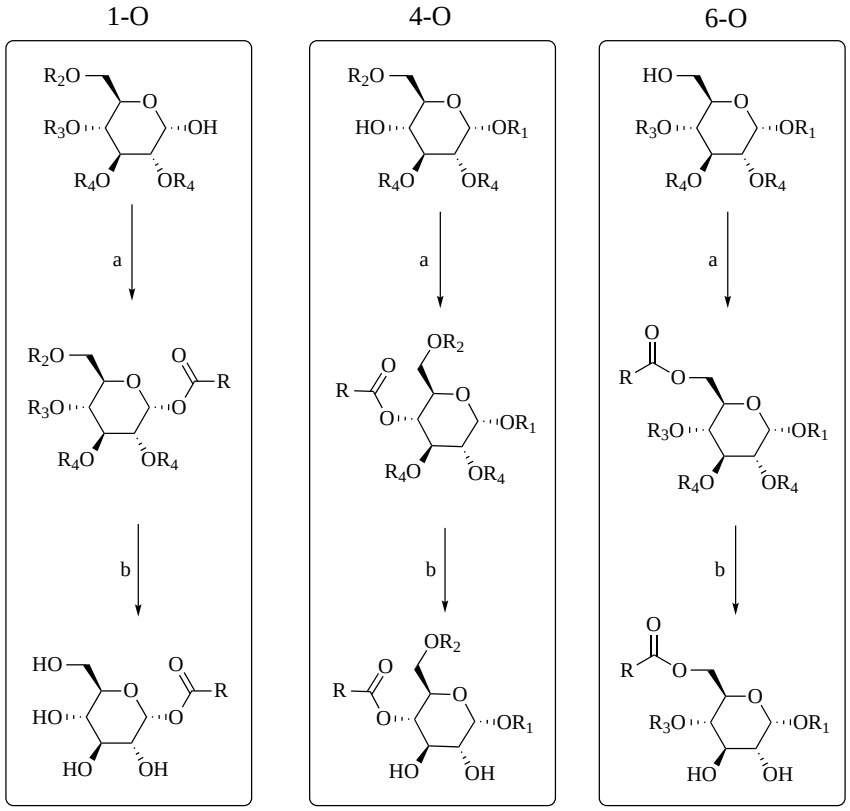

Scheme 1.3: Synthetic pathway to esterified compounds. a: esterification, b: mild deprotection of redundant protective groups. R_1 - R_4 represent various employed protective groups.

Esterification (a) and deprotection (b) in the synthesis towards sugar fatty acid esters (SFAEs).

Chapter 2 - Theory

2.1 Carbohydrates

Carbohydrates were originally defined as hydrates of carbon, with the general formula $C_m(H_2O)_n$ [4]. The definition of carbohydrates has been broadened in modern times to cover all polyhydroxy compounds containing a carbonyl functionality. This includes complex structural molecules, and a wide range of underlying compound classes, such as nucleic acids, a number of natural products and complex polymeric derivatives [5, 6]. Carbohydrates as a compound class is essential to life, and contribute to several biological mechanisms present in all living organisms. The roles played by carbohydrates range from controlling metabolic activity and structural building blocks to messengers in biosignaling pathways, and many other essential biological roles far beyond the scope of this thesis [5, 7]. Because of their abundance and biological importance, carbohydrates and their derivatives have been a field of extensive research for several centuries, since the first isolation of glucose in 1747 by Andreas Marggraf [8], and the first structural elucidation in 1884 by Emil Fischer [9]. In recent years, however, carbohydrate research in the pharmaceutical industry has exploded due to interesting bioactivities, such as inhibition of enzymes involved in

inflammation or carcinogenesis, for instance [10].

As mentioned previously, sugars play a central role in the synthesis of many natural products, either as building blocks for non-carbohydrate products, or as essential scaffolds in larger carbohydrates [11]. The high natural abundance of these compounds has its roots planted in one of the first chemical reactions mentioned in the modern education system, namely the photosynthesis (Scheme 2.1). Plants, algae, and certain bacteria, utilizes CO_2 to store energy from sunlight in the form of carbohydrates.

$$n\,CO_2 + n\,H_2O \underset{\text{Respiration}}{\overset{\text{Assimilation}\ h\nu,\ \text{ATP, NADPH}}{\rightleftharpoons}} (CH_2O)n + n\,O_2$$

Scheme 2.1: Overview of the photosynthetic generation of carbohydrates in plants and other microorganisms, such as algae.

The sugar molecules generated in photosynthesis may be further mediated in biological pathways to form highly complex, and in some cases bioactive, natural compounds, such as spectinomycin (Figure 2.1). Spectinomycin is a naturally occurring aminoglycoside antibiotic used for the treatment of gonorrhea, and originally found in the bacteria *Streptomyces spectabilis* [12]. The total synthesis carried out by Stephen Hanessian et al. of spectinomycin starts with D-glucose and requires 17 steps [12].

The following sections will mainly explore the chemistry and analysis of glucose derivatives, due to the stereochemistry found in the target molecule (**1a**). Other carbohydrates and carbohydrate derivatives are out of the scope of this thesis and are therefore omitted to deeper investigation.

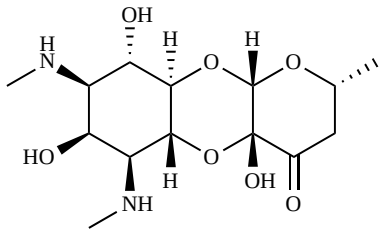

2.1a

Figure 2.1: Structure formula of spectinomycin, isolated from *Streptomyces spectabilis*.

2.1.1 General carbohydrate chemistry

Some carbohydrates, such as glucose, differ from many other compound classes due to the fact that they exist in an equilibrium of multiple conformations in the presence of water, as shown in Scheme 2.2. The open aldose cycles to a hemiacetal, which in the presence of water can open to the aldose form again.

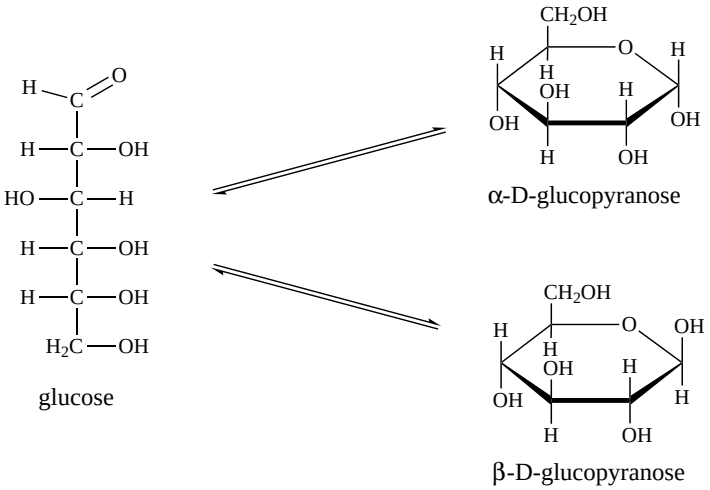

Scheme 2.2: The equilibrium between D-glucose (Fischer projection) and D-glucopyranose (Haworth projection) in aqueous media.

This equilibrium has for many years been studied thoroughly, but is

to this day still not fully understood [13]. Concepts, such as steric interractions, solvation, substituents and acidic/basic media, affects the equilibrium. It is believed that the addition of acid will protonate the ether function in the pyranose backbone, thus mediating an opening of the ring [14]. A proposed mechanism is showed in Scheme 2.3

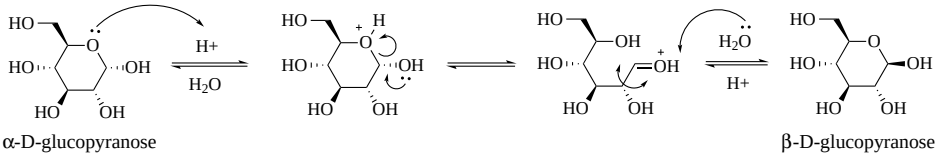

Scheme 2.3: Mechanism for the mediated ring opening and ring closing of α-D-glucopyranose.

Sugiyama et al. investigated this equilibrium on 2-*O*-methyl-glucopyranose as a model substrate in both acidic and basic media by NMR, and it became apparent that more α anomer was generated in acidic media, while more β anomer was generated in basic media. This was attributed to the hydrogen bonding acceptor/donor properties of the anomeric hydroxyl group [13].

An additional important observation regarding the anomeric composition of sugars in solution is the anomeric effect, also called the Edward-Lemieux effect [15]. The anomeric effect concerns heterocyclic systems, such as glucopyranose, and causes the steric unfavored axial position of the anomeric hydroxyl group to be present in much larger fractions than initially expected. The explanation for this effect comes partly from the dipole-dipole interactions between the ring-hetero atom and the anomeric substituents lone pairs, but lacking explanation of the differences in bond length and bond angles makes this description of the anomeric effect incomplete. The orbital-orbital interactions must also be considered, as non bonding electrons also

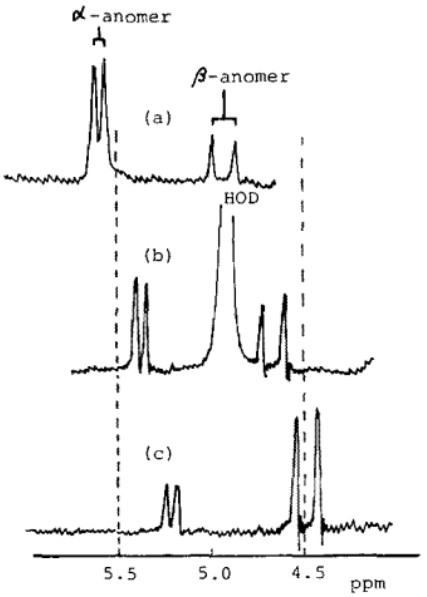

Figure 2.2: Partial ^{1}H-NMR (100 MHz) spectra of 2-*O*-Methyl-glucopyranose in HCOOH (a), D_2O (b) and Diethylamine (c) [13].

partake in the formation of the equilibrium [16]. A stabilizing overlap of the axial molecular orbital with the lone pair of the ring heteroatom delocalizes the electron lone pair, thus favoring the generation of the α anomer. Depending on the electronic effects of the anomeric substituent, the α:β ratio changes dramatically [16]. This hyperconjugation is visualized in Scheme 2.4 [17].

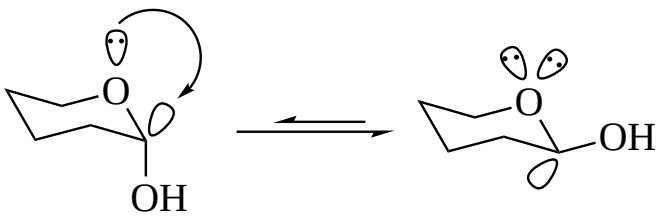

Scheme 2.4: Orbital interactions in the hyperconjugation of heterocycles.

2.1.2 Protective groups in carbohydrate synthesis

The synthesis of large and complex molecules is becoming increasingly feasible in organic chemistry, due to the development of new methodology. Highly selective synthetic techniques, such as cross coupling reactions, metathesis reactions, and enzymatic reactions, facilitates the synthesis of until recently almost impossible synthetic reactions [18, 19]. However, the reactions alone are often not sufficient in highly functionalised molecules. What happens if two competing functionalities, say ketone and aldehyde, are present in the same molecule? Normally aldehydes would react faster in nucleophilic substitution reactions, thus exluding the ketone transformation. Protecting the aldehyde, before proceeding with the reaction, might be the solution to such problems, where the ketone transformation is sought after [20]. The use of protective groups is often essential in the synthesis of complex organic molecules, as exemplified by the total synthesis of paclitaxel (Taxol®), completed simultaneously, and for the first time by Holton et al., and Nicolaou et al., in 1994 [21, 22]. Although this particular example is one of the extremes regarding total synthesis, use of protective groups is advantageous in all stages of synthetic work.

Due to the high functionality of carbohydrates, resulting from the many hydroxyl groups, they may prove useful as building blocks, or scaffolds, in fields such as natural product synthesis, advanced polymerisation or other complex fields of organic chemistry [23, 24]. However, this high functionality is not simple to utilise, due to the chemical similarity between the hydroxyl functions, and the vast amount of different protective groups and reaction conditions required to obtain a fully selective protected moiety. Thus, protective groups used in carbohydrate chemistry must have different regiospecific inclinations for

the hydroxyl groups [25]. Often such inclinations come down to spacial orientation of hydroxyl groups, promoting varying regioselectivity to different protective groups, as will be made clear in the following sections [26].

Popular protective group classes in carbohydrate chemistry include ethers, esters and acetals, although all groups compatible with hydroxyl functions can be utilised [25]. Because of their relevance and place in this thesis, a few well known types of protective groups are described in further details below. The most relevant protective groups for the overall project is TBDMS (*tert*-Butyldimethylsilyl) ethers, allyl ethers, benzyl ethers and the benzylidene acetal. Ethers are highly represented, as the reader already might be aware.

2.1.2.1 Triphenylmethyl ethers

The triphenylmethyl protective group, commercially available as the chloride, is classically used in carbohydrate chemistry to protect the sterically available primary position [27]. Trityl, as it is commonly abbreviated, is a highly bulky protective group. The single benzylic carbon is highly stabilised by resonance, promoting S_N1 reactivity. Scheme 2.5 shows the implementation of a trityl moiety in D-glucopyranose.

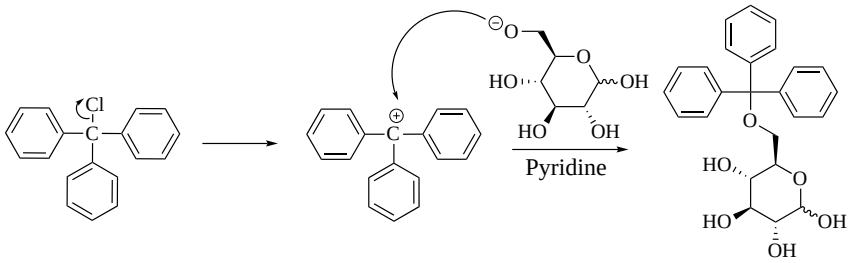

Scheme 2.5: Mechanism for the tritylation of the primary position in D-glucopyranose.

The rate of reaction is low, hence it is normal to use a catalyst, such as DMAP, upon introduction. Deprotection is commonly carried out in acidic media, or in the presence of Lewis acids [25]. The trityl group also imparts a strong UV activity, allowing more facile detection and monitoring by thin layer chromatography and/or high performance liquid chromatography.

2.1.2.2 Sulfonates

Sulfonyl ether functions are present in several compound classes with many different utilisations, however this section only explores two compounds with protective attributes in organic synthesis, namely methanesulfonyl (mesyl) and toluensulfonyl (tosyl) functions [28]. The general structure of sulfonyl ethers are shown in Figure 2.3.

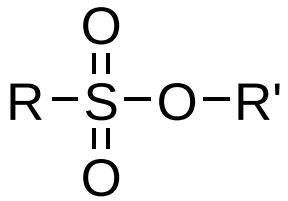

Figure 2.3: The general structure of an organic sulfonyl ether.

Mesyl and tosyl functions are commonly employed in the protection of

alcohols or amines, yielding the corresponding ethers and sulfoamides, respectively. [29]. Mesyl are more labile than their larger tosyl counterpart [25]. Concerning the latter, the para (ρ)-derivative is the most common, although meta (m) and ortho (o) derivatives also exist [30]. As with trityl, tosyl prefers the primary position due to steric effects. Therefore, in the event of a problematic tritylation, a tosylation might prove as a suitable alternative. The tosylation mechanism under basic conditions is shown in Scheme 2.6 [31].

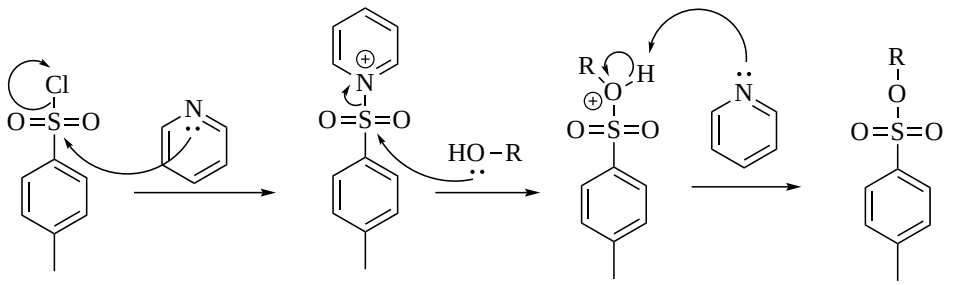

Scheme 2.6: General mechanism for the tosylation of alcohols.

In addition to the protective properties of tosyl functions, they also serve as good leaving groups compared to the poor leaving group potential inherited by the hydroxyls. To illustrate the leaving group potential of tosyl groups, the well known base catalyzed pinacol rearrangement, and insertion of a sulfonate ester are visualised in Scheme 2.7 and Scheme 2.8 [32].

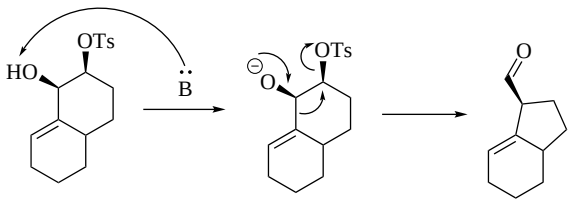

Scheme 2.7: Mechanism for the base catalyzed pinacol rearrangement on a model substrate.

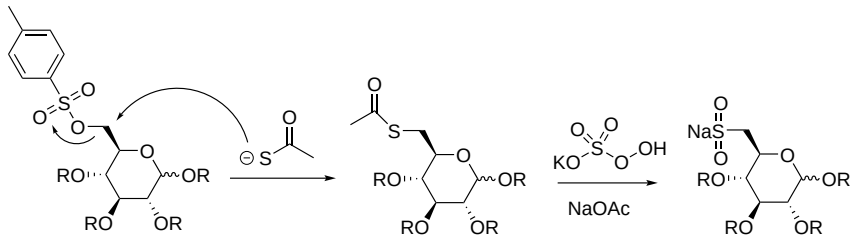

Scheme 2.8: The conversion from a tosyl to a sulfonate function in D-glucopyranose.

Deprotection of the tosyl moiety can be achieved by Birch reduction ($Na(s)/NH_3(l)$), or by employing other reducing agents in combination with Lewis acids [25]. Tosyl groups, similarly to trityl, also impart a highly useful UV-absorbance, making the reactions simple to follow by TLC or HPLC.

2.1.2.3 Silyl ethers

Silyl ethers have been widely used in organic synthesis, especially as protective groups for hydroxy functions [33]. Among their advantageous properties lies stability towards basic, oxidative and reductive conditions, thermal stability and the simple cleavage from their parent molecules [33]. The Si – O bonds are much stronger than normal C – O single bonds, thus acting as a driving force in many reactions [34]. The Si – F bond is even stronger, making fluoride anions exceptional reagents for the liberation of hydroxyl functionality, without many possible side reactions [35]. Some of the more well known types of silyl ethers are listed in Figure 2.4, according to their stability towards acidic (a) or basic (b) media [36].

As such, TMS is very labile towards most conditions, and is rarely used for anything else than the temporary masking of a given hydroxyl group [36]. This may prove useful in a number of reactions, where

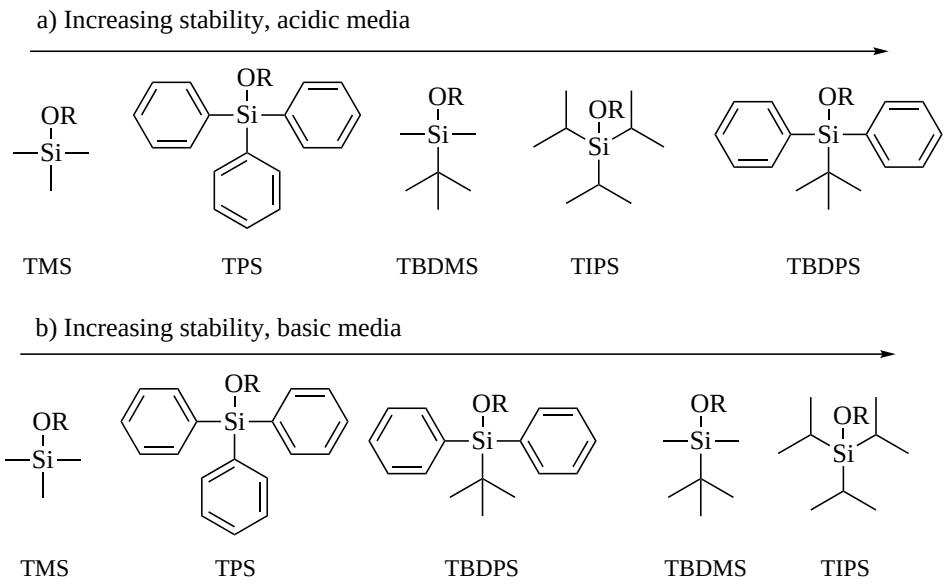

Figure 2.4: Common silyl ether derivatives used as protective groups ranked according to stability in acidic (a) and basic (b) media.

permanent protection is unwanted. One of these applications may be illustrated with the trapping of an carbonyl function on its enolate form, thus enabling specific reactivity, visualised in Scheme 2.9.

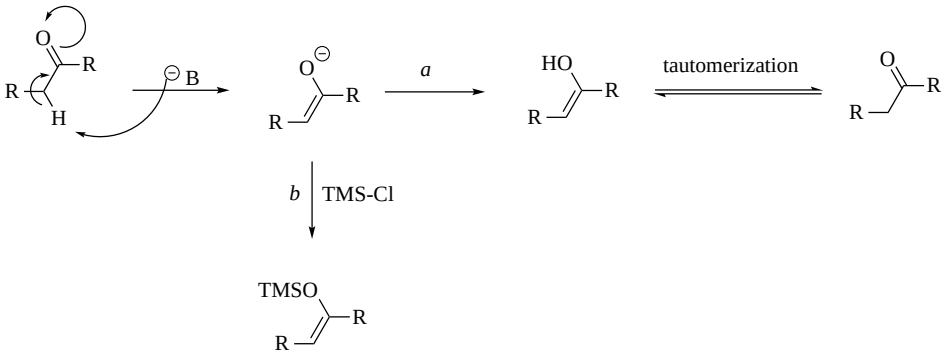

Scheme 2.9: The capture of the enolate form of a carbonyl using TMS.

The typical reagents for silylation are usually chlorides or triflates,

although a plethora of different silylating agents are available [37]. The high reactivity of the triflate derivative makes this reagent useful in the silylation of highly substituted intermediates with steric constraints, for example secondary or tertiary alcohols [38]. The downside is the relatively high nucleophilic nature of the triflate anion, mediating the generation of possible byproducts [39]. In addition to the silyl reagent, a base is required to drive the reaction towards full conversion [40]. Commonly used bases are DMAP, imidazole, 2,6-lutidine, NEt_3 or other Lewis bases, such as PPY. Scheme 2.10 shows the proposed silyl mechanism as presented by Patchinski et al., in the presence of such Lewis bases [40].

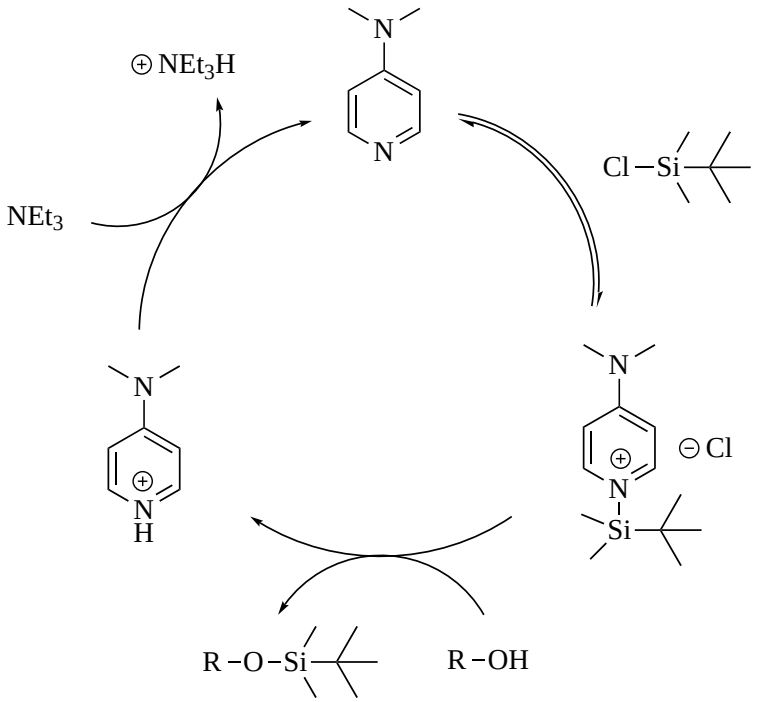

Scheme 2.10: Mechanism for the silylation with TBDMSCl using DMAP as activator on a general alcohol [40].

As mentioned earlier, silyl ethers are easily deprotected with fluoride

anions, or under acidic conditions, although since acidic conditions might cause unwanted side reactions in some situations, methods employing fluoride are generally preferred. Common commercial sources of fluoride are HF, NH_4F, or TBAF [25, 35, 36]. The proposed mechanism for deprotection of silyl ethers by fluoride anions is presented in Scheme 2.11 [35, 41].

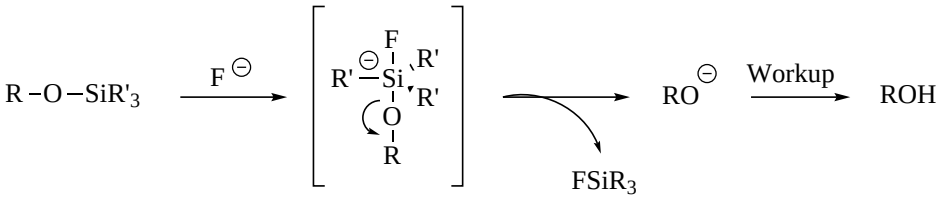

Scheme 2.11: The general mechanism for the deprotection of silyl ethers using fluoride anions.

2.1.2.4 Benzyl ethers

Benzyl ethers, typically abbreviated as BnOR, are frequently used as protective groups in carbohydrate synthesis, due to their high stability in both acidic and basic media, granted by the benzylic carbon [25, 42]. Although several derivatives exist, such as ρ-methoxybenzyl (PMB), regular non substituted benzyl ethers ($C_6H_6CH_2$) is the most common in sugar chemistry [42]. Because of their high stability and strong UV activity, benzyl ethers are usually applied as long term protective groups on hydroxyl functions, that must stay masked for several synthetic steps [42].

Benzyl ethers are highly versatile upon implementation, and can be introduced under reductive, basic, acidic or neutral conditions, depending on the properties of the starting material. In sugar chemistry, basic conditions using a relatively strong base, such as NaH, and BnBr in DMF, are the most common, thus resembling the well known

Williamson ether synthesis [43]. The protection of 1-*O*-methyl-α-D-glucopyranose under basic conditions is shown in Scheme 2.12 [42].

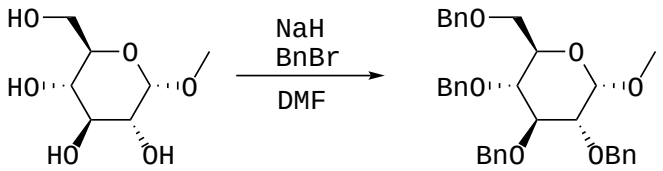

Scheme 2.12: Benzylation of 1-*O*-methyl-α-D-glucopyranose.

It is also possible to interchange the primary benzyl groups into acetate groups regioselectively using acetic anhydride, thus opening for selective functionalizations within the molecule, as shown in Scheme 2.13 [44, 45].

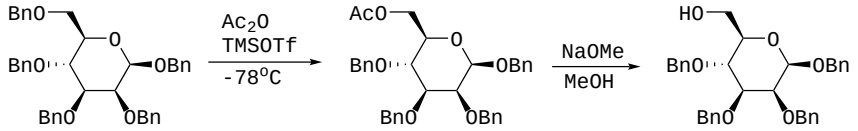

Scheme 2.13: Regioselective manipulation of primary benzyl group.

Deprotection of the benzyl moiety is usually achieved under reductive conditions, for example with catalytic hydrogenation, or Birch reduction [25, 46, 47]. Such conditions are, however, often incompatible with other functionality in the molecule, and this must be taken into account before deprotection is attempted. A good example to illustrate the problem of deprotection, related to carbohydrate synthesis, is the presence of a simple double bond within the molecule undergoing the debenzylation as shown in Scheme 2.14.

The labile allyl group is reduced to a propyl group under the respective conditions. Such problems can be avoided by masking the double bonds, for example as epoxide functions. However, it is always beneficial to reduce the amount of synthetic steps where possible [48].

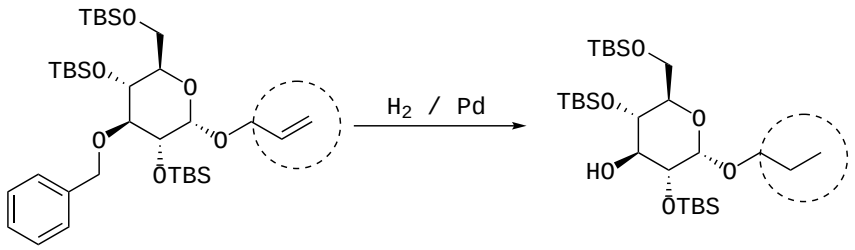

Scheme 2.14: Attempted catalytic hydrogenation of benzyl ether in the presence of labile double bond.

Catalytic hydrogenation of a benzyl ether is shown in Scheme 2.15, and yields toluene as the main byproduct, which is easily removed by evaporation under reduced pressure. Because palladium on carbon catalysts are heterogeneous, they can be easily filtered off after the reaction.

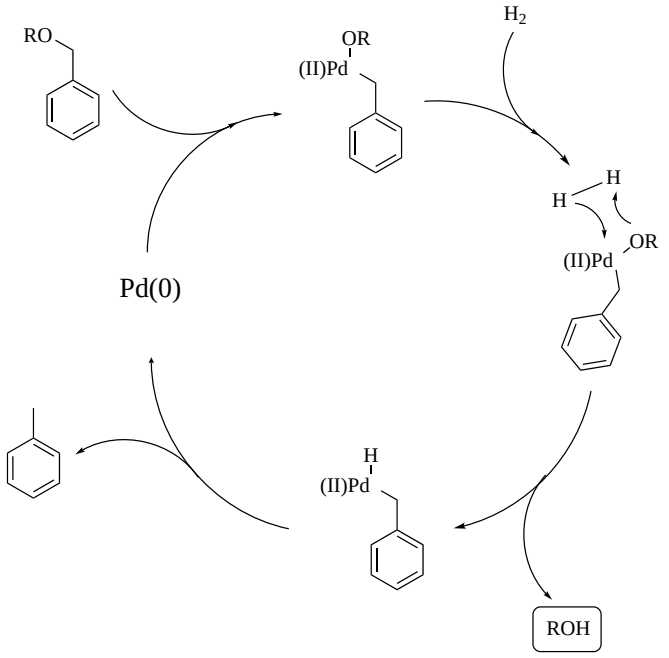

Scheme 2.15: Mechanism for the catalytic hydrogenation with palladium.

2.1.2.5 Allyl ethers

Another convenient group for the protection of alcohols is the allyl ether, which has high stability towards both acidic and basic media [25]. Although this group might seem like it is preceded by both silyl ethers and benzyl ethers in terms of popularity, and therefore usefulness, the allyl ether can contribute with unique modification potential, not inherited by the previously covered types of protective groups. Contrary to silyl ethers, for example, which are inherently used for their protective capacities, allyl ethers are also used as a handle for further development of the parent molecule, for example by oxidation or reduction [49]. As made clear from Scheme 2.14, double bonds and in particular allylic functions, are reactive under numerous conditions, therefore rigorous synthetic planning must be carried out to avoid such missteps.

Allyl ethers can be introduced in the same fashion as benzyl ethers, for example using Williamson conditions [43] (Scheme 2.12). Another method, frequently encountered in carbohydrate synthesis, is the Fischer glycosidation using allyl alcohol. This method was developed by Emil Fischer in the late 19^{th} century, and is the reaction between an aldose or ketose with an alcohol under acidic conditions [50]. Fischer glycosylation is an excellent technique to insert substituent selectively on the anomeric position, thus enabling regioselective functionalisation of that particular part of the molecule. Frequently used acids include HCl, but TMSCl has also been proven useful for obtaining high $\alpha : \beta$ ratio, due to its catalytic nature caused by the formation of the $ROSiMe_3$ intermediate [51]. The mechanism for a general Fischer glycosidation is quite similar to that of the anomerization mechanism in acidic media presented in Scheme 2.2, however the alcohol, or TMS ether intermediate, attacks the formed C=O double bond either from

above or below the ring structure, thus promoting the formation of two different anomers [52].

Deprotection of allyl ethers is accomplished under several conditions, but most notably using *t*BuOK to generate the much more labile 1-propenyl ether, which then conveniently can be removed by either acidic or basic conditions, as illustrated in Scheme 2.16 [53–55].

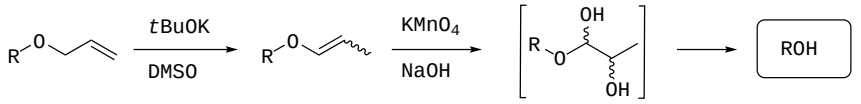

Scheme 2.16: Deprotection of allyl ether via the labile 1-propenyl ether.

Activation of the allyl group by transition metal catalysts is a more modern approach to the deprotection of allyl ethers. In such cases, the coordination of the transition metal in question enables the interaction between the π-allyl complex with mild reagents, such as weak nucleophiles, for deprotection [55–57]. While palladium reagents, such as $PdCl_2$ or $Pd(PPh_3)_4$, are widely used, rhodium derivatives, like the Wilkinson catalyst, $Rh(PPh_3)_3Cl$, also possess great deallylation potential [54, 56].

2.1.2.6 Benzylidene acetal

Acetals are extremely versatile protective groups, due to the masking potential of diols some of these derivatives can inherit, thus enabling protection of two neighbouring active sites at once [58]. This is particularly useful in carbohydrate synthesis, where many relatively similar hydroxyl groups are present in close quarters [59]. A very likely question that arises is whether this protective strategy is of any advantage at all, considering that during deprotection of said acetal, two resulting labile groups would be liberated at the same time, and the regioselec-

tivity is therefore seemingly lost. The last statement is only true for complete removal of the acetal moiety, and does not occur in the case of partial opening of acetal protective groups [60].

There are several acetal protective groups with specific reactivities and selectivities, some whom protect only one hydroxyl group, like THP or MOM, while others protect two, like the isopropylidene acetal or 1,3-dioxolane analogues [25]. This thesis shall focus on the benzylidene acetal, due to high stability and UV activity, but most importantly its high crystallinity and tendency to affect anomeric ratio, as will be made clear later on [61]. The benzylidene acetal is commonly introduced on carbohydrate substrates using benzaldehyde dimethyl acetal under acidic conditions. On pyranose substrates the reaction is regioselective for the protection of the hydroxyls present at the C-6 and C-4 carbons in the pyranose ring [61]. Scheme 2.17 shows the proposed mechanistic acetalization of benzylidene on α-D-glucipyranose [62].

As mentioned previously, the benzylidene acetal is frequently taken advantage of in carbohydrate synthesis, because of its simple and reliable implementation process. The aromatic system furnishes easy detection by UV, which makes further analyses much easier. However, the most important reason for utilising this acetal, is the regioselective opening under reductive conditions [60]. Concerning glucopyranose substrates, and depending on the reductive agent, and Lewis acids used, one can either expect cleavage of the O-6 or O-4 bond, thus liberating the resulting hydroxyl group at specific positions. Tanaka et al., have presented a method for the reduction of benzylidene acetals using DIBAL−H, containing a small review of other established methods, such as the use of $LiAlH_4$ and $AlCl_3$, which readily reduces the O-6 bond. The $LiAlH_4/AlCl_3$ methodology is also presented by

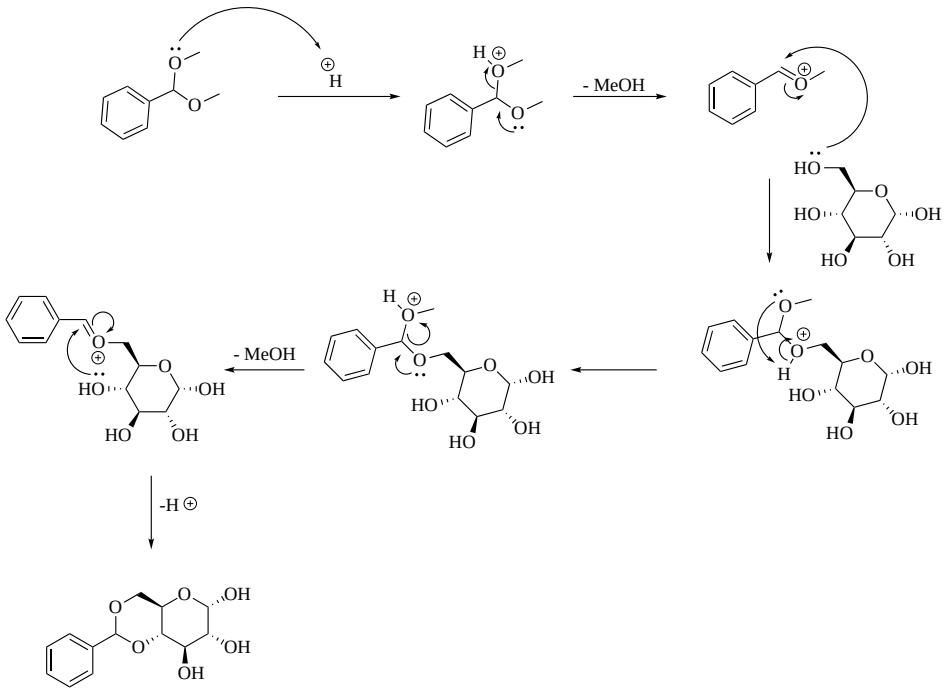

Scheme 2.17: Proposed mechanism for the reaction between benzylidene dimethyl acetal with α-D-glucopyranose under acidic conditions.

Lipták et al., [63, 64]. Other reagents, such as $NaBH_3CN$ and HCl, or Et_3SiH and TFA, showed high selectivity for the reduction of the O-4 bond in pyranose substrates [63, 65, 66]. These conditions are relatively mild, however, reductive conditions must be used with great care considering side reactions, especially, removal of other protective groups.

2.2 Carboxylic acids

Carboxylic acids are one of the fundamental functional groups in organic chemistry, and belong to the family of carbonyl compounds together with ketones, aldehydes, esters and many other similar ana-

logues of carbon-oxygen double bond containing compounds [67].

As will be made clear in the sections presented herein, carboxylic acids inherit several unique chemical properties, making them useful in a wide range of reactions [67].

2.2.1 Carboxylic acid reactivity

As all organic chemists know, carboxylic acids consists of a carbonyl group bonded directly to a hydroxyl group, which in turn weakens the O−H bond, thus imparting acidity. This acidity depends strongly on the stability of the resulting carboxylate anion, which is highly dependant on the electronic effects resulting from the rest of the molecule [68]. If the carboxylate anion is connected to a conjugated system, then the resulting negative charge can be stabilized by delocalization or resonance, and the acidity of the system increases. However if the resulting negative charge is not stabilized, or even destabilized by electron donating groups, then the acidity of the system is reduced [68]. Some carboxylic acids and their pKa values are showed in Table 2.1 [34].

Table 2.1: Carboxylic acids and their pKa values at 25°C.

Name	formula	pKa
Stearic acid	$C_{17}H_{35}COOH$	10.15
Linolenic acid	$C_{17}H_{31}COOH$	8.28
Acetic acid	CH_3COOH	4.76
Formic acid	HCOOH	3.77
Trifluoroacetic acid	CF_3COOH	0.52

The carboxyl group shows unique reactivity, and steric availability, due to the nearly planar structure, resulting from the sp^2-hybridization of the carbon atom. This can be illustrated by the calculated bond

angles of formic acid using the 6-31G* basis set, a common set of functions used to model chemical bonds in Hartree-Fock calculations, as illustrated in Figure 2.5 [15, 69].

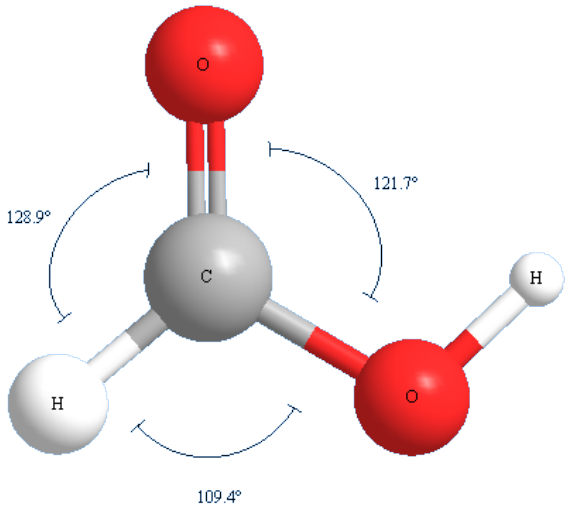

Figure 2.5: Bond angles and structure of formic acid calculated from the 6-31G* basis set.

The carbon in carbonyl groups is relatively electron poor, and therefore susceptible to nucleophilic attacks. This, along with the acidic proton, are two properties that define the reactivity of carboxylic acids [70]. Well known transformations of carboxylic acids include reduction reactions, decarboxylations, formation of acid halides, amide formation, anhydride formation, and many other reactions [32, 67, 71]. Regarding the synthesis of compound **1a** (Figure 1.1), esterification reactions are of particular interest and will be explored further in the section to come.

2.2.2 Esterification reactions

Esterification is the process in which two components, traditionally carboxylic acids and alcohols, react to form an ester product (RCOOR), often through the elimination of water [72]. Conversely, the addition of water, also known as hydrolysis, to ester bonds constitute the inverse reaction, thus establishing an equilibrium between the molecular species present in solution [73].

Since both reactions occur under relatively similar conditions, small changes in the equilibrium driving forces will have a big effect on the outcome of the reaction. Using Le Chatelier's principle, the removal of water from the reaction vessel promotes the formation of the ester product, while the presence of water promotes the hydrolysis to alcohol and acid [73]. This simple equilibrium is visualised in Scheme 2.18.

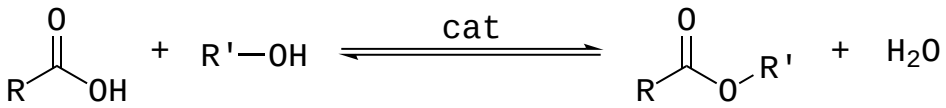

Scheme 2.18: Ester formation equilibrium

There are numerous methods to form esters, depending on the substrates involved. Some methods circumvent the equilibrium stage, by changing the mechanism of reaction entirely, for example using acid halides instead of carboxylic acids as one of the reagents [74]. Some esterification methods common in carbohydrate research are further explained in the following sections.

2.2.2.1 Fischer esterification

The process known as Fischer esterification involves the stirring of a carboxylic acid in the presence of alocohol, usually with some form of

acid catalyst, either Brønsted or Lewis acids. The reaction was first described by Emil Fischer and Arthur Speier in the late 19^{th} century, and is still fairly common in academic, educational and industrial settings. The frequent use has its roots in the mechanistic and practical simplicity, as well as reliability [75, 76]. The general mechanism for Fischer esterifications is shown in Scheme 2.19 [77].

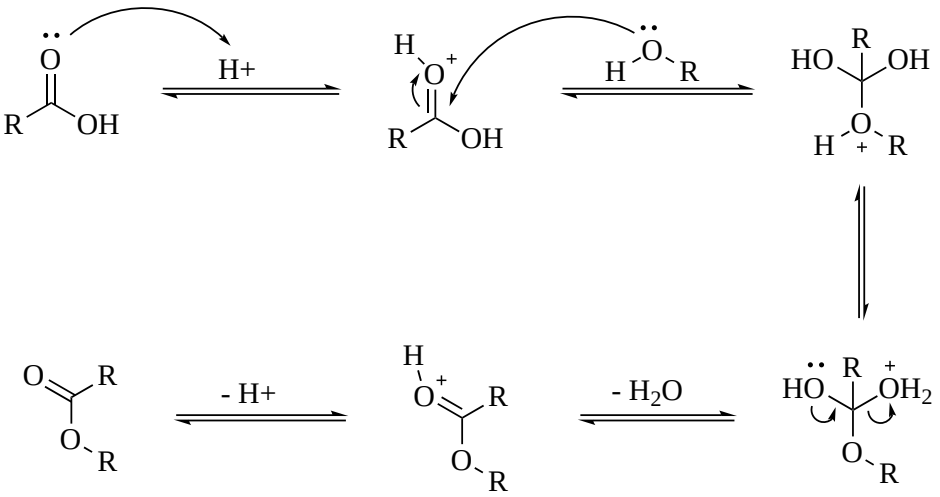

Scheme 2.19: General mechanism for the Fischer esterification

2.2.2.2 Steglich esterification

Steglich esterification is a variation of classical esterifications between a carboxylic acid and an alcohol, where a promoter, typically a carbodiimide, is utilized to initiate reactivity [78]. In addition to the carbodiimide, a base catalyst, such as DMAP, is employed to increase the rate of reaction and avoid formation of certain byproducts [78]. The reaction was first employed in esterifications by Wolfgang Steglich in 1978, using dicyclohexylcarbodiimide (DCC) as the coupling reagent and DMAP as the catalyst [79]. In recent years, several new carbodiimide derivatives have found their place as coupling reagents in

the Steglich reaction. Among those is N-(3-dimethylaminopropyl)-N-ethylcarbodiimide (EDCI), which is used partly for the water soluble urea byproduct, making workup of the reactions easier [80].

The reaction conditions used for most Steglich esterifications are mild, and proceeds at room temperature, thus appearing suitable for highly functionalized and sensitive substrates. In addition, the high rate of reaction allows for esterifications at sterically crowded positions [78]. Another convenient property of the carbodiimide activators is their water scavenging ability, thus forcing the formation of ester product [78]. The general mechanism for Steglich esterifications is shown in Scheme 2.20 [81].

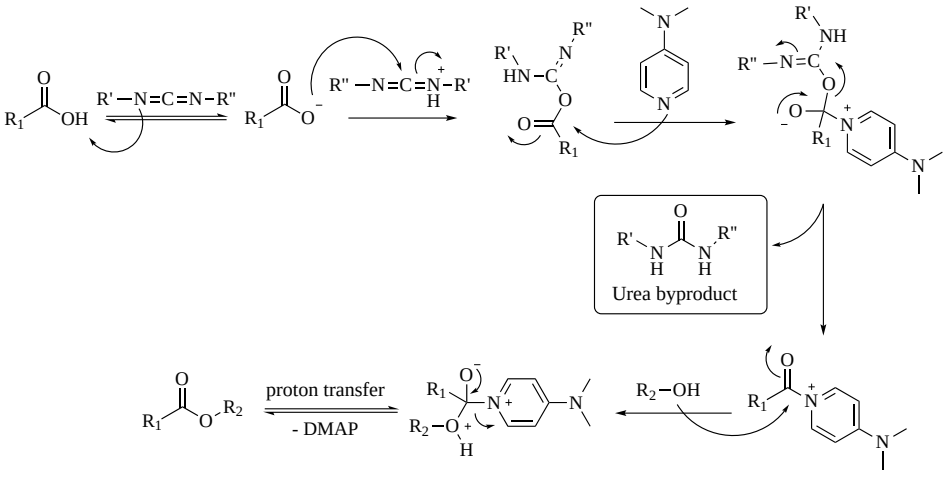

Scheme 2.20: General mechanism for the Steglich esterification

2.2.2.3 Enzymatic esterification

The utilisation of enzymes is becoming increasingly popular in organic synthesis, due to the stereo selectivity and the possibility of running organic reactions in aqueous media, useful for highly polar reactants. Low consumption of organic solvents, toxic reagents, and simple re-

covery of the product, make bio catalytic reactions sought after in cosmetics and food industry [82].

Lipase A and B from *Candida antarctica*, abbreviated CAL-A and CAL-B respectively, are common enzymes used to catalyse the acylation of hydroxyl groups in natural compounds, such as flavonoids [83]. CAL-B also possess high enantioselectivity to chiral substrates, yielding enantiomerically pure product from racemic mixtures [84]. Enzymes are also frequently encountered in carbohydrate synthesis for the mild reaction conditions and stereo selectivity [85]. Sterically crowded positions are, however, often not compatible with the active site of the enzyme, thus limiting the esterification potential of highly functionalized substrates [86, 87]. Enzymatic esterification is not employed in the work presented herein, however it might be applicable in the esterification of unprotected sulfoquinovose (Chapter 5).

2.2.2.4 Transesterification

Transesterifiation is the process of interchanging one organic substituent from an ester in the presence of a catalyst, to another organic group from an alcohol, as visualized in Scheme 2.21.

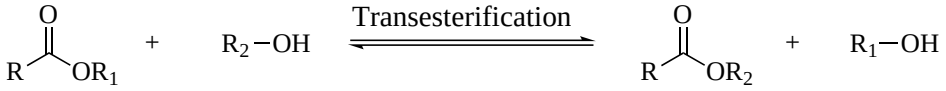

Scheme 2.21: Simple schematic representation of transesterification.

To drive the equilibrium forward, it is common to use a small R_1 group and a bulky R_2 group, such that the resulting small and volatile alcohol byproduct can be distilled off during the reaction, yielding pure ester product [88, 89].

2.3 Sugar fatty acid esters

Sugar fatty acid esters (SFAEs) are important target molecules for synthesis, due to their wide range of industrial and medicinal applications [90, 91]. The general structure of SFAEs contains a type of carbohydrate, typically a mono- or di-saccharide, and one or multiple lipid chains bonded through an ester bond [91]. Sucrose monostearate is a fairly simple SFAE structure, shown in Figure 2.6.

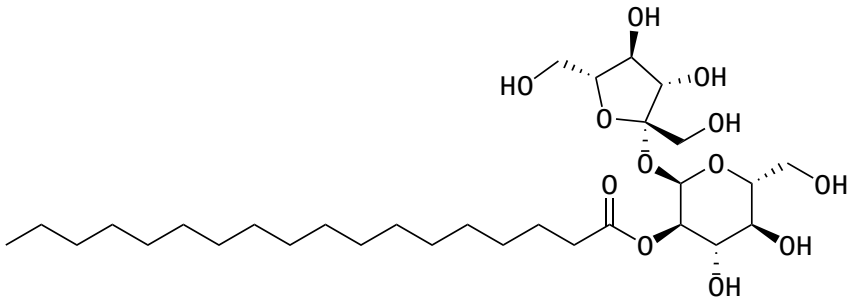

2.5a

Figure 2.6: Sucrose monostearate.

With the hydrophilic head group and long hydrophobic tail, SFAEs fall under the category of non-ionic surfactants and prove to be suitable emulsifiers in industry, cosmetics, food and pharmaceuticals due to their low toxicity [92]. Sucrose monostearate (**2.5a**) can appear as several analogues, depending on the location of the resulting fatty acid chain however the surfactant properties are nevertheless persistent, and with the nonexistent toxicity, these type of surfactants are frequently used as food emulsifiers around the world [92].

In recent years it has been discovered that certain SFAEs also posses antimicrobial properties, indicating untapped bioactivity potential [93].

2.4 Biological assessment

Compound **1a** was found to affect the PLA_2 enzyme, responsible for the release of arachidonic acid (20:4), which is essential in the inflammatory cascade [3, 94]. The inflammatory cascade is a highly complex biochemical process that releases signal molecules as a response to some phenomenon, for example contact with reactive or toxic substances. These signal molecules contribute with blood flow, swelling of tissue and heightened cell growth of the affected area as a fighting or healing response. The inflammatory cascade is partly illustrated in Scheme 2.22 [95–97].

Heightened cell growth is one responses from the inflammatory cascade, thus chronic inflammation and cancer are tightly connected [98]. Molecules that inhibit either LOX, COX or the Phospholipase enzymes, might also inhibit tumour growth, proving as valuable anticancer drug candidates. Biological evaluation of synthesised compounds similar in structure to the target compound (**1a**), contribute to a structure activity relationship study (SAR) toward new pharmacophores. In the branch of science known as medicinal chemistry, biological studies combine with organic or structural chemistry to discover molecules with applications in the treatment of various conditions. Such discoveries are often attributed to structure activity relationship studies, in which a structural moiety inherit some biological effect. This biological effect is then attempted replicated on other model substrates to either enhance or in other ways modify the biological response, thus creating a library of potentially active compounds [99, 100].

Fatty acids are known to possess pharmacological effects, especially

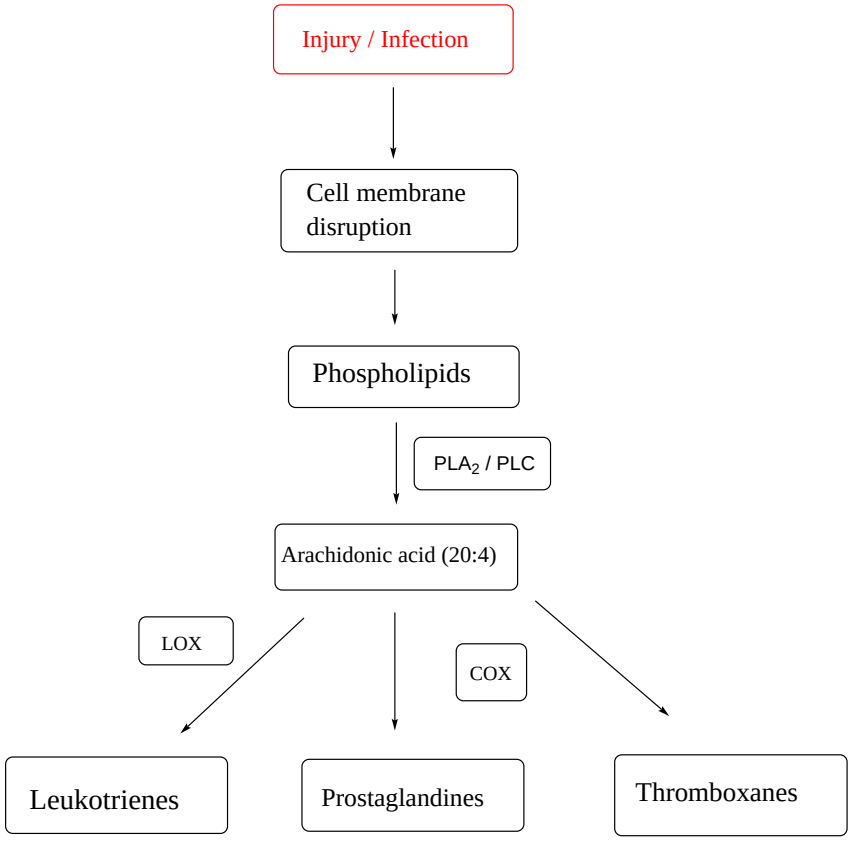

Scheme 2.22: Schematic overview of the inflammatory cascade, from injury to release of signal molecules promoting an inflammatory response. LOX: lipooxygenase, COX: cyclooxygenase.

unsaturated fatty acids, such as α-linolenic acid [101, 102]. Glucose pharmacophores have already been investigated in the inhibition of sodium-dependent glucose co-transporters for the treatment of diabetes [103]. Sugar fatty acid ester, are therefore becoming a compound class interesting for pharmaceutical study.

There are numerous ways to study a compounds biological activity. In the section below, a spectrophotometric assay measuring cell viability

after treatment, is explained in further detail. Deeper investigation on the topics of biological activity and assessment are out of the scope of this thesis.

2.4.1 MTT-assay

MTT (Scheme 2.23) is a tetrazole derivative appearing as a yellow bromine salt. If MTT comes in contact with a reducing agent, it will quickly react to form a formazan compound (Scheme 2.23), with a strong purple colour [104]. In the mitochondria of cells, an enzyme named mitochondrial reductase readily reduces MTT to its corresponding formazan, thus indicating the viability of present cells [105]. Scheme 2.23 illustrates the structure of both MTT and the resulting formazan after contact with mitochondrial reductase.

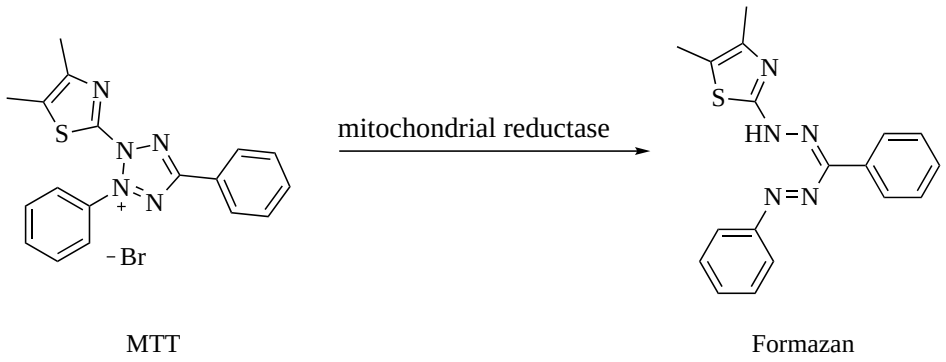

Scheme 2.23: Structure of MTT, faint yellow, and the produced formazan, purple, by reduction.

By comparing absorbance to applied compound concentration, cell viability (%) can be assessed relative to the concentration of applied compound. There are several other colorimetric assays apart from MTT explored in literature [106].

Chapter 3 - Results and Discussion

Results regarding extensive research on protective strategy, selective deprotections and functionalization of α-D-glucopyranosides are presented in the following sections. This chapter is structured in four main parts, which is listed below, to provide clarity and guidance to the reader.

Section 3.1 covers protective strategy in the synthesis towards 1-*O*, 4-*O* and 6-*O* hydroxy-α-D-glucopyanosides. Section 3.2 investigate esterification techniques, and the attempted optimization of a working esterification procedure yielding sugar fatty acid esters. Section 3.3 concerns biological evaluation of esterified compounds. Section 3.4 explores the characterisation of selected synthesised compounds by various spectroscopic methods.

3.1 Synthesis of α-D-glucopyranoside intermediates

The nO terminology is employed throughout this chapter, however it might be confusing to some, thus a short clarification is in order. An n-O intermediate where $n = 1, 2, 3, ...$ relates to a pyranose backbone where all the hydroxyl groups, except the one present at carbon n, are protected with various substituents. For example, 6-O and 4-O will describe compound **10** and **12**, respectively, because of their free hydroxyl groups at the given positions. Figure 3.1 explains the n-O concept further.

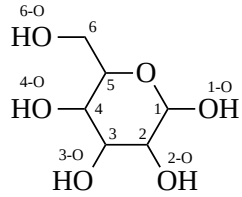

Figure 3.1: Employed numbering system when referring to individual positions within the pyranose backbone.

3.1.1 The route to a 6-*O* intermediate

Early in the synthetic planning, two different protective pathways were investigated for their synthetic advantages towards a 6-O intermediate. The two paths were based on the works of Hanashima et al., and Izumi et al., in the synthesis towards SQAGs and selective implementation of benzylidene acetals, respectively [1, 51]. Both paths start from α-D-glucopyranose (**SD1**, Scheme 3.1) and progress with glycosylation at 1-O using allyl alcohol. The synthetic overview of these two pathways is visualised in Scheme 3.1.

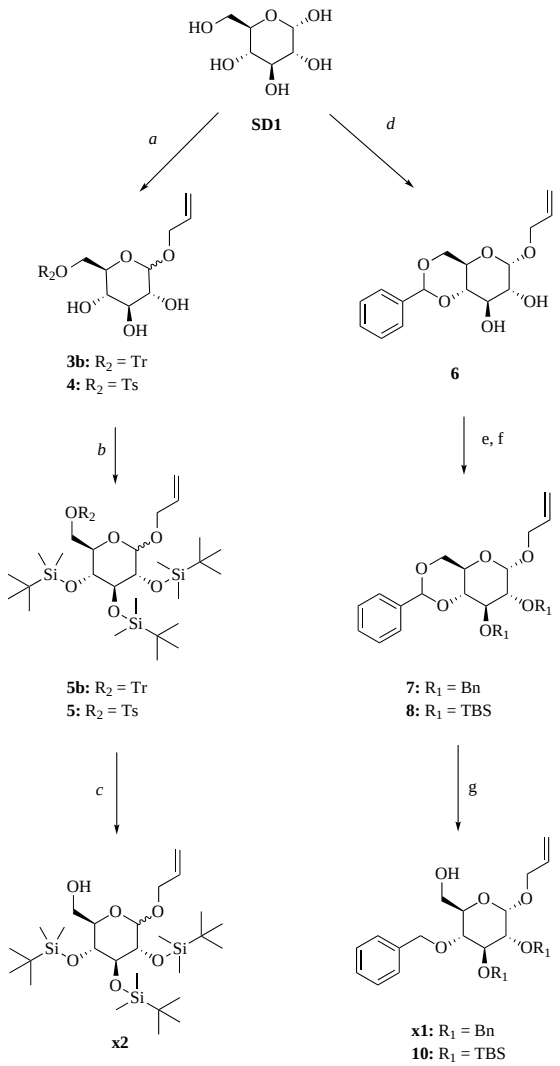

Scheme 3.1: Two pathways in the synthesis towards 6-*O*-α-D-glucopyranoside intermediates. Path 1, *a*: 1) Allyl-OH, TMS-Cl, 60°C, 5h. 2) Ts (**4**)/Tr (**3b**)-Cl, DMAP, pyridine, rt, 16h; *b*: TBDMS-OTf, 2,6-lutidine, DCM, 0°C, 5h; *c*: K_2CO_3, LiBr, DMF, rt, 1h, not attempted. Path 2, *d*: 1) Allyl-OH, TMS-Cl, 60°C, 5h. 2) $PhCH(OMe)_2$, ρ-TsOH, ACN, rt, 5h; *e* (**7**): BnBr, NaH, THF, TBAI, 60°C, 2h; *f* (**8**): TBDMS-Cl, imidazole, DMF, rt, 2d; *g*: $LiAlH_4$, $AlCl_3$, CH_2Cl_2/Et_2O, reflux, 1.5h.

Experimental work was first conducted on path 1, because of the promising work presented by Keisuke et al., in the synthesis toward functionalized sugar derivatives [107]. First, Fischer glycosidation using allyl alcohol in the presence of TMS-Cl, as described by Izumi et al. and illustrated in Scheme 3.2 was carried out [51].

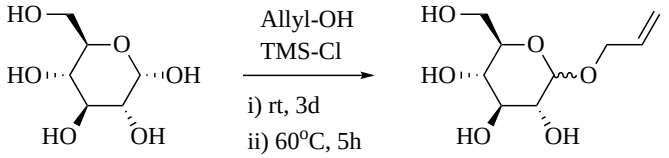

Scheme 3.2: Ficher glycosidation of α-D-glucopyranose.

It is important to notice that glycosidation reactions (Scheme 3.2) follow a mechansim which yields two possible products, even from anomerically pure starting material (2.1.1). The resulting α/β mixture (Scheme 2.2, Scheme 2.3) must be taken into account when discussing the viability of competing pathways, and possible purification potential from sequential steps.

The glycosidation was conducted using two different methods, i and ii (Scheme 3.2), where ii provided less β anomer (20 %), compared to i (26 %), under more time efficient reaction conditions, thus making it the method of choise. The product was purified by silica gel flash chromatography (20:1 DCM/MeOH), however, due to the highly polar nature of both the product and resulting byproducts, this was not successful. Further purification work was omitted, as further advance in the synthetic pathway was achievable using the crude mixture as starting material [51, 107].

The next segment of path 1, step *a* progressed with protection of 6-*O* with a bulky group showing high selectivity for primary alcohols.

Both trityl (2.1.2.1) and tosyl (2.1.2.2) groups were deemed suitable alternatives, and the results are listed in Table 3.1.

Table 3.1: Results from path 1 *a*. Constant reaction parameters: DMAP (31 mg/g SM), pyridine (30 mL/g SM), rt, 16h.

entry	reagent (eq)	scale (g)	yield (%)
1	TrCl (1.2)	1.0	-[a]
2	TrCl (2.0)	5.0	-[a]
3	TsCl (1.0)	0.5	24*[b]
4	TsCl (1.2)	2.0	73*[a]
5	TsCl (2.0)	10.0	48*[a]

a: H_2O. *b*: NEt_3(1 eq) /H_2O. * = product mixture.

Selective 6-*O*-tritylation gave disappointing results, when compared to general literature procedures [27, 108]. The reaction was attempted purified by recrystallization from ethanol, using water as an anti solvent. However, this was unsuccessful, yielding a complex mixture of species, which could not be individually identified by NMR.

The problematic tritylation might be attributed to the crude starting material, resulting in several inseparable tritylated analogues to the main product, where the trityl or allyl groups occupied different positions within the molecule. 6-*O*-Trityl-D-glucopyranoside could also be present in the product mixture, contributing to the separability issues. This hypothesis was strengthened with the successful selective 6-*O*-tritylation of commercially available 1-*O*-methyl-α-D-glucopyranoside (Scheme 3.3).

Tritylation of 1-*O*-methyl-α-D-glucopyranoside (Scheme 3.3) progressed as expected from literature, yielding compound **3** (66 %) as a white solid [109]. Previous work within the research group also suggests that 1-*O*-methylated derivatives are more crystalline, and

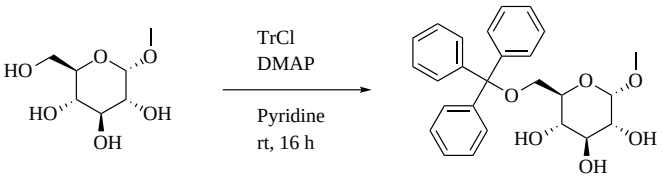

3

Scheme 3.3: Selective 6-*O*-tritylation of 1-*O*-methyl-α-D-glucopyranoside.

therefore more easily purified than their allylic counterparts. Crystallinity is highly affected by the purity of the sample, thus pure 1-*O*-methyl-6-*O*-trityl-α-D-glucopyranoside is expected to inherit a higher recrystallisation potential then the allylic derivative, appearing as an anomeric mixture.

The tosyl counterpart gave more promising results (Table 3.1), however separation from the starting material, as well as anomeric separation was not achieved, yielding a compound mixture. From this mixture, the product could be identified with certainty. The yields presented in Table 3.1 refer to product mixture after silica gel flash chromatography (20:1 EtOAc/MeOH).

At this point a new strategy towards a 6-*O* intermediate had to be investigated, seeing no anomeric resolution following path 1. Path 2 step *d* (Scheme 3.4) starts with Fischer glycosidation using allyl alcohol. The crude residue, and without further work up, was reacted with benzaldehyde dimethyl acetal under acidic conditions (Scheme 3.4).

After completion of the reaction, the mixture was precipitated, crashing out the product as a light brown solid, which could then be filtered off. Precipitation media are listed for each entry in Table 3.2. The brown solid was recrystallized from ethanol and water. Results re-

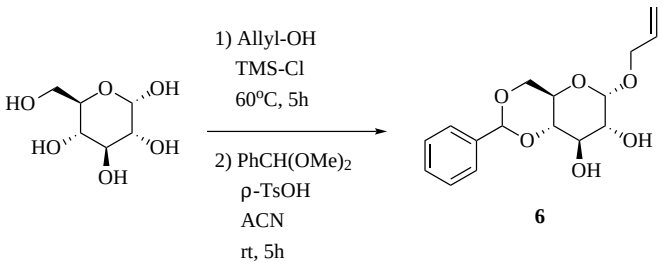

Scheme 3.4: Synthesis of compound **6**.

garding the acetalization are listen in Table 3.2.

Table 3.2: Acetalization of 1-*O*-allyl-α-D-glucopyranoside. Constant reaction parameters: ρ-TsOH (0.1 eq), ACN, rt, 5 h. Work-up procedure are listed for each entry together with yields.

entry	acetal (eq)	additives	SM (g)	yield (%)
1	1.5	-	0.5	48[c]
2	1.5	-	10.2	50[c]
3	1.5	DMF[a]	5.0	39[d]
4	2.5	DMF[a]	5.1	41[e]
5	1.5	-	2.2	43[e]
6	1.5	TBAI[b]	0.5	22[c]

a: 5 vol% *b*: 15 mol% *c*: H_2O/$NaHCO_3$ *d*: H_2O/*n*-pentane *e*: *n*-pentane

The starting material was not soluble in ACN, so the reaction progressed as a suspension. The effect of completely dissolving the reagents in DMF (entry 3, 4), or using TBAI as a phase transfer catalyst (entry 6) were investigated for potential yield increasing measures, however, to no avail. The best yield from this one pot procedure over two steps (Fischer glycosylation before subsequent acetalization) was 50% (entry 2), using neat ACN as the solvent and without any additives. When conducting the work-up, the product was crashed out in a large volume of solvent, in which it has very low solubility. As DMF is both a strong solvent and miscible in water, it is conceivable

that some product may have been lost in filtration, thus reducing the yield in reactions where DMF was used as additive (entry 3, 4). TBAI caused some unknown by reaction, leaving dark crusts in the product even after recrystallization (entry 6). Because of the poor yield obtained from the parallel with TBAI, no further work was conducted on the analysis of said byproducts. The appearance of product from entry 1 and 6, Table 3.2, are displayed in Figure 3.2.

Figure 3.2: The apperance of entry 1 (right) and entry 6 (left) listed in Table 3.2.

^{1}H-NMR was conducted on the crude mixture before recrystallization to investigate the α:β relationship (Figure 3.3), revealing 22% β anomer as indicated by Figure 3.3.

The α anomer is highly crystalline compared to the β anomer, which appeared more like a viscous residue, with a high solubility in heated ethanol. This radical difference in physical properties provided a reliable method towards anomeric separation, yielding pure α-D-glucopyranoside from recrystallization. The observed difference in crystallinity is not readily apparent, however, one possibility is the intramolecular hydrogen bonding network occurring between 1-O and

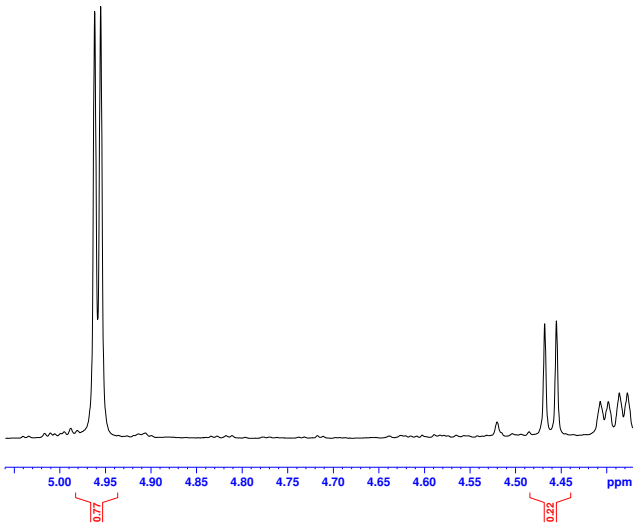

Figure 3.3: ^{1}H-NMR (600 MHz, $CDCl_3$) of the crude mixture from Table 3.2, entry 5. α proton: 4.96 ppm, β proton: 4.46 ppm.

2-*O*. This network is deemed stronger in the β anomer, due to the equatorial position of the anomeric substituent, leaving 1-*O* in the same plane as 2-*O*. This may in turn reduce the crystallinity of the β anomer due to lower availability for intramolecular H-bonding [110]. The spacial orientation of the anomeric substituent in both α and β D-glucopyranoside is visualised in Figure 3.4.

To illustrate the hydrogen bonding between 1-*O* and 2-*O* in compound **6** further, a minimized energy conformational analysis was computed using Chem3D.

The energy conformations show longer hydrogen bond length of the α anomer (3.1 Å) compared to the β anomer (2.5 Å). Strong intramolecular hydrogen bonding might reduce the crystallinity, while strong intermolecular hydrogen bonding have been proved to increase crys-

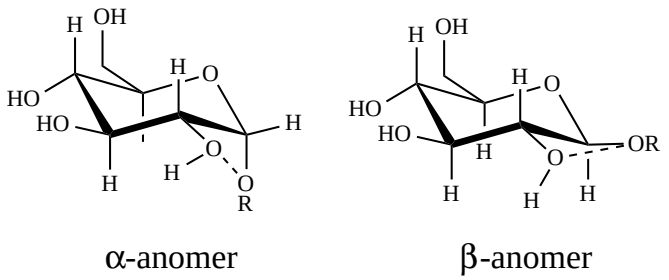

Figure 3.4: The chair conformation of α and β glucopyranoside. Arrows represent hydrogen bonding between 1-*O* and 2-*O*.

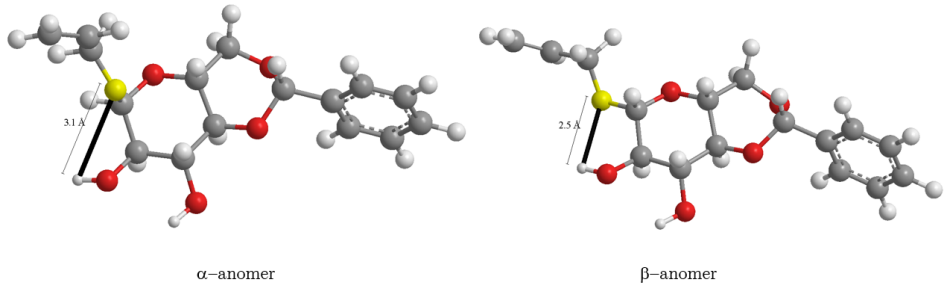

Figure 3.5: Calculated hydrogen bond length (black line) of alfa (left, 3.1 Å) and beta (right, 2.5 Å) 1-*O*-allyl-4,6-*O*-benzylidene-D-glucopyranoside. Structures are shown in the calculated minimized energy conformation using Chem3D. Yellow: anomeric oxygen, red: oxygen, white: hydrogen, grey: carbon.

tallinity in polymers [111]. The origin of the heightened crystallinity observed for the α anomer remains ambiguous.

Additional protection of compound **6** (step *e*, *f* Scheme 3.1) produced a fully protected α-D-glucopyranoside moiety. As mentioned in theory (2.1.2.4), benzyl ethers are attractive protective groups in carbohydrate synthesis due to their sturdiness and ease of implementation, making them excellent in trial reactions. In this case, basic conditions (NaH) were deemed as preferable, due to possible hydrolysis of the

benzylidene acetal under acidic conditions.

The benzylation proceeded according to Scheme 3.5, and the results for the benzylation of compound **6** are presented in Table 3.3.

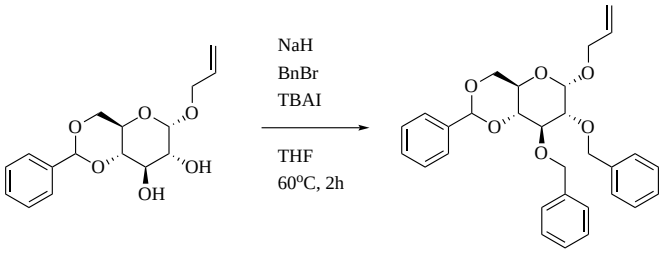

6 **7**

Scheme 3.5: Synthesis of compound **7** under basic conditions.

Table 3.3: Benzylation of compound **6**. Constant reaction parameters: NaH (4.5 eq), TBAI (10 mol%), THF (25 mL / g), 60°C.

Entry	SM (g)	BnBr (eq)	time (h)	yield (%)
1	0.20	3	1	62
2	0.21	3	2	73
3	1.03	4	2	86

The reaction progressed according to literature, with higher amount of benzyl bromide yielding better results [107, 112]. TBAI was primarily used as a phase transfer catalyst, however it has also been reported to increase the rate of benzylation reactions [113, 114]. Full conversion of the starting material was observed after 2 hours.

Protecting the hydroxyls at C-2 and C-6 of compound **6** was also carried out using TBDMS groups, due to their application in the total synthesis of compound **1a** (Scheme 1.1). In addition, TBDMS groups have the great advantage of mild deprotection using fluoride anions

[36]. Because the SFAEs synthesised herein, should possess a similar, yet simpler structure to that of compound **1a**, deprotection after esterification is wanted. Investigation on the deprotection of silyl ethers on esterified compounds were, therefore, highly interesting in the larger total synthesis project. Global deprotection of benzyl ethers is not possible on SFAEs, because of the reductive conditions employed during such reactions. Deeper investigation on the deprotection of SFAEs is described in 3.2.

Two different silylation techniques were explored on compound **6** (Scheme 3.6).

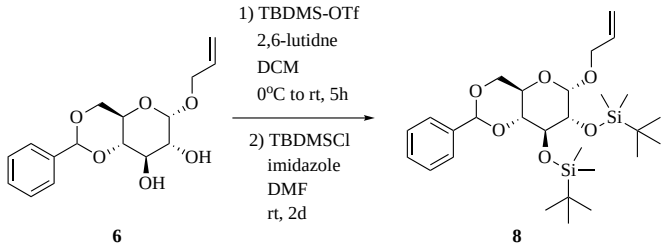

Scheme 3.6: Synthesis of **8** using two silylation techniques (1 and 2).

Results from the silylation of **6**, using method 1 and 2, are listed in Table 3.4.

Silylation of **6** using 2,6-lutidine and TBDMS-OTf (entry 1 and 2, Table 3.4) yielded poor results, compared to previous work by Tanaka et al. [115]. Silylation lasting four hours in the presence of 2,6-lutidine and TBDMS-OTf in 5 and 3 equivalents, entry 1, remained as a colourless solution throughout the reaction. The presence of byproducts were observed after full conversion of the starting material, as indicated by HPLC (method A, 6.1.1.2). This byproduct, although not isolated, is believed to be the mono-silylated analogue of compound **8**, based on

Table 3.4: Silylation of compound **6**. Constant reaction parameters: 1) DCM (15 mL / g), 0°C → rt. 2) DMF (30 mL / g), rt.

Entry (1)	SM (g)	cat (eq)	silyl reagent (eq)	time (h)	yield (%)
1[b]	0.26	5.0	3.0	5	43
2[b]	1.00	2.0	2.5	12	-[a]
3[c]	0.25	1.5	2.0	24	-[a]
4[c]	1.03	3.0	2.0	48	38
5[c]	1.07	5	3,4	24	34
6[c]	2.05	7.5	6.3	72	93
7[c]	3.01	7.5	6.3	72	84
8[c]	3.05	10.0	10.0	48	78
9[c]	3.75	7.5	6.3	72	82
10[c]	5.00	5	5	72	79

a: no product could be isolated for analysis.

b: cat = 2,6-lutidine, silyl reagent = TBDMSOTf.

c: cat = imidazole, silyl reagent = TBDMSCl.

the NMR integrals.

When employing TBDMS-OTf and 2,6-lutidine in 2.5 and 2 equivalents, entry 2, the reaction turned deep green after addition of the triflate reagent. The crude mixture was analysed by ^{1}H-NMR and HPLC (method A, 6.1.1.2), and no presence of product **8** could be observed. The volatile triflate reagent is highly reactive towards water, thus residual water or other reactive species could have caused a side reaction, preventing product formation.

Additional variance of reaction parameters could have resulted in higher yields using TBDMS-OTf and 2,6-lutidine (Scheme 3.6). Further experimentation stopped because classical insertion of TBDMS using the chloride together with imidazole (entry 3 - 10) Scheme 3.6) gave compound **8** in excellent yields (Table 3.4) [40]. Obtaining com-

pound **8** was a breakthrough in the synthesis towards SFAEs, considering its availability to form both a 4-*O* and 6-*O* intermediate.

The last step in the synthesis towards a 6-*O* intermediate boiled down to the regioselective opening of the benzylidene acetal. Extensive research on regioselective cleavage of benzylidene acetals on carbohydrate derivatives have been conducted by several research groups, especially on benzylated or acetylated derivatives. Few has attempted reductive cleavage in the presence of TBDMS-ethers [63, 65, 66, 116–118]. Wang et al. cleaved the ρ-methoxy benzylidene acetal in the presence of TBDMS ethers on β-mannopyranosides [119].

The reductive opening of the benzylidene acetal yielding a 6-*O* intermediate is presented in Scheme 3.7.

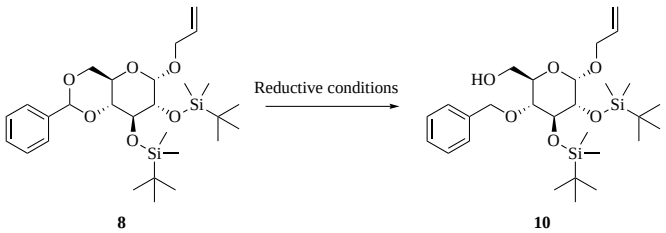

Scheme 3.7: Regioselective cleavage of benzylidene acetal **8** in the synthesis towards a 6-*O* intermediate (**10**).

The reductive cleavage of **8** were attempted multiple times under different conditions, results are listed in Table 3.5.

Regioselective opening of the benzylidene acetal **8** to yield a 6-*O* intermediate **10** proved a considerable challenge. Although rigorous experimentation has been conducted by other research groups, most have been in the presence of benzyl ethers, possessing higher stability towards Lewis acids and most reducing agents, contrary to the TBDMS ethers employed in this work.

Table 3.5: Reductive cleavage of benzylidene acetal **8**. Reducing agent and Lewis acid/catalyst are given for each respective entry. Starting material was dissolved in 60 mL/g solvent. Fraction of DCM:Et_2O = 7:4.

Entry	SM (g)	red agent (eq)	LS/cat (eq)	solvent	temp (°C)	time (h)	yield (%)
1[b]	0.26	2.5	2.5	DCM/Et_2O	50	2	32
2[b]	0.52	2.0	2.0	DCM/Et_2O	40	1	70
3[b]	1.60	2.5	2.5	DCM/Et_2O	50	2	-[a]
4[b]	1.72	2.5	2.5	DCM/Et_2O	rt	2	38
5[c]	1.07	10.0	2.0	DCM	0	4	-[a]
6[d]	1.05	10.0	8.1	ACN	0	8	-[a]
7[e]	0.57	3.0	-	Toluene	-10	15	-[a]
8[b]	7.02	4.5	4.0	DCM/Et_2O	40	1	-[a]
9[b]	1.05	1.5	1.5	DCM/Et_2O	rt	4	55
10[b]	0.53	1.0	1.0	DCM/Et_2O	-10	16	-[a]

a: no product could be isolated for analysis.
b: $LiAlH_4$, $AlCl_3$.
c: Et_3SiH, $AlCl_3$.
d: $NaBH_4$, TCT.
e: DIBAL−H.

The most promising method listed in Table 3.5 employed $LiAlH_4$ and $AlCl_3$, where $AlCl_3$ is believed to coordinate to the 6-*O* oxygen, thus allowing $LiAlH_4$ to donate a hydrogen. The mechanism is visualised in Scheme 3.8.

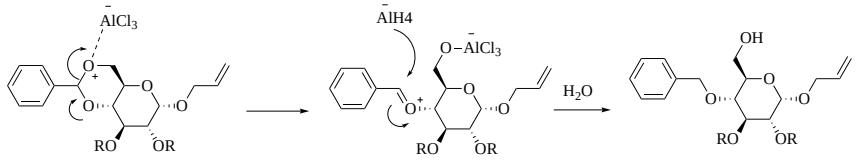

Scheme 3.8: The proposed mechanism for the 6-*O* reduction of **8** [31]

While silyl ethers possess some stability towards reductive conditions, high temperature in conjugation with bombardment of several equivalents $LiAlH_4$ and $AlCl_3$ resulted in the reduction of not only the benzylidene acetal, but also present silyl groups. All reactions presented

in Table 3.5 were monitored by HPLC (6.1.1.2, method A) using the pure benzylidene acetal (**8**) as a point of reference ($t_R = 53$ min).

As can be seen from Table 3.5, several attempts gave no product that could be isolated, either because of severe byproduct formation, or no conversion of the starting material. Employing $LiAlH_4$ and $AlCl_3$ in high equivalents (entry 3 and 8) yielded the formation of one main byproduct, and although not isolated, the byproduct is assumed completely desilylated, due to the exhibited polarity observed by HPLC ($t_R = 9$ min, Figure 3.7), and the observed 6-OH proton in NMR. The assumed byproduct structure is shown in Figure 3.6. The chromatogram (Figure 3.7) is presented underneath. The peak at $t_R = 8.715$ is assumed compound **10a** (Figure 3.6).

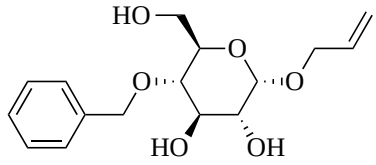

10a

Figure 3.6: Assumed structure of formed byproduct in the synthesis towards compound **10**

Previous research within the group has been conducted on the 3-*O* benzylated analogue to compound **10a**, with a retention time of $t_R = 8$ min using the same chromatographic method.

Attempted reduction of the benzylidene acetal employing $Et_3SiH/AlCl_3$, $NaBH_4$/TCT, DIBAL-H and $LiAlH_4/AlCl_3$ at low temperature (entry 5, 6, 7, 10, Table 3.5) gave no, or very little, conversion of starting material. Observing no reduction of the benzylidene acetal, indicates too mild reaction conditions. As

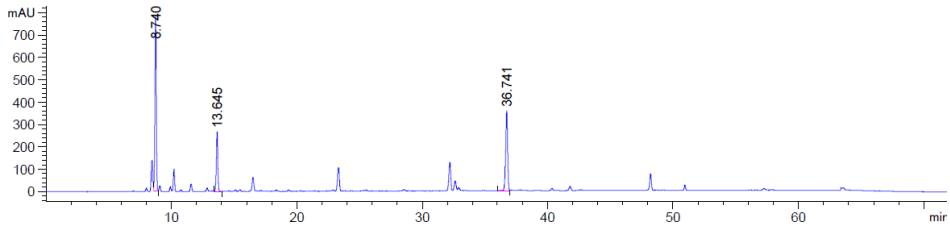

Figure 3.7: HPLC of entry 8 (Table 3.5), DAD detection, 214 nm.

DIBAL-H is highly reactive, the observed low conversion was quite unexpected (entry 7). DIBAL-H reacts violently with any residual impurities, such as water. The toluene used in entry 7 was dried over activated molecular sieves, however this might not have been enough. Residual water would have been detrimental for the reaction, thus contributing to the abysmal conversion observed in entry 7. The reduction mechanisms of $LiAlH_4$ and DIBAL-H is quite different. $LiAlH_4$ donates H^- which then directly attacks any electrophilic position, acting as a nucleophilic reducing agent. DIBAL-H is first attacked by any free electron pairs forming an X-Al bond, where X is any heteroatom containing lone pairs, such as oxygen or nitrogen, thus acting as an electrophilic reducing agent [120]. This mechanistic difference might attribute to DIBAL-H's high reactivity towards water. Further investigation of the regioselective opening of the benzylidene acetal (**8**) was deemed counterproductive for the goal of this thesis. If more time was allocated to investigation of benzylidene cleavage, the employment DIBAL-H and other reducing agents, could have been explored in more detail. Nevertheless, a method yielding

6-*O* intermediate **10** in high yield was discovered, running the reaction in relatively small scale (500 mg) and with 2 equivalents of both $LiAlH_4$ and $AlCl_3$, making the reaction conditions considerable milder. Purification using silica flash chromatography was simple, due to full conversion of the starting material, producing compound **10** in 70% yield.

3.1.2 The route to a 4-*O* intermediate

The secondary hydroxyls in position 2-4 are fairly similar in nature, and often not readily chemically distinguishable. Therefore, selective functionalization on one of the above groups often comes down to spacial orientation [26, 121]. Conveniently, the benzylidene acetal synthesised when pursuing a 6-*O* intermediate (**8**, Scheme 3.6) already protects the 4-*O* hydroxyl selectively relative to the silyl groups present at 2-*O* and 3-*O*. Because of this, all literature concerning a regioselctive cleavage of benzylidene acetals yielding the 4-*O* hydroxyl were of particular interest. The works of DeNinno et al,. and Tananka et al,. were examined closely [63, 66].

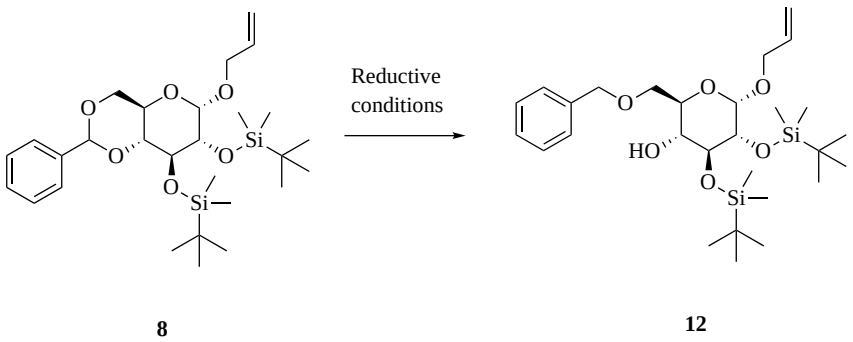

8 **12**

Scheme 3.9: Regioselective reduction of benzylidene acetal **8**.

Results from the regioselective clevage of benzylidene acetal **8** towards a 4-*O* intermediate **12** are presented in Table 3.6.

Utilizing Et_3SiH and $BF_3 \cdot Et_2O$ only formed byproducts, as indicated by HPLC (method A). The use of Et_3SiH and $BF_3 \cdot Et_2O$ have previously been reported as efficient and highly selective cleavage of benzylidene acetals, yielding the 4-*O* derivative [63]. Therefore, no conversion of the presented acetal (**8**) to 4-*O* intermediate (**12**), was surprising at first. Delving further into literature revealed the desilylation poten-

Table 3.6: Reductive cleavage of benzylidene acetal **8**. Reducing agent and Lewis acid/catalyst are given for each respective entry.

Entry	SM (g)	red agent (eq)	LS/cat (eq)	solvent	temp (°C)	time (h)	yield (%)
1[b]	0.51	3	2	DMF	rt	4	-[a]
2[b]	1.52	12	2	DCM	0	4	-[a]
3[c]	0.27	5	5	DCM	0 → rt	4	99
4[c]	2.97	4	4	DCM	0 → rt	5	87
5[c]	1.51	5	5	DCM	rt	4	64
6[c]	1.57	5	5	DMF	0 → rt	4	38
7[c]	5.08	10	10	DCM	0 → rt	5	47

a: no product could be isolated for analysis.
b: Et_3SiH, $BF_3 \cdot Et_2O$.
c: Et_3SiH, TFA.

tial of BF_3^- and $BF_3 \cdot Et_2O$, thus the formed byproduct is assumed the 6-*O* benzylated analogue of byproduct **10a** as indicated by NMR [122]. The structure is shown in Figure 3.8.

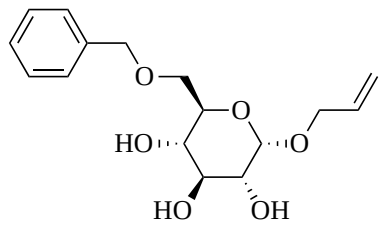

12a

Figure 3.8: Assumed structure of byproduct **12a**

The above observations excluded any continuation of work using $BF_2 \cdot EtO_2$ as Lewis acid. A new method, employing trifluoroacetic acid (TFA) in conjugation with Et_3SiH was attempted, and the results are listed in Table 3.6 (entries 3 - 7). Yields ranging from medium to high were obtained, divulging 5 equivalents Et_3SiH and TFA as the most promising conditions. Mediocre yield was obtained using DMF

as reaction solvent, possibly attributed to a lower rate of reaction when conducting the reduction in highly polar solvents. Employing Et_3SiH and TFA in 5 equivalents, using DCM as the reaction solvent, produced the product in very high yield. Compound **12** was deemed a novel compound, considering its absence form explored literature. The protection strategy towards a 4-*O* intermediate was highly successful, providing a novel compound with possibility of functionalization at 4-*O*. This might be advantageous in other carbohydrate fields, such as glycosidic 1-4 linkages [123].

3.1.3 The route to a 1-*O* intermediate

The route to a 1-*O* intermediate progressed somewhat differently than the 6-*O* and 4-*O* pathways. A schematic overview is given in Scheme 3.10

First of all, advances in the synthesis towards a 1-*O* intermediate was conducted after most of the esterification work presented in 3.2. Establishing suitable esterification conditions was at the time highly prioritised. As a consequence, some of the reactions presented herein have only been attempted a few times before proceeding in the synthetic pathway. Step *a* (Scheme 3.10) was done as previously reported in Scheme 3.1 to obtain compound **6** in high anomeric purity. Compound **6** was thereafter hydrolysed in the process of deacetalization, yielding compound **1** (Scheme 3.10) also in high anomeric purity.

The reader must be made aware that this particular method, yielding pure compound **1**, could have been conducted in the process of obtaining compound **3b** and **4** in the route towards a 6-*O* intermediate. Avoiding tritylation or tosylation on crude starting material could potentially improve the results in these reactions. However, progressing

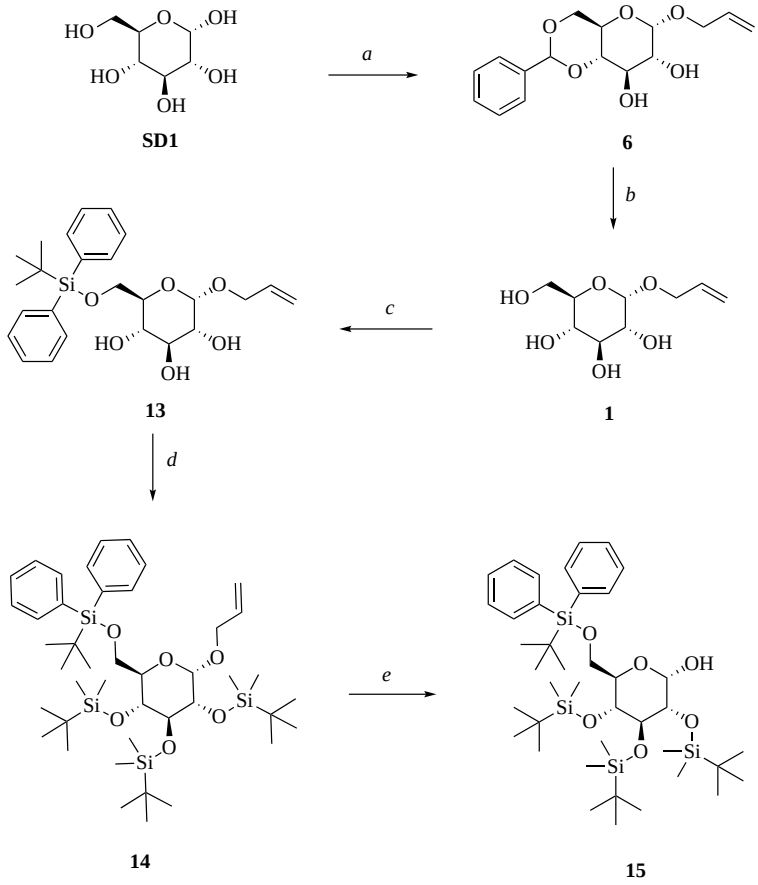

Scheme 3.10: Synthetic overview in the route towards a 1-*O* intermediate. *a*: 1) Allyl-OH, TMS-Cl, 60°C, 5h. 2) $PhCH(OMe)_2$, *ρ*-TsOH, ACN, rt, 5h; *b*: 8:5 $AcOH/H_2O$, 100°C, 1h; *c*: TBDPS-Cl, imidazole, DMF, 0°C → rt, 24h; *d*: 1) TBDMS-Cl, imidazole, DMF, rt, 3d. 2) TBDMS-OTf, 2,6-lutidine, DCM, 0°C → rt, 24h; *e*: $Pd(PPh_3)_4$, K_2CO_3, MeOH, 68°C, 12h.

with acetalization, purification and deacetalization before conducting the tritylation or tosylation would increase the number of steps in the synthetic pathway dramatically (Scheme 3.1), decreasing the overall yield and thus favouring path 2 (Scheme 3.1).

Results from Scheme 3.10 step *b* are visualized in Scheme 3.11.

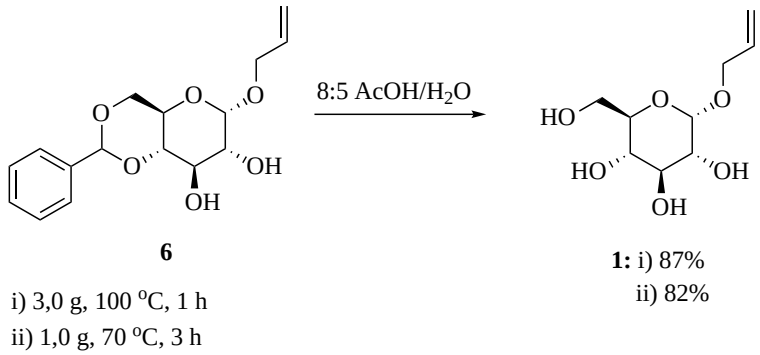

Scheme 3.11: Deacetalization of **6**, mixture of acetic acid and water (8:5, 25 mL / g SM).

The reaction proceeded according to literature in high yields [1, 107].

Further progress in the synthetic pathway towards a 1-*O* intermediate was carried out with the selective silylation of the primary hydroxyl using TBDPS-Cl. The bulky nature of the TBDPS group causes high selectivity towards the primary hydroxyl present at position 6. The method is already well established in literature, and because of the successful first attempt, further experimentation was deemed unnecessary. The procedure and results are listed in Scheme 3.12.

Expected results according to already established literature procedures were observed [124]. Introducing the TBDPS group enables detection by UV, thus simplifying further analysis using UV absorbing detectors (6.1.1.2). As already stated in the theory section (2.1.2.3, Figure 2.4), TBDPS has relatively high stability towards acidic conditions, however its stability towards bases is lacklustre. Fear for the unwanted removal of TBDPS therefore arose, when imidazole was employed in the subsequent silylation of 2-*O*, 3-*O* and 4-*O* with TBDMS. Results in the synthesis towards compound **14** is listed in Scheme 3.13.

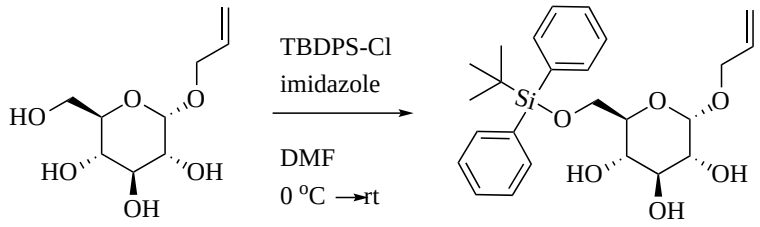

1 **13:** 85%

Scheme 3.12: Selective insertion of TBDPS on the primary hydroxyl in compound **1**. Reagent quantities: SM (2.17 g), TBDPS-Cl (1.14 eq), imidazole (1.74 eq), DMF (40 mL).

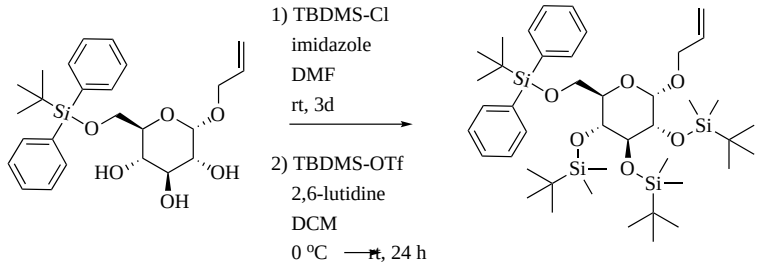

13 **14:** 72%

Scheme 3.13: Total silylation of compound **13**. Reagent quantities: 1) SM (3.56 g), TBDMS-Cl (9 eq), imidazole (9 eq), DMF (80 mL). 2) TBDMS-OTf (2.5 eq), 2,6-lutidine (5 eq), DCM (70 mL).

No analogues to compound **14** was found in litterature, however both silylation techniques are thoroughly described as general procedures (2.1.2.3). Compound **14** was isolated as a viscous clear oil.

The final step towards a 1-*O* intermediate is the selective deallylation of compound **14**. There are several methods by which deprotection of allyl ethers is achieved (2.1.2.5). Wilkinson catalyst, in conjugation with either acidic, or oxidative conditions, has been previously applied in carbohydrate synthesis [24]. In this project, a literature procedure employing the Wilkinson catalyst to isomerize the allyl group into

a prop-1-enyl ether seamed like a good starting point. The method progressed with oxidative removal of the prop-1-enyl ether using Hg^{2+}. Unfortunately, both mercury(II)chloride and mercury(II)oxide was not easy to obtain in short notice. Therefore, another method employing palladium catalysis was used in the synthesis towards compound **15**. The deallylation of compound **14** is showed in Scheme 3.14.

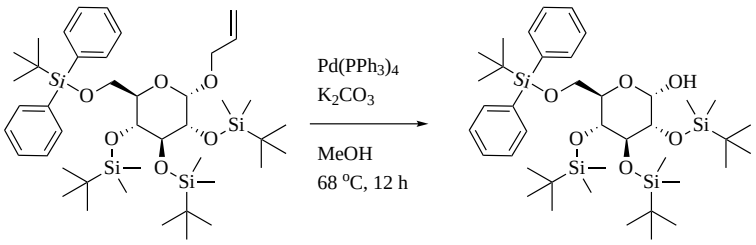

14 **15**

Scheme 3.14: Deallylation employing tetrakis-palladium making the allyl group labile for nucleophilic attack.

The crude mixture was attempted purified by silica gel flash chromatography, however some by products were present even after purification, indicated by ^{1}H-NMR (600 MHz, $CDCl_3$). Among these byproducts a characteristic β proton signal at 4.35 ppm was observed, shown in Figure 3.9. Because of the high anomeric purity of the starting material, anomerization befell during the reaction, thus leaving this deprotection strategy futile.

No mention of anomerization or any change in stereochemistry was found on the subject of palladium catalyzed deallylations [56]. Tanaka et al,. reported both starting material and product as an anomeric mixture when conducting the anomeric deallylation using Wilkinson catalyst [115].

Removal of the allyl group was deemed successful due to the absences

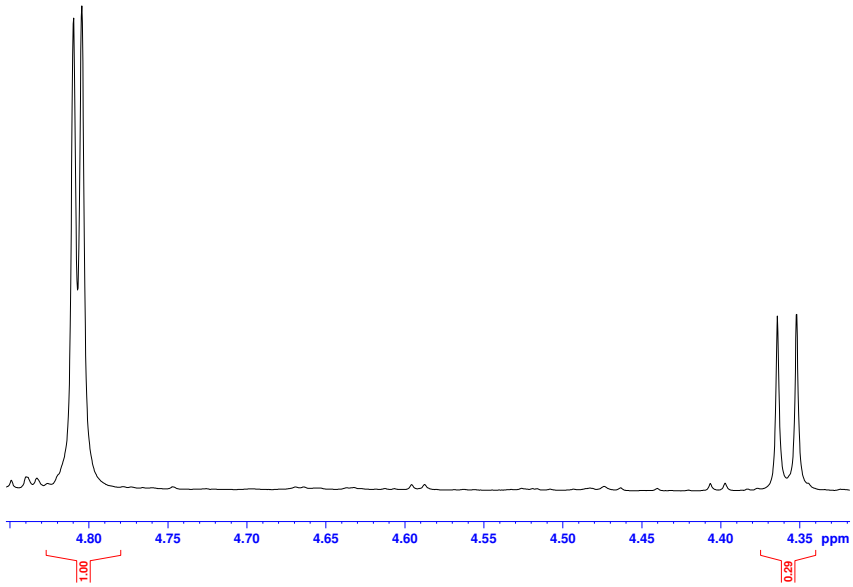

Figure 3.9: ^{1}H-NMR (600 MHz, $CDCl_3$) of compound **15** illustrating the presence of both an α (4.80 ppm) and β (4.36 ppm) signal.

of the allylic protons indicated by the partial ^{1}H-NMR (600 MHz, $CDCl_3$) spectra shown in Figure 3.10.

Although anomerization was observed, the separability of anomers, either 1-*O* intermediate or esterified compound, by preparative chromatography might be high. Also, synthesizing anomeric derivatives of target compounds will add to the library of potentially interesting drug candidates in the establishment of a structure activity relationship study. The synthesis of compound **14** and **15** is not described in literature, making these assumed novel compounds. Due to time constrains, no further work in the synthesis towards 1-*O* intermediates was conducted.

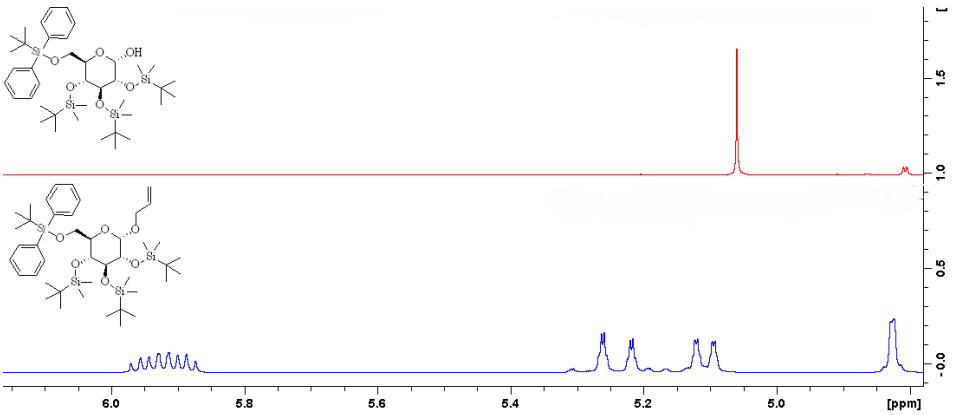

Figure 3.10: Partial ^{1}H-NMR (600 MHz, $CDCl_3$) of compound **14** (bottom) and **15** (top), illustrating the absence of allylic protons.

3.2 Synthesis of sugar fatty acid esters

Esterification was primarily conducted on substrates **10** and **12** respectively. As mentioned previously, the motivation for this work was the mild conditions required in the esterification of target molecule **1a** (Figure 1.1). Several conditions were investigated for their ability to introduce the fatty acids under mild conditions. Deprotection of the silyl ethers were conducted in the presence of TBAF, to avoid any potential hydrolysis of the ester under acidic desilylation conditions. A schematic overview is presented in Scheme 3.15.

3.2.1 Esterification

The preceding synthetic work, obtaining selectively protected α-D-glucopyranoside intermediates **10** and **12**, were fruitful. The primary 6-*O* intermediate and the secondary 4-*O* intermediate retain different steric hindrance around their respective hydroxyl group, thus imparting a varying degree of esterification potential. The possible difference in esterification potential is highly interesting in this research groups future work (see chapter 5).

Methods for esterification were carefully selected, and due to the acid labile silyl ethers, classical Fischer conditions were excluded. Three esterification methods of the primary position is shown in Scheme 3.16.

Results for the attmepted esterifications are shown in Table 3.7.

Method iii, using TMS-Cl as promotor, did not yield SFAE product as seen from Table 3.7. Mechanistically, the esterification is thought to progresses through the *in situ* generation of HCl, which acts as an acid catalyst [78]. TMS-Cl also has water scavenging properties,

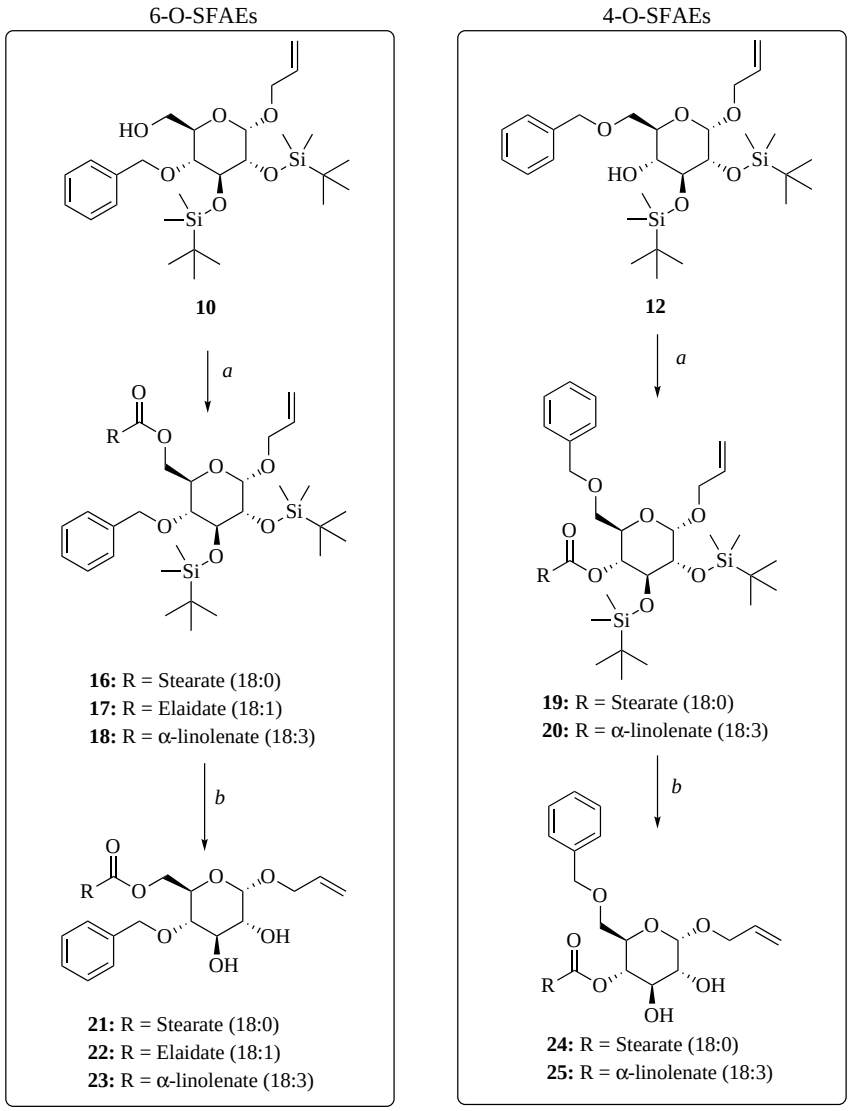

Scheme 3.15: Synthetic strategy towards SFAEs. *a*: Fatty acid, EDCI, DMAP, DCM, rt, 24 h. *b*: TBAF, THF, rt, 12 - 24 h.

thus driving the esterification equilibrium forward. In entry 1 and 2 Table 3.7 only free fatty acid and 6-*O* intermediate could be observed when monitoring the reaction using HPLC. This observation

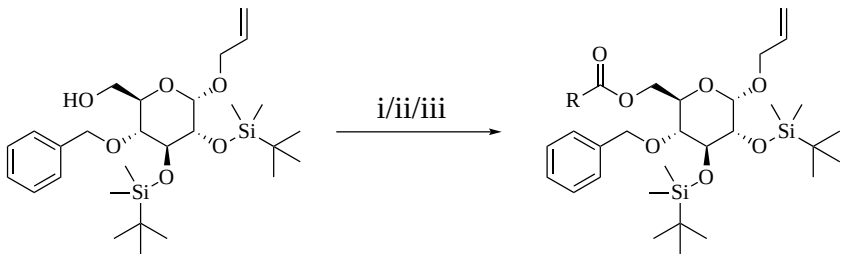

10

i: fatty acid, EDCI, DMAP, DCM
ii: fatty acid, DCC, DMAP, DCM
iii: fatty acid, TMSCl, DCM

16: R = Stearate (18:0)
17: R = Elaidate (18:1)
18: R = α-linolenate (18:3)

Scheme 3.16: Method i, ii and iii employed in the synthesis towards 6-*O* SFAEs.

Table 3.7: Methods attempted during the esterification of 6-*O* intermediate **10**. Constant reaction parameters: DCM (50 mL / g).

Entry	SM (g)	fatty acid (eq)	promotor (eq)	cat (eq)	temp (°C)	time (h)	yield (%)
$1^{b,e}$	0.10	1.0	0.6	-	rt	20	-[a]
$2^{b,e}$	0.15	2.0	1.0	-	40	20	-[a]
$3^{b,f}$	0.10	1.0	2.5	1.5	rt	5	14
$4^{b,f}$	0.10	1.0	4.5	2.5	rt	24	25
$5^{b,g}$	0.05	1.0	2.5	1.5	rt	5	22
$6^{b,g}$	0.14	1.5	4.5	2.5	rt	24	67
$7^{c,g}$	0.15	1.0	4.5	2.5	rt	24	39
$8^{c,g}$	0.05	1.0	2.0	-	rt	5	-[a]
$9^{d,g}$	0.05	1.0	4.5	2.5	rt	24	19
$10^{d,g}$	0.31	1.5	4.5	2.5	rt	24	48

a: no product could be isolated for analysis.
b: fatty acid: stearic acid.
c: fatty acid: elaidic acid.
d: fatty acid: α-linolenic acid.
e: promotor: TMS-Cl.
f: promotor: DCC, cat: DMAP.
g: promotor: EDCI, cat: DMAP.

is attributable to the small reaction scale, causing residual moisture to affect the equilibrium, or spending the sparse amount of present

reaction promotor.

Entry 3 to 10 employed two variations of the Steglich esterification (2.2.2.2). DCC has somewhat higher steric limitation than EDCI, possibly explaining the lower than average yield in entry 3 and 4. After these esterification experiments (Table 3.7), method i (Scheme 3.16) was chosen as the general approach for future esterifications. 4,5 equivalents of promotor and 2,5 equivalents of DMAP gave the best results. Increasing the fatty acid equivalents also provided somewhat higher yield, however the surplus of reactant had a tendency to furnish purification impediments.

The esterification of the 4-*O* position of compound **12** progressed according to Scheme 3.17.

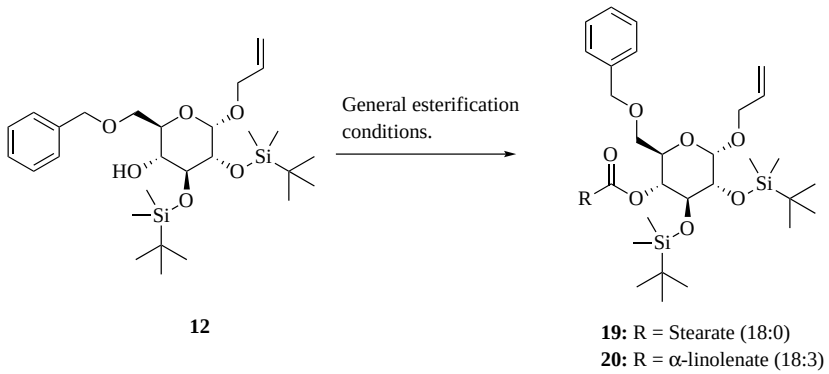

Scheme 3.17: Esterification of compound **12** under Steglich conditions.

Results from the esterification of 4-*O* intermediate **12** are listed in Table 3.8.

SFAEs were synthesised from 4-*O* intermediate **12** in low yields (Table 3.8). Varying several of the reaction conditions were attempted to increase the lacklustre conversion from starting material. Increasing

Table 3.8: Methods attempted during the esterification of 4-*O* intermediate **12**. Constant reaction parameters: Solvent = DCM except entry 5 and 6, C = 50 mL / g.

Entry	SM (g)	fatty acid (eq)	promotor (eq)	cat (eq)	temp (°C)	time (h)	yield (%)
1[b,f]	0.20	1.0	4.5	2.5	rt	24	10
2[b,f]	0.24	1.0	4.5	2.5	rt	72	11
3[b,e]	0.19	1.0	4.5	2.5	rt	24	5
4[b,f]	0.15	5.0	4.5	2.5	rt	24	22
5[b,f,h]	0.15	1.0	4.5	2.5	60 °C	24	18
6[b,f,g]	0.16	1.0	4.5	2.5	rt	24	-[a]
7[d,f]	0.22	1.0	4.5	2.5	rt	24	-[a]
8[c,f]	0.20	1.0	4.5	2.5	rt	24	12
9[c,f]	0.95	1.5	4.5	2.5	rt	24	20
10[c,f]	0.15	1.0	4.5	2.5	rt	24	8

a: no product could be isolated for analysis.
b: fatty acid: stearic acid.
c: fatty acid: α-linolenic acid.
d: fatty acid: elaidic acid.
e: promotor: DCC, cat: DMAP.
f: promotor: EDCI, cat: DMAP.
g: Solvent = DMF.
h: Solvent = Chloroform.

the equivalents of fatty acid (entry 4), or increasing the reaction temperature (entry 5) increased the total yield to around 20%. DMF was attempted as reaction solvent (entry 6), because of the high polarity which may cause increased rate of reaction. DMF is also sometimes used as reaction solvent in literature, however no product could be isolated [79, 125]. Residual moisture could have affected the reduction, and could have been countered by running the reaction in the presence of activated molecular sieves, however, this was not attempted.

Entry 7 was not purified before deprotection of the silyl ethers with TBAF, expecting the deprotection to run smoothly resulting in a higher overall yield. This did, however, not work, and the attempt

resulted in a complex mixture of inseparable compounds which will be further explored in 3.2.2.

As previously stated, the main difference between the esterification potential of **10** (Table 3.7) and **12** (Table 3.8) are the steric hindrance of the hydroxyl groups. The primary hydroxyl of intermediate **10** is relatively available for intermolecular interactions. The three dimensional structure of intermediate **12** reveal a highly obstructed hydroxyl, only available through a cavity in between the benzyl and TBDMS groups. A solvent accessible surface model covering the structure has been employed to illustrate this steric conundrum, visualized in Figure 3.11.

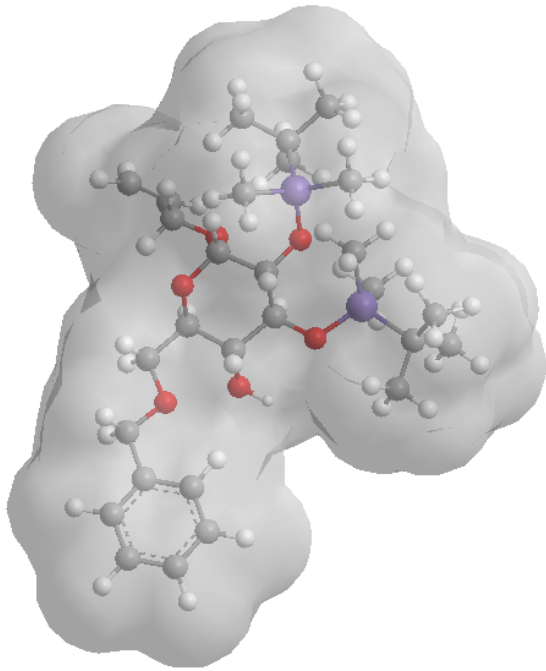

Figure 3.11: 3D structure of compound **12** showing the solvent accesible surface. Model constructed using Chem3D®. White = hydrogen, gray = carbon, red = oxygen, purple = silicon.

The striking difference between the surfaces of the two intermediates

are expressed with Figure 3.12, revealing the highly accessible hydroxyl of compound **10**.

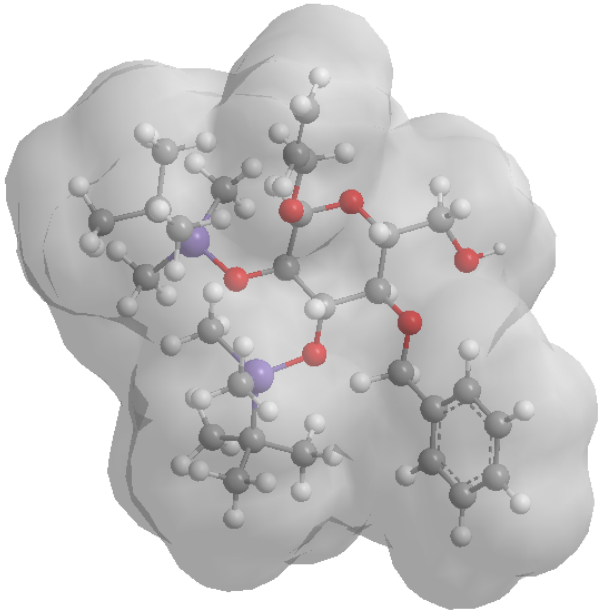

Figure 3.12: 3D structure of compound **10** showing the solvent accesible surface. Model constructed using Chem3D®. White = hydrogen, gray = carbon, red = oxygen, purple = silicon.

In the works presented by Prof. Junzo Otera and Dr. Joji Nishikido, a statement is made regarding the Steglich esterification. This statement posit the Steglich esterifications inclination to remain unaffected by steric constrains of the starting materials [78]. The results presented in Table 3.7 and Table 3.8 contradict no steric influence considering steric variation, as the main difference between compound **10** and **12**.

3.2.2 Desilylation

Deprotection of the TBDMS ethers from the esterified compounds were carried out primarily using TBAF in THF, as described by

Crouch et al., [36]. The motivation for this step, was to reduce the potential toxic effect exhibited by remaining silyl protective groups, and to simplify the SFAEs structure [127]. Deprotection of the benzyl ether was not conducted for the following reasons: the lack of a deprotection stategy compatible with the ester moiety, and benzyl ethers inherit some previously reported interesting biological activity, thus justifying their presence during biological evaluation studies [128, 129]. Deprotection was conducted according to Scheme 3.18 and the results are presented in Table 3.9.

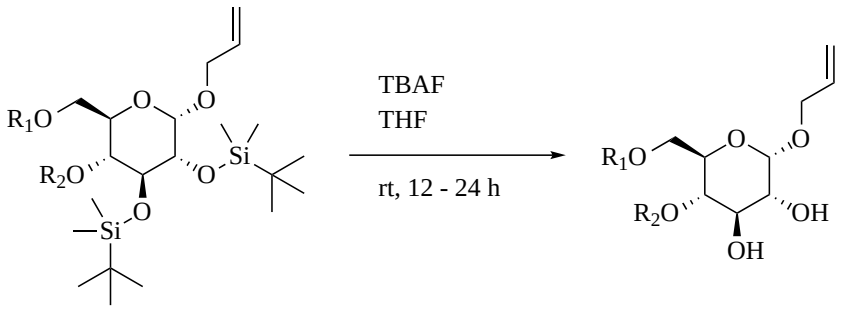

16, 17, 18: R_1 = ester
R_2 = Bn
19, 20: R_1 = Bn
R_2 = ester

21, 22, 23: R_1 = ester
R_2 = Bn
24, 25: R_1 = Bn
R_2 = ester

Scheme 3.18: Deprotection of redundant TBDMS groups using TBAF in THF.

The products were extracted according to the procedure described in 6.3.7. The crude mixture was then purified by preparative HPLC, as described in 6.1.1.2. Generally, the deprotection of the 6-*O* sugar fatty acid esters progressed as expected, yielding a major peak on HPLC. However for the 4-*O* esters, two or even three closely eluting peaks were observed (Figure 3.13), having much lower intensity than for the 6-*O* compounds.

Table 3.9: Results from the deprotection of TBDMS. Constant reaction parameters: TBAF (3 eq), THF (15 mL/ g), rt. Purification was conducted using preparatory HPLC (6.1.1.2).

Entry	precursor	scale (mg)	time (h)	yield (%)
1	16	100	12	60
2	17	90	24	73
3	18	98	24	-[a]
4	19	112	24	10
5	20	500	12	34

a: no product could be isolated for analysis.

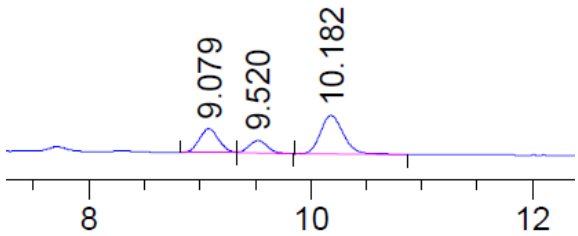

Figure 3.13: Partial HPLC spectra of compound **24** (entry 4), method C.

Upon isolation and analysis of each individual compound, it was discovered that the closely eluting components were in fact 2-*O* and 3-*O* analogues of the 4-*O* esters. This means that ester migration is mediated by the conditions employed upon deprotection of the silyl ethers. TBAF produces HF *in situ*, thus providing an acidic media, in which the esters can migrate [130, 131]. No migration is observed for the 6-*O* esters, thus promoting a higher overall yield in entry 1 and 2 (Table 3.9). The migration pattern observed in the 4-*O* SFAEs is illustrated in Scheme 3.19.

The lack of migration in the 6-*O* SFAEs is logically explained by the interfering benzyl ether located at 4-*O*. Even in the absence of the

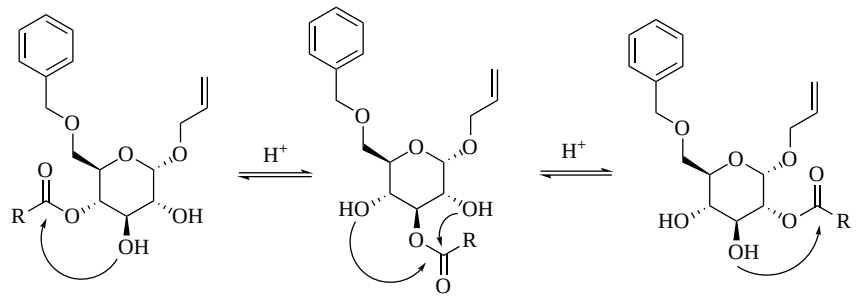

Scheme 3.19: migration pattern observed during the desilylation of 4-*O* SFAEs.

benzyl group, less migration would be expected from the 6-*O* ester, due to higher nucleophilicity of the primary hydroxyl, thus shifting the migration equilibrium towards 6-*O* ester formation.

The discovery of this migration pattern was attributed to the works of Daiqiang Xu et al., showing TBAF in THF to deacetylate positions 2-*O* and 3-*O* on cellulose derivatives [132]. Although detrimental to the current esterification work, the observed migration indicates potential for producing several SFAE analogues from simplified starting materials in a diversity oriented manner. The low yield gave problems with handling the material, but also with subsequent analysis. In the case of compound **24**, the 2-*O*-esterified analogue was the major product, and the only derivative in high enough quantity for carbon NMR. The 3-*O* and 4-*O* analogues were confirmed by proton NMR, where coupling with the respective sugar protons could be observed, confirming the ester placement. Observed acyl migration is further explained in 3.4.

In the preparation of compound **25**, less time was devoted to the deprotection (12 h). With lower reaction time, less migration were observed yielding the 4-*O*-ester as the major product. Being able to

control the extent of migration opens the possibility of synthesising several product analogues to the target compound **1a**, thus establishing a structure activity relationship (SAR) study. The establishment of such SAR study is highly relevant to the future of this research group.

3.3 Biological evaluation

Biological evaluation was conducted in collaboration with another member of the research group and presented as a subordinate goal after the synthesis of sugar fatty acid esters. To determine the SFAEs effect on cell viability, the MTT procedure (2.4.1) was employed, assessing cell metabolic activity using the MTT tetrazole derivative. General experimental procedure for the MTT assay can be found in 6.4.

Compound **22** was the first SFAE to be synthesised, thus also the first to be tested *in vitro* on F98 glioma cancer cell lines. After conducting the MTT and obtaining raw data, the cell viability (%) was plotted against compound concentration (μM). The results are shown in Figure 3.14.

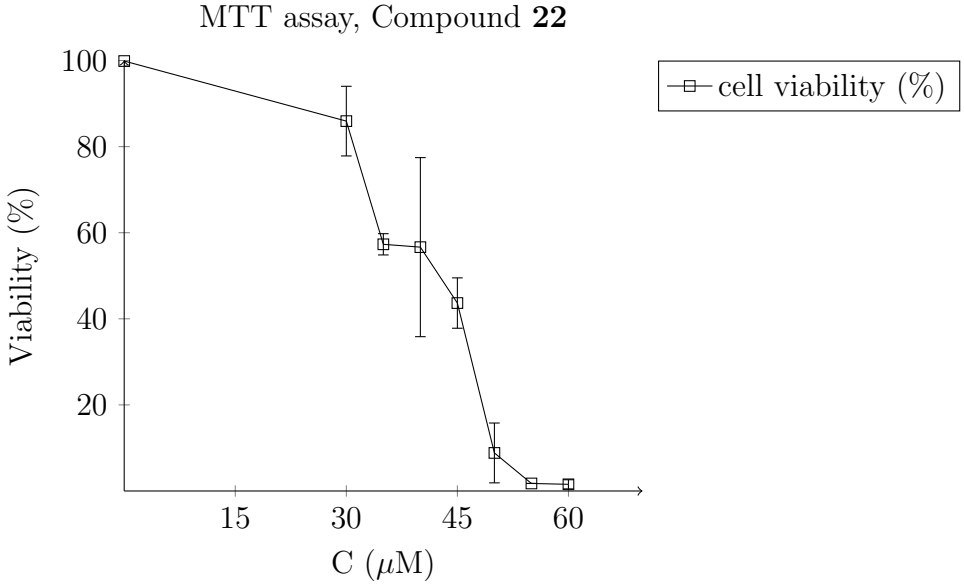

Figure 3.14: Cell viability (%) as a function of applied compound (μM) in DMSO. Error bars show the calculated standard deviation of cell viability among dishes with equal compound application.

Figure 3.14 shows a slow and steady decline of cell viability in dishes treated with a concentration ranging from 0 to 30 μM. In dishes treated with concentrations above 30 μM there is observed a steep decline in cell viability to around 50 % living cells in the average dish. The amount of living cells present are more or less constant even with a 50% increase in compound application. This indicates a cell metabolic resistance against compound **22**. In dishes treated with a compound solution of 50 μM, the viability suddenly dropped close to zero revealing the cell lines toleration limit towards compound **22**.

These results indicate some form of biological activity from compound **22**, however it is difficult to assess whether this is a toxic response, or if the compound inherits some other activity.

Solvent (DMSO) employed in the MTT study was also investigated for potential interfering toxic effects, however no biological activity was observed, leaving the viability of cells close to 100 % (Figure 3.15).

The observed increase in cell viability might be attributed to the cells resistance to the outside media. At 120 μL DMSO the cell viability dropped significantly. This might be due to exceeding the tolerability of the cell lines towards DMSO.

Further biological evaluation of other compound analogues, such as **21** and **25**, have been conducted, however data is still being processed and results are not yet ready to be presented. Continued work will be conducted on compound analogues to establish a structure-activity relationship.

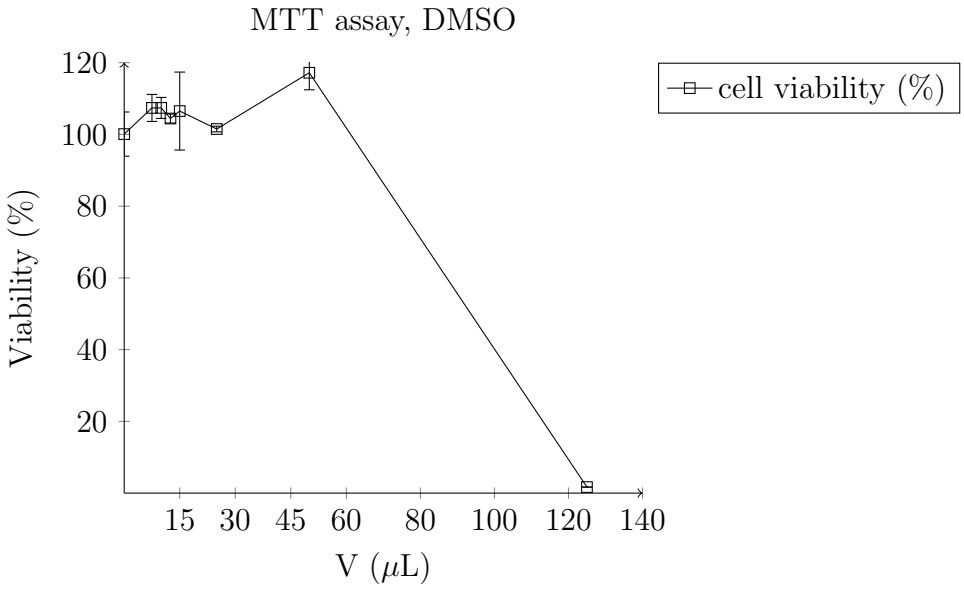

Figure 3.15: Cell viability (%) as a function of volume DMSO (μL). Error bars show the calculated standard deviation of cell viability among dishes with equal DMSO application.

3.4 Spectroscopic characterisation

In the following section, spectroscopic characterisation and analysis will be presented for chosen compounds. Detailed spectroscopic data for each synthesised compound are listed together with experimental work, thus only compounds that require some form of additional discussion will be treated herein. Some of the simple α-D-glucopyranosides have already sufficient spectroscopic data presented in literature, while others have been fully characterised by other members of the research group, and are therefore not shown.

Generally ^{1}H-NMR, ^{13}C-NMR, COSY, HSQC and HMBC sufficed to elucidate the complete structure of all compounds and assign all shifts, barring overlapping peaks such as in aromatics. In some cases, NOESY and selective HSQC and HMBC experiments were required to aid in shift assignment. Aromatic shifts are assigned where possible. Solvent impurities, such as chloroform, dichlorometane, water, ethyl acetate, grease and *n*-pentane, are present throughout some of the analysed samples. Residual signals were identified using the work presented by Fulmer et al,. [133].

3.4.1 Characterisation of α-D-glucopyranoside intermediates

Due to their high relevance regarding the synthetic goal of this thesis and lack of their spectroscopic data in literature, compound **8**, **10** and **12** have been chosen for deeper spectroscopic characterisation. Their structure and numbered positions are shown in Figure 3.16.

All shifts except for aromatic and TBDMS were assigned with ^{1}H-NMR, ^{13}C-NMR, H,H-COSY, HSQC and HMBC. Aromatic shifts

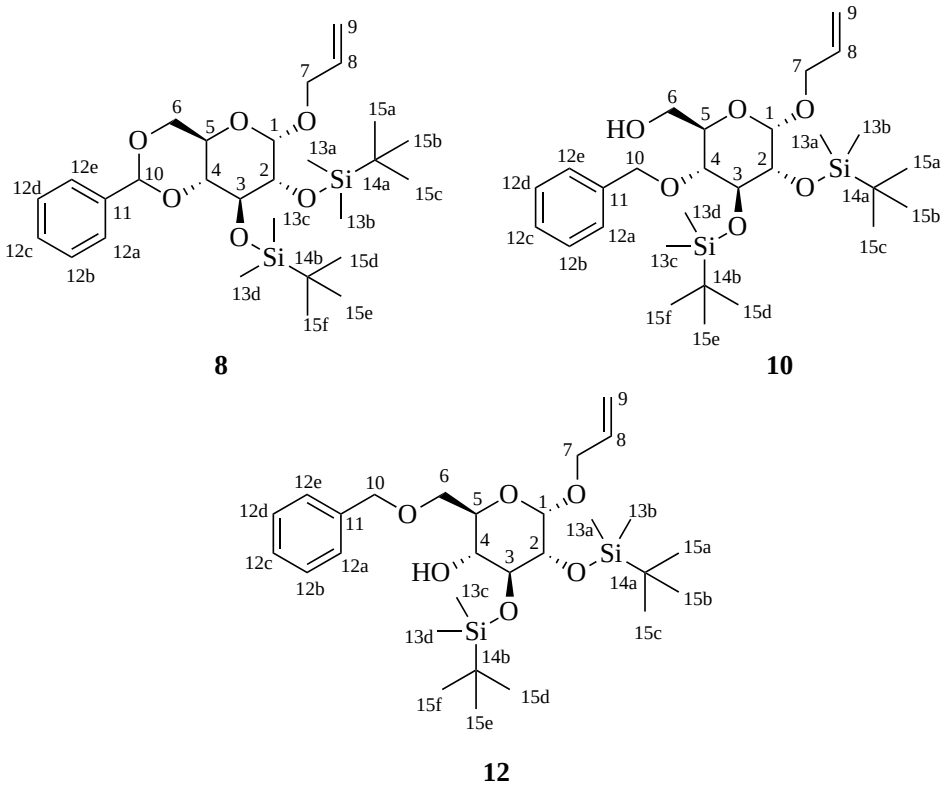

Figure 3.16: Numbered positions for compounds **8**, **10** and **12**, respectively.

proved difficult to resolve from one another, even with NOESY. NOESY was, however, very applicable in the assignment of the silyl ethers, as shown in Figure 3.17.

Utilising through space interactions, as observed in Figure 3.17, the two TBDMS ethers could be placed accordingly. The allylic side group was expected to give the strongest through space interactions, however the highest intensity peaks were observed for the interactions between the hydroxyl at 4-*O* and the silyl alkyl groups in compound **12**.

Table 3.10: ^{1}H-NMR ($CDCl_3$, 600 MHz, ppm) chemical shifts for compounds **8**, **10** and **12**. Samples taken at 25 °C using TMS as internal standard. Multiplicities are given in parenthesis behind each respective shift.*: Shifts could not be individually resolved against analogous positions.

H	**8**	**10**	**12**
1	4.81 (d)	4.76 (d)	4.81 (d)
2	3.64 (dd)	3.58 (dd)	3.58 (dd)
3	4.01 (m)	4.00 (t)	3.84 (t)
4	3.38 (t)	3.35 (t)	3.46 (t(b))
5	3.86 (td)	3.67 (m)	3.77 (m)
6a	3.68 (t)	3.67 (m)	3.69 (m)
6b	4.23 (dd)	3.73(m)	3.69 (m)
7a	4.01 (ddt)	4.14(ddt)	4.18 (ddt)
7b	4.20 (ddt)	3.92(ddt)	3.97 (ddt)
8	5.96 (dddd)	5.92(dddd)	5.93 (dddd)
9a	5.32 (m)	5.30(m)	5.29 (m)
9b	5.22 (m)	5.18 (m)	5.17 (m)
10a	5.44 (s)	4.89 (d)	4.63 (d)
10b	-	4.60 (d)	4.55 (d)
12a	7.45-7.48 (m)	7.27-7.36 (m)*	7.26 - 7.36 (m)*
12b	7.32-7.37 (m)	7.27-7.36 (m)*	7.26 - 7.36 (m)*
12c	7.32-7.37 (m)	7.27-7.36 (m)*	7.26 - 7.36 (m)*
12d	7.32-7.37 (m)	7.27-7.36 (m)*	7.26 - 7.36 (m)*
12e	7.45-7.48 (m)	7.27-7.36 (m)*	7.26 - 7.36 (m)*
13a	0.09 (s)	0.11 (s)*	0.07 (s)
13b	0.11 (s)	0.10 (s)*	0.09 (s)
13c	0.04 (s)	0.06 (s)	0.11 (s)
13d	-0.13(s)	0.12 (s)	0.13 (s)
15a	0.92 (s)*	0.92* (s)	0.908 (s)*
15b	0.92 (s)*	0.92* (s)	0.908 (s)*
15c	0.92 (s)*	0.92* (s)	0.908 (s)*
15d	0.80 (s)*	0.93* (s)	0.912 (s)*
15e	0.80 (s)*	0.93* (s)	0.912 (s)*
15f	0.80 (s)*	0.93* (s)	0.912 (s)*
OH	-	1.61 (m)	2.14 (s)

Table 3.11: ^{13}C-NMR ($CDCl_3$, 150 MHz, ppm) chemical shifts for compounds **8**, **10** and **12**. Samples taken at 25 °C using TMS as internal standard. *: Shifts could not be individually resolved between analogous positions.

C	**8**	**10**	**12**
1	99.2	98.8	98.3
2	74.6	74.4	73.6
3	71.9	74.0	75.0
4	82.8	79.0	72.4
5	62.6	71.2	70.3
6	69.2	62.0	69.8
7	68.9	68.6	68.5
8	133.9	134.1	134.1
9	118.0	117.4	117.7
10	102.4	74.8	73.5
11	137.4	138.4	138.2
12a	126.5	127.5*	128.4*
12b	128.1	128.4*	127.7*
12c	129.1	127.6*	127.7*
12d	128.1	128.4*	127.7*
12e	126.5	127.5*	128.4*
13a	-4.4	-3.3	-4.3
13b	-3.0	-4.3	-3.7
13c	-3.4	-4.0	-3.3
13d	-4.3	-3.0	-4.2
14a	18.2	18.4	18.3
14b	18.3	18.1	18.3
15a	26.1	26.2	26.1*
15b	26.1	26.2	26.1*
15c	26.1	26.2	26.1*
15d	26.0	26.4	26.2*
15e	26.0	26.4	26.2*
15f	26.0	26.4	26.2*

^{1}H coupling constants (Hz) for compound **8**, **10** and **12** are listed in Table 3.12.

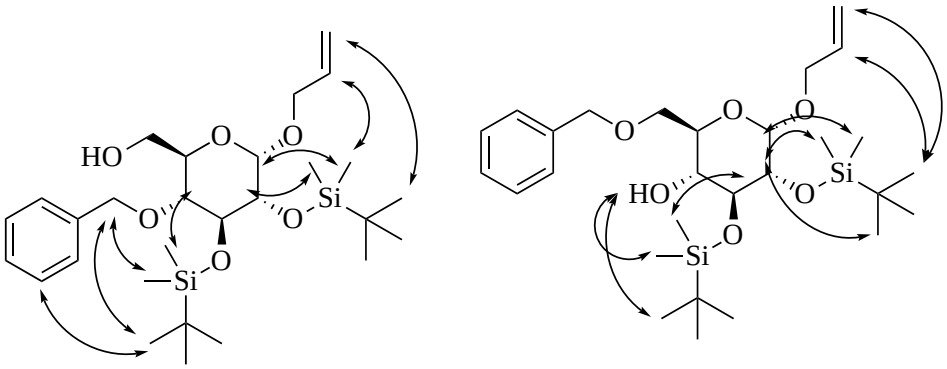

10 **12**

Figure 3.17: Through space hydrogen interactions as observed by 2D-NOESY for compound **10** and **12**.

Table 3.12: ^{1}H coupling constants (Hz) resolved for compound **8**, **10** and **12**. - marks unresolved coupling resulting for multiplets.

Coupling (H-H)	**8**	**10**	**12**
1-2	3.6	3.4	3.3
2-3	8.8	9.1	8.9
3-4	9.3	8.9	8.5
4-5	9.9	9.2	8.9
5-6a	10.7	-	-
5-6b	4.9	-	4.1
6a-6b	10.2	-	-
7a-7b	12.8	12.8	12.8
7a-8	5.5	5.7	5.4
7b-8	6.6	6.0	6.3
8-9a	17.0	16.2	17.0
8-9b	10.3	10.5	10.4
9a-9b	1.6	1.7	1.7
10a-10b	-	11.9	12.3

Observed J-values corresponds with structural elements present in the molecules **8**, **10** and **12**. Lastly, the shift assignment of two synthesised SFAEs are presented herein. Providing detailed assignment of the

silylated precursors in this section was deemed unnecessary. Numbered position within the molecules **22** and **25** are illustrated in Figure 3.18. These positions will be referred to in resulting tables.

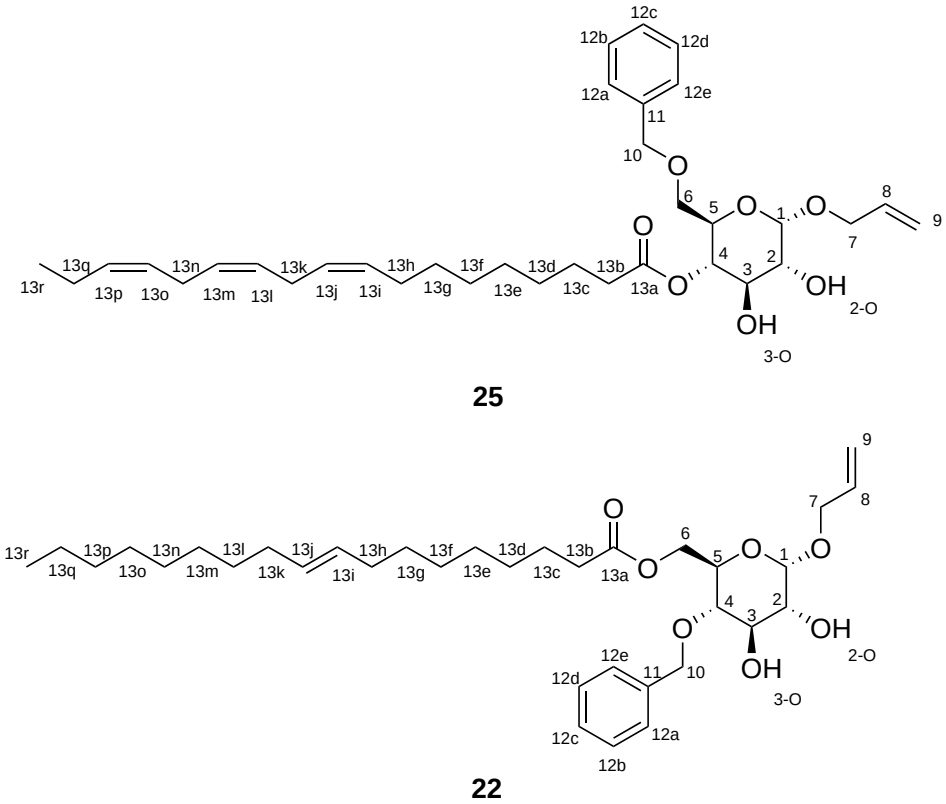

Figure 3.18: Numbered positions on SFAEs **22** and **25**.

Shifts belonging to the pyranose backbone were easily assigned with regular 2D experiments, however the numerous fatty acid ester shifts were difficult to distinguish with conventional methods. For compound **22**, selective HSQC and HMBC experiments with a carbon dimension spanning δ 20 - 40 ppm were utilised. Compound **25** was not analysed in this manner, which is clearly reflected from Table 3.14 and Table 3.16.

Table 3.13: ^{1}H-NMR ($CDCl_3$, 600 MHz, ppm) chemical shifts for compounds **22** and **25**. Samples taken at 25 °C using TMS as internal standard. *: Shifts could not be accurately resolved relative to analogous positions or due to overlapping signals. Sugar protons, fatty acid ester shifts are presented in another table for practical reasons.

H	**22**	**25**
1	4.92 (d)	4.98 (d)
2	3.52 (dd)	3.62 (dd)
3	3.90(t)	3.85 (t)
4	3.42 (dd)	4.94 (t(b))
5	3.85 (ddd)	3.90 (m)
6a	4.29 (dd)	3.52 (m)
6b	4.34 (dd)	3.52(m)
7a	4.02 (ddt)	4.24(ddt)
7b	4.20 (ddt)	4.06(ddt)
8	5.96 (dddd)	5.93(dddd)
9a	5.21 (m)	5.31(m)
9b	5.28 (m)	5.22 (m)
10a	4.66 (d)	4.57 (d)
10b	4.87 (d)	4.50 (d)
12a,e	7.34 (m)	7.27-7.36 (m)*
12b,d	7.35 (m)	7.27-7.36 (m)*
12c	7.30 (m)	7.27-7.36 (m)*
$2O$	-*	-*
$3O$	-*	-*

Another highly interesting aspect is the deshielding provided by the ester bond on the hydrogen present at position 4 in compound **25**. The proton, appearing as a broad triplet, has a shift value close to the anomeric proton (4.94 / 4.98 ppm). This observation was the key determinant for the correct assignment of ester position, highly relevant for the SFAEs where the ester is located directly on the pyranose ring ($2O$, $3O$ and $4O$).

Table 3.14: ^{1}H-NMR ($CDCl_3$, 600/800 MHz, ppm) chemical shifts for compounds **22** and **25**. Samples taken at 25 °C using TMS as internal standard. *: Shifts could not be accurately resolved relative to analogous positions or due to overlapping signals. Ester shifts.

H	**22**	**25**
13b	2.31 (td)	2.23 (m)
13c	1.62 (p)	1.55 (m)
13d	1.305 (m)	1.30 (m)*
13e	1.28 (m)	1.30 (m)*
13f	1.26 (m)	1.30 (m)*
13g	1.316 (m)	1.30 (m)*
13h	1.95 (m)	2.06(m)*
13i	5.37(m)*	5.35 (m)
13j	5.37 (m)*	5.35 (m)
13k	1.96 (m)	2.81 (m)
13l	1.323 (m)	5.35 (m)
13m	1.26 (m)*	5.35 (m)
13n	1.26 (m)*	2.81 (m)
13o	1.26 (m)*	5.35 (m)
13p	1.25 (m)	5.35 (m)
13q	1.29 (m)	2.06*
13r	0.88 (t)	0.97

^{1}H-NMR ($CDCl_3$, 600 MHz) of various migrated esters analogous to compound **24** are shown below, to illustrate the deshielded ester position Figure 3.19.

Table 3.15: ^{13}C-NMR ($CDCl_3$, 150 MHz, ppm) chemical shifts for compounds **22** and **25**. Samples taken at 25 °C using TMS as internal standard. *: Shifts could not be individually resolved against analogous positions. Sugar carbons.

C	22	25
1	97.1	97.2
2	72.6	72.8
3	75.6	73.1
4	77.0*	71.0
5	69.0	69.1
6	62.8	68.6
7	68.6	68.7
8	133.4	133.5
9	118.2	118.1
10	74.8	73.5
11	138.4	138.0
12a,e	128.1	127.8*
12b,d	128.6	128.8*
12c	128.0	127.7*

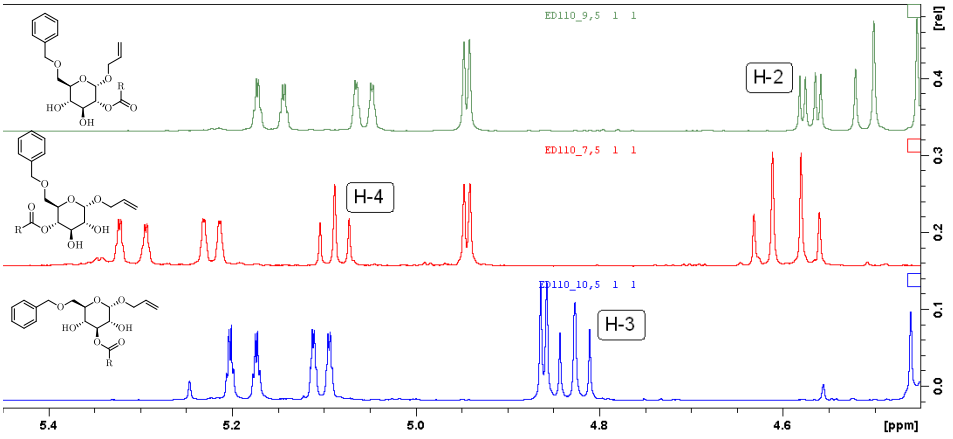

Figure 3.19: $2O$, $3O$ and $4O$ esters obteined during the deprotection of compound **19** in the synthesis towards **24**.

Table 3.16: ^{13}C-NMR ($CDCl_3$, 150/200 MHz, ppm) chemical shifts for compound **22** and **25**. Samples taken at 25 °C using TMS as internal standard. *: Shifts could not be individually resolved against analogous positions. Ester carbons.

C	**22**	**25**
13a	173.5	173.6
13b	34.2	34.2
13c	24.9	24.8*
13d	29.14	29.11*
13e	29.16	29.16*
13f	28.9	29.1*
13g	29.60	29.6*
13h	32.56	27.2
13i	130.2	128.2-132.0*
13j	130.5	128.2-132.0*
13k	32.61	25.5/25.5*
13l	29.66	128.2-132.0*
13m	29.19	128.2-132.0*
13n	29.5	25.5/25.5*
13o	29.3	128.2-132.0*
13p	31.9	128.2-132.0*
13q	22.7	20.6
13r	14.1	14.3

Chapter 4 - Conclusion

A large ongoing total synthesis project, towards 1-*O*-(3-*O*-linolenoyl-6-deoxy-6-sulfo-α-D-glucopyranosyl)glycerol (**1a**), previously extracted from *Schlerochloa dura*, was the motivation for the work presented in this thesis. Strategies employing regioselective protection of α-D-glucopyranosides in the synthesis towards 1-*O*, 4-*O* and 6-*O* intermediates have been explored. Furthermore, the development of a working esterification procedure, and subsequent esterification of α-D-glucopyranoside intermediates with various fatty acids, yielded sugar fatty acid esters. As a subordinate goal, the bioactivity of one SFAE was assessed with *in vitro* MTT methodology on F98 glioma cancer cell lines.

Regarding the protective chemistry, α-D-glucopyranosides were obtained in high anomeric purity, utilizing the crystallinity inherited by 1-*O*-allyl-4,6-*O*-benzylidene-α-D-glucopyranoside (**6**). Attempts made utilizing regioselective tritylation or tosylation of 6-*O* gave no anomeric resolution. Anomerization was observed in the synthesis of 1-*O* intermediate **15**, with α:β= 78:22, thus curbing further development on the pathway towards a 1-*O*-ester in this particular work. Synthesis of 4-*O* and 6-*O* intermediates were conducted through the re-

gioselective reduction of 1-*O*-allyl-2,3-di-*O*-(*tert*-butyldimethylsilyl)-4,6-*O*-benzylidene-α-D-glucopyranoside (**8**). Substantial examples on clevage of silylated benzylidene derivatives are lacking in literature.

Esterification of the 6-*O* and 4-*O* intermediates produced SFAEs in medium and low yields, respectively. The observed difference in average conversion of starting material between esterification of the two intermediates are presumably due to steric hindrance of the 4-*O* position, which did not correspond to previously reported literature as described in 3.2.1. Selective HMBC and HSQC experiments were employed in the assignment of fatty acid ester shifts, which in succession confirmed no migration of C=C double bonds in synthesised unsaturated esters. After desilylation of SFAEs in the 4-*O* position, a tendency for the esters to migrate on the sugar backbone was observed. Placement of esters were confirmed by NMR spectroscopy.

Chapter 5 - Future work

All work presented in the preceding chapters have been a contribution to the total synthesis of **1a** (Scheme 5.1).

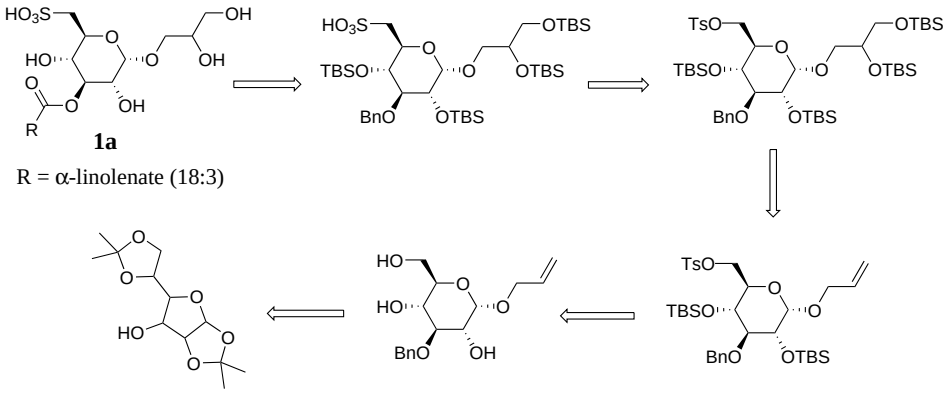

Scheme 5.1: Reterosynthetic analysis for the generation of **1a** from 1,2:5,6-Di-*O*-isopropylidene-α-D-glucofuranose.

As of writing this thesis, ongoing work on the anomeric resolution of 1-*O*-allyl-3-*O*-benzyl, and oxidation of the allylic group with OsO_4 is being completed by other members of the research group. This thesis has established a method in which esterification and subsequent desilylation are successful on model substrates to **1a**, while a working procedure for the insertion of SO_3H has already been optimized by other group members.

Establishing a mild deprotection strategy for the 3-*O*-benzyl ether is the only step left uninvestigated, as seen in the retrosynthetic analysis presented in Scheme 5.1. Although examination of the debenzylation is the final piece of the synthetic puzzle, a lot of work remains before target molecule **1a** falls within reach. Establishing working procedures on model substrates are one thing, executing them in the final synthesis is another. In one of the last steps of the total synthesis of **1a**, esterification of the 3-*O* position is required. The 3-*O* position is, in a similar manner to the 4-*O* position explored in this thesis, highly sterically hindered with TBDMS group at both 2-*O* and 4-*O*. Further investigation of the observed sterical effects in the Steglich esterification is therefore of interest to this project.

Work from this thesis showed migration of fatty acid esters among the secondary alcohols on the sugar backbone. Initially, this meant a lower potential yield of target molecule **1a**. However, synthesising several analogues of **1a** can be advantageous, having in mind a need of building a molecule library for SAR investigation towards SQAGs. One can imagine an simpler starting material, with multiple free hydroxyl groups, in which a single esterification process might yield several esterified derivatives in a diversity oriented manner.

If more time were been devoted to this project, the exploration of new protective patterns, and the synthesis of multiple SFAE analogues could have been carried out. Furthermore, biological evaluation of other synthesised SFAEs, either with MTT assays or photodynamic therapy, would have founded a library of compounds compatible with SAR studies.

Chapter 6 - Experimental

Reagents, starting materials and other consumables mentioned in this chapter were purchased from Sigma-Aldrich and have been used without further purification, unless stated otherwise. Temperatures above or below room temperature was obtained using oil or ice bath. Deviations from general procedures and modification of reaction conditions are described in further detail for each respective synthesis.

6.1 Instruments

6.1.1 Chromatography

Instrumental details and methods for low and high resolution chromatographic techniques are listed herein.

6.1.1.1 Low resolution chromatography

Thin layer chromatography, TLC, was carried out using silica on alumina plates, 60 F-254 Merck. Detection was accomplished by UV-light (254 nm), and a visualizing reagent solution of 1% $KMnO_4$ and K_2CO_3 in water.

Column flash chromatography was performed using silica gel 60Å (40 - 64 nm) as the stationary phase. Mobile phase composition is mentioned for each synthesised compound.

6.1.1.2 High Performance Liquid Chromatography

High Performance Liquid Chromatography was executed using an Agilent UHPLC system, consisting of the following: Agilent 1290 Infinity binary pump VL, G4220B, Agilent 1290 Infinity, G4226A auto sampler, Agilent 1260 TCAA, G1316A degasser, and a 1260 DAD, G4212-60007 Diode Array Detector.

A Zorbax Bonus-RP 250 x 4.6 mm column with a Zorbax Bonus-RP 12.5 x 4.6 mm guard column was used with C18 as the stationary phase.

Preparative HPLC was performed on an Agilent preparative HPLC system with the following equipment: Agilent 1260 Infinity Bin-Pump VL, G1361A, Agilent 1260 ALS G2260A autosampler, Agilent 1260 TCC G1316A degasser, Agilent 1260 FC-PS G1364B sample collector and an Agilent 126 G1315D diode array detector.
Separation and method development was preformed on a Zorbax XDB-C18, 21.2 x 150 mm preparative column.

Software employed for operation of the system and data analysis was Agilent Chemstation Open LAB.

Underneath follows a list of chromatographic methods employed in this work:

Chromatographic method A: Gradient elution starting at 80:20 ACN:H_2O to 100% ACN over 50 min, Isocratic at 100% ACN for

10 min. Flowrate: 1 mL/min.

Chromatographic method B: Isocratic elution with 100% ACN over 30 min. Flowrate: 1 mL/min.

Chromatographic method C: Isocratic elution with 99:1 ACN:H_2O over 20 min. Flowrate: 1 mL/min (analytical), 20 mL/min (preparative).

Chromatographic method D: Isocratic elution with 95:5 ACN:H_2O over 20 min. Flowrate: 1 mL/min (analytical), 20 mL/min (preparative).

6.1.2 Nuclear Magnetic Resonance Spectroscopy

1D and 2D NMR experiments were conducted on the following three instruments:

Bruker 400 MHz Avance III HD system, equipped with a 5 mm SmartProbe Z-gradient probe.

Bruker 600 MHz Avance III HD system, equipped with a 5 mm cryogenic CP-TCI Z-gradient probe.

Bruker 800 MHz Avance III HD system, equipped with a 5 mm cryogenic CP-TCI Z-gradient probe.

Chloroform-d was used as solvent with TMS as a reference compound, except in the analysis of compound **1**, which employed dimethylsulfoxide-d_6 due to solubility issues. All coupling constants (J) are denoted in Hertz (Hz) and reported with one decimal digit. Data were processed with Bruker TopSpin version 3.5.5 and 4.0.6. Residual solvent signals and other common impurities were identified

using the works of Fulmer et al. [133]. Experiments conducted in this thesis: ^{1}H, ^{13}C, HSQC, H,H-COSY, HMBC, NOESY, selective HSQC and selective HMBC, from Bruker® user library of experiments.

Spectroscopic data ar listed individually for each synthesised compound.

6.1.3 Infrared Spectroscopy

Infrared spectroscopy was recorded using a Bruker Alpha FRIT ECO-ATR spectrometer. Opus 7.5 software was used to process spectra.

6.1.4 Mass Spectroscopy

Accurate mass determination in positive and negative mode was performed on a "Synapt G2-S" Q-TOF instrument from Water TM. Samples were ionized by the use of ASAP probe (APCI), or ESI probe. Calculated exact mass and spectra processing was done by Waters TM Software Masslynx V4.1 SCN871.

6.1.5 Melting point analysis

Melting points was obtained using a Sanyo Gallenkamp manual melting point apparatus.

6.1.6 Optical rotation

Optical rotation was measured using a Anton Paar Modular Circular Polarimeter 5100. Constant wavelength (λ), cell length (l) and temperature (°C) for all analysis, λ= 589 nm, l = 2.5 mm, T = 20 °C.

Specific rotation was automatically calculated from equation 6.1 by the instrument.

$$[\alpha]_D^T = \frac{100\alpha}{l * c} \tag{6.1}$$

Where α is the observed rotation of polarized light, T is the temperature in °C, l is the cell length in dm and c is the compound concentration in g/100 mL.

6.1.7 Anhydrous solvents

Pure anhydrous solvents were obtained from a Braun MB SPS-800 system and collected in flasks containing 3Å activated molecular sieves.

6.2 Synthesis of glucopyranoside intermediates

6.2.1 Synthesis of 1-*O*-methyl-6-*O*-trityl-α-D-glucopyranoside (3)

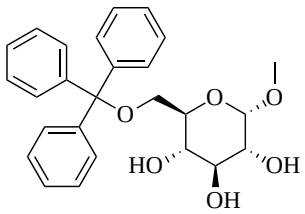

3

To a solution of 1-*O*-methyl-α-D-glucopyranoside (6.16 g, 32 mmol) in DMF (50 mL) was added TrCl (11.2 g, 40 mmol, 1.3 eqv.), DMAP (290 mg, 2 mmol, 6 mol%), and NEt_3 (8.02 mL, 58 mmol, 1.8 eqv.). The solution was stirred under nitrogen atmosphere at room temperature for 16 hours. The reaction was stopped with the addition of water (50.2 mL), and the mixture was extracted with DCM (3 x 100 mL). The organic phase was dried with brine followed by $MgSO_4$. The solvent was removed under reduced pressure and the resulting residue was dissolved in EtOAc (50.2 mL) and precipitated from *n*-pentane (500 mL). The precipitate was filtered off and recrystallised from EtOH using water as an anti solvent yielding **3** (9,10 g, 21 mmol, 66 %) as a white solid, $R_f = 0.2$ (1:1 EtOAc/ *n*-pentane), t_R (HPLC, method A) = 9 min, MP: 145-149 °C, $[\alpha]_D^{20} = 55.9°$(c 1.00, CH_2Cl_2), **^{1}H-NMR** (600 MHz, $CDCl_3$) δ: 7.44-7.47 (m, 6H, Ar), 7.28-7.32 (m, 6H, Ar), 7.22-7.25 (m, 3H, Ar), 4.77 (d, 1H, $J = 3.9$, CH), 3.67 (m, 2H, CH), 3.52 (m, 2H, CH) 3.43 (s, 3H, CH_3), 3.39 (m, 2H, CH), 2.77 (s, 1H, OH), 3.58 (s, 1H, OH), 2.19 (m, 1H, $J = 7.9$, OH). **^{13}C-NMR** (150 MHz, $CDCl_3$) δ: 143.7 (C_q-Ar), 128.6 (Ar), 127.9 (Ar), 127.2 (Ar), 99.1 (CH), 87.1 (C_q), 74.8 (CH), 72.3 (CH), 71.9 (CH), 69.8

(CH), 64.0 (CH), 55.3 (CH_3), HRMS (ESI+) m/z: 459.1784 $[M+Na]^+$ for $C_{26}H_{28}O_6Na$, IR (cm^{-1}): 3374, 3086, 2929, 1447, 1364, 1145, 1044, 900, 763, 736, 699, 632.

6.2.2 Synthesis of 1-*O*-allyl-6-*O*-tosyl-D-glucopyranoside (4)

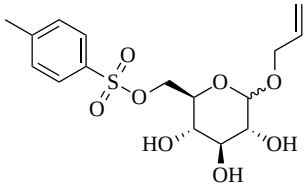

4

A suspension of α-D-glucose (2.02 g, 11 mmol) in allyl alcohol (38.2 mL, 561 mmol, 50 eqv.) and TMSCl (10.1 mL, 78 mmol, 7 eqv.) was stirred at 60°C for 5 hours before being concentrated under reduced pressure. The brown resiude was then co-evaporated with toluene (20 mL) before being dissolved in pyridine (50 mL). To the solution was added ρ-TsCl (2,20 g, 11 mmol, 1 eqv.) and DMAP (65 mg, 0.5 mmol, 5 mol%). The reaction was stirred at room temperature for 16 hours. After completion of the reaction, the solvent was removed under reduced pressure, prior to addition of ice water (20 mL) and EtOAc (10 mL). The aqueous phase was extracted with EtOAc (3x 50 mL) and the resulting organic phase was dried over $MgSO_4$, filtered and concentrated under reduced pressure. The resulting light brown residue was purified by silica flash chromatography (20:1 DCM/MeOH) to yield **4** (2.52 g, 6.7 mmol, 73%) as a brown oil containing an anomeric mixture and by products. R_f = 0.25 (20:1 DCM/ MeOH), $[\alpha]_D^{20}$ = 63.9°(c 1.00, CH_2Cl_2), ^{1}**H-NMR** (600 MHz, $CDCl_3$) δ: 7.77-7.87 (m, 2H, Ar), 7.31-7.36 (m, 2H, Ar), 5.90 (m, 1H, CH), 5.10-5.34 (m, 2H, CH_2), 4.73-4.93 (m, 1H, J = 3.7, CH), 3.40-4.44 (m, 10H, CH), 3.16 (s, 1H, OH), 2.43 (m, 3H, CH_3). HRMS (ESI+) m/z: 397.0933 $[M+Na]^+$ for $C_{16}H_{22}O_8NaS$, IR (cm^{-1}): 3360, 2923, 1645, 1356, 1175, 1027, 928, 836, 666, 508.

6.2.3 Synthesis of 1-*O*-allyl-2,3,4-tri-O-(*tert*-butyldimethylsilyl)-6-*O*-tosyl-D-glucopyranoside (5)

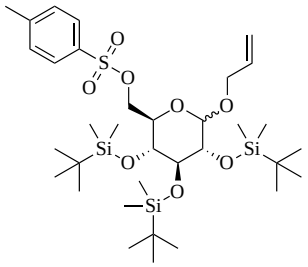

5

A stirred solution of 1-*O*-allyl-6-*O*-tosyl-D-glucopyranoside (**4**, 5.0 g, 13 mmol) and 2,6-lutidine (6.2 mL, 54 mmol, 4.1 eqv.) in DCM (100 mL) was cooled to 0°C before being added TBDMS-*O*Tf (14 mL, 47 mmol, 3.6 eqv.) dropwise under inert atmosphere. The reaction was stirred at 0°C for 5 hours before being quenched with water (60 mL). The mixture was then extracted with DCM (3 x 100 mL), and the organic phase was dried over $MgSO_4$, filtered and concentrated under reduced pressure. The resulting volatile oil was then purified by silica flash chromatography (20:1 n-pentane/EtOAc) to yield the product **5** (7.0, 9.8 mmol, 75%) as a clear oil containing several by products. R_f = 0.7 (main) + 0.6 + 0.3 (20:1 n-pentane/ EtOAc). A pure enough sample for further analysis could not be obtained.

6.2.4 Synthesis of 1-*O*-allyl-4,6-*O*-benzylidene-α-D-glucopyranoside (6)

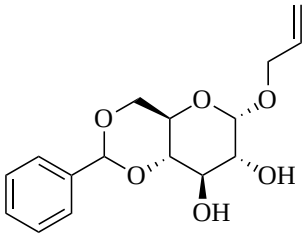

6

To a suspension of α-D-glucose (10.2 g, 56 mmol) in allyl alcohol (200 mL, 2.80 mol, 50 eqv.) was added TMSCl (36 mL, 392 mmol, 7 eqv.). The reaction mixture was stirred at 60°C for 5 hours before removal of the solvent by evaporation under reduced pressure. The resulting residue was co-evaporated with toluene (20 mL). The brown residue (9.01 g) was added MeCN (100 mL), Benzaldehyde dimethyl acetal (9.21 mL, 61 mmol, 1.1 eqv.) and ρ-toluene sulfonic acid (777 mg, 4 mmol, 7 mol%). The suspension was stirred at room temperature for 5 hours before being precipitated in saturated $NaHCO_3$ solution (600 mL). The resulting precipitate was filtered and recrystallised from heated EtOH using water as an anti solvent yielding the product (**6**, 8.64 g, 28 mmol, 50 %) as white crystals, R_f = 0.4 (10:1 n-pentane/ EtOAc), t_R (HPLC, method A) = 12 min, MP: 130 - 134 °C, $[\alpha]_D^{20} = 67.9°$(c 1.00, CH_2Cl_2), ^{1}**H-NMR** (600 MHz, $CDCl_3$) δ: 7.48-7.51 (m, 2H, Ar), 7.34-7.39 (m, 3H, Ar), 5.93 (m, 1H, CH), 5.54 (s, 1H, CH-Ar), 5.33 (dd, 1H, J = 17.3, 1.4, CH), 5.26 (m, 1H, J = 10.4, 1.4, CH), 4.97 (d, 1H, J = 4.0, CH) 4.29 (dd, 1H, J = 10.4, 4.9, CH), 4.26 (m, 1H, J = 12.2, 5.4, CH), 4.07 (m, 1H, J = 12.2, 6.3, CH), 3.97 (t, 1H, J = 9.3, CH), 3.86 (td, 1H, J = 9.9, 4.9, CH), 3.74 (t, 1H, J = 10.4, CH), 3.65 (m, 1H, CH), 3.52 (t, 1H, J = 9.3, CH), 2.64 (s, 1H, OH), 2.19 (d, 1H, J = 9.3, OH). ^{13}**C-NMR** (150 MHz, $CDCl_3$) δ: 137.03 (C_q-Ar), 133.3 (CH), 129.3 (Ar), 128.3 (Ar), 126.3 (Ar), 118.4 (CH_2), 101.9 (CH), 97.8 (CH),

80.9 (CH), 72.9 (CH), 71.9 (CH), 68.9 (CH_2), 68.9 (CH_2), 62.6 (CH), HRMS (ESI+) m/z: 331.1156 $[M+Na]^+$ for $C_{16}H_{20}O_6Na$, IR (cm^{-1}): 3425, 2916, 2867, 1376, 1071, 1029, 993, 926, 752, 699.

6.2.5 Synthesis of 1-*O*-allyl-2,3-di-*O*-(benzyl)-4,6-*O*-benzylidene-α-D-glucopyranoside (7)

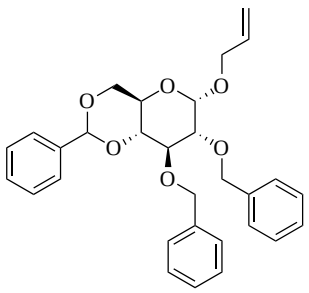

7

1-*O*-allyl-4,6-*O*-benzylidene-α-D-glucopyranoside (**6**, 1.03 g, 3.34 mmol), NaH (360 mg, 15 mmol, 4.5 eqv.) and TBAI (123 mg, 0.3 mmol, 10 mol%) was dissolved in dry THF (25 mL). BnBr (1.62 mL, 13.6 mmol, 4.1 eqv.) was added to the mixture while stirring at room temperature. After addition of all reagents, the mixture was heated to 60°C under vigorous stirring. After 2 hours the reaction was stopped with the addition of water (40 mL), and the resulting solution was extracted with EtOAc (3 x 70 mL) before being dried over $MgSO_4$, filtered and evaporated under reduced pressure. The crude product was purified by silica flash chromatography (20:1 n-pentane/EtOAc) to yield the product **7** (1.40 g, 3.04 mmol, 86 %) as a white, crystalline solid, R_f = 0.70 (20:1 n-pentane/ EtOAc), t_R (HPLC, method A) = 36.20 min, MP: 145-147 °C, $[\alpha]_D^{20}$ = 24.0°(c 1.00, CH_2Cl_2), ^{1}**H-NMR** (400 MHz, $CDCl_3$) δ: 7.46-7.51 (m, 2H, Ar), 7.27-7.41 (m, 13H, Ar), 5.94 (dddd, 1H, J = 17.1, 10.3, 6.6, 5.3), 5.55 (s, 1H, CH-Ar), 5.33 (m, 1H, J = 17.1, 1.5, CH), 5.24 (m, 1H, J = 10.3, 1.5, CH), 4.92 (d, 1H, J = 11.2, CH_2) 4.84 (d, 1H, J = 11.2, CH_2), 4.83 (d, 1H, J = 12.1, CH_2), 4.80 (d, 1H, J = 3.9, CH), 4.75 (d, 1H, J = 12.1, CH_2), 4.26 (dd, 1H, J = 10.3, 4.9, CH), 4.19 (m, 1H, J = 13.0, 5.3, 1.4, CH), 4.08 (t, 1H, J = 9.2, CH), 4.04 (m, 1H, J = 13.0, 6.7, 1.4 , CH), 3.89 (td, 1H, J= 10.3, 4.9, CH), 3.70 (t, 1H, J = 10.3, CH), 3.60 (dd, 1H, J = 19.5, 9.4, CH), 3.56 (d, 1H, J = 9.4, CH). ^{13}**C-NMR** (100 MHz, $CDCl_3$)

δ: 138.8 (C_q-Ar), 138.2 (C_q-Ar), 137.4 (C_q-Ar), 133.6 (CH), 128.9 (Ar), 120.4 (Ar), 128.3 (Ar), 128.2 (Ar), 128.1 (Ar), 128.0 (Ar), 127.9 (Ar), 127.6 (Ar), 126.0 (Ar), 118.4 (CH), 101.2 (CH-Ar), 96.8 (CH), 82.2 (CH), 79.2 (CH), 78.6 (CH), 75.4 (CH_2), 73.6 (CH_2), 69.0 (CH), 68.5 (CH), 62.5 (CH), HRMS (ESI+) m/z: 511.2097 $[M+Na]^+$ for $C_{30}H_{32}O_6Na$, IR (cm^{-1}): 3063, 2916, 2865, 1496, 1369, 1087, 1028, 999, 747, 697, 656.

6.2.6 Synthesis of 1-*O*-allyl-2,3-di-*O*-(*tert*-butyldimethylsilyl)-4,6-*O*-benzylidene-α-D-glucopyranoside (8)

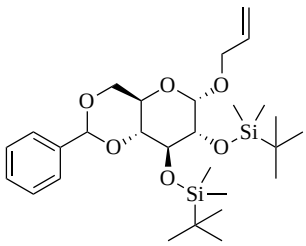

8

1-*O*-allyl-4,6-*O*-benzylidene-α-D-glucopyranoside (**6**, 2.05 g, 6.4 mmol), *tert*-butyldimethylsilylchloride (6.1 g, 41 mmol, 6.4 eqv.) and imidazole (3.3 g, 48 mmol, 7.5 eqv.) was sirred in DMF (50 mL) for 3 days until sufficient progress of the reaction was observed. The mixture was concentrated under reduced pressure to 10 mL, then added a saturated aqueous solution of $NaHCO_3$ (30 mL) and DCM (50 mL). The aqueous phase was extracted with DCM (3x 75 mL). The organic phase was washed with a saturated salt solution, before being dried over $MgSO_4$, filtered and evaporation of the solvent under reduced pressure. The solidified crude residue was then purified by silica flash chromatography (20:1, n-pentane/EtOAc) to yield the product (**8**, 3.2 g, 5.9 mmol, 93%) as a clear oil, R_f = 0.85 (20:1 EtOAc/ n-pentane), t_R (HPLC, method A) = 53 min, $[\alpha]_D^{20}$ = 36.0°(c 1.00, CH_2Cl_2), ^{1}**H-NMR** (600 MHz, $CDCl_3$) δ: 7.45-7.48 (m, 2H, Ar), 7.33-7.37 (m, 3H, Ar), 5.96 (dddd, 1H, J = 17.0, 10.3, 6.6, 5.5, (CH)), 5.44 (s, 1H, CH-Ar), 5.32 (m, 1H, J = 17.2, 1.6, CH), 5.22 (m, 1H, J = 10.4, 1.7, CH), 4.81 (d, 1H, J = 3.6, CH) 4.23 (dd, 1H, J = 10.2, 4.9, CH_2), 4.20 (m, 1H, J = 12.8, 5.5, 1.3, CH_2), 4.01 (m, 2H, CH), 3.86 (td, 1H, J = 10.1, 4.9 CH), 3.68 (t, 1H, J = 10.3, CH), 3.65 (dd, 1H, J = 8.8, 3.6, CH), 3.38 (t, 1H, J = 9.4, CH), 0.92 (s, 9H, CH_3), 0.80 (s, 9H, CH_3), 0.11 (s, 3H, CH_3–Si), 0.09 (s, 3H, CH_3–Si), 0.04 (s, 3H, CH_3–Si), -0,01 (s,

3H, CH_3–Si). ^{13}**C-NMR** (150 MHz, $CDCl_3$) δ: 137.4 (C_q-Ar), 133.9 (CH), 129.0 (Ar), 128.1 (Ar), 126.5 (Ar), 118.1 (CH_2), 102.4 (CH-Ar), 99.2 (CH), 82.8 (CH), 74.6 (CH), 71.9 (CH), 69.2 (CH_2), 68.8 (CH_2), 62.5 (CH), 26.1 (CH_3), 26.0 (CH_3), 18.3 (C_q-Si), 18.2 (C_q-Si), -3.4 (CH_3-Si), -3.9 (CH_3-Si), -4.3 (CH_3-Si), -4.4 (CH_3-Si), HRMS (ESI+) m/z: 559.2886 $[M+Na]^+$ for $C_{28}H_{48}O_6Si_2Na$, IR (cm^{-1}): 2952, 2929, 2857, 1471, 1385, 1251, 1171, 1088, 1047, 931, 858, 837, 760, 668.

6.2.7 Synthesis of 1-*O*-allyl-2,3-di-*O*-(*tert*-butyldimethylsilyl)-6-*O*-benzyl-α-D-glucopyranoside (12)

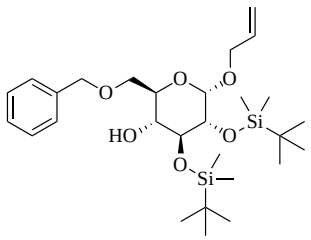

12

1-*O*-allyl-2,3-di-*O*-(*tert*-butyldimethylsilyl)-4,6-*O*-benzylidene-α-D-glucopyranoside (**8**, 0.27 g, 0.51 mmol) was dissolved in anhydrous DCM (6 mL) and stirred at 0°C, before being added Et_3SiH (0,40 mL, 2.5 mmol, 5 eqv.). To the cooled mixture was added TFA (0,19 mL, 2.5 mmol, 5 eqv.) dropwise and under an inert atmosphere of nitrogen. The reaction was left stirring at 0°C for 4 hours before being added a saturated aquous solution of $NaHCO_3$ (10 mL). The aqueous phase was extracted with DCM (3 x 50 mL), and the resulting organic phase was washed with a saturated salt solution before being dried over Na_2SO_4, filtered and evaporated under reduced pressure. The crude oil was purified by silica flash chromatography (20:1 n-pentane/EtOAc) to yield the product **12** (0,26 g, 0.50 mmol, 99%) as a white crystaline wax, R_f = 0.78 (20:1 n-pentane/ EtOAc), t_R (HPLC, method A) = 49 min, MP: 47-48 °C, $[\alpha]_D^{20}$ = 48.0°(c 1.00, CH_2Cl_2), ^{1}**H-NMR** (600 MHz, $CDCl_3$) δ: 7.27-7.36 (m, 5H, Ar), 5.93 (dddd, 1H, J = 17.0, 10.4, 6.3, 5.4, CH), 5.29 (m, 1H, J = 17.0, 1.7, CH), 5.17 (m, 1H, J = 10.4, 1.7, CH) 4.81 (d, 1H, J = 3.3, CH), 4.63 (d, 1H, J = 12.1, CH_2), 4.55 (d, 1H J = 12.1, CH_2), 4.18 (m, 1H, J = 12.8, 5.4, CH_2), 3.96 (m, 1H, J = 12.8. 6.4, CH_2) 3.83 (t, 1H, J = 8.5, CH), 3.77 (m, 1H, J = 9.4, 4.1, CH), 3.69 (m, 1H, J = 4.6, 3.3, CH_2), 3.58 (dd, 1H, J = 8.9, 3.3, CH), 3.46 (t, 1H, J = 8.9, CH), 2.14 (s, 1H, OH), 0.91 (s, 9H,

CH_3), 0.91 (s, 9H, CH_3), 0.13 (s, 3H, CH_3–Si), 0.11 (s, 3H, CH_3–Si), 0.09 (s, 3H, CH_3–Si), 0.07 (s, 3H, CH_3–Si). **^{13}C-NMR** (150 MHz, $CDCl_3$) δ: 138.1 (C_q-Ar), 134.1 (CH), 128.4 (Ar), 127.7 (Ar), 117.6 (CH_2), 98.3 (CH), 74.9 (CH), 73.6 (CH), 73.5 (CH_2), 72.4 (CH), 70.3 (CH), 69.7 (CH_2), 68.5 (CH_2), 26.2 (CH_3), 26.1 (CH_3), 18.3 (C_q-Si), -3.3 (CH_3–Si), -3.7 (CH_3–Si), -4.2 (CH_3–Si), -4.3 (CH_3–Si), HRMS (ESI+) m/z: 561.3039 $[M+Na]^+$ for $C_{28}H_{50}O_6Si_2Na$, IR (cm^{-1}): 3617, 3519, 2951, 2928, 2856, 1472, 1251, 1144, 1054, 861, 836, 776, 697, 669.

6.2.8 Synthesis of 1-*O*-allyl-2,3,6-tri-*O*-(benzyl)-α-D-glucopyranoside (9)

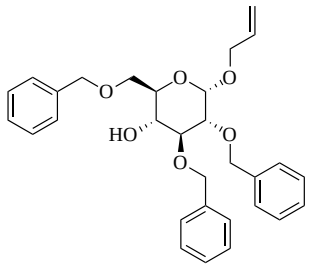

9

To a stirred solution of 1-*O*-allyl-2,3-di-*O*-(benzyl)-4,6-*O*-benzylidene-α-D-glucopyranoside (**7**, 0.52 g, 1.1 mmol) in DCM (20 mL) at 0°C was added Et_3SiH (2.0 mL, 12 mmol, 12 eqv.) before being added $BF_3 \cdot Et_2O$ (0.26 mL, 2.1 mmol, 2 eqv.) dropwise. The reaction was continued stirring at 0°C for 4 hours before being added a saturated aquous solution of $NaHCO_3$ (10 mL) and extracted with DCM (3 x 75 mL). The organic phase was washed with brine (100 mL) before being dried over $MgSO_4$, filtered and evaporated under reduced pressure. The crude oil was purified by silica flash chromatography (10:1 *n*-pentane/EtOAc) to yield the product **9** (0.37 g, 0.76 mmol, 72%) together with by products as a oil, R_f = 0.37 (11:1 *n*-pentane/EtOAc), t_R (HPLC, method A) = 39 min, ^{1}**H-NMR** (400 MHz, $CDCl_3$) δ: 7.26-7.39 (m, 15H, Ar), 5.94 (dddd, 1H, J = 17.1, 10.3, 6.7, 5.2, CH), 5.32 (m, 1H, J = 17.1, 1.4, CH_2), 5.21 (m, 1H, J = 10.3, 1.4, CH_2), 5.01 (d, 1H, J = 11.5, CH_2), 4.84 (d, 1H, J = 3.7, CH) 4.74 (m, 2H, CH_2), 4.50-4.70 (m, 3H, CH_2), 4.17 (m, 1H, J = 12.8, 5.3, CH_2), 4.01 (m, 1H, J = 12.8, 6.6, CH_2), 3.79 (m, 2H, CH), 3.67 (m, 1H, CH), 3.62 (m, 1H, CH), 3.54 (dd, 1H, J = 9.6, 3.7, CH), 2.33 (d, 1H, J = 2.3, OH). ^{13}**C-NMR** (150 MHz, $CDCl_3$) δ: 134.5 (Ar), 133.7 (CH), 130.0 (C_q), 129.7 (C_q), 128.9 (C_q), 128.5 (Ar), 128.5 (Ar), 128.4 (Ar), 128.4 (Ar), 128.4 (Ar), 128.4 (Ar), 128.3 (Ar), 128.3 (Ar), 128.3 (Ar), 128.0 (Ar), 128.0 (Ar), 127.9 (Ar), 127.8 (Ar), 127.8 (Ar), 118.2 (CH_2),

95.6 (CH), 81.5 (CH), 79.6 (CH), 75.4 (CH_2), 73.5 (CH), 72.9 (CH_2), 70.7 (CH), 70.2 (CH_2), 69.4 (CH_2), 68.2 (CH_2). Spectroscopic data present in literature [134].

6.2.9 Synthesis of 1-*O*-allyl-6-*O*-benzyl-α-D-glucopyranoside (11)

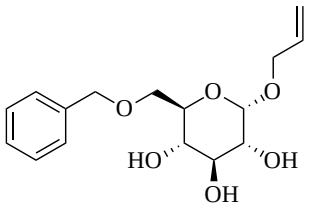

11

To a solution of 1-*O*-allyl-2,3-di-*O*-(*tert*-butyldimethylsilyl)-4,6-*O*-benzylidene-α-D-glucopyranoside (**8**, 1.52 g, 2.84 mmol) in DCM (40 mL) was added Et_3SiH (5.63 mL, 33.9 mmol, 12 eqv.) before being added $BF_3 \cdot Et_2O$ (0.70 mL, 5.66 mmol, 2 eqv.) dropwise at 0°C. The reaction was stirred under these conditions for 4 hours before being added a saturated aqueous solution of $NaHCO_3$ (20 mL) and extracted with DCM (3 x 100 mL). The organic phase was washed with brine (50 mL) before being dried over $MgSO_4$, filtered and evaporated under reduced pressure. The crude oil was purified by silica flash chromatography (10:1 *n*-pentane/EtOAc) to yield the compound **11** (0.29 g, 0.94 mmol, 33%) together with other compounds as a clear oil, R_f = 0.10 (4:1 *n*-pentane/EtOAc), t_R (HPLC) = 8 min, ^{1}**H-NMR** (600 MHz, $CDCl_3$) δ: 7.24-7.35 (m, 5H, Ar), 5.91 (m, 1H, CH), 5.28 (m, 1H, J = 17.1, 1.5, CH_2), 5.19 (m, 1H, J = 10.3, 1.5, CH_2), 4.91 (d, 1H, J = 3.9, CH), 4.61 (d, 1H, J = 12.1, CH_2), 4.55 (d, 1H, J = 12.1, CH_2), 4.21 (m, 1H, J = 12.9, 5.0, CH_2), 4.03 (m, 1H, J = 12.9, 6.6, CH_2), 3.75 (m, 1H, CH), 3.69 (m, 3H, CH/CH_2), 3.50 (m, 2H, CH), 2.37 (s, 1H, OH), 2.00 (d, 1H, J = 9.3, OH). ^{13}**C-NMR** (150 MHz, $CDCl_3$) δ: 136.9 (C_q-Ar), 132.5 (CH), 127.2 (Ar), 126.5 (Ar), 126.5 (Ar), 116.6 (CH_2), 96.5 (CH), 73.8 (CH_2), 72.4 (CH), 72.3 (CH), 71.4 (CH), 71.2 (CH), 69.2 (CH_2), 69.2 (CH), 68.4 (CH), 67.3 (CH).

6.2.10 Synthesis of 1-*O*-allyl-2,3-di-*O*-(*tert*-butyldimethylsilyl)-4-*O*-benzyl-α-D-glucopyranoside (10)

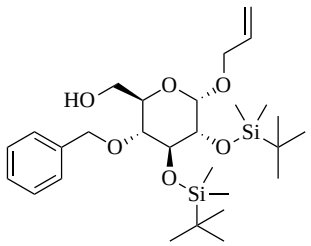

10

1-*O*-allyl-2,3-di-*O*-(*tert*-butyldimethylsilyl)-4,6-*O*-benzylidene-α-D-glucopyranoside (**8**, 0.52 g, 0.9 mmol) was dissolved in a mixture of anhydrous DCM and Et_2O (7:4, 50 mL). To the stirred solution was added $LiAlH_4$ (70 mg, 1.8 mmol, 2 eqv.) slowly in 3 portions, and the mixture was then heated to reflux (40°C). After 3 minutes the reaction vessel was added $AlCl_3$ (0,25 g, 1.8 mmol, 2 eqv.) dissolved in anhydrous Et_2O (10 mL) dropwise. The mixture was stirred under the given conditions for 1 hour before being stopped with the dropwise addition of water (20 mL). The two phase dispersion was then extracted with DCM (3x 100 mL) and the organic phase was dried over Na_2SO_4, filtered and the solvents removed under reduced pressure to yield the crude product as a transparent syrup. Purification was conducted using silica flash chromatography (20:1 n-pentane/EtOAc) to yield the product **10** (0.35, 0.63 mmol, 70%) as a white crystalline wax. R_f = 0.70 (20:1 n-pentane/ EtOAc) t_R (HPLC) = 48 min, MP: 49-50 °C, $[\alpha]_D^{20}$ = 59.9°(c 1.00, CH_2Cl_2), ^{1}**H-NMR** (600 MHz, $CDCl_3$) δ: 7.27-7.36 (m, 5H, Ar), 5.92 (m, 1H, J = 16.2, 10.5, 6.0, 5.7, CH), 5.30 (m, 1H, J = 16.2, 1.7, CH_2), 5.18 (m, 1H, J = 10.5, 1.7, CH_2), 4.89 (d, 1H, J = 11.7, CH_2), 4.76 (d, 1H, J = 3.4, CH), 4.60 (d, 1H, J = 11.7, CH_2), 4.14 (m, 1H, J = 12.8, 5.7, CH_2) 4.00 (t, 1H, J = 8.9, CH), 3.92 (m, 1H, J = 12.8, 5.7, CH_2), 3.71-3.76 (m, 1H, CH), 3.63-3.69 (m, 2H,

CH_2), 3.58 (dd, 1H, J = 8.9, 3.4, CH), 3.36 (t, 1H, J = 9.2, CH), 0.93 (s, 9H, CH_3), 0.92 (s, 9H, CH_3), 0.12 (s, 3H, CH_3–Si), 0.11 (s, 3H, CH_3–Si), 0.09 (s, 3H, CH_3–Si), 0.06 (s, 3H, CH_3–Si). **^{13}C-NMR** (150 MHz, $CDCl_3$) δ: 138.4 (C_q-Ar), 134.0 (CH), 128.3 (Ar), 127.5 (Ar), 127.4 (Ar), 117.3 (CH_2), 98.9 (CH), 79.0 (CH), 74.8 (CH_2), 74.3 (CH), 74.0 (CH), 71.2 (CH), 68.6 (CH_2), 61.9 (CH_2), 26.4 (CH_3), 26.2 (CH_3), 18.3 (C_q-Si), 18.0 (C_q-Si), -3.0 (CH_3–Si), -3.3 (CH_3–Si), -4.0 (CH_3–Si), -4.3 (CH_3–Si). HRMS (ESI+) m/z: 561.3049 $[M+Na]^+$ for $C_{28}H_{50}O_6Si_2Na$, IR (cm^{-1}): 3594, 3498, 2953, 2928, 2856, 1472, 1388, 1252, 1209, 1086, 1029, 935, 862, 837, 776, 670.

6.2.11 Synthesis of 1-*O*-allyl-α-D-glucopyranoside (1)

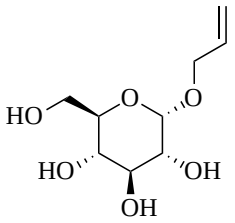

1

A suspension of 1-*O*-allyl-4,6-*O*-benzylidene-α-D-glucopyranoside (**1**, 3.0 g, 9.7 mmol) in AcOH and water (8:5, 75 mL) was heated to 100°C and stirred for 1 hour. After the required reaction time, the solution was evaporated under reduced pressure, yielding a yellow oil which then was kept under vacuum for 3 days to give the product (**1**, 1.86 g, 87 %) with presence of minor residual solvent, R_f = 0.10 (9:1 EtOAc/ MeOH), MP: 99-102 °C, $[\alpha]_D^{20}$ = 93.9°(c 1.00, CH_2Cl_2), ^{1}**H-NMR** (400 MHz, DMSO−d_6) δ: 5.91 (m, 1H, J = 15.8, 10.4, 5.3, CH), 5.32 (m, 1H, J = 17.2, 1.3, CH_2), 5.14 (m, 1H,J = 10.4, 1.3, CH_2), 4.67 (dd, 1H, J = 3.6, CH), 4.12 (m, 1H, J = 13.6, 4.7, CH_2), 3.92 (m, 1H, J = 13.6, 5.6, CH_2) 3.62 (m, 1H, J = 11.6, 1.9, CH_2), 3.40-3.47 (m, 2H, CH/CH_2), 3.36 (m, 1H, J = 15.5, 9.7, 5.7, 1.9, CH), 3.21 (dd, 1H, J = 9.7, 3.6, CH), 3.06 (t, 1H, J = 9.2, CH). ^{13}**C-NMR** (100 MHz, $CDCl_3$) δ: 135.3 (CH), 116.8 (CH_2), 98.3 (CH), 73.7 (CH), 73.3 (CH), 72.4 (CH), 70.8 (CH), 67.5 (CH_2), 61.4 (CH_2). HRMS (ESI+) m/z: 243.038 $[M+Na]^+$ for $C_9H_{16}O_6Na$. IR (cm^{-1}): 3340, 2923, 1422, 1255, 1145, 1100, 1076, 1024, 929, 601, 554. Spectroscopic data corresponds with those previously reported in literature [135].

6.2.12 Synthesis of 1-*O*-allyl-6-*O*-(*tert*-butyldiphenylsilyl)-α-D-glucopyranoside (13)

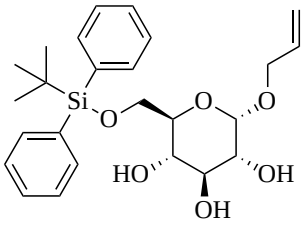

13

A stirred solution of 1-*O*-allyl-α-D-glucopyranoside (**1**, 2.17 g, 9.9 mmol) and imidazole (1.17 g, 17.2 mmol, 1.7 eqv.) in DMF (40 mL) was cooled to 0°C and then added TBDPS-Cl (3 mL, 11.3 mmol, 1.1 eqv.) dropwise. The reaction was then stirred under an atmosphere of nitrogen, and allowed to reach room temperature. After 24 hours the reaction was terminated by the addition of a saturated aqueous solution of $NaHCO_3$ (40 mL), before being extracted with EtOAc (3 x 80 mL). The organic phase was dried over Na_2SO_4, filtered and evaporated under reduced pressure. The crude residue was purified by silica flash chromatography (20:1 n-pentane/EtOAc) to yield the product **13** (3.85 g, 8.4 mmol, 85%) as a clear oil. R_f = 0.35 (4:1 EtOAc/ *n*-pentane) t_R (HPLC, method A) = 10.2 min, $[\alpha]_D^{20}$ = 40.0°(c 1.00, CH_2Cl_2), **^{1}H-NMR** (600 MHz, $CDCl_3$) δ: 7.67-7.71 (m, 4H, Ar), 7.35-7.43 (m, 6H, Ar), 5.88 (dddd, 1H, J = 17.0, 10.5, 6.4, 5.4, CH), 5.26 (m, 1H, J = 17.0, 1.5, CH_2), 5.16 (m, 1H, J = 10.5, 1.5, CH_2), 4.88 (d, 1H, J = 3.9, CH), 4.17 (m, 1H, J = 12.9, 5.4, CH_2), 3.99 (dd, 1H, J = 12.9, 6.4, CH_2), 3.87 (m, 2H, J = 10.8, 3.9, CH_2), 3.77 (t, 2H, J = 9.2, CH), 3.68 (m, 1H, J = 9.4, 4.8, CH), 3.52 (m, 2H, J = 9.3, CH/OH), 3.31 (s, 1H, OH), 2.87 (s, 1H, OH), 1.05 (m, 9H, CH_3). **^{13}C-NMR** (150 MHz, $CDCl_3$) δ: 135.7 (Ar), 135.6 (Ar), 133.6 (CH), 133.2 (C_q-Ar), 133.1 (C_q-Ar), 129.8 (Ar), 127.7 (Ar), 127.7 (Ar), 117.9 (CH_2), 97.1 (CH), 74.7 (CH), 72.1 (CH), 71.6 (CH), 71.3 (CH), 68.3 (CH_2), 64.3 (CH_2), 26.8 (CH_3),

26.8 (CH_3), 19.2 (C_q-Si). HRMS (ESI+) m/z: 481.2021 $[M+Na]^+$ for $C_{25}H_{34}O_6SiNa$, IR (cm^{-1}): 3238, 3071, 3049, 2929, 2856, 1427, 1144, 1111, 1044, 1005, 930, 822, 740, 701, 613, 504. Spectroscopic data has been compared to the mannose analogue found in literature [124].

6.2.13 Synthesis of 1-*O*-allyl-2,3,4-tri-*O*-(*tert*-butyldimethylsilyl)-6-*O*-(*tert*-butyldiphenylsilyl)-α-D-glucopyranoside (14)

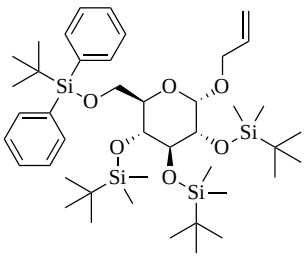

14

1-*O*-allyl-6-*O*-(*tert*-butyldiphenylsilyl)-α-D-glucopyranoside (**13**, 3.56 g, 7.8 mmol), imidazole (4.70 g, 69 mmol) and TBDMS-Cl (10.5 g, 70 mmol) was dissolved in DMF (80 mL) and stirred at room temperature for 3 days. The reaction was terminated by the addition of a saturated solution of $NaHCO_3$ (100 mL), and the mixture was extracted with DCM (3x 200 mL) before being dried over Na_2SO_4, filtered and evaporated under reduced pressure. The resulting orange crude mixture was then eluted through a silica pad (15:1 n-pentane/EtOAc) to yield several product analogues, indicated by proton NMR, as a clear syrup. The product mixture was then dissolved in anhydrous DCM (70 mL) and cooled to 0°C. To the stirred solution under an atmosphere of nitrogen was added 2,6−lutidine (3 mL, 26 mmol) before being added TBDMS-Triflate (3 mL, 13 mmol) dropwise. After addition of the reagents the reaction vessel was slowly warmed to room temperature and left to stir for 24 hours. The reaction was terminated by the addition of water (50 mL) and the aqueous phase was extracted with DCM (3x 100 mL). The organic phase was dried over Na_2SO_4, filtered and evaporated under reduced pressure and purified by silica flash chromatography (30:1 n-pentane/EtOAc) to yield the product **14** (4.50 g, 5.62 mmol, 72%) as a clear syrup, $R_f = 0.75$ (15:1 *n*-pentane/EtOAc) t_R (HPLC, method A) = 60 min, $[\alpha]_D^{20} = 40.0°$(c 1.00, CH_2Cl_2), ^{1}**H-NMR** (600

MHz, $CDCl_3$) δ: 7.63-7.74 (m, 4H, Ar), 7.30-7.42 (m, 6H, Ar), 5.92 (m, 1H, J = 17.2, 10.5, 6.0, 5.3, CH), 5.24 (m, 1H, J = 17.2, 1.7, CH_2), 5.11 (m, XH, J = 10.5, 1.7, CH_2), 4.83 (d, 1H, J = 2.8, CH), 4.32 (m, 1H, J = 12.8, 1.5, CH_2) 4.04 (m, 1H, CH), 3.99 (m, 1H, J = 6.1, 1.5, CH_2), 3.90 (dd, 1H, J = 10.7, 1.8, CH), 3.83 (m, 2H, CH/CH_2), 3.75 (m, 2H, CH/CH_2), 3.48 (m, 1H, CH), 1.05 (m, 9H, CH_3), 0.89 (m, 18H, CH_3), 0.78 (m, 9H, CH_3), 0.08 (m, 15H, CH_3), -0.06 (s, 3H, CH_3). **^{13}C-NMR** (150 MHz, $CDCl_3$) δ: 135.9 (C_q-Ar), 135.6 (C_q-Ar), 133.6 (CH), 129.4 (Ar), 129.4 (Ar), 127.5 (Ar), 127.5 (Ar), 127.4(Ar), 116.2 (CH_2), 95.4 (CH), 74.5 (CH), 74.5 (CH), 73.9 (CH), 72.7 (CH), 71.8 (CH), 68.2 (CH), 63.9 (CH), 26.8 (CH_3), 26.8 (CH_3), 26.0 (CH_3), 26.0 (CH_3), 25.9 (CH_3), 25.8 (CH_3), 25.8 (CH_3), 19.3 (C_q), 18.4 (C_q), 18.0 (C_q), 17.9 (C_q), -3.5 (CH_3), -3.9 (CH_3), -4.2 (CH_3), -4.5 (CH_3), -4.7 (CH_3), -4.8 (CH_3). HRMS (ESI+) m/z: 823.4617 $[M+Na]^+$ for $C_{43}H_{76}O_6NaSi_4$, IR (cm^{-1}): 2952, 2928, 2855, 1471, 1252, 1157, 1095, 1064, 882, 776, 701, 505.

6.2.14 Synthesis of 2,3,4-tri-*O*-(*tert*-butyldimethylsilyl)-6-*O*-(*tert*-butyldiphenylsilyl)-α-D-glucopyranoside (15)

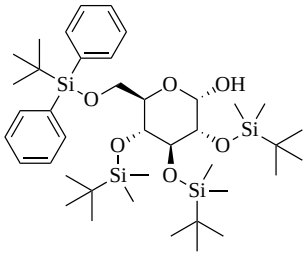

15

1-*O*-allyl-2,3,4-tri-*O*-(*tert*-butyldimethylsilyl)-6-*O*-(*tert*-butyldiphenylsilyl)α-D-glucopyranoside (**14**, 233 mg, 0.29 mmol) was dissolved in MeOH (5 mL), and added $Pd(PPh_3)_4$ (6 mg, 5.2 μmol, 2 mol%) under an atmosphere of nitrogen. The mixture was stirred for 5 minutes before being added K_2CO_3 (0.20 g, 1.5 mmol, 5 eqv.). The reaction was heated to 68°C and stirred under an atmosphere of nitrogen for 12 hours, before being terminated with the addition of mildly acidic water (5 mL, pH = 4). The aqueous phase was extracted with EtOAC (3x 40 mL) and the organic phase was dried over $MgSO_4$, filtered and evaporated under reduced pressure. The crude residue was eluted through a pad of silica (15:1 *n*-pentane/EtOAc), yielding the product **15** (0.12 g, 0.16 mmol, 56%) together with several by products. $[\alpha]_D^{20}$ = 16.0°(c 1.00, CH_2Cl_2), ^{1}**H-NMR** (600 MHz, $CDCl_3$) δ: 7.50-7.62 (m, 4H, Ar), 7.21-7.36 (m, 6H, Ar), 4.90 (d, 1H, J = 3.3, CH), 3.71-3.84 (m, 1H, CH), 3.70 (m, 1H, CH), 3.62 (m, 2H, CH_2), 3.55 (m, 1H, CH), 3.45 (t, 1H, J = 9.1, CH), 3.33 (m, 1H, CH), 3.29 (dd, 1H, J = 9.3, 3.3, CH), 0.95 (m, 9H, CH_3), 0.81 (m, 18H, CH_3), 0.70 (s, 9H, CH_3), 0.00 (m, 18H, CH_3),. HRMS (ESI+) m/z: 783.4304 $[M+Na]^+$ for $C_{40}H_{72}O_6NaSi_4$, IR (cm^{-1}): 3395, 3432, 3072, 2955, 2929, 2857, 1472, 1389, 1253, 1112, 1093, 1006, 836, 778, 701, 611, 505.

6.3 Synthesis of sugar fatty acid esters

6.3.1 General esterification procedure

To a pre dried reaction vessel with a magnetic stirring bar was added a regioselectively protected α-D-glucopyranoside, fatty acid, DMAP and anhydrous DCM. The reactants were stirred under a nitrogen atmosphere before being added EDCI. The reaction progressed at the desired temperature until formation of product subsided (18 - 24 hours). The reaction was terminated with the addition of water, and the aqueous phase was extracted with DCM. The organic phase was washed with brine, dried over Na_2SO_4, filtered and evaporated under reduced pressure. The crude residue was purified by silica flash chromatography (30:1 n-pentane/EtOAc) to yield the targeted compound.

For details related to each individual synthesis, see the sections presented herein.

6.3.2 Synthesis of 1-*O*-allyl-2,3-di-*O*-(*tert*-butyldimethylsilyl)-4-*O*-benzyl-6-*O*-elaidate-α-D-glucopyranoside (17)

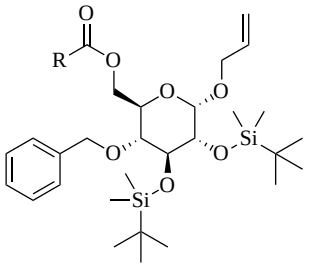

17: R = Elaidate (18:1)

Compound **17** was prepared according to the procedure described in 6.3.1. 1-*O*-allyl-2,3-di-*O*-(*tert*-butyldimethylsilyl)-4-*O*-benzyl-α-D-glucopyranoside (**10**, 150 mg, 0.28 mmol), Elaidic acid (78.6 mg, 0.28 mmol, 1.0 eqv.), DMAP (85.0 mg, 0.70 mmol, 2.5 eqv.) and EDCI (0.22 mL, 1.25 mmol, 4.5 eqv.) was dissolved in DCM (10.2 mL). The reaction progressed at room temperature for 20 hours, and after purification by silica flash chromatography (30:1 n-pentane/EtOAc) yielded the product **17** (90 mg, 0.11 mmol, 39%) together with by product as a faint yellow oil. R_f = 0.60 (20:1 *n*-pentane/EtOAc), t_R (HPLC, method B) = 25 min, $[\alpha]_D^{20}$ = 31.969°(c 1.00, CH_2Cl_2), ^{1}**H-NMR** (600 MHz, $CDCl_3$) δ: 7.26-7.34 (m, 5H, Ar), 5.93 (m, 1H, CH), 5.37 (m, 2H, CH), 5.30 (m, 1H, J = 17.2, 1.6, CH_2), 5.18 (m, 1H, J = 10.4, 1.26, CH_2), 4.88 (d, 1H, J = 11.5, CH_2), 4.77 (dd, 1H, J = 3.3, CH), 4.47 (m, 1H, J = 11.5, CH_2), 4.32 (dd, 1H, J = 12.2, 2.2, CH_2), 4.22 (m, 1H, CH), 4.13 (m, 3H, J = 12.2, 5.1, CH_2), 4.03 (dd, 1H, J = 8.3, 2.7, CH), 4.00 (t, 1H,J = 8.8, CH), 3.95 (dd, 1H, J = 8.4, 6.0, CH), 3.92 (m, 1H,J = 12.8, 6.0, CH), 3.85 (m, 1H, J = 10.0, 2.1, CH), 3.60 (dd, 1H, J = 9.1, 3.3, CH), 3.30 (dd, 1H, J = 9.8, 8.8, CH), 2.32 (td, 2H, J = 15.3, 7.5, 3.8, CH_2), 1.95 (m, 2H, CH_2), 1.61 (m, 2H, CH_2), 1.26 (m, 24H, CH_2), 0.92 (s, 9H, CH_3), 0.91 (s, 9H, CH_3), 0.88 (t, 3H, J = 7.05, CH_3), 0.11 (m, 14H, CH_3). ^{13}**C-NMR** (150 MHz, $CDCl_3$) δ:

173.5 (C_q), 138.0 (C_q-Ar), 133.9 (CH), 130.5 (CH), 130.2 (CH), 128.4 (Ar), 127.6 (Ar), 127.4 (Ar), 117.9 (CH_2), 98.7 (CH), 79.6 (CH), 75.1 (CH_2), 74.3 (CH), 74.1 (CH), 69.1 (CH), 68.6 (CH_2), 67.8 (CH_2), 34.2 (CH_2), 32.5 (CH_2), 32.0 (CH_2), 29.71 (CH_2), 29.67 (CH_2), 29.6 (CH_2), 29.5 (CH_2), 29.3 (CH_2), 29.2 (CH_2), 29.2 (CH_2), 29.1 (CH_2), 29.0 (CH_2), 27.0 (CH_3), 26.8 (CH_3), 26.4(CH_3), 26.2 (CH_3), 25.7 (CH_3), 25.3 (CH_3), 24.9 (CH_2), 22.7 (CH_2), 18.3 (C_q), 18.1 (C_q), 18.0 (C_q), 14.3 (CH_3), -3.0 (CH_3), -3.3 (CH_3), -4.0 (CH_3), -4.3 (CH_3), -5.0 (CH_3), -5.2 (CH_3). HRMS (ESI+) m/z: 825.5497 $[M+Na]^+$ for $C_{46}H_{82}O_7NaSi_2$, IR (cm^{-1}): 2926, 2855, 1741, 1462, 1371, 1252, 1158, 1074, 1021, 835, 776, 697, 671.

6.3.3 Synthesis of 1-*O*-allyl-2,3-di-*O*-(*tert*-butyl-dimethylsilyl)-4-*O*-benzyl-6-*O*-stearate-α-D-glucopyranoside (16)

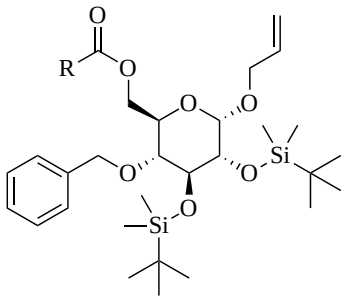

16: R = Stearate (18:0)

Compound **16** was prepared according to the procedure described in 6.3.1. 1-*O*-allyl-2,3-di-*O*-(*tert*-butyl-dimethylsilyl)-4-*O*-benzyl-α-D-glucopyranoside (**10**, 140 mg, 0.26 mmol), Stearic acid (111 mg, 0.39 mmol, 1.5 eqv.), DMAP (79.4 mg, 0.65 mmol, 2.5 eqv.) and EDCI (0.21 mL, 11.7 mmol, 4.5 eqv.) was dissolved in DCM (12.2 mL). The reaction progressed at room temperature for 24 hours, and after purification by silica flash chromatography (30:1 n-pentane/EtOAc) yielded the product **16** (144 mg, 0.17 mmol, 67%) as a clear oil, R_f = 0.63 (15:1 *n*-pentane/EtOAc) t_R (HPLC, method B) = 24 min, $[\alpha]_D^{20}$ = 67.935°(c 1.00, CH_2Cl_2), ^{1}**H-NMR** (600 MHz, $CDCl_3$) δ: 7.27-7.35 (m, 5H, Ar), 5.93 (m, 1H, CH), 5.30 (m, 1H, J = 17.2, 1.5, CH_2), 5.18 (m, 1H, J = 10.4, 1.5, CH_2), 4.88 (d, 1H, J = 11.3 , CH_2), 4.77 (d, 1H, J = 3.5, CH), 4.47 (d, 1H, J = 11.3, CH) 4.32 (dd, 1H, J = 11.9, 2.1, CH_2), 4.14 (m, 2H, J = 4.9, CH_2), 4.00 (t, 1H, J = 8.8, CH), 3.92 (m, 1H, J = 12.8, 6.0, CH_2), 3.85 (m, 1H, J = 14.8, 10.1, 4.8, 2.1, CH), 3.60 (dd, 1H, J = 9.1, 3.5, CH), 3.30 (dd, 1H, J = 9.9, 8.9, CH), 2.32 (td, 2H, J = 15.3, 7.4, 3.6, CH_2), 1.61 (m, 2H, J = 7.1, 6.9, CH_2), 1.26 (m, 30H, CH_2), 0.94 (s, 9H, CH_3), 0.91 (s, 9H, CH_3), 0.94 (t, 3H, J = 7.14, CH_3), 0.12 (s, 3H, CH_3), 0.10 (s, 3H, CH_3), 0.09 (s, 3H, CH_3), 0.05 (s, 3H, CH_3). ^{13}**C-NMR** (150 MHz,

$CDCl_3$) δ: 173.5 (C_q), 138.0 (C_q-Ar), 133.9 (CH), 128.4 (Ar), 127.6 (Ar), 127.4 (Ar), 117.4 (CH_2), 98.7 (CH), 79.6 (CH), 75.0 (CH_2), 74.3 (CH), 74.1 (CH), 69.1 (CH), 68.6 (CH_2), 63.2 (CH_2), 34.2 (CH_2), 31.9 (CH_2), 29.7 (CH_2), 29.7 (CH_2), 29.6 (CH_2), 29.5 (CH_2), 29.4 (CH_2), 29.3 (CH_2), 29.2 (CH_2), 26.4 (CH_3), 26.2 (CH_3), 24.9 (CH_2), 22.7 (CH_2), 18.3 (C_q), 18.0 (C_q), 14.1 (CH_3), -3.0 (CH_3), -3.3 (CH_3), -4.0 (CH_3), -4.3 (CH_3). HRMS (ESI+) m/z: 827.5653 $[M+Na]^+$ for $C_{46}H_{84}O_7NaSi_2$, IR (cm^{-1}): 2925, 2854, 1741, 1463, 1252, 1156, 1108, 1050, 861, 837, 776.

6.3.4 Synthesis of 1-*O*-allyl-2,3-di-*O*-(*tert*-butyldimethylsilyl)-4-*O*-benzyl-6-*O*-α-linolenate-α-D-glucopyranoside (18)

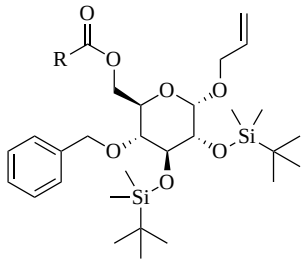

18: R = α–linolenate (18:3)

Compound **18** was prepared according to the procedure described in 6.3.1. 1-*O*-allyl-2,3-di-*O*-(*tert*-butyldimethylsilyl)-4-*O*-benzyl-α-D-glucopyranoside (**10**, 310 mg, 0.56 mmol), α-linolenic acid (0,26 mL, 0.86 mmol, 1.5 eqv.), DMAP (176 mg, 1.44 mmol, 2.5 eqv.) and EDCI (0.46 mL, 2.59 mmol, 4.5 eqv.) was dissolved in DCM (10.5 mL). The reaction progressed at room temperature for 24 hours, and after purification by silica flash chromatography (30:1 n-pentane/EtOAc) yielded the product **18** (223 mg, 0.27 mmol, 48%) as a clear oil, $R_f = 0.64$ (15:1 *n*-pentane/EtOAc) t_R (HPLC, method B) = 25 min, $[\alpha]_D^{20} = 79.9°$(c 1.00, CH_2Cl_2), **^{1}H-NMR** (600 MHz, $CDCl_3$) δ: 7.14-7.27 (m, 5H, Ar), 5.83 (m, 1H, J = 16.3, 10.5, 5.7, CH), 5.25 (m, 7H, CH_2), 5.08 (m, 1H, J = 10.4, 1.4, CH_2), 4.79 (d, 1H, J = 11.3, CH_2), 4.68 (d, 1H, J = 3.4, CH), 4.38 (d, 1H, J = 11.3, CH_2) 4.23 (dd, 1H, J = 11.9, 2.1, CH), 4.05 (m, 2H, J = 5.0, CH_2), 4.91 (t, 1H, J = 8.9, CH), 3.83 (m, 1H, J = 12.8, 6.1, CH_2), 3.76 (m, 1H, J = 14.8, 10.0, 4.8, 2.0, CH), 3.51 (dd, 1H, J = 9.1, 3.4, CH), 3.21 (dd, 1H, J = 9.9, 8.8, CH), 2.71 (m, 2H, CH_2), 2.22 (m, 2H, J = 7.4, 3.8, CH_2), 1.96 (m, 2H, CH_2), 1.51 (m, 2H, CH_2), 1.20 (m, 9H, CH_2), 0.87 (t, 3H, J = 7.62, CH_3), 0.85 (s, 8H, CH_3), 0.82 (s, 10H, CH_3), 0.03 (s, 3H, CH_3), 0.01 (s, 3H, CH_3), 0.00 (s, 3H, CH_3), -0.04 (s, 3H, CH_3). **^{13}C-NMR** (150 MHz, $CDCl_3$) δ: 173.5 (C_q), 138.0 (C_q-Ar), 133.9 (CH), 131.9

(CH), 130.2 (CH), 128.3 (Ar), 128.3 (Ar), 128.2 (CH), 127.7 (CH), 127.6 (CH), 127.4 (Ar), 127.1 (Ar), 117.4 (CH_2), 98.6 (CH), 79.6 (CH), 75.0 (CH_2), 74.2 (CH), 74.1 (CH), 69.1 (CH), 68.5 (CH_2), 63.2 (CH_2), 34.1 (CH_2), 29.2 (CH_2), 29.1 (CH_2), 27.2 (CH_2), 26.4 (CH_3), 26.2 (CH_3), 26.2 (CH_3), 25.5 (CH_2), 24.9 (CH_2), 20.5 (CH_2), 18.3 (C_q), 18.0 (C_q), 14.3 (CH_3), -3.0 (CH_3), -3.3 (CH_3), -4.0 (CH_3), -4.3 (CH_3). HRMS (ESI+) m/z: 821.5184 $[M+Na]^+$ for $C_{46}H_{78}O_7NaSi_2$, IR (cm^{-1}): 3011, 2953, 2928, 2856, 1740, 1472, 1360, 1252, 1156, 1107, 1050, 861, 838, 777, 697.

6.3.5 Synthesis of 1-*O*-allyl-2,3-di-*O*-(*tert*-butyldimethylsilyl)-4-*O*-stearate-6-*O*-benzyl-α-D-glucopyranoside (19)

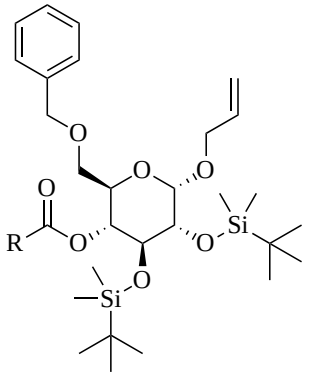

19: R = Stearate (18:0)

Compound **19** was prepared according to the procedure described in 6.3.1. 1-*O*-allyl-2,3-di-*O*-(*tert*-butyldimethylsilyl)-6-*O*-benzyl-α-D-glucopyranoside (**12**, 150 mg, 0.28 mmol), stearic acid (396 mg, 1.39 mmol, 5 eqv.), DMAP (85.0 mg, 0.69 mmol, 2.5 eqv.) and EDCI (0.22 mL, 1.25 mmol, 4.5 eqv.) was dissolved in dichloromethane (11.3 mL). The reaction progressed at room temperature for 24 hours, and after purification by silica flash chromatography (30:1 n-pentane/EtOAc) yielded the product **19** (56 mg, 62 μmol, 22%) as a faint yellow oil together with excess stearic acid. $R_f = 0.55$ (15:1 *n*-pentane/EtOAc), t_R (HPLC, method C) = 26 min, $[\alpha]_D^{20} = 45.958°$(c 1.00, CH_2Cl_2), ^{1}**H-NMR** (400 MHz, $CDCl_3$) δ: 7.22-7.33 (m, 5H, Ar), 5.86 (dddd, 1H, J = 16.9, 10.5, 6.3, 5.5, CH), 5.22 (m, 1H, J = 17.0, 1.5, CH_2), 5.10 (m, 1H, J = 10.2, 1.5, CH_2), 4.73 (d, 1H, J = 3.6, CH), 4.56 (d, 1H, J = 12.3, CH_2), 4.47 (d, 1H, J = 12.3, CH_2), 4.10 (m, 1H, J = 12.9, 5.4, CH_2), 3.89 (m, 1H, J = 12.9, 6.5, CH_2), 3.76 (t, 1H, J = 8.5, CH), 3.69 (m, 1H, CH_2), 3.62 (m, 2H, J = 7.3, 3.6, CH), 3.51 (dd, 1H, J = 8.7, 3.4, CH), 3.39 (m, 1H, J = 8.5, 3.8, CH), 1.54 (m, 4H, CH_2), 1.18 (m, 35H, CH_2), 0.84 (s, 9H, CH_3), 0.83 (s, 9H, CH_3), 0.81 (t, 3H, J = 6.91, CH_3), 0.05 (s, 3H, CH_3), 0.04 (s, 3H, CH_3), 0.01 (s, 3H, CH_3), 0.00 (s, 3H, CH_3). ^{13}**C-NMR** (100 MHz, $CDCl_3$)

δ: 172.9 (C_q), 137.1 (C_q-Ar), 133.0 (CH), 127.4 (Ar), 126.7 (Ar), 116.5 (CH_2), 97.3 (CH), 73.9 (CH), 72.6 (CH), 72.5 (CH_2), 71.4 (CH), 69.3 (CH), 68.6 (CH_2), 67.5 (CH_2), 59.1 (CH_2), 33.4 (CH_2), 30.9 (CH_2), 28.7 (CH_2), 28.6 (CH_2), 28.6 (CH_2), 28.4 (CH_2), 28.3 (CH_2), 28.2 (CH_2), 28.1 (CH_2), 25.1 (CH_3), 25.1 (CH_3), 24.0 (CH_2), 21.7 (CH_2), 17.2 (C_q), 13.2 (CH_3), -4.4 (CH_3), -4.8 (CH_3), -5.2 (CH_3), -5.3 (CH_3). HRMS (ESI+) m/z: 827.5653 $[M+Na]^+$ for $C_{46}H_{84}O_7NaSi_2$, IR (cm^{-1}): 2926, 2855, 1746, 1463, 1362, 1252, 1142, 1107, 1049, 861, 838, 777, 697.

6.3.6 Synthesis of 1-*O*-allyl-2,3-di-*O*-(*tert*-butyldimethylsilyl)-4-*O*-α-linolenate-6-*O*-benzyl-α-D-glucopyranoside (20)

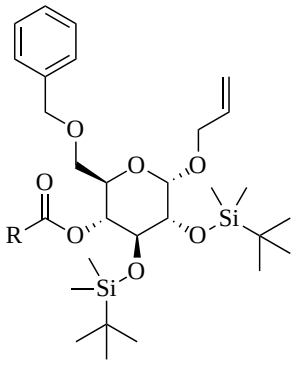

20: R = α-linolenate (18:3)

Compound **20** was prepared according to the procedure described in 6.3.1. 1-*O*-allyl-2,3-di-*O*-(*tert*-butyldimethylsilyl)-6-*O*-benzyl-α-D-glucopyranoside (**12**, 0.95 g, 1.8 mmol), α-linolenic acid (0.80 mL, 2.6 mmol, 1.5 eqv.), DMAP (0.54 g, 4.4 mmol, 2.5 eqv.) and EDCI (1.4 mL, 7.9 mmol, 4.5 eqv.) was dissolved in DCM (45 mL). The reaction progressed at room temperature for 24 hours, and after purification by silica flash chromatography (30:1 n-pentane/EtOAc) yielded the product **20** (0.30 g, 0.36 mmol, 20%) as a faint yellow oil. R_f = 0.57 (15:1 *n*-pentane/EtOAc), t_R (HPLC) = 23.5 min, $[\alpha]_D^{20}$ = 35.965°(c 1.00, CH_2Cl_2), ^{1}**H-NMR** (600 MHz, $CDCl_3$) δ: 7.24-7.37 (m, 5H, Ar), 5.96 (dddd, 1H, J = 16.8, 10.4, 6.3, 5.5, CH), 5.36 (m, 6H, CH), 5.30 (m, 1H, J = 1.7, CH_2), 5.19 (m, 1H, J = 10.4, 1.7, CH_2), 4.86 (dd, 1H, J = 10.2, 8.8, CH), 4.83 (d, 1H, J = 3.5, CH) 4.53 (d, 1H, J = 11.9, CH_2), 4.47 (d, 1H, J = 11.9, CH_2), 4.20 (ddt, 1H, J = 12.9, 5.4, 1.4, CH_2), 3.98 (m, 2H, J = 8.9, 5.3, 1.4, CH + CH_2), 3.84 (dt, 1H, J = 10.3, 4.4, CH), 3.66 (dd, 1H, J = 8.9, 3.3, CH), 3.43 (m, 2H, CH_2), 2.81 (m, 4H, CH_2), 2.25 (m, 1H, J = 6.6, 2.3, CH_2), 2.14 (m, 1H, J = 6.7, 2.3, CH_2), 2.06 (m, 4H, CH_2), 1.50 (m, 2H, CH_2), 1.29 (m, 11H, CH_2), 0.98 (t, 3H, J = 7.5, CH_3), 0.91 (s, 9H, CH_3), 0.83 (s, 9H, CH_3), 0.08 (m, 9H, CH_3), 0.04 (s, 3H, CH_3). ^{13}**C-NMR** (150

MHz, $CDCl_3$) δ: 172.6 (C_q), 137.9 (C_q-Ar), 134.0 (CH), 131.9 (CH), 130.2 (CH), 128.3 (CH), 128.3 (CH), 128.2 (CH), 127.8 (Ar), 127.8 (Ar), 127.6 (Ar), 127.1 (CH), 117.8 (CH_2), 98.3 (CH), 74.1 (CH), 73.5 (CH_2), 72.2 (CH), 72.0 (CH), 69.7 (CH_2), 67.0 (CH), 68. 6(CH_2), 34.6 (CH_2), 29.6 (CH_2), 29.2 (CH_2), 29.2 (CH_2), 29.1 (CH_2), 27.2 (CH_2), 26.2 (CH_3), 25.9 (CH_3), 25.6 (CH_2), 25.5 (CH_2), 24.7 (CH_2), 20.6 (CH_2), 18.3 (C_q), 17.9 (C_q), 14.4 (CH_3), -3.0 (CH_3), -3.5 (CH_3), -4.3 (CH_3), -4.4 (CH_3). HRMS (ESI+) m/z: 821.5184 $[M+Na]^+$ for $C_{46}H_{78}O_7NaSi_2$, IR (cm^{-1}): 2926, 2855, 1746, 1462, 1377, 1362, 1251, 1156, 1141, 1106, 1048, 861, 838, 777, 732, 697.

6.3.7 General procedure for the deprotection of silylated compounds

To a solution of silylated α-D-glucopyranoside in anhydrous THF and under an atmosphere of nitrogen was added a 1M solution of TBAF in THF. The reaction was stirred at room temperature for 12-24 hours before being terminated by the addition of water. The aqueous phase was extracted with EtOAc and the resulting organic phase was washed with brine, before being dried over $MgSO_4$, filtered and evaporated under reduced pressure. The crude product was purified using preperative HPLC (see section 6.1.1.2) to yield the pure sugar fatty acid ester.

For details related to each individual synthesis, see the sections herein.

6.3.8 Synthesis of 1-*O*-allyl-4-*O*-benzyl-6-*O*-elaidate-α-D-glucopyranoside (22)

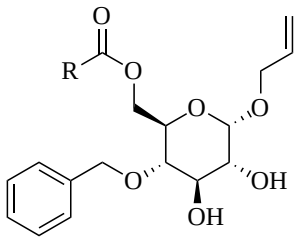

22: R = Elaidate (18:1)

Compound **22** was prepared according to the procedure described in 6.3.7. 1-*O*-allyl-2,3-di-*O*-(*tert*-butyldimethylsilyl)-4-*O*-benzyl-6-*O*-elaidate-α-D-glucopyranoside (**17**, 90 mg, 0.11 mmol) dissolved in THF (2 mL) was added 1M TBAF in THF (0.34 mL, 0.34 mmol, 3 eqv.). The reaction progressed at room temperature for 24 hours, and after purification by preperative HPLC yielded the product **22** (48 mg, 80 *mu*mol, 73%) as a faint yellow oil, $R_f = 0.40$ (10:1 *n*-pentane/EtOAc), t_R (HPLC,

method B) = 7.3 min, $[\alpha]_D^{20} = 36.0°$(c 1.00, CH_2Cl_2), ^{1}**H-NMR** (600 MHz, $CDCl_3$) δ: 7.30-7.34 (m, 5H, Ar), 5.89 (dddd, 1H, J = 17.1, 10.4, 6.2, 5.4, CH), 5.37 (m, 2H, CH), 5.28 (m, 1H, J = 17.1, 1.5, CH_2), 5.21 (m, 1H, J = 10.4, 1.5, CH_2), 4.92 (d, 1H, J = 3.9, CH) 4.87 (d, 1H, J = 11.0, CH_2), 4.65 (d, 1H, J = 11.0, CH_2), 4.34 (dd, 1H, J = 12.0, 2.3, CH_2), 4.29 (dd, 1H, J = 12.0, 4.7, CH_2), 4.20 (ddt, 1H, J = 12.4, 5.2, 1.4, CH_2), 4.02 (ddt, 1H, J = 12.8, 6.3, 1.2, CH_2), 3.90 (t, 1H, J = 9.2, CH), 3.85 (ddd, 1H, J = 6.9, 4.7, 2.2, CH), 3.52 (dd, 1H, J = 9.3, 3.9, CH), 3.42 (dd, 1H, J = 9.9, 8.9, CH). 2.31 (td, 2H, J = 15.3, 7.3, 3.8, CH_2), 1.95 (m, 4H, CH_2), 1.74 (m, 1H, OH), 1.62 (m, 2H, CH_2), 1.26 (m, 20H, CH_2), 0.88 (t, 3H, J = 6.99, CH_3). ^{13}**C-NMR** (150 MHz, $CDCl_3$) δ: 173.5 (C_q), 137.9 (C_q-Ar), 133.3 (CH), 130.5 (CH), 130.2 (CH), 128.6 (Ar), 128.1 (Ar), 128.0 (Ar), 118.1 (CH_2), 97.1 (CH), 77.0 (CH), 75.6 (CH), 74.7 (CH_2), 72.6 (CH), 69.0 (CH), 68.7 (CH_2), 62.8 (CH_2), 34.2 (CH_2), 32.6 (CH_2), 31.9 (CH_2), 29.7 (CH_2), 29.6 (CH_2), 29.6 (CH_2), 29.5 (CH_2), 29.3 (CH_2), 29.2 (CH_2), 29.2 (CH_2), 29.1 (CH_2), 28.0 (CH_2), 24.9 (CH_2), 22.7 (CH_2), 14.1 (CH_2). HRMS (ESI+) m/z: 597.3767 $[M+Na]^+$ for $C_{34}H_{54}O_7Na$, IR (cm^{-1}): 3398, 2922, 2852, 1738, 1649, 1454, 1356, 1240, 1146, 1042, 966, 927, 735, 679.

6.3.9 Synthesis of 1-*O*-allyl-4-*O*-benzyl-6-*O*-stearate-α-D-glucopyranoside (21)

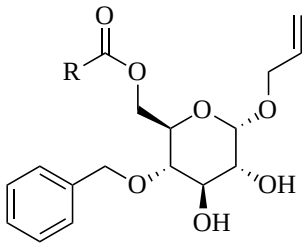

21: R = Stearate (18:0)

Compound **21** was prepared according to the procedure described in 6.3.7. 1-*O*-allyl-2,3-di-*O*-(*tert*-butyldimethylsilyl)-4-*O*-benzyl-6-*O*-stearate-α-D-glucopyranoside (**16**, 100 mg, 0.12 mmol) dissolved in THF (1.7 mL) was added 1M TBAF in THF (0.37 mL, 0.37 mmol, 3 eqv.). The reaction progressed at room temperature for 24 hours, and after purification by preperative HPLC yielded the product **21** (43 mg, 72 μmol, 60%) as a clear oil. $R_f = 0.48$ (12:1 *n*-pentane/EtOAc), t_R (HPLC, method C) = 11 min, $[\alpha]_D^{20} = 52.0°$(c 1.00, CH_2Cl_2), ^{1}**H-NMR** (600 MHz, $CDCl_3$) δ: 7.25-7.37 (m, 5H, Ar), 5.90 (m, 1H, J = 16.7, 10.4, 6.1, 5.4, CH), 5.37 (m, 2H, CH), 5.29 (m, 1H, J = 17.2, 1.1, CH_2), 5.18 (m, 1H, J = 10.4, CH_2), 4.95 (d, 1H, J = 11.2, CH) 4.90 (d, 1H, J = 3.8, CH_2), 4.65 (d, 1H, J = 11.2, CH_2), 4.32 (dd, 1H, J = 12.1, 2.3, CH_2), 4.27 (dd, 1H, J = 12.0, 4.8, CH_2), 4.18 (m, 1H, J = 12.9, 5.2, CH_2), 4.02 (m, 1H, J = 12.9, 6.2, CH_2), 3.97 (td, 1H, J = 9.33, 2.22, CH), 3.85 (ddd, 1H, J = 6.99, 4.83, 2.13, CH), 3.62 (m, 2H, CH_2), 3.42 (t, 1H, J = 9.5, CH). 3.33 (m, 6H, CH_2), 2.30 (td, 2H,J = 15.4, 7.6, 3.6, CH_2), 1.64 (m, 6H, CH_2), 1.45 (sext, 5H, J = 14.8, 7.4, CH_2), 1.25 (m, 25H, CH_2), 0.88 (t, 3H, J = 6.8, CH_3). ^{13}**C-NMR** (150 MHz, $CDCl_3$) δ: 173.6 (C_q), 138.4 (C_q-Ar), 133.8 (CH), 128.4 (Ar), 128.1 (Ar), 127.8 (Ar), 117.6 (CH_2), 97.5 (CH), 77.4 (CH), 75.3 (CH), 74.6 (CH_2), 72.6 (CH), 68.9 (CH), 68.5 (CH_2), 63.1 (CH_2), 59.0 (CH_2), 34.2 (CH_2), 31.9 (CH_2), 29.7 (CH_2), 29.7 (CH_2), 29.6 (CH_2),

29.5 (CH_2), 29.4 (CH_2), 29.3 (CH_2), 29.2 (CH_2), 24.9 (CH_2), 24.2 (CH_2), 22.7 (CH_2), 19.8 (CH_2), 13.7. HRMS (ESI+) m/z: 599.3924 $[M+Na]^+$ for $C_{34}H_{56}O_7Na$, IR (cm^{-1}): 3288, 2958, 2923, 2853, 1738, 1456, 1380, 1147, 1093, 1041, 1029, 926, 885, 738, 698.

6.3.10 Synthesis of 1-*O*-allyl-4-*O*-stearate-6-*O*-benzyl-α-D-glucopyranoside (24)

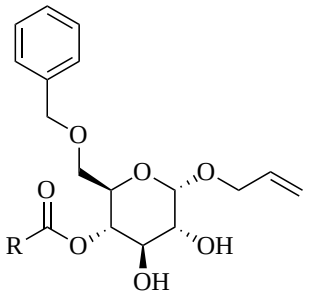

24: R = Stearate (18:0)

Compound **24** was prepared according to the procedure described in 6.3.7. 1-*O*-allyl-2,3-di-*O*-(*tert*-butyldimethylsilyl)-4-*O*-stearate-6-*O*-benzyl-α-D-glucopyranoside (**19**, 112 mg, 0.14 mmol) dissolved in THF (2.1 mL) was added 1M TBAF in THF (0.42 mL, 0.42 mmol, 3 eqv.). The reaction progressed at room temperature for 24 hours, and after purification by preperative HPLC yielded the product **24** (8.4 mg, 14μmol, 10%) as a clear oil, R_f = 0.39 (9:1 *n*-pentane/EtOAc), t_R (HPLC, method C) = 10 min, $[\alpha]_D^{20} = 28.0°$(c 1.00, CH_2Cl_2).

2-*O*-esterified analogue:

^{1}**H-NMR** (600 MHz, $CDCl_3$) δ: 7.15-7.25 (m, 5H, Ar), 5.74 (dddd, 1H, J = 17.2, 10.5, 5.9, 5.2, CH), 5.16 (m, 1H, J = 17.2, 1.6, CH_2), 5.06 (m, 1H, J = 10.5, 1.6, CH_2), 4.94 (d, 1H, J = 3.7, CH), 4.57 (dd, 1H, J = 10.0, 3.7, CH), 4.51 (d, 1H, J = 12.1, CH_2) 4.44 (d, 1H, J = 12.1, CH_2), 4.04 (ddt, 1H, J = 13.1, 5.2, 1.5, CH_2), 3.87 (m, 2H, J = 13.1, 9.8, 6.0, 3.0, 1.5, CH/CH_2), 3.68 (dt, 1H, J = 9.7, 4.4, CH), 3.64 (dd, 1H, J = 10.2, 4.4, CH_2), 3.58 (dd, 1H, J = 10.2, 4.4, CH_2), 3.54 (td, 1H, J = 9.4, 2.2, CH), 2.60 (d, 1H, J = 2.2, OH), 2.25 (t, 2H, J = 7.5, CH_2), 2.23 (d, 1H, J = 3.5, OH), 1.51 (quint, 2H, J = 14.7, 4.4, CH_2), 1.13 (m, 28H, CH_2), 0.75 (t, 3H, J = 7.1,

CH_3). ^{13}**C-NMR** (150 MHz, $CDCl_3$) δ: 173.8 (C_q), 137.8 (C_q), 133.5 (CH), 128.5 (Ar), 129.9 (Ar), 127.7 (Ar), 117.6 (CH_2), 95.2 (CH), 73.7 (CH_2), 73.2 (CH), 72.3 (CH), 71.7 (CH), 69.9 (CH_2), 69.5 (CH), 68.4 (CH_2), 34.2 (CH_2), 31.9 (CH_2), 29.7 (CH_2), 29.7 (CH_2), 29.7 (CH_2), 25.0 (CH_2), 22.7 (CH_2), 14.1 (CH_3). HRMS (ESI+) m/z: 599.3924 $[M+Na]^+$ for $C_{34}H_{56}O_7Na$, IR (cm^{-1}): 3421, 2923, 2853, 1738, 1650, 1594, 1455, 1376, 1215, 1154, 1099, 1051, 926, 861, 767, 733, 697.

4-*O*-esterified analogue:

^{1}**H-NMR** (600 MHz, $CDCl_3$) δ: 7.14-7.26 (m, 5H, Ar), 5.81 (dddd, 1H, J = 17.2, 10.4, 6.2, 5.4, CH), 5.19 (m, 1H, J = 17.2, 1.5, CH_2), 5.10 (m, 1H, J = 10.4, 1.5, CH_2), 4.86 (d, 1H, J = 3.9, CH), 4.83 (t, 1H, J = 9.7, CH), 4.45 (d, 1H, J = 12.1, CH_2) 4.37 (d, 1H, J = 12.1, CH_2), 4.12 (ddt, 1H, J = 12.8, 5.3, 1.4, CH_2), 3.94 (ddt, 1H, J = 12.8, 6.3, 1.3, CH_2), 3.78 (m, 1H, CH), 3.71 (t(b)), 1H, J = 9.4, CH_2), 3.50 (m, 1H, CH), 3.40 (m, 2H, CH), 2.40 (s, 1H, OH), 2.10 (m, 2H, CH_2), 1.99 (d, 1H, J = 8.9, OH), 1.42 (m, 4H, CH_2), 1.13 (m, 28H, CH_2), 0.76 (t, 3H, J = 7.0, CH_3).

3-*O*-esterified analogue:

^{1}**H-NMR** (600 MHz, $CDCl_3$) δ: 7.27-7.36 (m, 5H, Ar), 5.91 (m, 1H, J = 17.1, 10.4, 6.0, 5.5, CH), 5.31 (m, 1H, J = 17.1, 1.5, CH_2), 5.22 (m, 1H, J = 10.4, 1.5, CH_2), 5.09 (t, 1H, J = 9.5, CH), 4.94 (d, 1H, J = 3.8, CH), 4.62 (d, 1H, J = 12.1, CH_2) 4.57 (d, 1H, J = 12.1, CH_2), 4.24 (m, 1H, J = 12.8, 5.4, CH_2), 4.04 (m, 1H, J = 12.8, 6.3, CH_2), 3.80 (m, 1H, CH), 3.76 (dd, 1H, J = 10.4, 4.4, CH_2), 3.70 (m, 2H, CH), 3.63 (td, 1H,J = 13.4, 10.1, 3.8, CH), 2.62 (d, 1H,J = 4.1, OH), 2.41 (td, 2H,J = 15.5, 7.5, 1.3, CH_2), 1.65 (m, 3H, CH_2), 1.25 (m, 30H, CH_2), 0.88 (t, 3H,J = 7.0, CH_3).

6.3.11 Synthesis of 1-*O*-allyl-4-*O*-α-linolenate-6-*O*-benzyl-α-D-glucopyranoside (25)

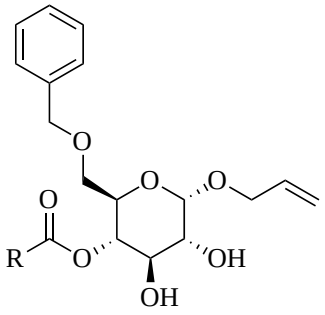

25: R = α-linolenate (18:3)

Compound **25** was prepared according to the procedure described in 6.3.7. 1-*O*-allyl-2,3-di-*O*-(*tert*-butyldimethylsilyl)-4-*O*-α-linolenate-6-*O*-benzyl-α-D-glucopyranoside (**20**, 500 mg, 0.63 mmol) dissolved in THF (8 mL) was added 1M TBAF in THF (1.56 mL, 1.56 mmol). The reaction progressed at room temperature for 24 hours, and after purification by preperative HPLC yielded the product **25** (128 mg, 0.21 mmol, 34%) as a clear oil. R_f = 0.43 (10:1 *n*-pentane/EtOAc), t_R (HPLC, method C) = 9 min, $[\alpha]_D^{20}$ = 63.9°(c 1.00, CH_2Cl_2), **^{1}H-NMR** (600 MHz, $CDCl_3$) δ: 7.25-7.35 (m, 5H, Ar), 5.93 (dddd, 1H, J = 16.8, 10.4, 6.2, 5.4, CH), 5.35 (m, 6H, CH), 5.31 (m, 1H, CH_2), 5.22 (m, 1H, J = 10.4, 1.5, CH_2), 4.98 (d, 1H, J = 3.9, CH), 4.94 ((t(b)), 1H, J = 9.7, CH), 4.57 (d, 1H, J = 12.1, CH_2), 4.50 (m, XH, J = 12.1, CH_2), 4.24 (ddt, 1H, J = 12.8, 5.3, 1.5, CH_2), 4.06 (ddt, 1H, J = 12.8, 6.3, 1.3, CH_2), 3.90 (m, 1H, CH), 3.85 (t, 1H,J = 9.4, CH), 3.62 (dd, 1H, J = 9.4, 3.9, CH), 3.52 (m, 2H, CH_2), 2.81 (m, 4H, CH_2), 2.23 (m, 2H, CH_2), 2.06 (m, 4H, CH_2), 1.55 (m, 2H, CH_2), 1.28 (m, 10H, CH_2), 0.97 (t, 3H, J = 7.5, CH_3). **^{13}C-NMR** (150 MHz, $CDCl_3$) δ: 173.6 (C_q), 137.8 (C_q), 133.5 (CH), 132.0 (CH), 130.2 (CH), 128.3 (CH), 128.3 (CH), 128.2 (CH), 127.8 (Ar), 127.8 (Ar), 127.7 (Ar), 127.1 (CH), 118.0 (CH_2), 97.2 (CH), 73.5 (CH_2), 73.1 (CH), 72.8 (CH), 71.0 (CH), 69.1 (CH), 68.7 (CH_2), 68.6 (CH_2), 34.2

(CH_2), 29.6 (CH_2), 29.2 (CH_2), 29.1 (CH_2), 29.1 (CH_2), 27.2 (CH_2), 25.6 (CH_2), 25.5 (CH_2), 24.8 (CH_2), 20.5 (CH_2), 14.3 (CH_3). HRMS (ESI+) m/z: 593.3452 $[M+Na]^+$ for $C_{34}H_{50}O_7Na$, IR (cm^{-1}): 3406, 3010, 2927, 2855, 1739, 1454, 1363, 1244, 1155, 1084, 1040, 927, 734, 676.

6.4 General procedure for biological assesment

Biological evaluation was conducted on F98 glioma rat cancer cell lines. An unknown amount of cells were counted, using a hemocytometer, before being centrifuged, dispersed in replenished growth medium and transferred to a new container. Cells are assumed to grow exponentially according to equation 6.2

$$N(t) = R^t N_0 \tag{6.2}$$

Where N_0 is the counted number of cells after splitting, R = 2 and t is the number of days cells are left to grow. After 3 days, the cells were split evenly into dishes, and applied a varying concentration of compound. Three parallel runs were conducted, to establish a standard deviation between the samples. After 2 days of treatment, the dishes were applied MTT (Stock solution, C = 5 g/L), and resulting crystals of formazan were removed and dissolved in *i-Pr*-OH. After the formazan crystals were completely dissolved, the solution was transferred to cuvettes and analysed using a spectrophotometer. Absorbance and compound concentration was averaged compared to control dishes, and average cell viability (%) were plotted against compound concentration (μM).

Bibliography

(1) Hanashima, S.; Mizushina, Y.; Yamazaki, T.; Ohta, K.; Takahashi, S.; Sahara, H.; Sakaguchi, K.; Sugawara, F. *Bioorg. Med. Chem.* **2001**, *9*, 367–376.

(2) Bukhari, S. M.; Feuerherm, A. J.; Boulfrad, F.; Zlatkovic, B.; Johansen, B.; Simic, N. *J. Serb. Chem. Soc.* **2014**, *79*, 779–791.

(3) Bukhari, S. M.; Feuerherm, A. J.; Tunset, H. M.; Isaksen, S. M.; Saether, M.; Thvedt, T. H. K.; Gonzalez, S. V.; Schmid, R.; Brunsvik, A.; Fuglseth, E.; Zlatkovic, B.; Johansen, B.; Simic, N. *J. Serb. Chem. Soc.* **2016**, *81*, 1–12.

(4) El Khadem, H., *Carbohydrate chemistry: monosaccharides and their oligomers*; Academic Press: 2012, p 266.

(5) Namdari, S.; Goel, D. P.; Romanowski, J.; Glaser, D.; Warner, J. J. *J. Shoulder. Elbow. Surg.* **2011**, *20*, 1016–1024.

(6) Pigman, W. W.; Goepp, R. M., *Chemistry of the carbohydrates*; Academic Press: 1948.

(7) Samuelsson, G., *Drugs of natural origin : a textbook of pharmacognosy*; Apotekarsocieteten: 1999, p 551.

(8) Andreas Sigismund Marggraf *Histoire de l'académie royale des sciences et belles-lettres de Berlin* **1747**, *3*, 79–90.

(9) Hudson, C. S. *J. Chem. Educ.* **2009**, *18*, 353.
(10) C.Ooi, V.; Liu, F. *Curr. Med. Chem.* **2000**, *7*, 715–729.
(11) Lichtenthaler, F. W. *ACS Symp. Ser. Am. Chem. Soc.* **2003**, *841*, 47–83.
(12) Hanessian, S.; Roy, R. *J. Am. Chem. Soc.* **1979**, *101*, 5839–5841.
(13) Sugiyama, H.; Usui, T. *Agric. Biol. Chem.* **1980**, *44*, 3001–3002.
(14) Shendurse, A.; Khedkar, C., *The Encyclopedia of Food and Health: Glucose: Properties and analysis*; Oxford: Academic Press: 2016, pp 239–247.
(15) Wolfe, S.; Rauk, A.; Tel, L. M. *J. Chem. SOC.* **1971**, 136–145.
(16) Kamerling, J. P. In *Comprehensive Glycoscience: From Chemistry to Systems Biology*; Elsevier: 2007; Vol. 1-4, pp 1–38.
(17) Juaristi, E.; Cuevas, G., *The anomeric effect*; CRC Press: Boca Raton, 1995.
(18) Suzuki, A. *J. Organomet. Chem.* **1999**, *576*, 147–168.
(19) Gais, H. J.; D, K., *Enzyme Catalysis in Organic Synthesis*; Wiley-VCH: 1995, pp 165–261.
(20) Smith, M. B., *Organic Synthesis: Protecting Groups*, 2010, pp 587–622.
(21) Holton, R. A. et al. *J. Am. Chem. Soc.* **1994**, *116*, 1599–1600.
(22) Masters, J. J.; Link, J. T.; Snyder, L. B.; Young, W. B.; Danishefsky, S. J. *Angew. Chem., Int. Ed. Engl.* **1995**, *34*, 1723–1726.
(23) D'Onofrio, J.; Coppola, C.; Fabio, G. D.; De Napoli, L.; Montesarchio, D. *Eur. J. Org. Chem.* **2007**, *2007*, 3849–3858.
(24) Tanaka, H.; Kawai, K.; Fujiwara, K.; Murai, A. *Tetrahedron* **2002**, *58*, 10017–10031.

(25) Wuts, P. G. M.; Greene, T. W.; Greene, T. W., *Greene's protective groups in organic synthesis.* Wiley-Interscience: 2007.

(26) Codée, J. D. C.; Ali, A.; Overkleeft, H. S.; van der Marel, G. A. *Comptes Rendus Chimie* **2011**, *14*, 178–193.

(27) Jones, G. B.; Hynd, G.; Wright, J. M.; Sharma, A. *J. Org. Chem.* **2000**, *65*, 263–265.

(28) Sach, N. W.; Richter, D. T.; Cripps, S.; Tran-Dubé, M.; Zhu, H.; Huang, B.; Cui, J.; Sutton, S. C. *Org. Lett.* **2012**, *14*, 3886–3889.

(29) Jia, H.; Li, Q.; Bayaguud, A.; She, S.; Huang, Y.; Chen, K.; Wei, Y. *Scientific Reports* **2017**, *7*, DOI: 10.1038/s41598-017-12633-8.

(30) Kice, J. L.; Bowers, K. W. *J. Am. Chem. Soc.* **1962**, *84*, 605–610.

(31) Carey, F. A.; Sundberg, R. J., *Advanced Organic Chemistry: Part A: Structure and Mechanisms*; Advanced Organic Chemistry; Springer US: 2007.

(32) Ollis, W. D., *Advanced Organic Chemistry*; 4601; Springer US: Boston, MA, 1958; Vol. 181, pp 6–7.

(33) Sartori, G.; Ballini, R.; Bigi, F.; Bosica, G.; Maggi, R.; Righi, P. *Chem. Rev.* **2004**, *104*, 199–250.

(34) Haynes, W. M., *CRC Handbook of Chemistry and Physics*, 95th ed.; CRC Press: 2014.

(35) Zhang, W.; Robins, M. J. *Tetrahedron Lett.* **1992**, *33*, 1177–1180.

(36) Nelson, T. D.; Crouch, R. D. *Synthesis* **1996**, *1996*, 1031–1069.

(37) Gleispach, H. *J. Chromatogr.* **1974**, *91*, 407–412.

(38) Uhlig, W. *Chemische Berichte* **1996**, *129*, 733–739.

(39) Dhakal, B.; Bohé, L.; Crich, D. *J. Org. Chem* **2017**, *82*, 9263–9269.

(40) Patschinski, P.; Zhang, C.; Zipse, H. *J. Org. Chem.* **2014**, *79*, 8348–8357.

(41) Oguri, H.; Hishiyama, S.; Oishi, T.; Hirama, M. *Synlett* **1995**, *1995*, 1252–1254.

(42) Stick, R. V.; Williams, S. J. In *Carbohydrates: The Essential Molecules of Life (Second Edition)*, Stick, R. V., Williams, S. J., Eds., Second Edi; Elsevier: Oxford, 2009, pp 35–74.

(43) Williamson, A. *Lond. Edinb. Dubl. Phil .Mag.* **1850**, *37*, 350–356.

(44) Lu, W.; Navidpour, L.; Taylor, S. D. *Carbohydr. Res.* **2005**, *340*, 1213–1217.

(45) Alzeer, J.; Vasella, A. *Helv. Chim. Acta* **1995**, *78*, 177–193.

(46) Llàcer, E.; Romea, P.; Urpí, F. *Tetrahedron Lett.* **2006**, *47*, 5815–5818.

(47) Ohno, S.; Wilde, M.; Mukai, K.; Yoshinobu, J.; Fukutani, K. *J. Phys. Chem. C* **2016**, *120*, 11481–11489.

(48) Martin, M. G.; Ganem, B. *Tetrahedron Lett.* **1984**, *25*, 251–254.

(49) Vermeulen, N. A.; Delcamp, J. H.; White, M. C. *J. Am. Chem. Soc.* **2010**, *132*, 11323–11328.

(50) Fischer, E. *Berichte der deutschen chemischen Gesellschaft* **1895**, *28*, 1145–1167.

(51) Izumi, M.; Fukase, K.; Kusumoto, S. *Biosci. Biotechnol. Biochem.* **2002**, *66*, 211–214.

(52) Bishop, C. T.; Cooper, F. P. *Can. J. Chem.* **1962**, *40*, 224–232.

(53) Gigg (nèe Cunningham), J.; Gigg, R. *J. Chem. Soc. C* **1966**, 82–86.

(54) Vutukuri, D.; Bharathi Rao Pandi Rajasekaran, Z. Y.; Karthik; Tran, M.-H.; Thayumanavan, S. *J. Org. Chem* **2003**, *68*, 1146–1149.

(55) Corey, E. J.; Suggs, J. W. *J. Org. Chem.* **1973**, *38*, 3224.
(56) Guibé, F. *Tetrahedron* **1998**, *54*, 2967–3042.
(57) Boss, R.; Scheffold, R. *Angew. Chem., Int. Ed. Engl.* **1976**, *15*, 558–559.
(58) Demchenko, A. V.; Pornsuriyasak, P.; De Meo, C. *J. Chem. Educ.* **2006**, *83*, 782.
(59) Boltje, T. J.; Li, C.; Boons, G.-J. *Org. Lett.* **2010**, *12*, 4636–4639.
(60) Johnsson, R.; Ohlin, M.; Ellervik, U. *J. Org. Chem.* **2010**, *75*, 8003–8011.
(61) Guo, J.; Ye, X.-S. *Molecules* **2010**, *15*, DOI: 10 . 3390 / molecules15107235.
(62) Cordes, E. H.; Bull, H. G. *Chem. Rev.* **1974**, *74*, 581–603.
(63) Tanaka, N.; Ogawa, I.; Yoshigase, S.; Nokami, J. *Carbohydr. Res.* **2008**, *343*, 2675–2679.
(64) Lipták, A.; Jodál, I.; Nánási, P. *Carbohydr. Res.* **1975**, *44*, 1–11.
(65) Debenham, S. D.; Toone, E. J. *Tetrahedron: Asymmetry* **2000**, *11*, 385–387.
(66) DeNinno, M. P.; Etienne, J. B.; Duplantier, K. C. *Tetrahedron Lett.* **1995**, *36*, 669–672.
(67) Solomons, T. W. G.; Fryhle, C.; Snyder, S., *Organic Chemistry, 11th Edition*; Organic Chemistry; Wiley: 2012.
(68) Siggel, M. R. F.; Streitwieser, A.; Thomas, T. D. *J. Am. Chem. Soc.* **1988**, *110*, 8022–8028.
(69) Davidson, E. R.; Feller, D. *Chem. Rev.* **1986**, *86*, 681–696.
(70) Bender, M. L. *Chem. Rev.* **1960**, *60*, 53–113.
(71) Dub, P. A.; Ikariya, T. *ACS Catal.* **2012**, *2*, 1718–1741.
(72) Reid, E. E. *Ind. Eng. Chem.* **1937**, *29*, 1344–1350.

(73) Stefanidis, D.; Jencks, W. P. *J. Am. Chem. Soc.* **1993**, *115*, 6045–6050.

(74) Ono, N.; Yamada, T.; Saito, T.; Tanaka, K.; Kaji, A. *Bull. Chem. Soc. Jpn.* **1978**, *51*, 2401–2404.

(75) Fischer, E.; Speier, A. *Berichte der deutschen chemischen Gesellschaft* **1895**, *28*, 3252–3258.

(76) Wade, P. A.; Rutkowsky, S. A.; King, D. B. *J. Chem. Educ.* **2006**, *83*, 927.

(77) Liu, Y.; Lotero, E.; Goodwin, J. G. *J. Mol. Catal. A: Chem.* **2006**, *245*, 132–140.

(78) Otera, J. *Org. Process Res. Dev.* **2004**, *8*, 814–814.

(79) Neises, B.; Steglich, W. *Angew. Chem., Int. Ed. Engl.* **1978**, *17*, 522–524.

(80) Mitachi, K.; Kurosu, Y. E.; Hazlett, B. T.; Kurosu, M. *J. Pept. Sci* **2016**, *22*, 186–191.

(81) Lutjen, A. B.; Quirk, M. A.; Barbera, A. M.; Kolonko, E. M. *Bioorg. Med. Chem.* **2018**, *26*, 5291–5298.

(82) Raveendran, S.; Parameswaran, B.; Ummalyma, S. B.; Abraham, A.; Mathew, A. K.; Madhavan, A.; Rebello, S.; Pandey, A. *Food Technol. Biotechnol.* **2018**, *56*, 16–30.

(83) Passicos, E.; Santarelli, X.; Coulon, D. *Biotechnol. Lett.* **2004**, *26*, 1073–1076.

(84) Raza, S.; Fransson, L.; Hult, K. *Protein Sci.* **2001**, *10*, 329–338.

(85) Sutili, F. K.; Ruela, H. S.; Nogueira, D. D. O.; Leal, I. C. R.; Miranda, L. S. M.; De Souza, R. O. M. A. *Sustainable Chem. Processes* **2015**, *3*, 6.

(86) Nahmany, M.; Melman, A. *Org. Biomol. Chem.* **2004**, *2*, 1563–1572.

(87) Estell, D. A.; Graycar, T. P.; Miller, J. V.; Powers, D. B.; Wells, J. A.; Burnier, J. P.; Ng, P. G. *Science* **1986**, *233*, 659–663.

(88) Otera, J. *Chem. Rev.* **1993**, *93*, 1449–1470.

(89) Schuchardt, U.; Sercheli, R.; Vargas, R. M. *J. Braz. Chem. Soc.* **1998**, *9*, 199–210.

(90) Zheng, Y.; Zheng, M.; Ma, Z.; Xin, B.; Guo, R.; Xu, X. In *Polar Lipids: Biology, Chemistry, and Technology*; Elsevier: 2015; Vol. 5, pp 215–243.

(91) Pérez, B.; Anankanbil, S.; Guo, Z., *Fatty Acids: Synthesis of Sugar Fatty Acid Esters and Their Industrial Utilizations*; Elsevier BV: 2017, pp 329–354.

(92) Hill, K.; Ach, C. In *Sugar-Based Surfactants: Fundamentals and Applications*; 1; Wiley-Blackwell: 2008; Vol. 101, pp 1–20.

(93) Ferrer, M.; Perez, G.; Plou, F. J.; Castell, J. V.; Ballesteros, A. *Biotechnol. Appl. Biochem.* **2005**, *42*, 35.

(94) Davies, P.; Bailey, P. J.; Goldenberg, M. M.; Ford-Hutchinson, A. W. *Annu. Rev. Immunol.* **1984**, *2*, 335–357.

(95) Soberman, R. J.; Christmas, P. *J. Clin. Investig.* **2003**, *111*, 1107–1113.

(96) De Caterina, R.; Basta, G. *Eur. Hear. J.* **2001**, *3*, 42–49.

(97) Herskowitz, A.; Mangano, D. T. *Anesthesiology* **1996**, *85*, 957–960.

(98) Coussens, L. M.; Werb, Z. *Nature* **2002**, *420*, 860–867.

(99) Parascandol, J. *Trends Pharmacol. Sci.* **1980**, *1*, 417–419.

(100) Hughes, J. P.; Rees, S.; Kalindjian, S. B.; Philpott, K. L. *Br. J. Pharmacol.* **2011**, *162*, 1239–1249.

(101) Calder, P. C. *Br. J. Clin. Pharmacol.* **2013**, *75*, 645–662.

(102) Ren, J.; Chung, S. H. *J. Agric. Food Chem.* **2007**, *55*, 5073–5080.

(103) Tang, C.; Zhu, X.; Huang, D.; Zan, X.; Yang, B.; Li, Y.; Du, X.; Qian, H.; Huang, W. *J. Mol. Model.* **2012**, *18*, 2795–2804.

(104) Altman, F. P. *Prog. Histochem. Cytochem.* **1976**, *9*, III–51.

(105) Chacon, E.; Acosta, D.; Lemasters, J. J., *Primary Cultures of Cardiac Myocytes as In Vitro Models for Pharmacological and Toxicological Assessments*; Castell, J. V., Gómez-Lechón, M. J. B. T. .-.-. I. V. M. i. P. R., Eds.; Academic Press: San Diego, 1997, pp 209–223.

(106) Van Tonder, A.; Joubert, A. M.; Cromarty, A. D. *BMC Res. Notes* **2015**, *8*, 47.

(107) Ohta, K.; Miura, M.; Sakaguchi, K.; Sugawara, F.; Ishima, M.; Murata, H. Compound having tumor-resident property., 2010.

(108) Kohli, V.; Blöcker, H.; Köster, H. *Tetrahedron Lett.* **1980**, *21*, 2683–2686.

(109) Xia, M.-j.; Yao, W.; Meng, X.-b.; Lou, Q.-h.; Li, Z.-j. *Tetrahedron Lett.* **2017**, *58*, 2389–2392.

(110) Kurahashi, T.; Mizutani, T.; Yoshida, J.-i. *J. Chem. Soc., Perkin Trans. 1* **1999**, 465–474.

(111) McKiernan, R. L.; Heintz, A. M.; Hsu, S. L.; Atkins, E. D. T.; Penelle, J.; Gido, S. P. *Macromolecules* **2002**, *35*, 6970–6974.

(112) Mccloskey, C. M., *Advances in Carbohydrate Chemistry: Benzyl Ethers of Sugars*; Wolfrom, M. L., Tipson, R. S. B. T. .-.-. A. i. C. C., Eds.; Academic Press: 1957; Vol. 12, pp 137–156.

(113) Al-Douh, M.; Hamid, S.; Osman, H. *Univ. Aden J. Nat. Appl. Sci.* **2008**, *12*, 79–92.

(114) Mukherjee, C.; Liu, L.; Pohl, N. L. B. *Adv. Synth. Catal.* **2014**, *356*, 2247–2256.

(115) Tanaka, H.; Kawai, K.; Fujiwara, K.; Murai, A. *Tetrahedron* **2002**, *58*, 10017–10031.

(116) Lipták, A.; Jodál, I.; Nánási, P. *Carbohydr. Res.* **1975**, *44*, 1–11.

(117) Tatina, M.; Yousuf, S. K.; Aravinda, S.; Singh, B.; Mukherjee, D. *Carbohydr. Res.* **2013**, *381*, 142–145.

(118) Johnsson, R.; Ohlin, M.; Ellervik, U. *J. Org. Chem.* **2010**, *75*, 8003–8011.

(119) Wang, Y.; Cheon, H.; Kishi, Y. *Chem. - Asian J.* **2008**, *3*, 319–326.

(120) Ducry, L.; Roberge, D. M. *Org. Process Res. Dev.* **2008**, *12*, 163–167.

(121) Dimakos, V.; Taylor, M. S. *Chem. Rev.* **2018**, *118*, 11457–11517.

(122) Kawahara, S.-i.; Wada, T.; Sekine, M. *Tetrahedron Lett.* **1996**, *37*, 509–512.

(123) Sugiyama, H.; Nitta, T.; Horii, M.; Motohashi, K.; Sakai, J.; Usui, T.; Hisamichi, K.; Ishiyama, J.-i. *Carbohydr. Res.* **2000**, *325*, 177–182.

(124) Cmoch, P.; Pakulski, Z. *Tetrahedron: Asymmetry* **2008**, *19*, 1493–1502.

(125) Gilles, V.; Vieira, M. A.; Lacerda Jr., V.; Castro, E. V. R.; Santos, R. B.; Orestes, E.; Carneiro, J. W. M.; Greco, S. J. *J. Braz. Chem. Soc.* **2015**, *26*, 74–83.

(126) Hui, Y.; Webster, R. D. *Anal. Chem.* **2011**, *83*, 976–981.

(127) Mohammed, I. A.; Shahabuddin, S.; Khanam, R.; Saidur, R. *Polímeros* **2018**, *28*, 406–412.

(128) Powell, N. A.; Clay, E. H.; Holsworth, D. D.; Bryant, J. W.; Ryan, M. J.; Jalaie, M.; Edmunds, J. J. *Bioorg. Med. Chem. Lett.* **2005**, *15*, 4713–4716.

(129) Yokoyama, H.; Keithly, J.; Gausman, H. Plant bioregulatory composition and method using (benzyl substituted) trialkylamine ether compounds., 1993.

(130) Roslund, M. U.; Aitio, O.; Wärnå, J.; Maaheimo, H.; Murzin, D. Y.; Leino, R. *J. Am. Chem. Soc.* **2008**, *130*, 8769–8772.

(131) Ekholm, F. S.; Leino, R., *Acyl Migrations in Carbohydrate Chemistry*; Wiley Online Books; Wiley-VCH: 2018, pp 227–241.

(132) Xu, D.; Edgar, K. J. *Biomacromolecules* **2012**, *13*, 299–303.

(133) Fulmer, G. R.; Miller, A. J. M.; Sherden, N. H.; Gottlieb, H. E.; Nudelman, A.; Stoltz, B. M.; Bercaw, J. E.; Goldberg, K. I. *Organometallics* **2010**, *29*, 2176–2179.

(134) Yamanoi, T.; Inoue, R.; Matsuda, S.; Iwao, K.; Oda, Y.; Yoshida, A.; Hamasaki, K. *Heterocycles* **2009**, *77*, 445–460.

(135) Fang, T. T.; Bendiak, B. *J. Am. Chem. Soc.* **2007**, *129*, 9721–9736.

Appendices

A Spectroscopic data for compound 3

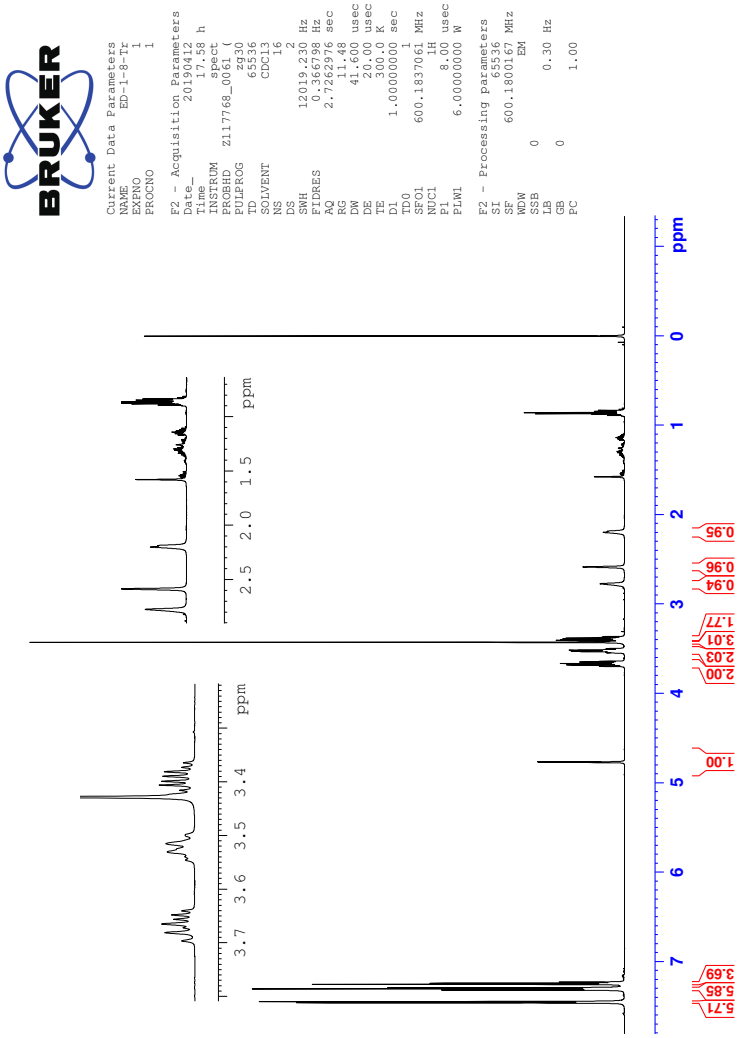

Figure 1: ^{1}H-NMR spectrum of compound **3**.

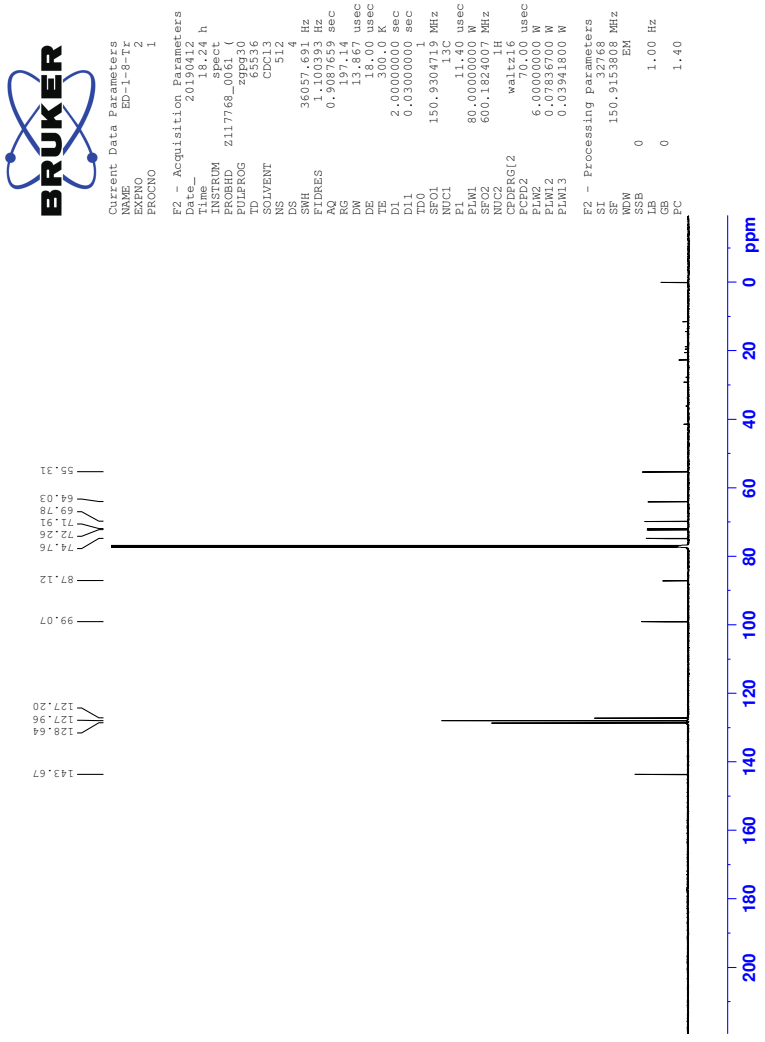

Figure 2: ^{13}C-NMR spectrum of compound **3**.

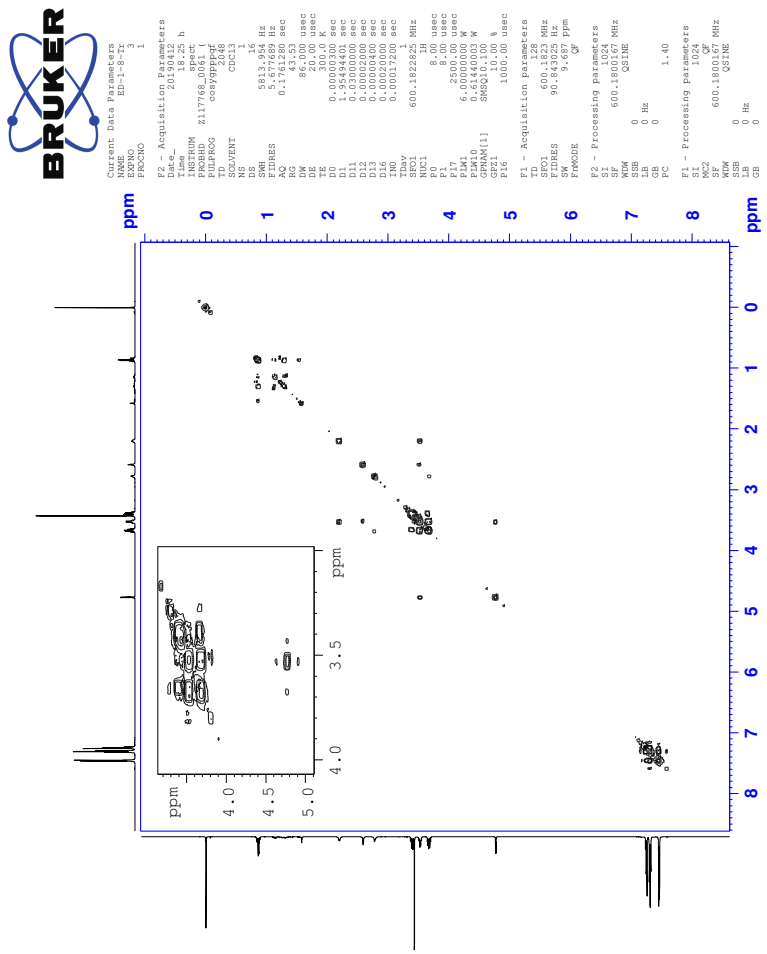

Figure 3: COSY spectrum of compound **3**.

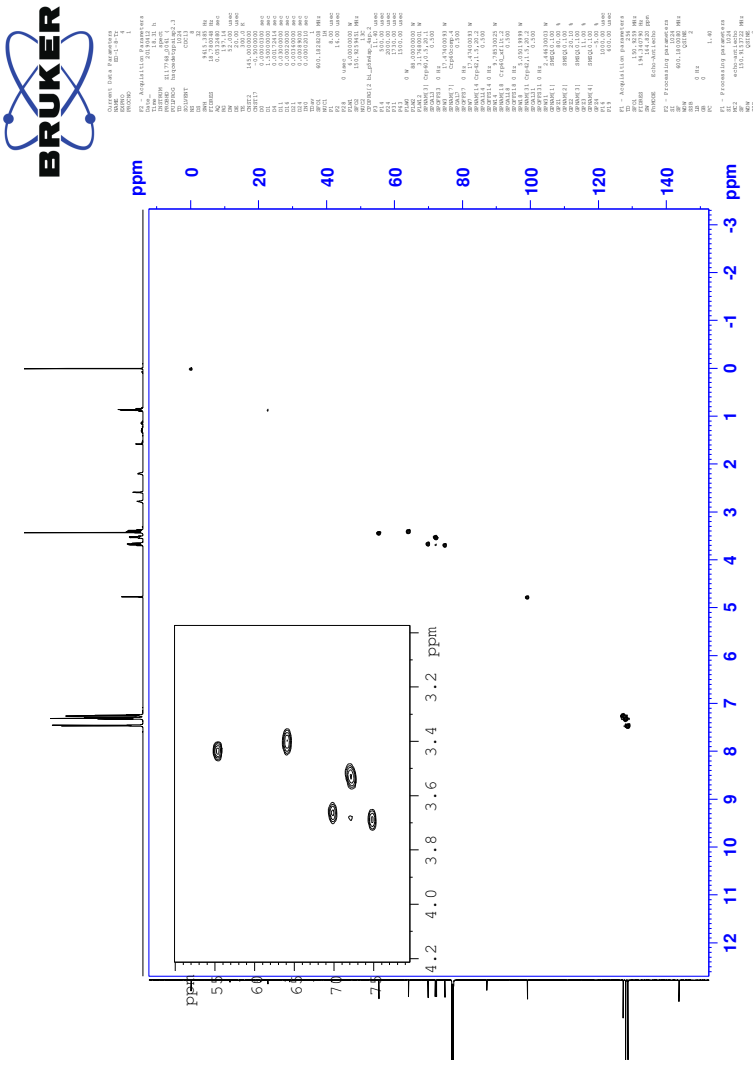

Figure 4: HSQC spectrum of compound **3**.

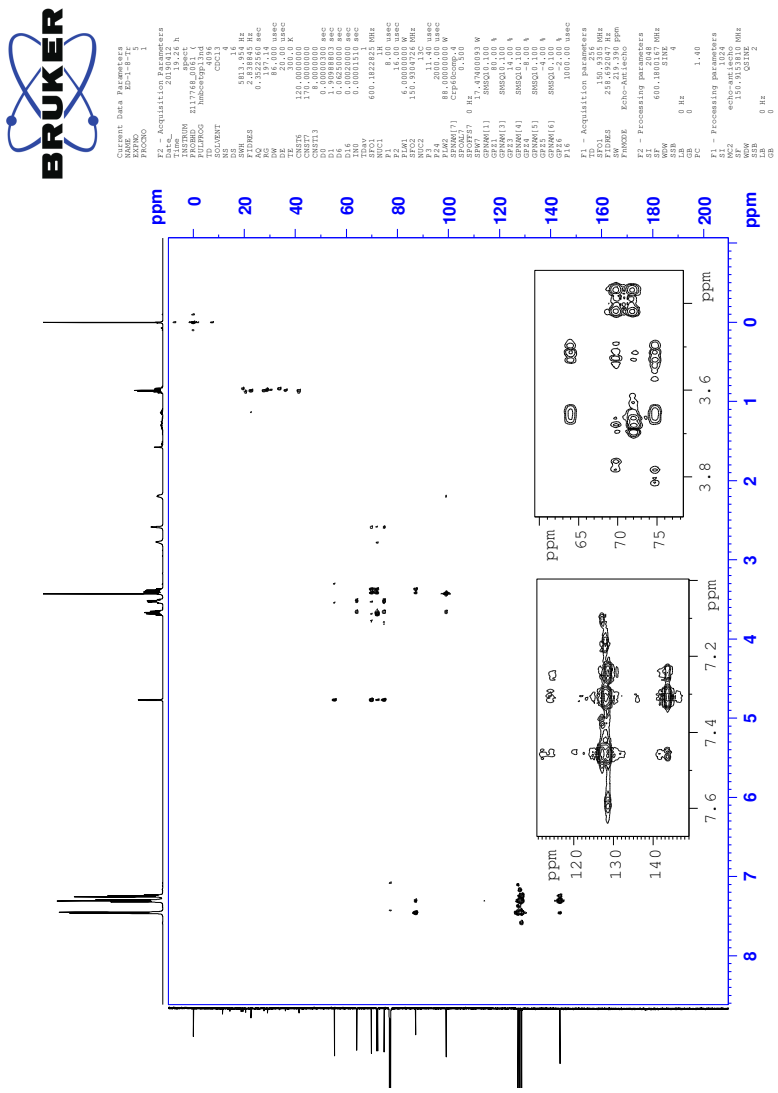

Figure 5: HMBC spectrum of compound **3**.

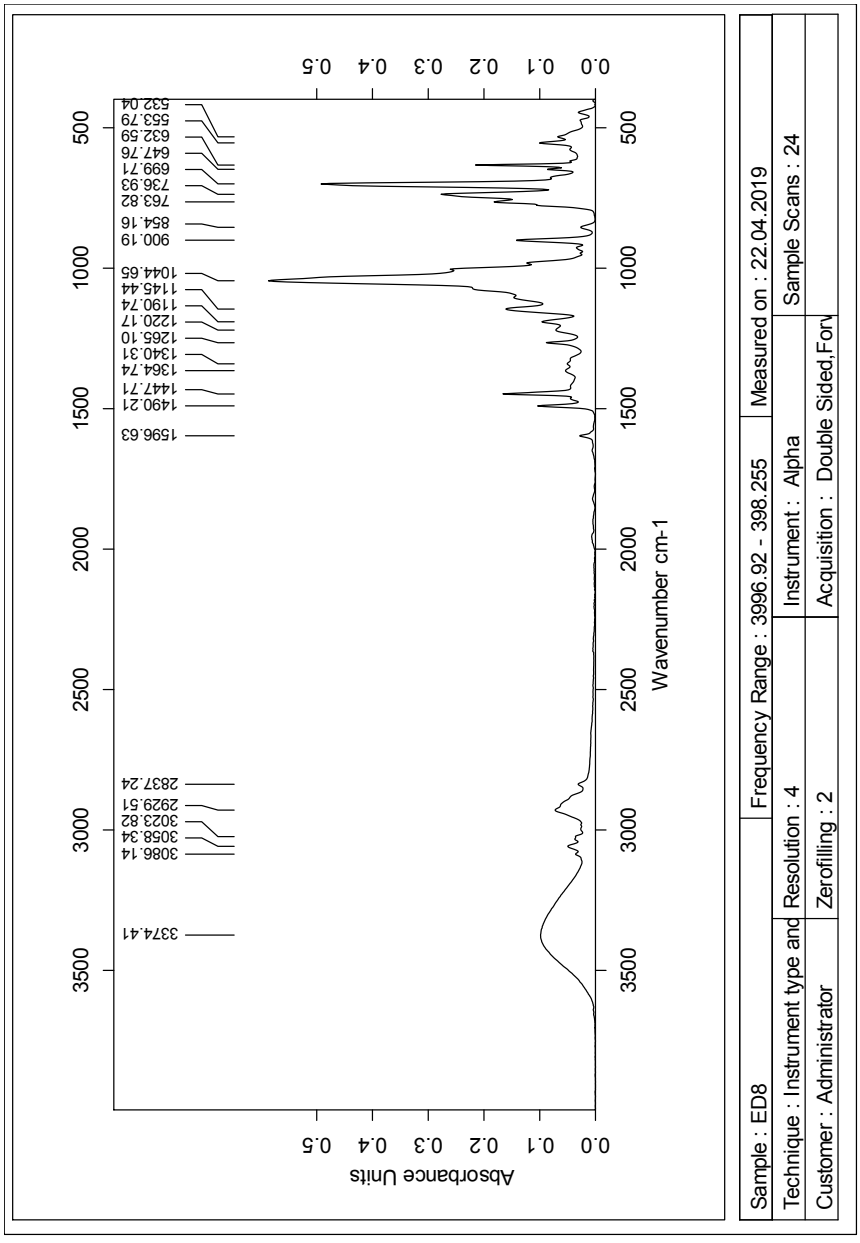

Figure 6: IR spectrum of compound **3**.

!\[p\]

Elemental Composition Report **Page 1**

Single Mass Analysis
Tolerance = 2.0 PPM / DBE: min = -50.0, max = 50.0
Element prediction: Off
Number of isotope peaks used for i-FIT = 3

Monoisotopic Mass, Even Electron Ions
619 formula(e) evaluated with 1 results within limits (all results (up to 1000) for each mass)
Elements Used:
C: 0-100 H: 0-150 O: 0-8 Na: 0-1 Br: 0-2

2019-368 29 (0.550) AM2 (Ar,35000.0,0.00,0.00); Cm (25:32)
1: TOF MS ES+

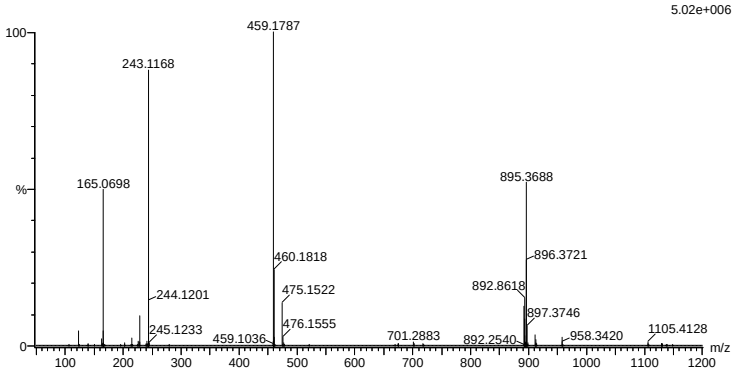

Minimum:				-50.0				
Maximum:		5.0	2.0	50.0				
Mass	Calc. Mass	mDa	PPM	DBE	i-FIT	Norm	Conf(%)	Formula
459.1787	459.1784	0.3	0.7	12.5	1179.6	n/a	n/a	C26 H28 O6 Na

Figure 7: MS results for compound **3**.

B Spectroscopic data for compound 4

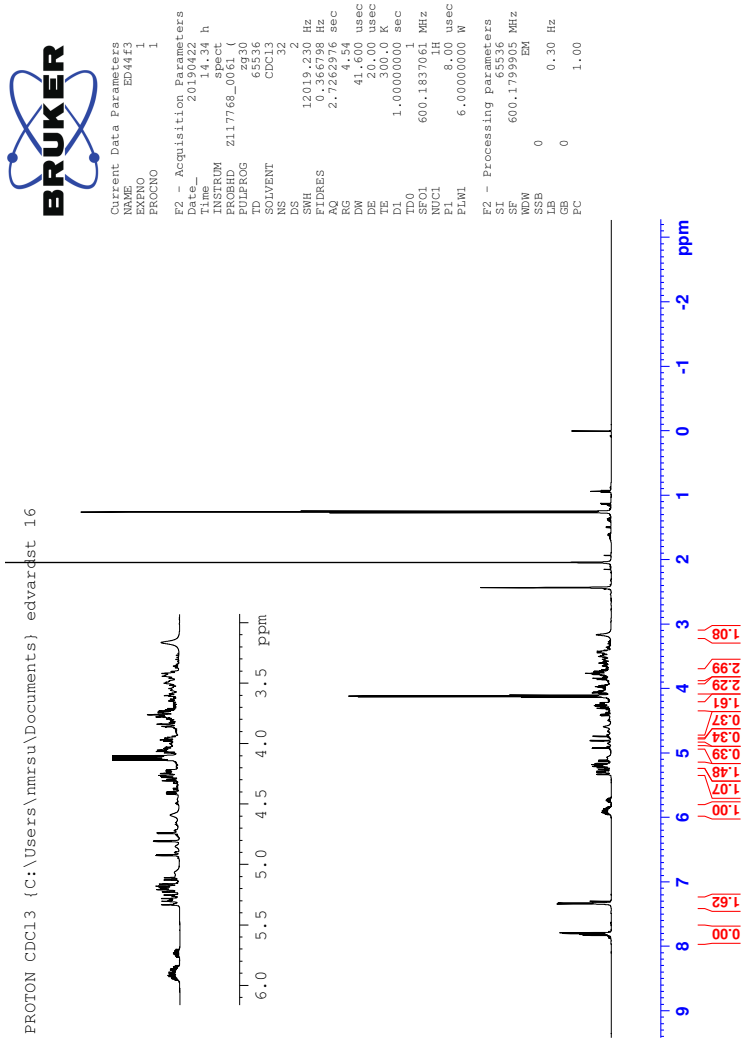

Figure 8: ^{1}H-NMR spectrum of compound **4**.

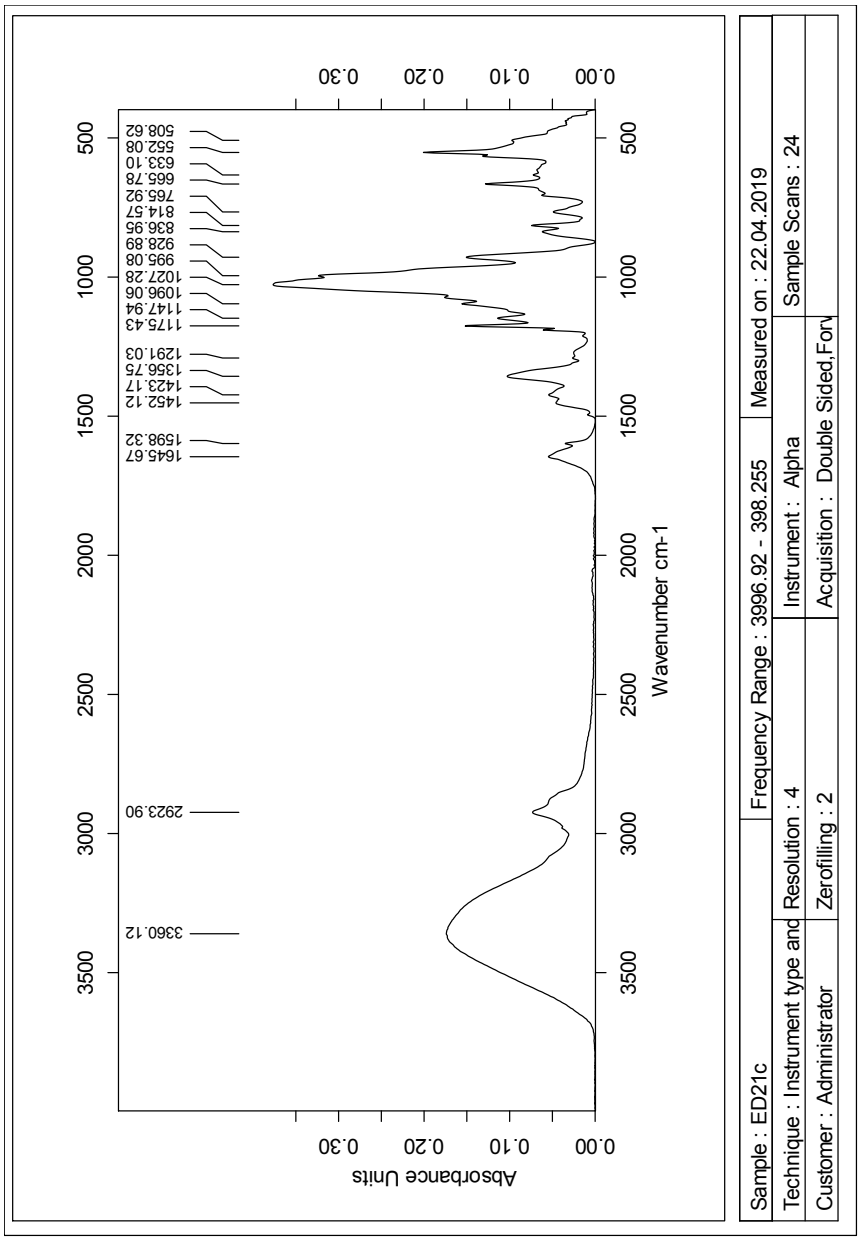

Figure 9: IR spectrum of compound **4**.

Elemental Composition Report **Page 1**

Single Mass Analysis
Tolerance = 2.0 PPM / DBE: min = -50.0, max = 50.0
Element prediction: Off
Number of isotope peaks used for i-FIT = 3

Monoisotopic Mass, Even Electron Ions
1438 formula(e) evaluated with 3 results within limits (all results (up to 1000) for each mass)
Elements Used:
C: 0-100 H: 0-150 O: 0-10 Na: 0-1 S: 0-2 K: 0-1
2019-367 21 (0.402) AM2 (Ar,35000.0,0.00,0.00); Cm (19:21)
1: TOF MS ES+

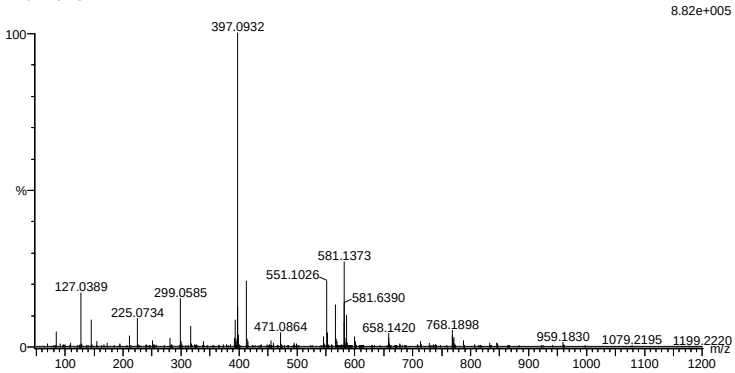

Minimum:				-50.0				
Maximum:		5.0	2.0	50.0				
Mass	Calc. Mass	mDa	PPM	DBE	i-FIT	Norm	Conf(%)	Formula
397.0932	397.0932	0.0	0.0	12.5	980.9	4.031	1.78	C22 H21 O3 S2
	397.0933	-0.1	-0.3	5.5	976.9	0.032	96.87	C16 H22 O8 Na S
	397.0935	-0.3	-0.8	0.5	981.2	4.302	1.35	C13 H26 O9 S K

Figure 10: MS results for compound **4**.

C Spectroscopic data for compound 6

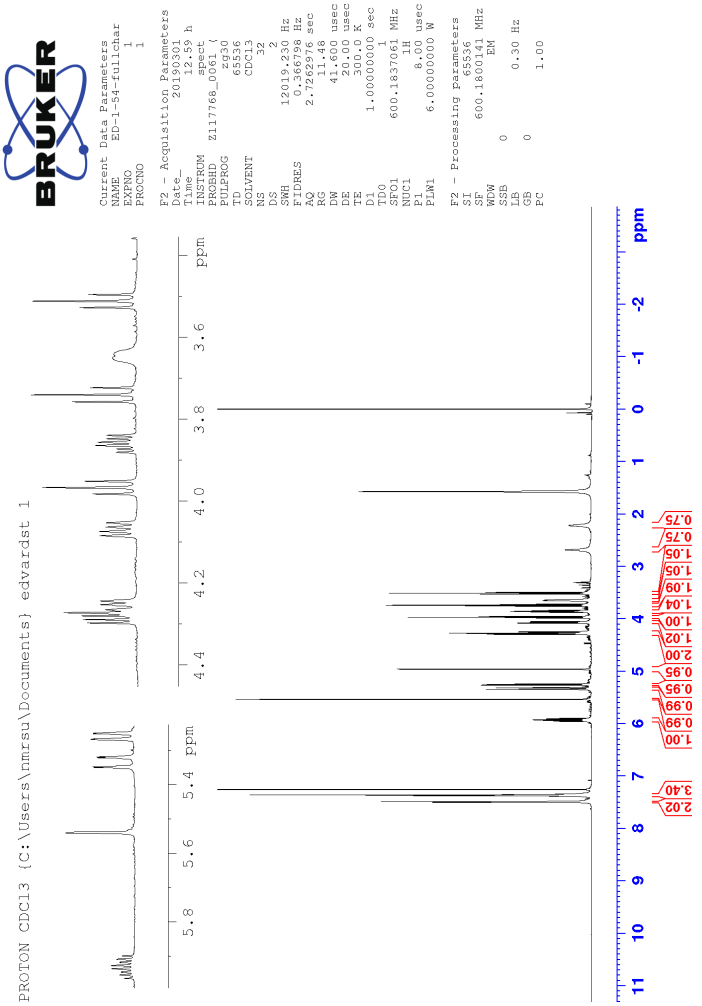

Figure 11: ^{1}H-NMR spectrum of compound **6**.

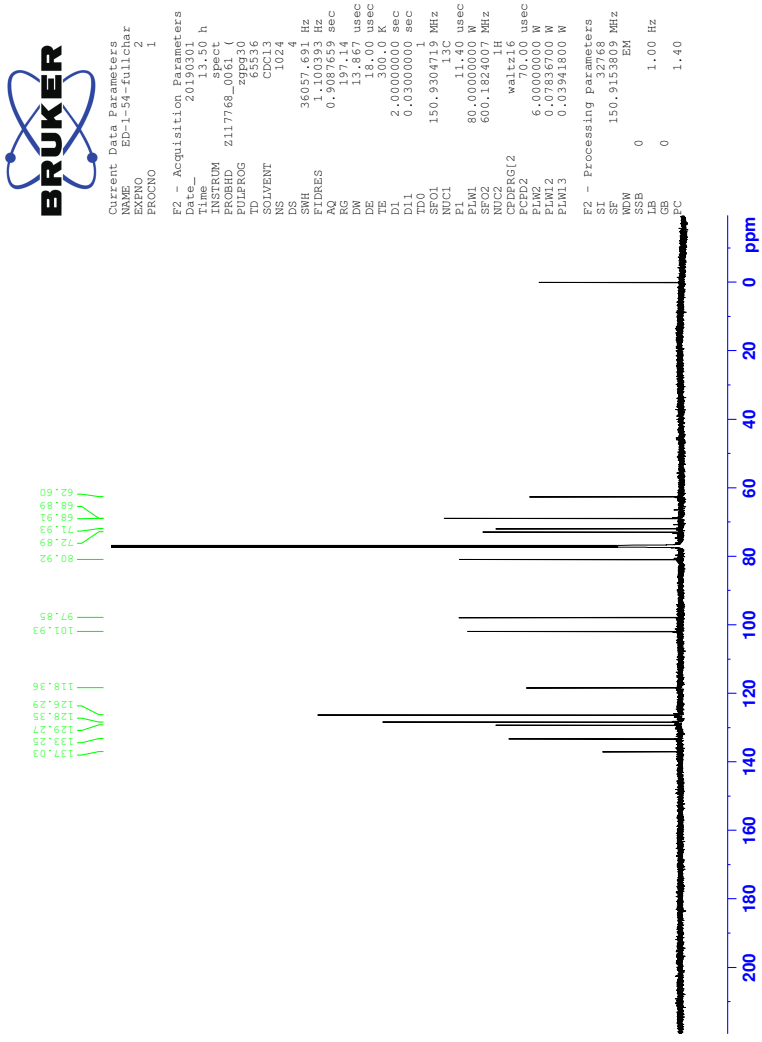

Figure 12: ^{13}C-NMR spectrum of compound **6**.

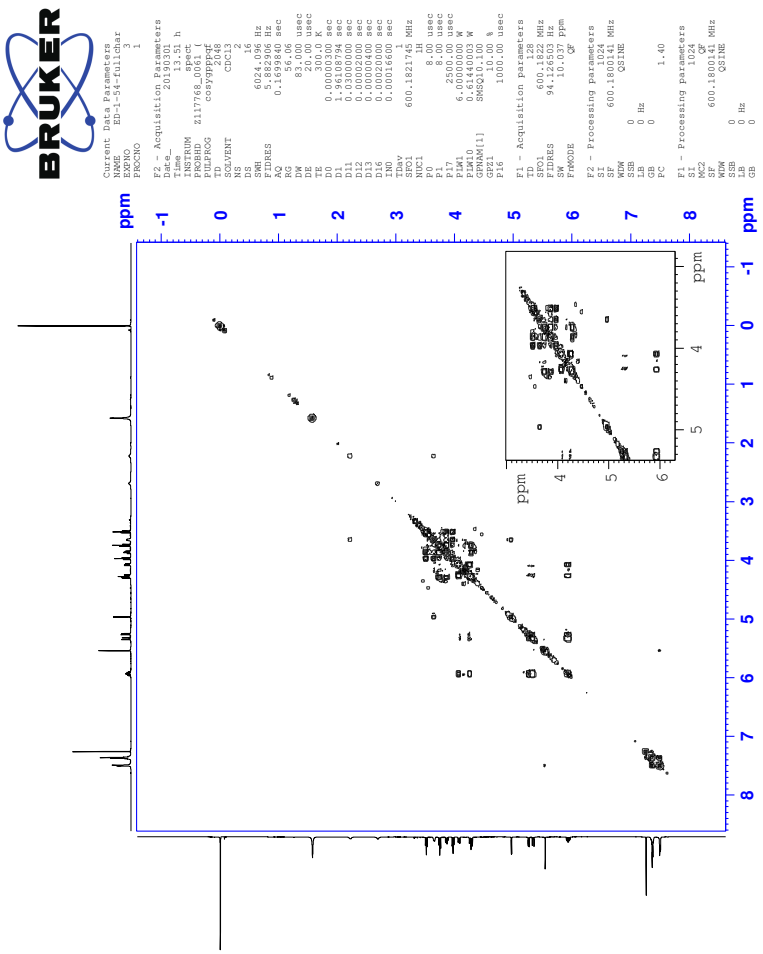

Figure 13: COSY spectrum of compound **6**.

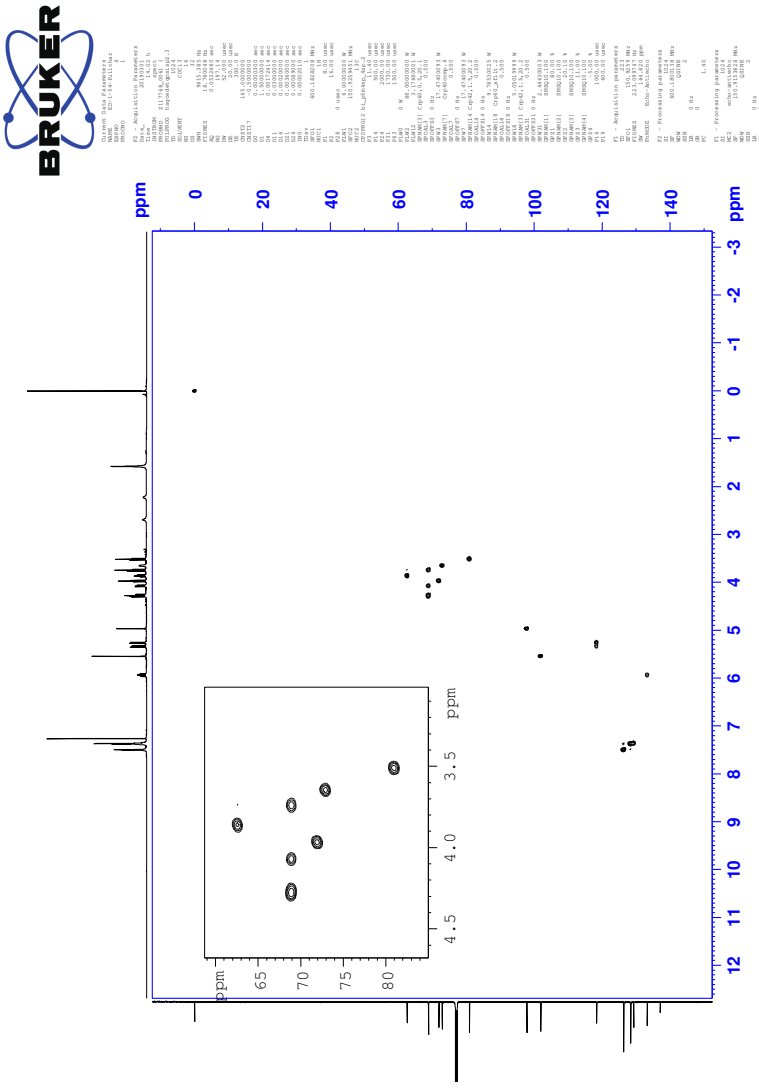

Figure 14: HSQC spectrum of compound **6**.

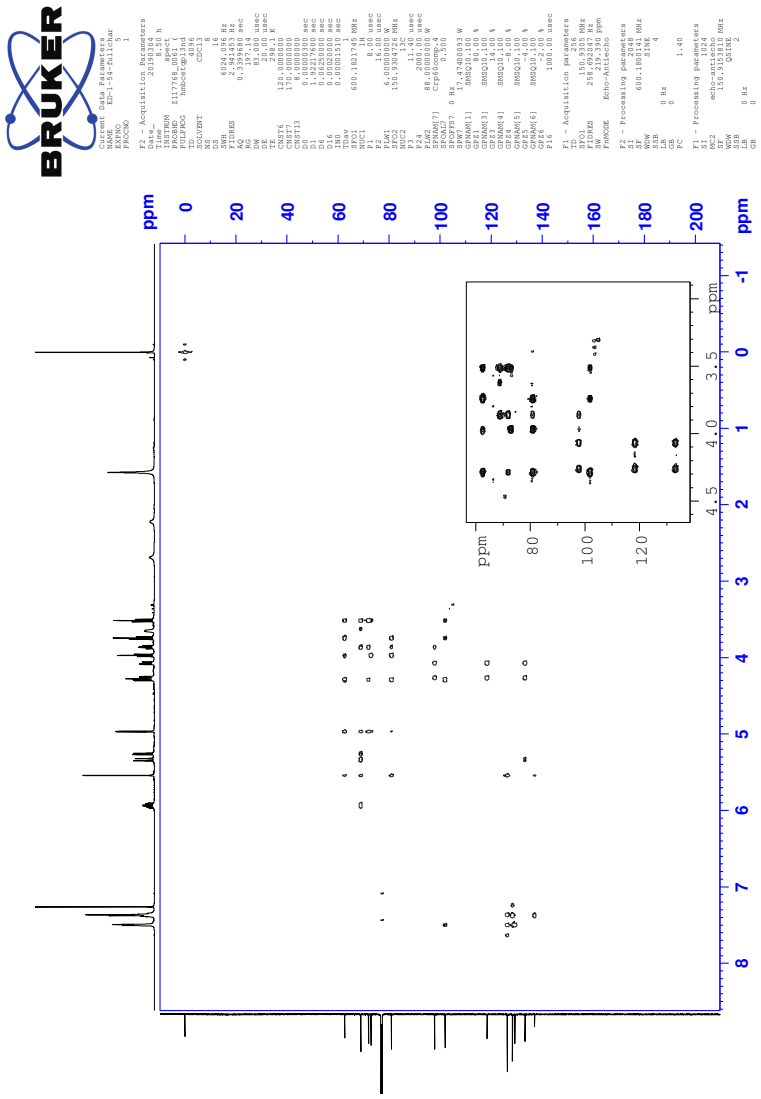

Figure 15: HMBC spectrum of compound **6**.

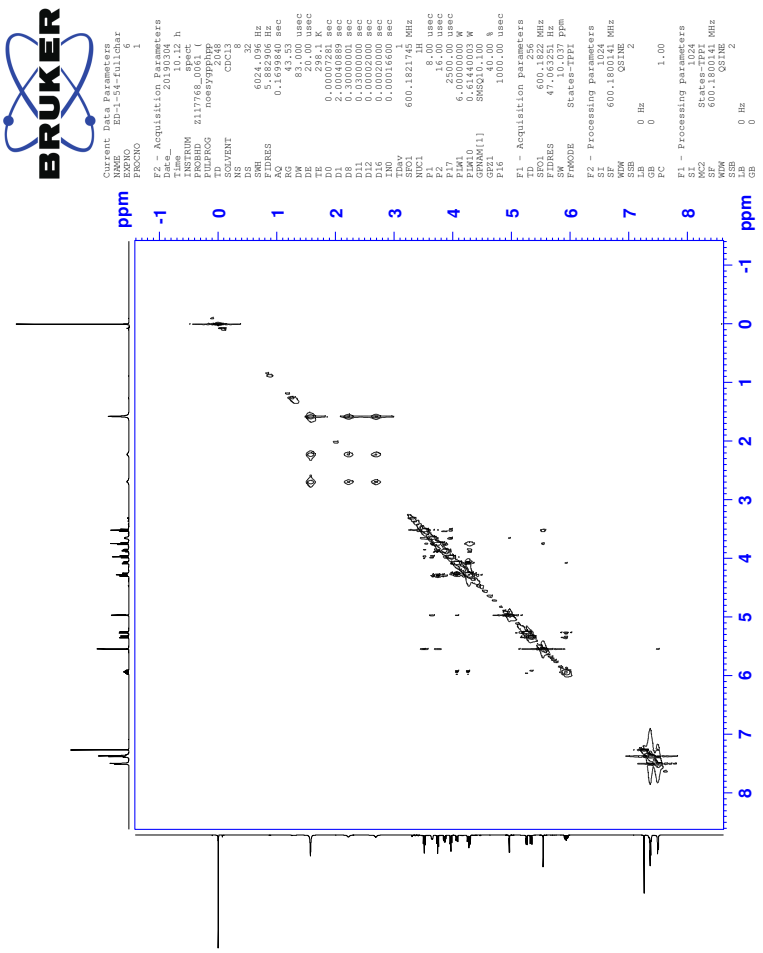

Figure 16: NOESY spectra of compound **6**.

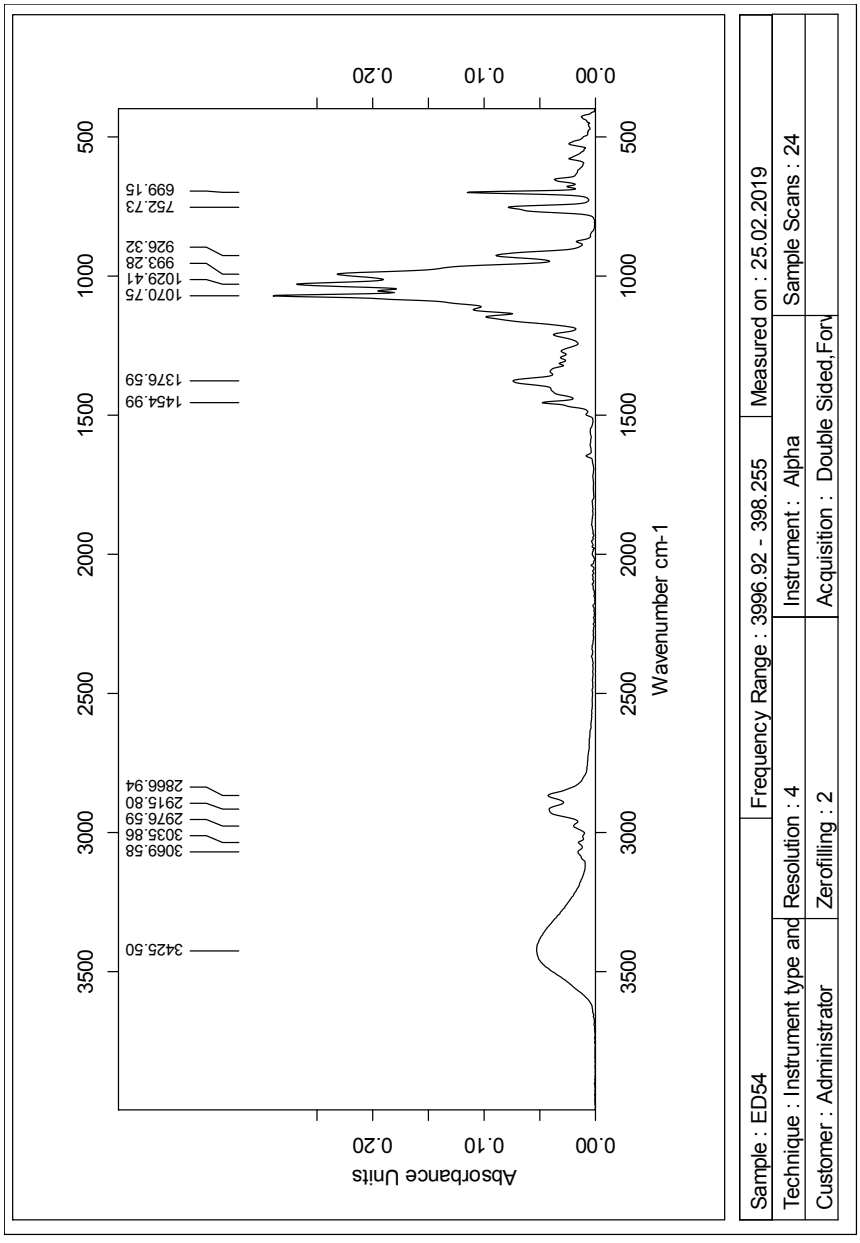

Figure 17: IR spectrum of compound **6**.

Elemental Composition Report **Page 1**

Single Mass Analysis
Tolerance = 3.0 PPM / DBE: min = -50.0, max = 50.0
Element prediction: Off
Number of isotope peaks used for i-FIT = 3

Monoisotopic Mass, Even Electron Ions
239 formula(e) evaluated with 1 results within limits (all results (up to 1000) for each mass)
Elements Used:
C: 0-100 H: 0-150 O: 0-10 Na: 0-1
svg_20190403_2019_260 22 (0.419) AM2 (Ar,35000.0,0.00,0.00); Cm (21:22)
1: TOF MS ES+

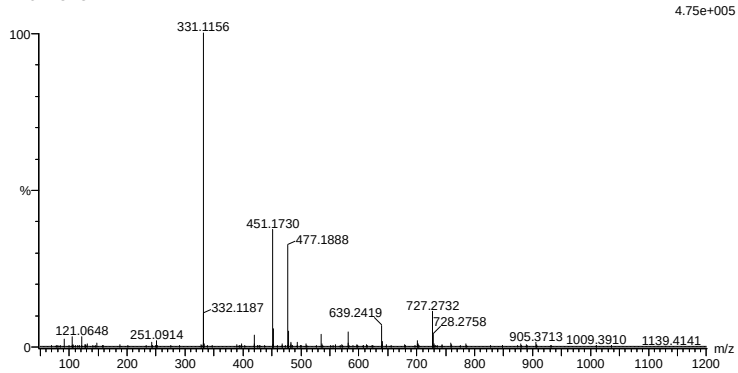

Minimum:				-50.0				
Maximum:		5.0	3.0	50.0				
Mass	Calc. Mass	mDa	PPM	DBE	i-FIT	Norm	Conf(%)	Formula
331.1156	331.1158	-0.2	-0.6	6.5	887.6	n/a	n/a	C16 H20 O6 Na

Figure 18: MS results for compound **6**.

D Spectroscopic data for compound 7

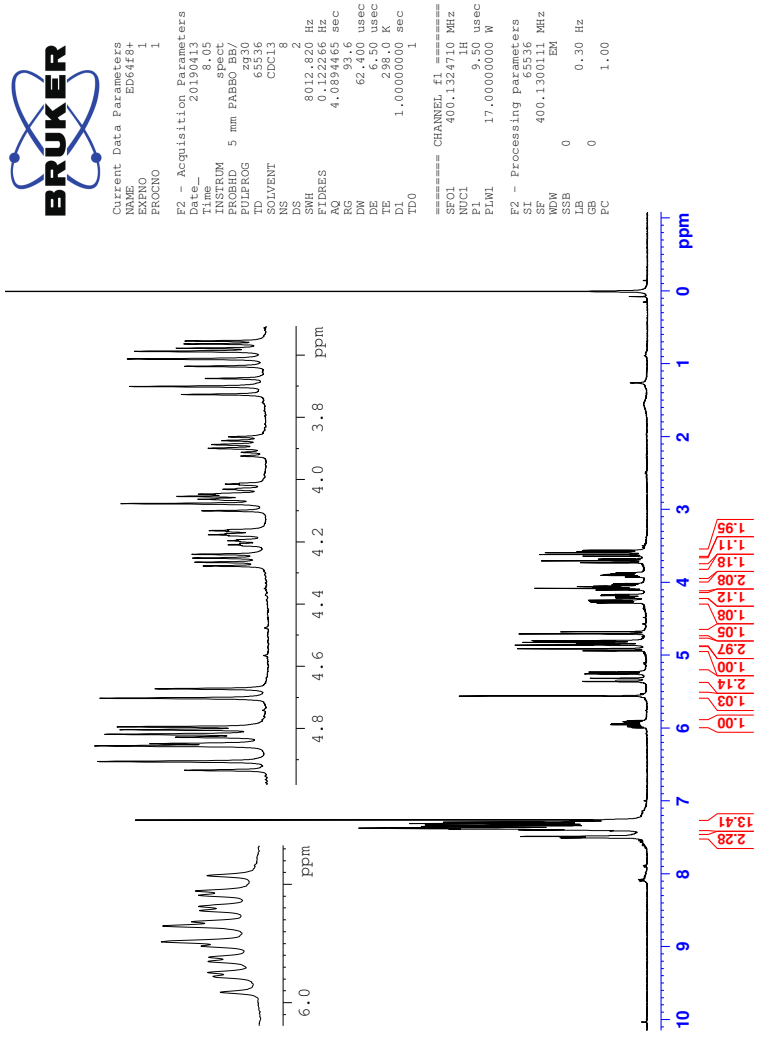

Figure 19: ^{1}H-NMR spectrum of compound **7**.

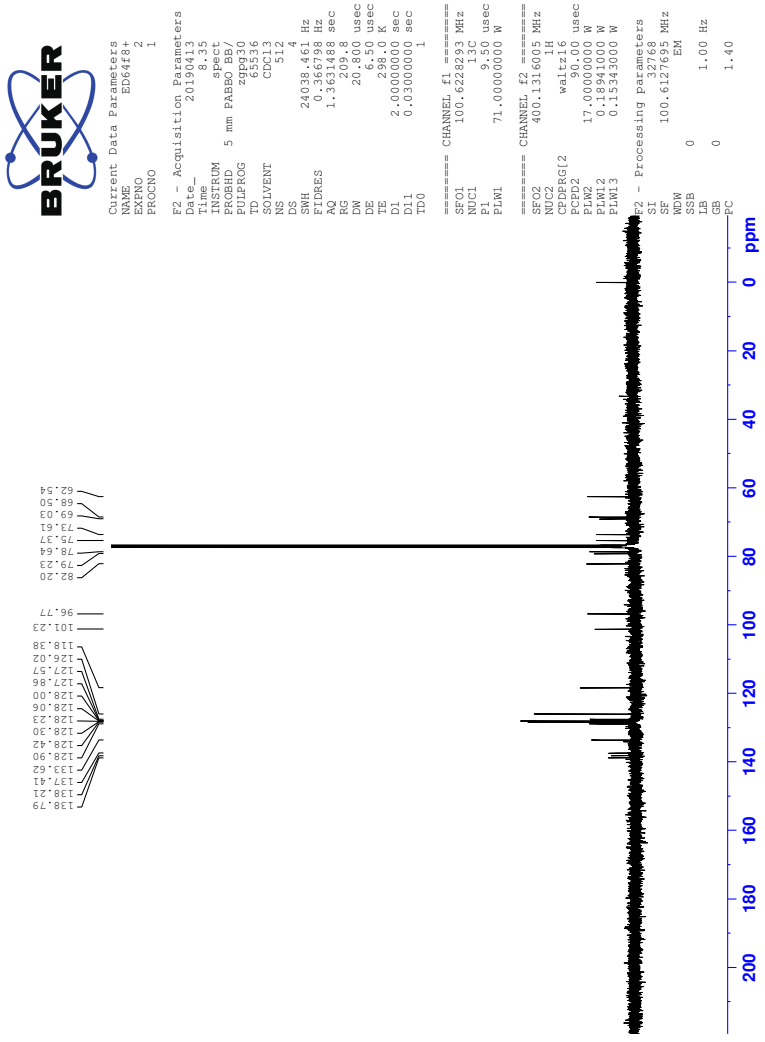

Figure 20: ^{13}C-NMR spectrum of compound **7**.

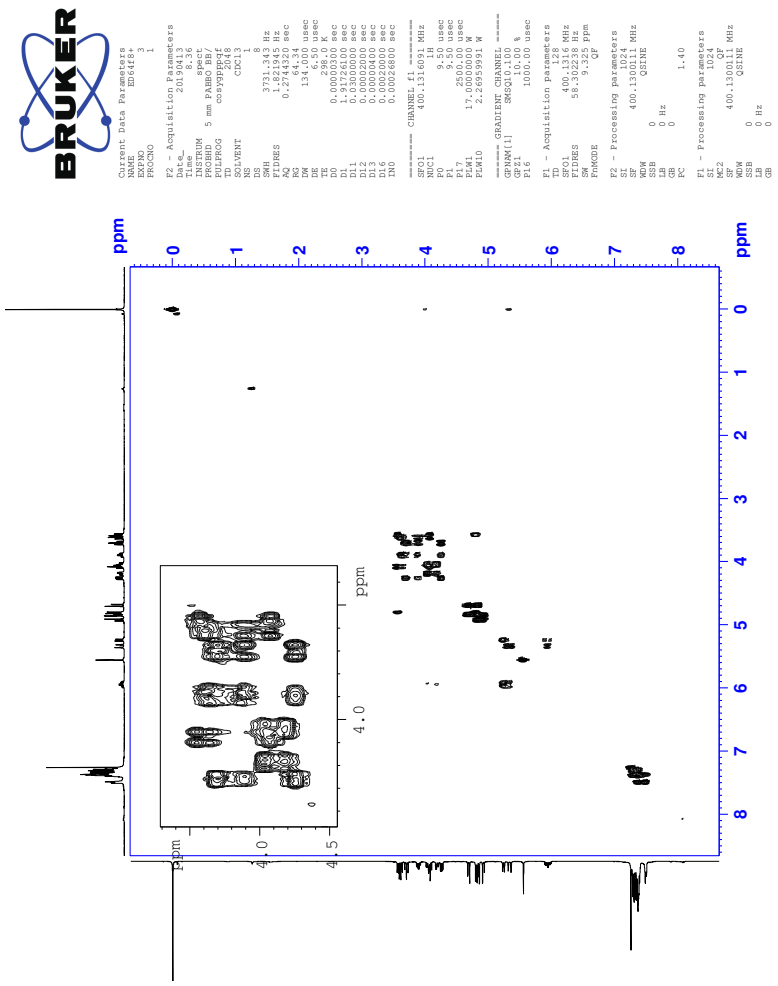

Figure 21: COSY spectrum of compound **7**.

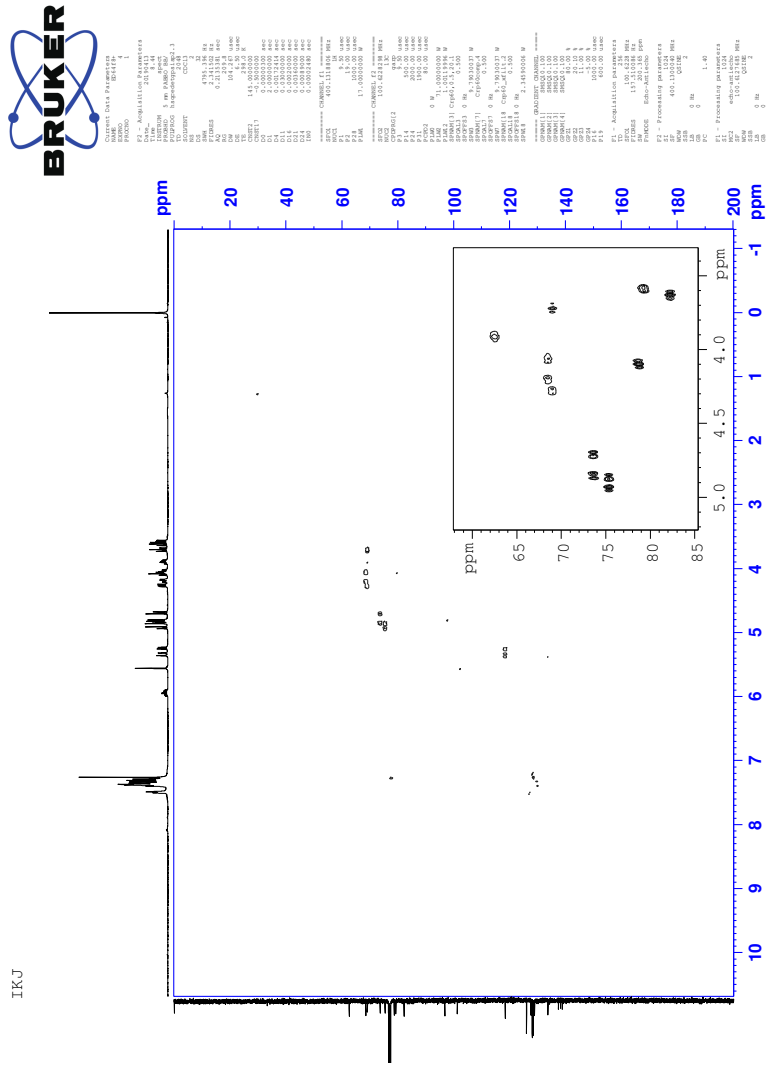

Figure 22: HSQC spectrum of compound **7**.

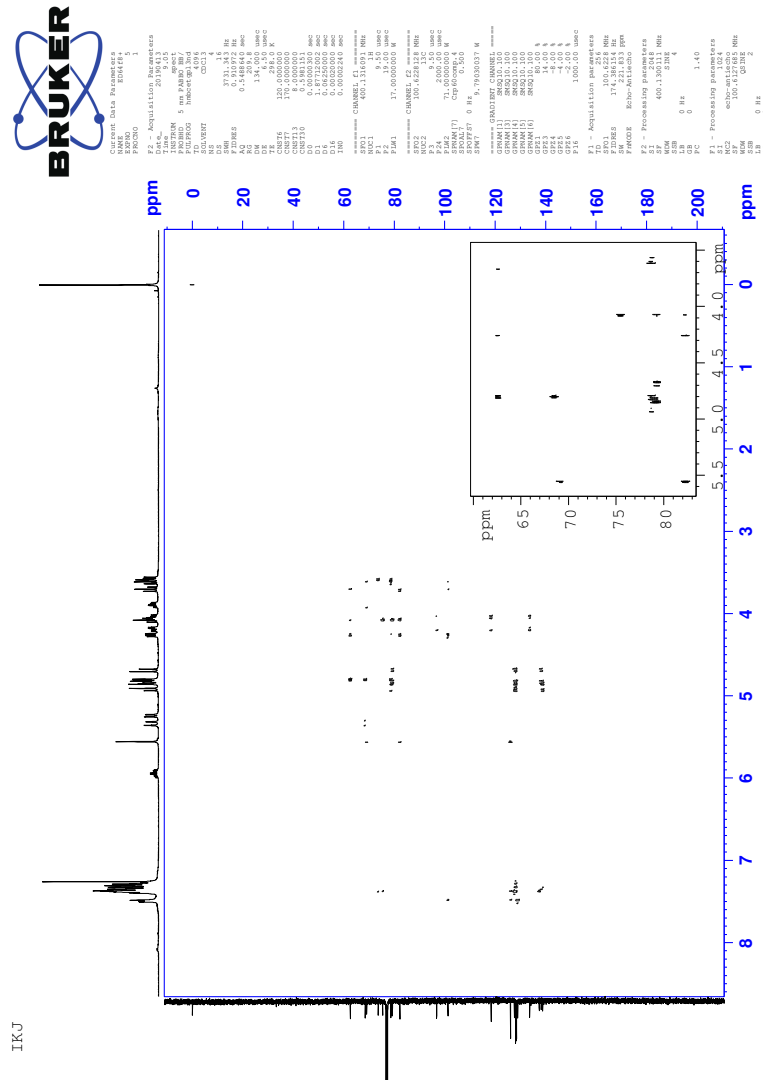

Figure 23: HMBC spectrum of compound **7**.

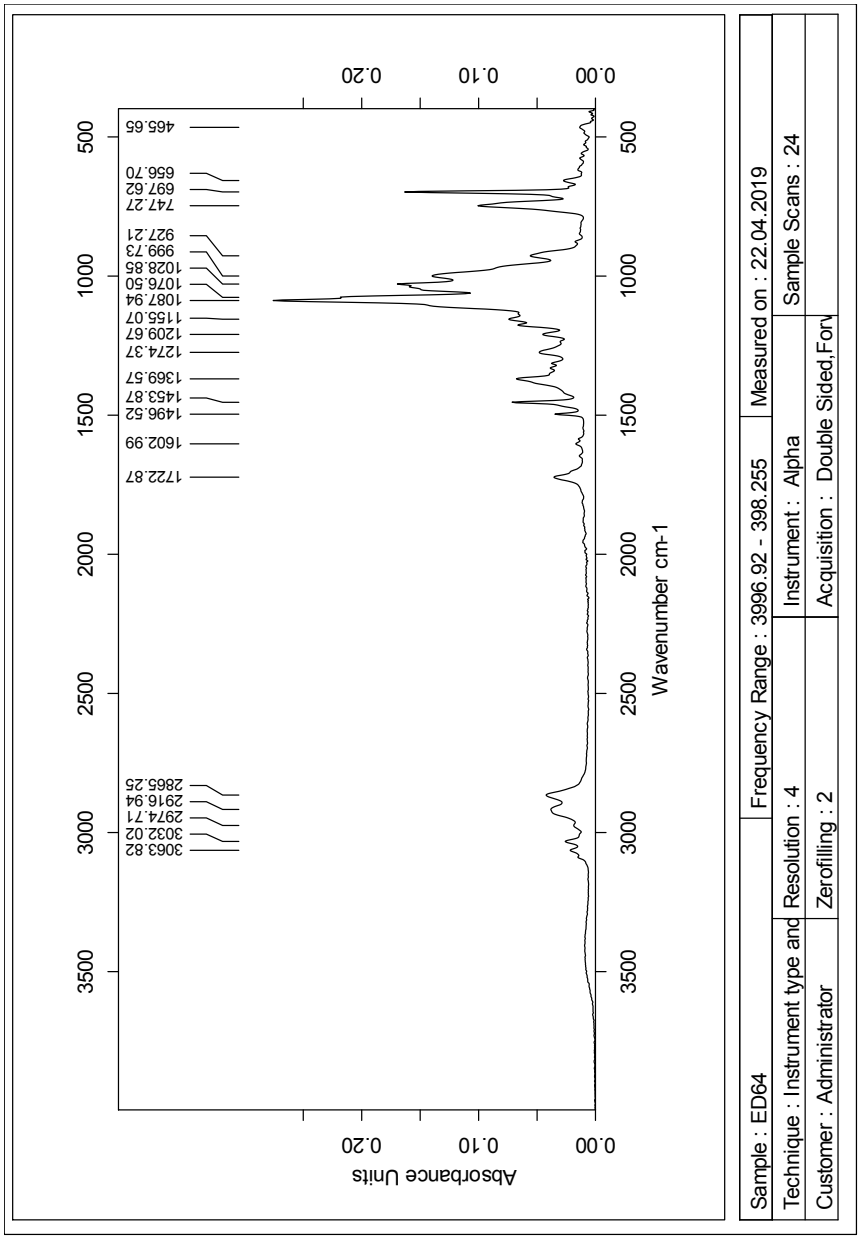

Figure 24: IR spectrum of compound **7**.

Elemental Composition Report **Page 1**

Single Mass Analysis
Tolerance = 2.0 PPM / DBE: min = -50.0, max = 50.0
Element prediction: Off
Number of isotope peaks used for i-FIT = 3

Monoisotopic Mass, Even Electron Ions
549 formula(e) evaluated with 2 results within limits (all results (up to 1000) for each mass)
Elements Used:
C: 0-100 H: 0-150 O: 0-10 Na: 0-1 K: 0-1
2019-366 28 (0.533) AM2 (Ar,35000.0,0.00,0.00); Cm (28:29)
1: TOF MS ES+

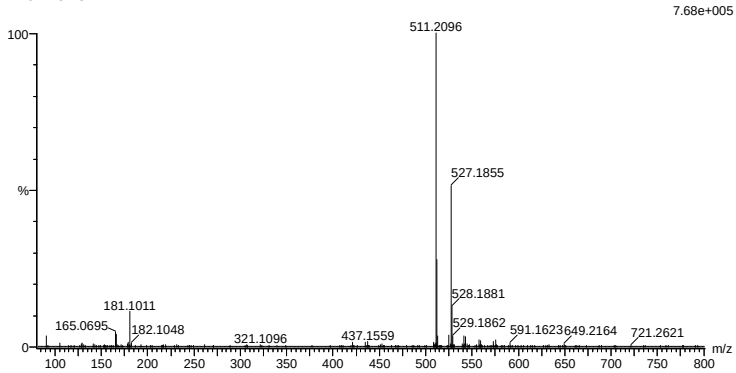

Minimum:				-50.0				
Maximum:		5.0	2.0	50.0				
Mass	Calc. Mass	mDa	PPM	DBE	i-FIT	Norm	Conf(%)	Formula
511.2096	511.2097	-0.1	-0.2	14.5	870.8	0.000	100.00	C30 H32 O6 Na
	511.2098	-0.2	-0.4	9.5	881.8	11.034	0.00	C27 H36 O7 K

Figure 25: MS results for compound **7**.

E Spectroscopic data for compound 8

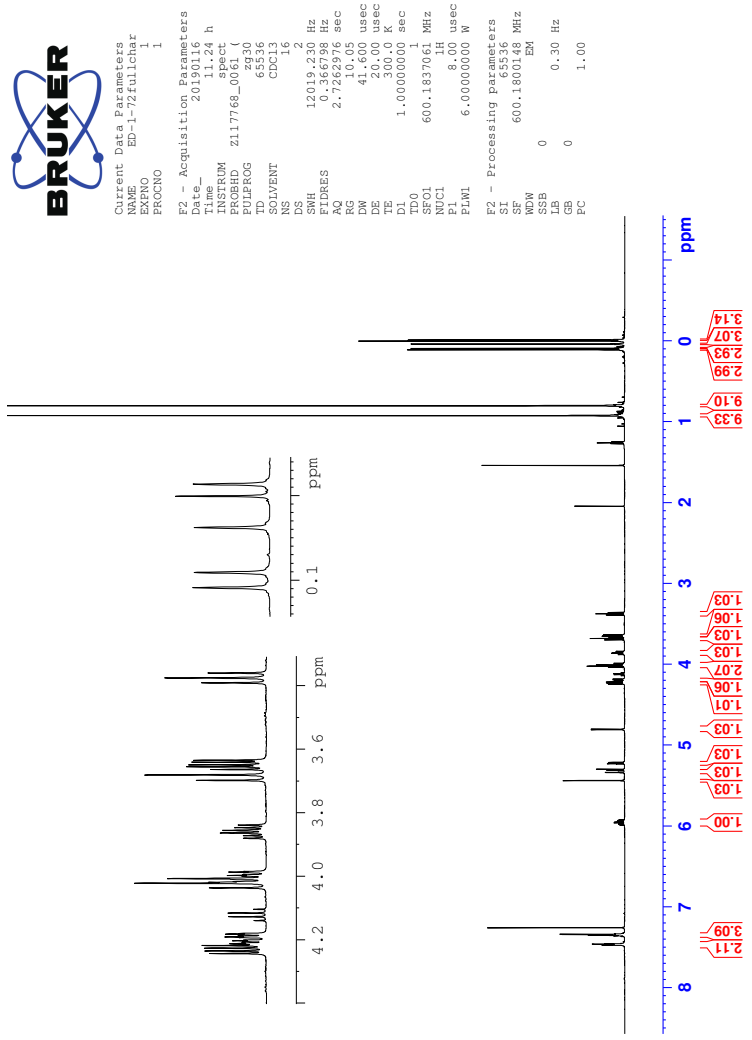

Figure 26: ^{1}H-NMR spectrum of compound **8**.

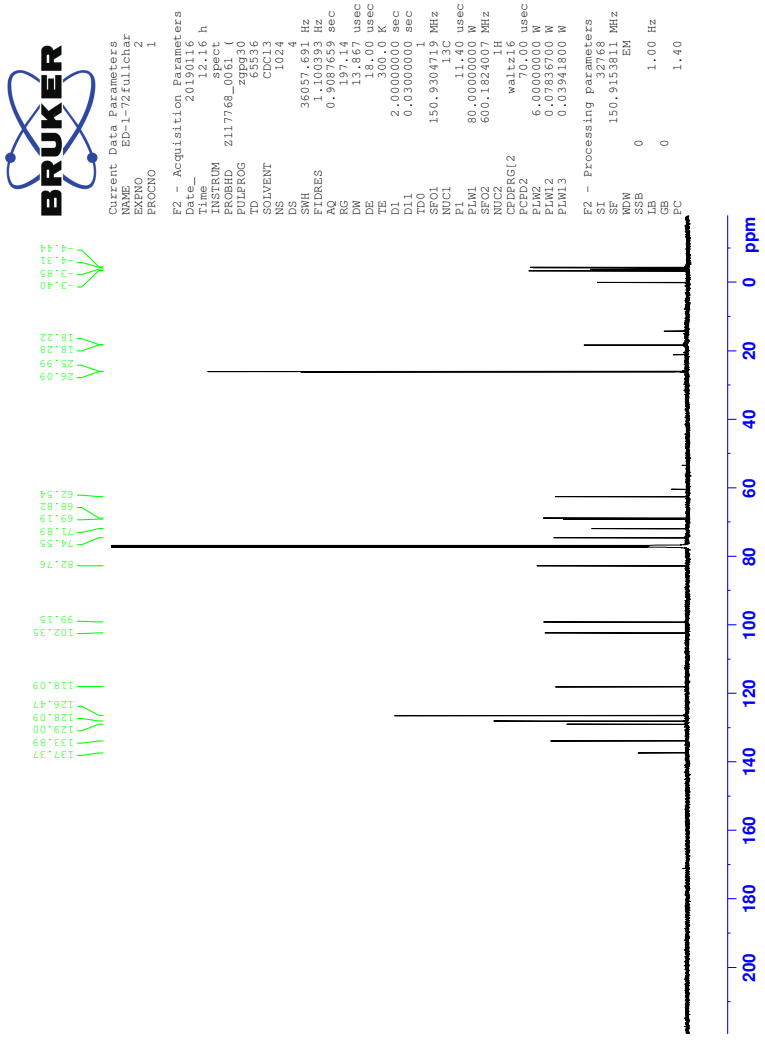

Figure 27: ^{13}C-NMR spectrum of compound **8**.

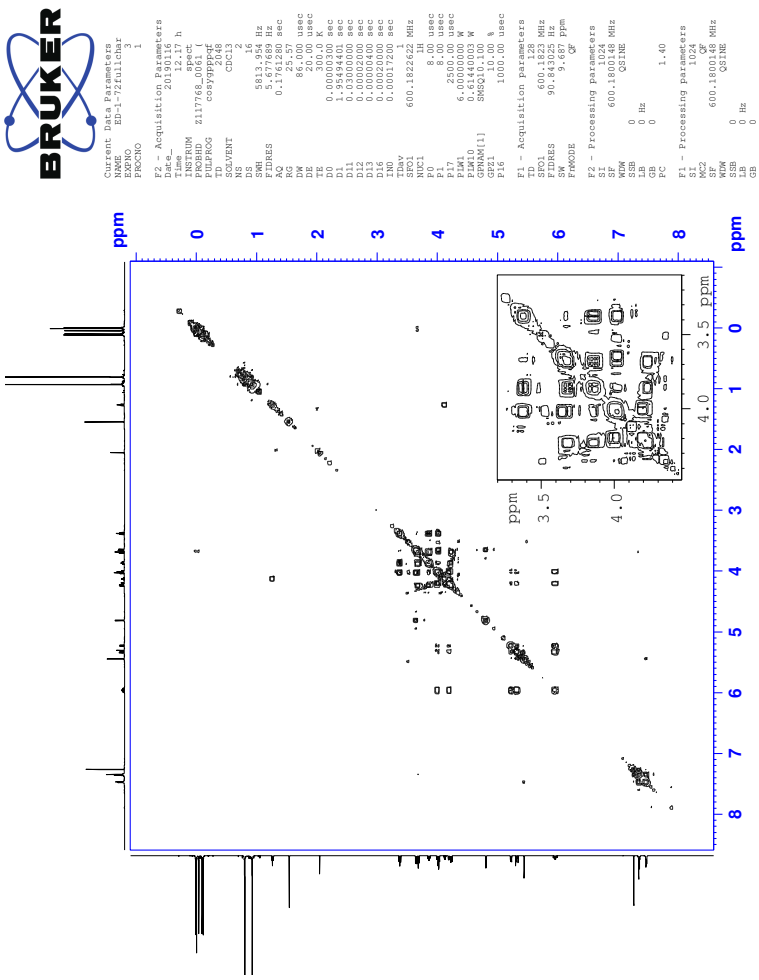

Figure 28: COSY spectrum of compound **8**.

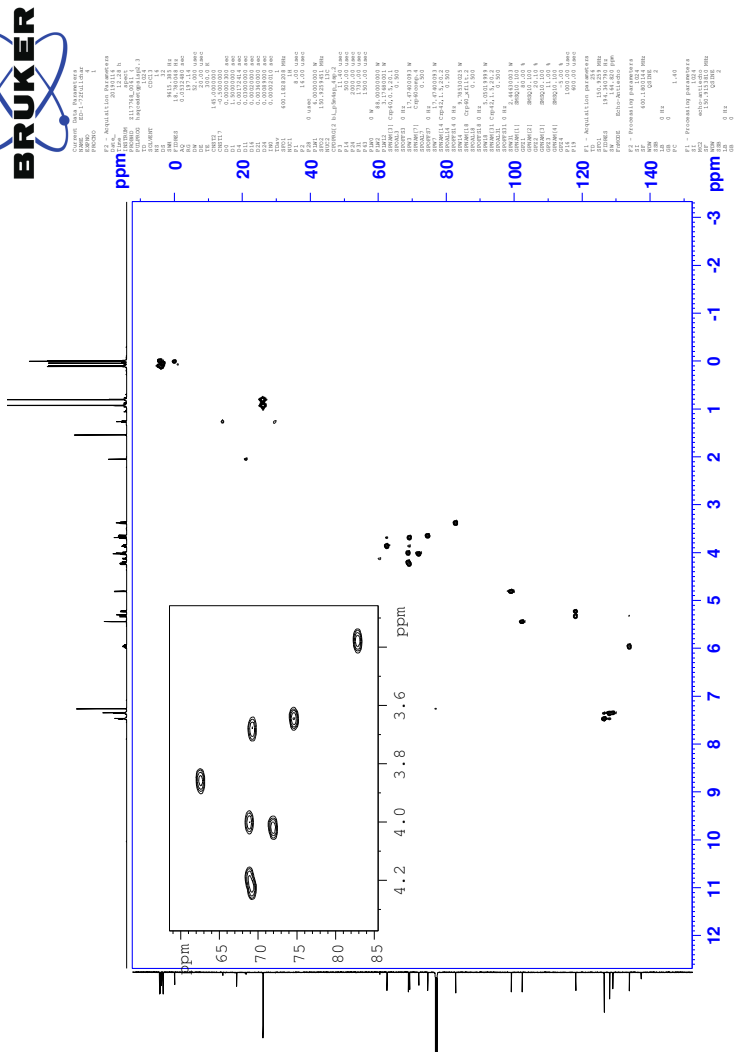

Figure 29: HSQC spectrum of compound **8**.

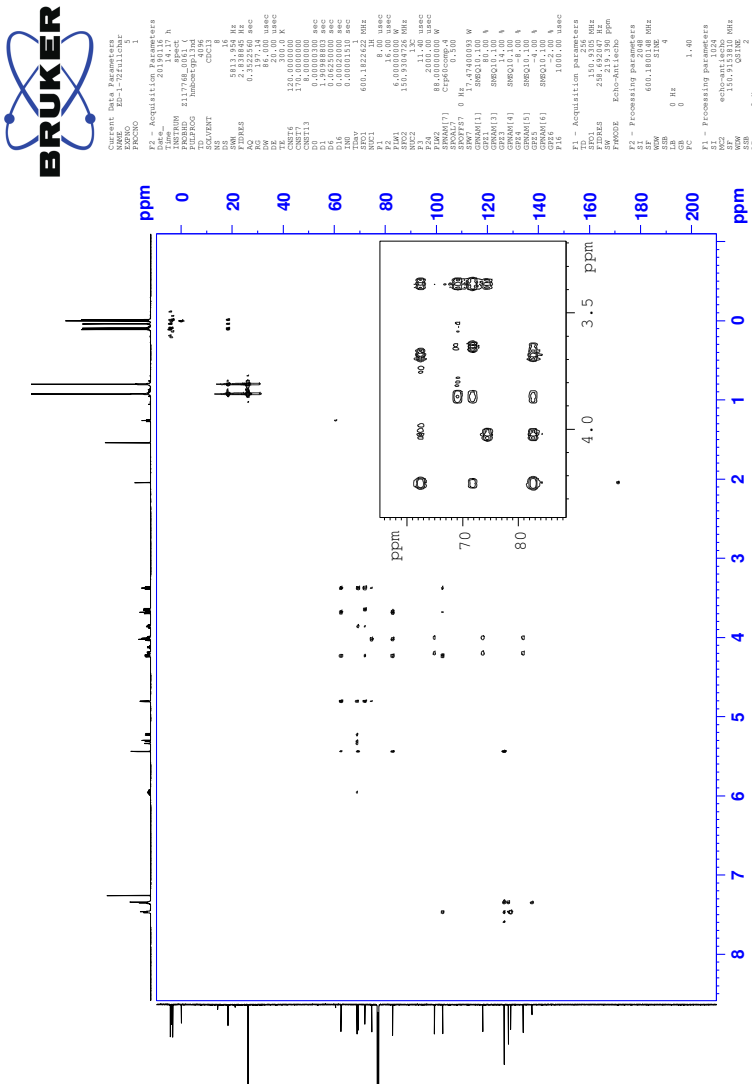

Figure 30: HMBC spectrum of compound **8**.

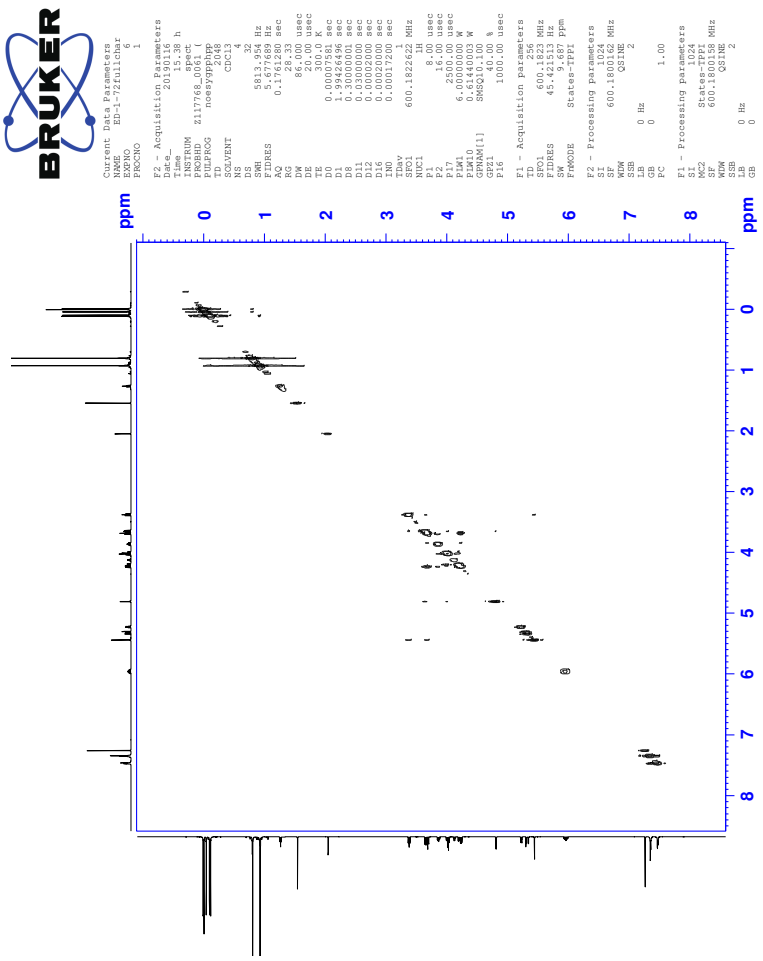

Figure 31: NOESY spectra of compound **8**.

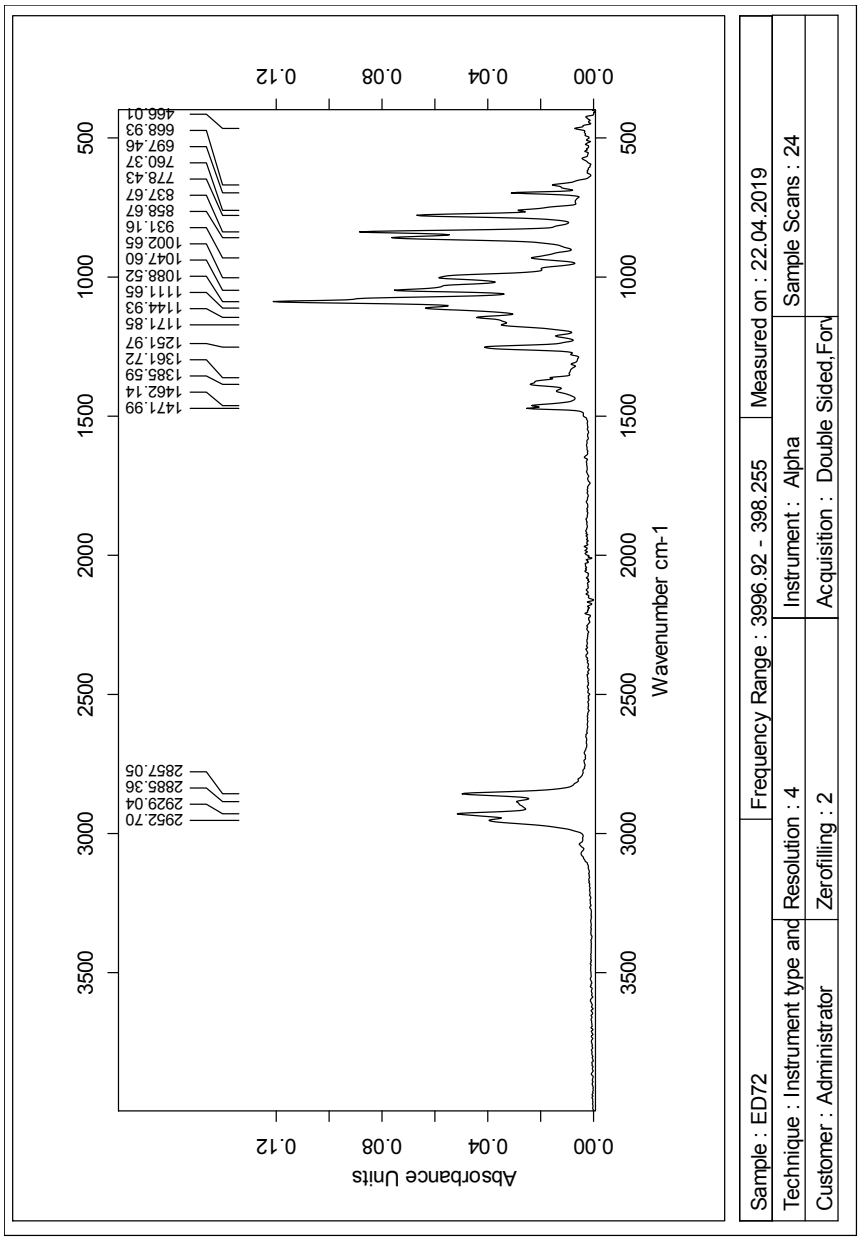

Figure 32: IR spectrum of compound **8**.

Elemental Composition Report **Page 1**

Single Mass Analysis
Tolerance = 4.0 PPM / DBE: min = -50.0, max = 50.0
Element prediction: Off
Number of isotope peaks used for i-FIT = 3

Monoisotopic Mass, Even Electron Ions
3335 formula(e) evaluated with 5 results within limits (all results (up to 1000) for each mass)
Elements Used:
C: 0-100 H: 0-150 N: 0-3 O: 0-10 Na: 0-1 Si: 0-2
svg_20190403_2019_265 18 (0.339) AM2 (Ar,35000.0,0.00,0.00); Cm (17:18)
1: TOF MS ES+

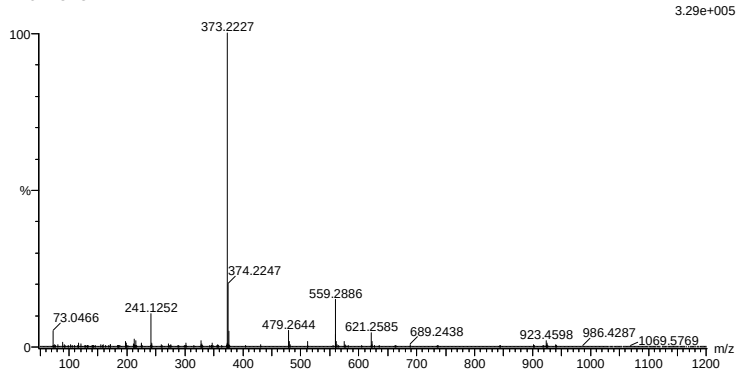

Minimum:				-50.0				
Maximum:		5.0	4.0	50.0				
Mass	Calc. Mass	mDa	PPM	DBE	i-FIT	Norm	Conf(%)	Formula
559.2886	559.2887	-0.1	-0.2	6.5	563.7	1.193	30.33	C28 H48 O6 Na Si2
	559.2883	0.3	0.5	7.5	566.4	3.852	2.12	C29 H44 O9 Na
	559.2880	0.6	1.1	14.5	563.0	0.473	62.30	C34 H43 O5 Si
	559.2871	1.5	2.7	5.5	565.6	3.070	4.64	C25 H47 N2 O8 Si2
	559.2907	-2.1	-3.8	10.5	567.6	5.107	0.61	C31 H43 O9

Figure 33: MS results for compound **8**.

F Spectroscopic data for compound 9

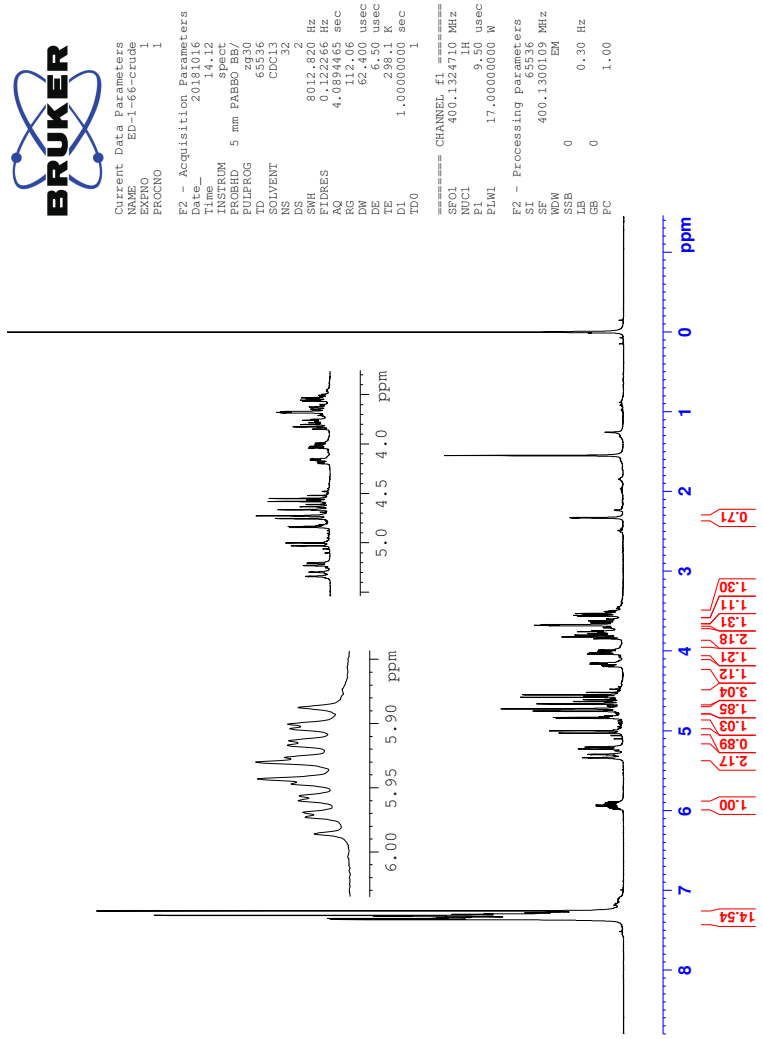

Figure 34: ^{1}H-NMR spectrum of compound **9**.

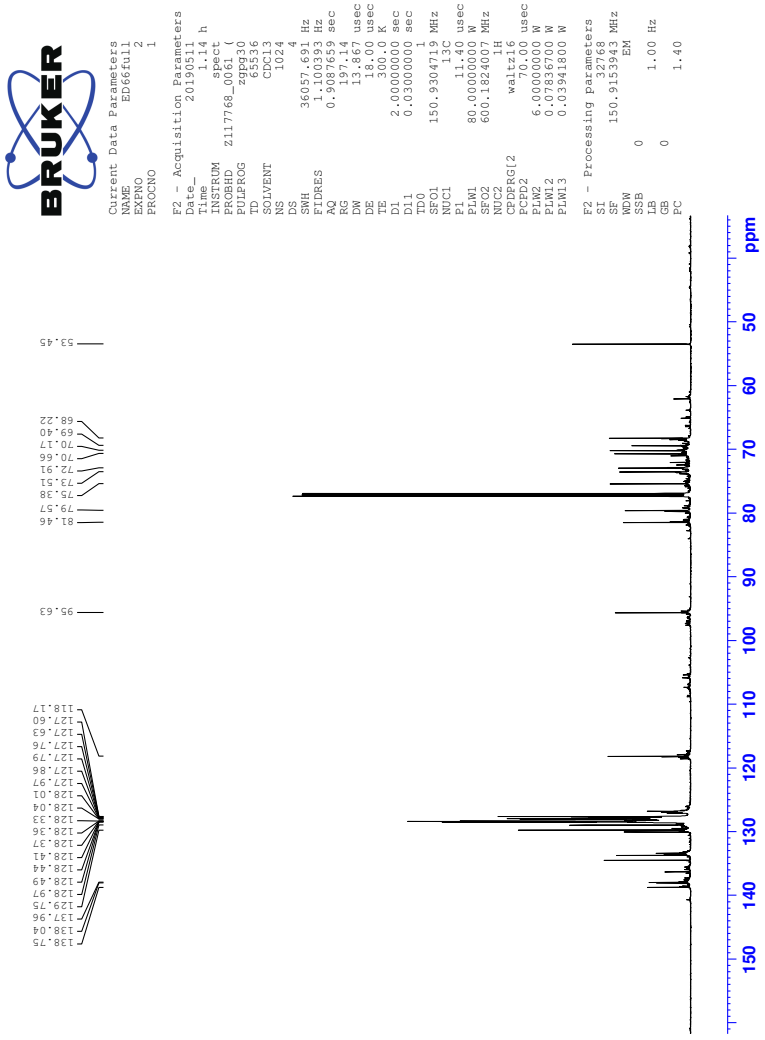

Figure 35: ^{13}C-NMR spectrum of compound **9**.

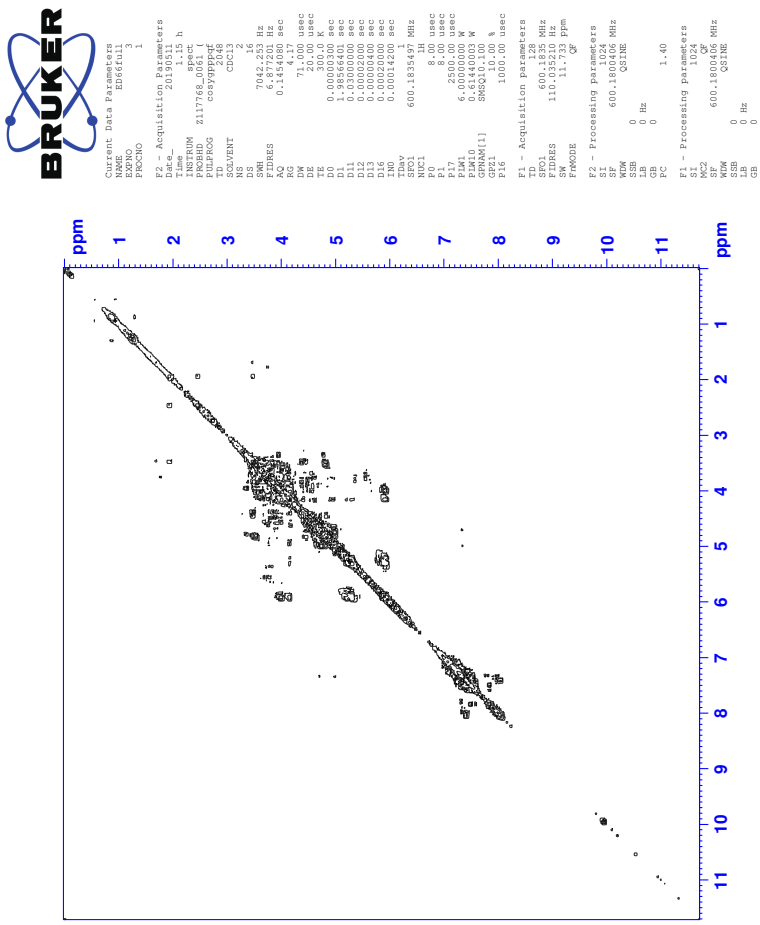

Figure 36: COSY spectrum of compound **9**.

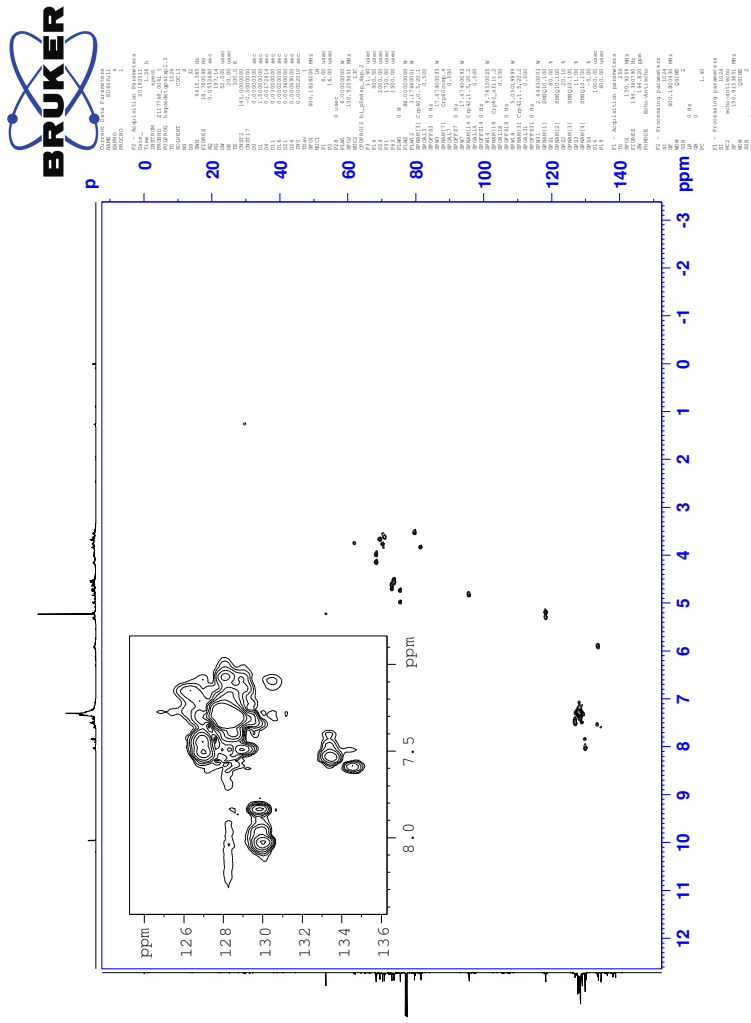

Figure 37: HSQC spectrum of compound **9**.

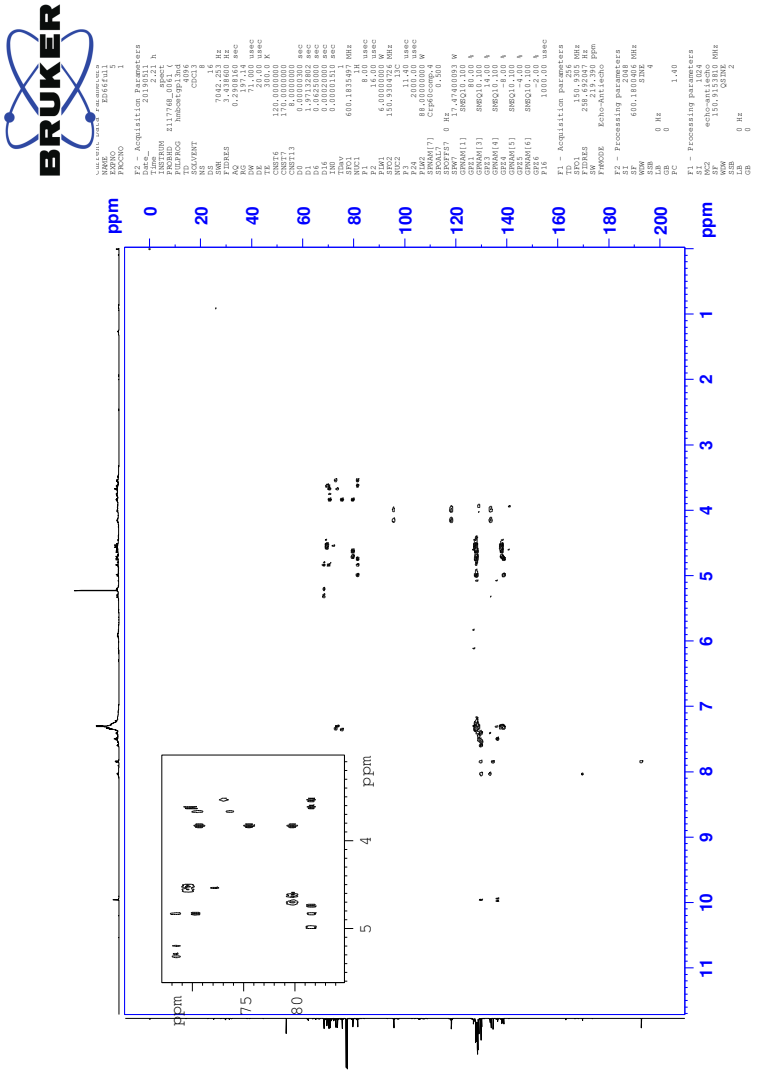

Figure 38: HMBC spectrum of compound **9**.

G Spectroscopic data for compound 10

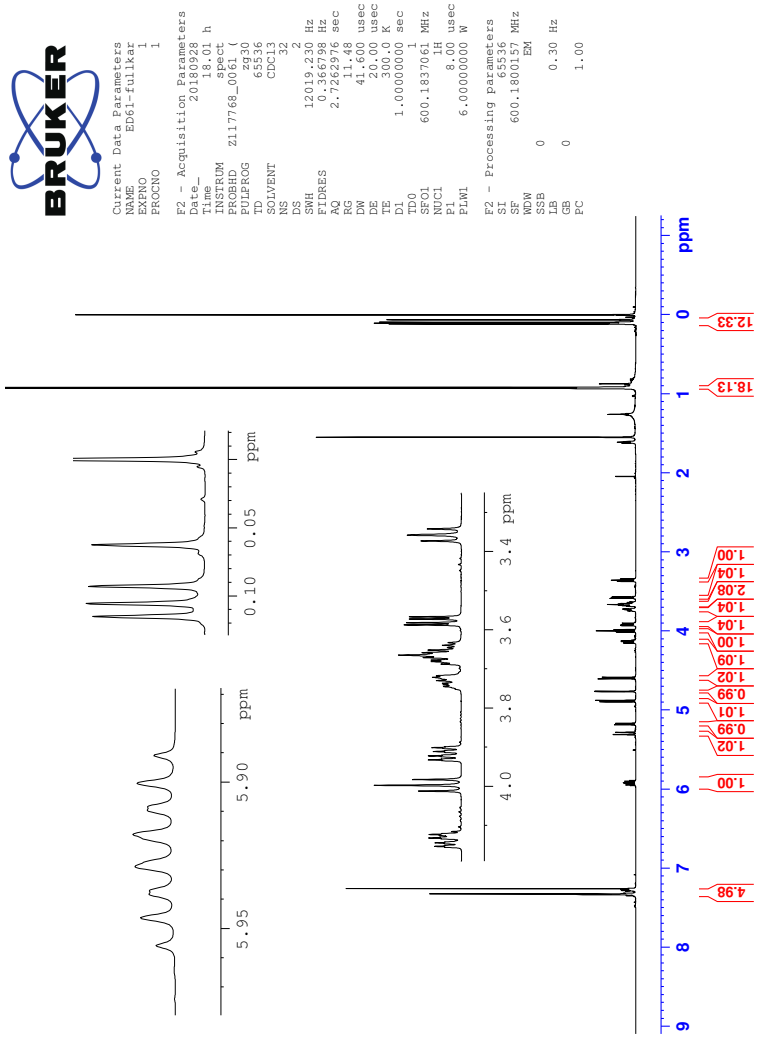

Figure 39: ^{1}H-NMR spectrum of compound **10**.

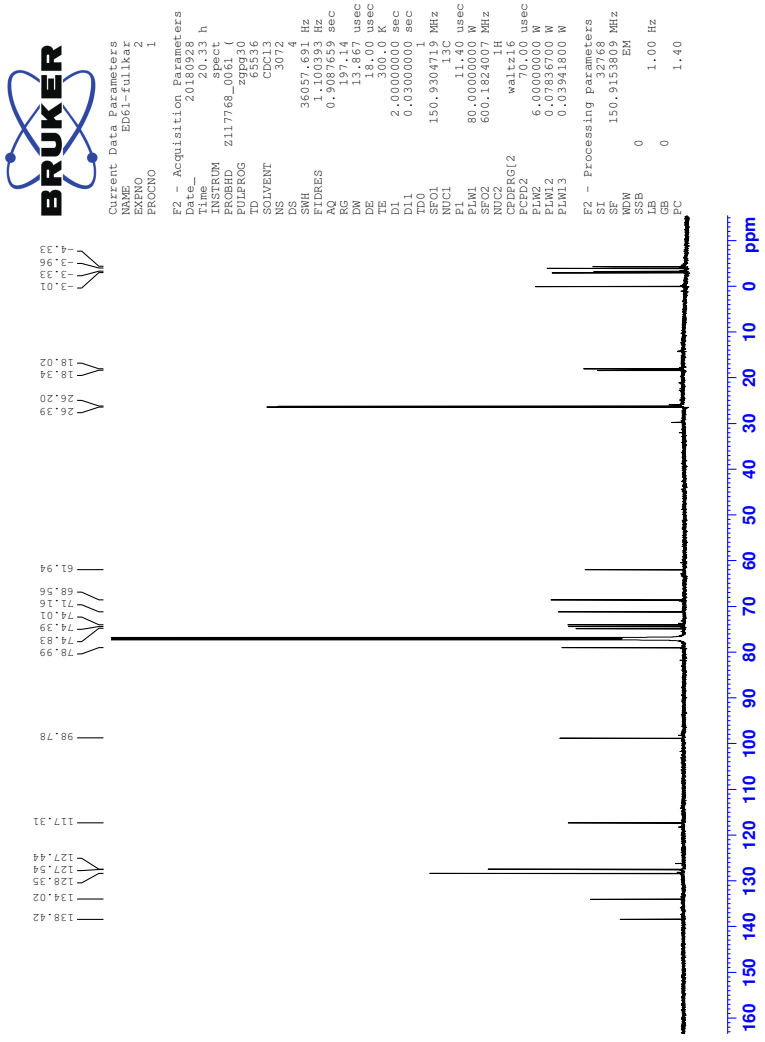

Figure 40: ^{13}C-NMR spectrum of compound **10**.

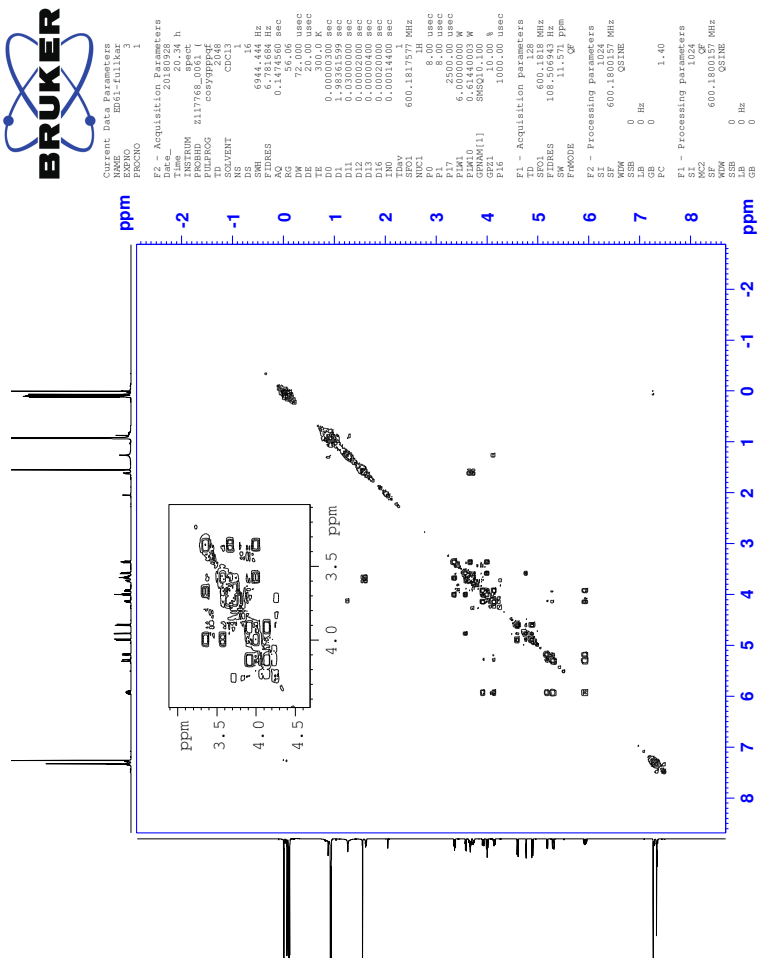

Figure 41: COSY spectrum of compound **10**.

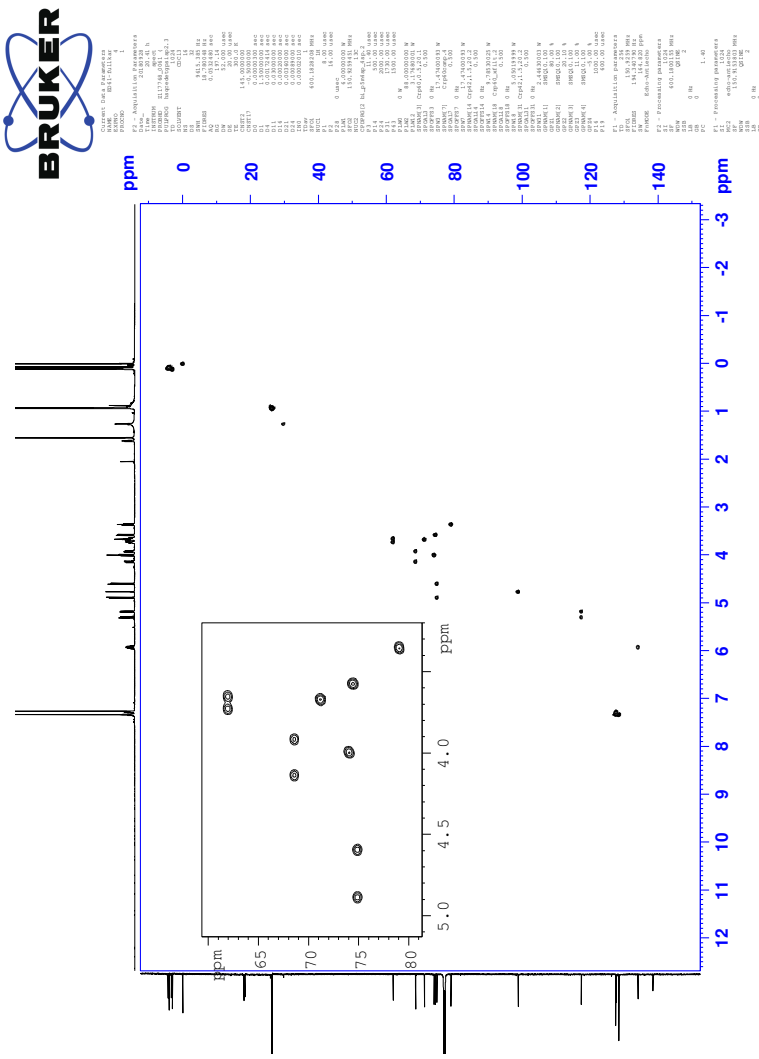

Figure 42: HSQC spectrum of compound **10**.

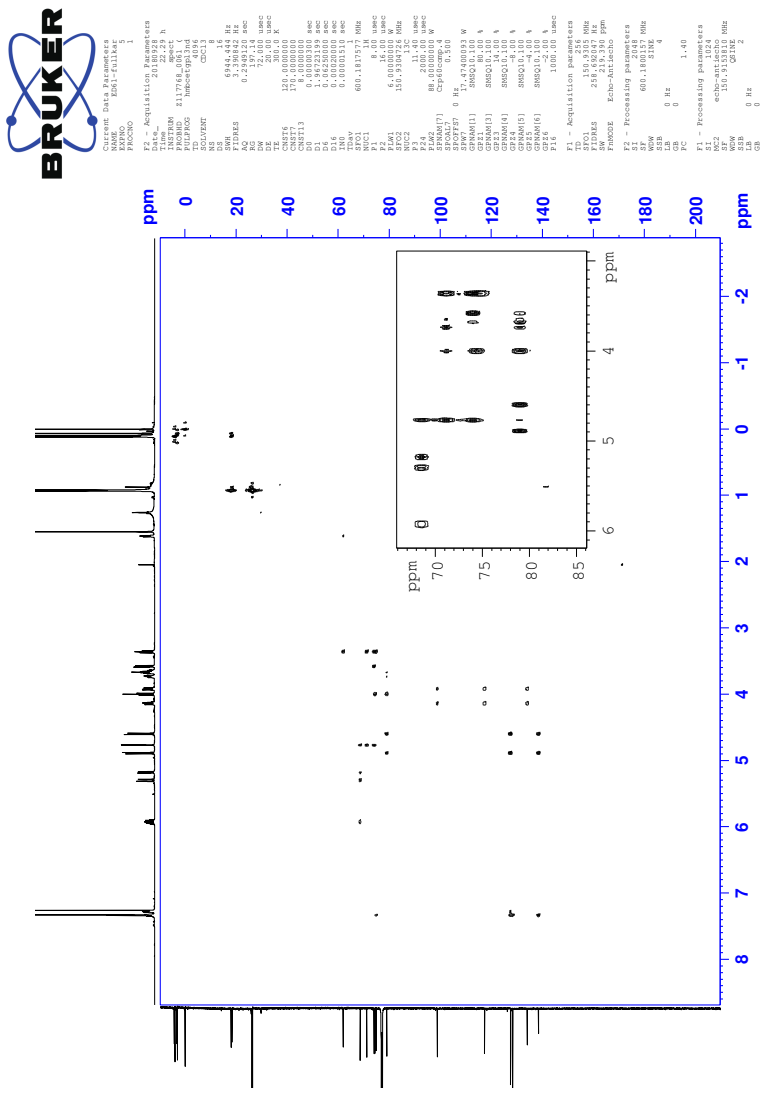

Figure 43: HMBC spectrum of compound **10**.

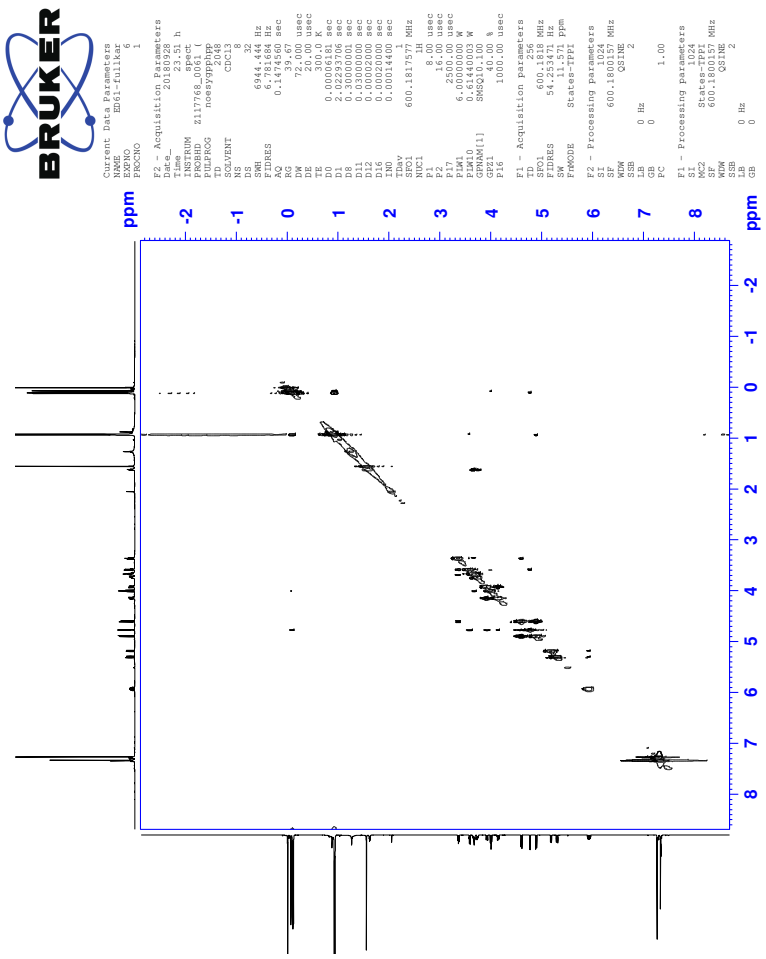

Figure 44: NOESY spectra of compound **10**.

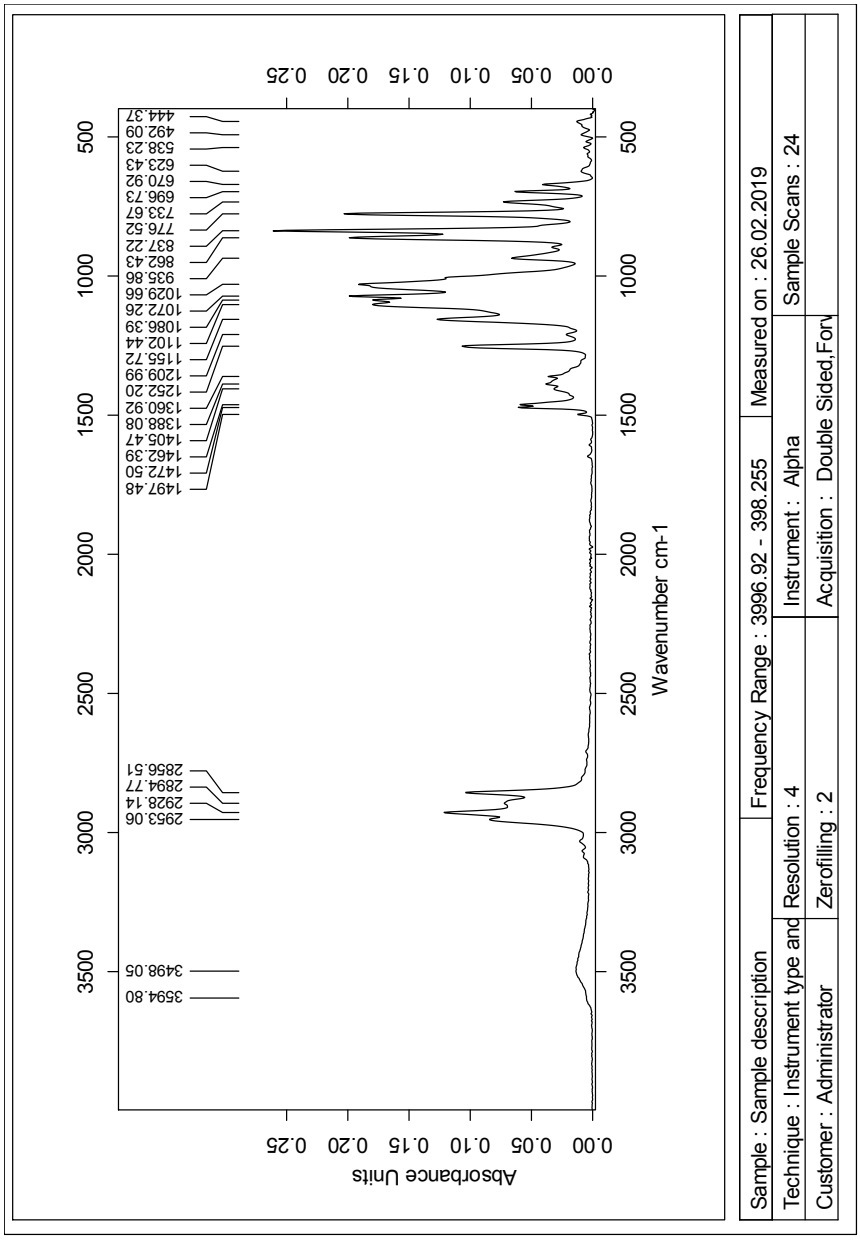

Figure 45: IR spectrum of compound **10**.

Elemental Composition Report **Page 1**

Single Mass Analysis
Tolerance = 4.0 PPM / DBE: min = -50.0, max = 50.0
Element prediction: Off
Number of isotope peaks used for i-FIT = 3

Monoisotopic Mass, Even Electron Ions
3337 formula(e) evaluated with 7 results within limits (all results (up to 1000) for each mass)
Elements Used:
C: 0-100 H: 0-150 N: 0-3 O: 0-10 Na: 0-1 Si: 0-2
svg_20190403_2019_266_2 22 (0.419) AM2 (Ar,35000.0,0.00,0.00); Cm (20:22)
1: TOF MS ES+

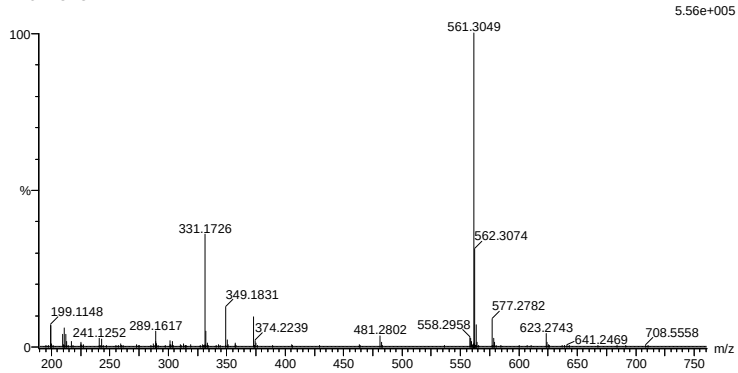

Minimum:				-50.0				
Maximum:		5.0	4.0	50.0				
Mass	Calc. Mass	mDa	PPM	DBE	i-FIT	Norm	Conf(%)	Formula
561.3049	561.3044	0.5	0.9	5.5	726.6	3.751	2.35	C28 H50 O6 Na Si2
	561.3040	0.9	1.6	6.5	722.9	0.053	94.81	C29 H46 O9 Na
	561.3036	1.3	2.3	13.5	729.5	6.684	0.13	C34 H45 O5 Si
	561.3064	-1.5	-2.7	9.5	727.1	4.262	1.41	C31 H45 O9
	561.3068	-1.9	-3.4	8.5	729.8	7.010	0.09	C30 H49 O6 Si2
	561.3071	-2.2	-3.9	1.5	727.5	4.688	0.92	C25 H50 O10 Na Si
	561.3027	2.2	3.9	4.5	728.6	5.829	0.29	C25 H49 N2 O8 Si2

Figure 46: MS results for compound **10**.

H Spectroscopic data for compound 11

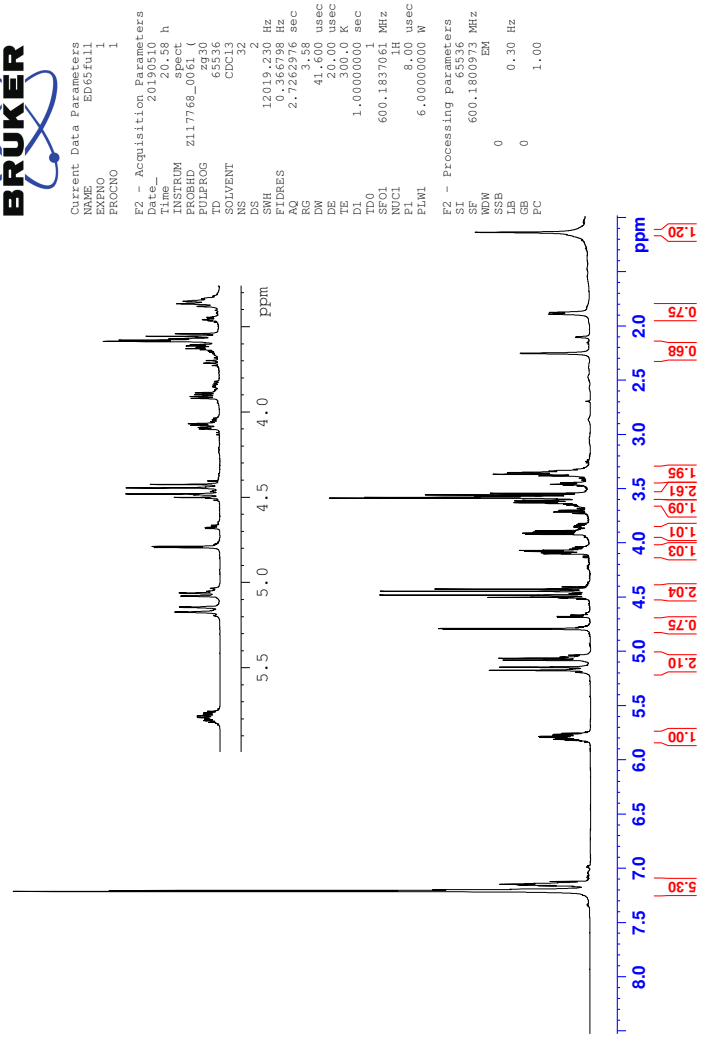

Figure 47: ^{1}H-NMR spectrum of compound **11**.

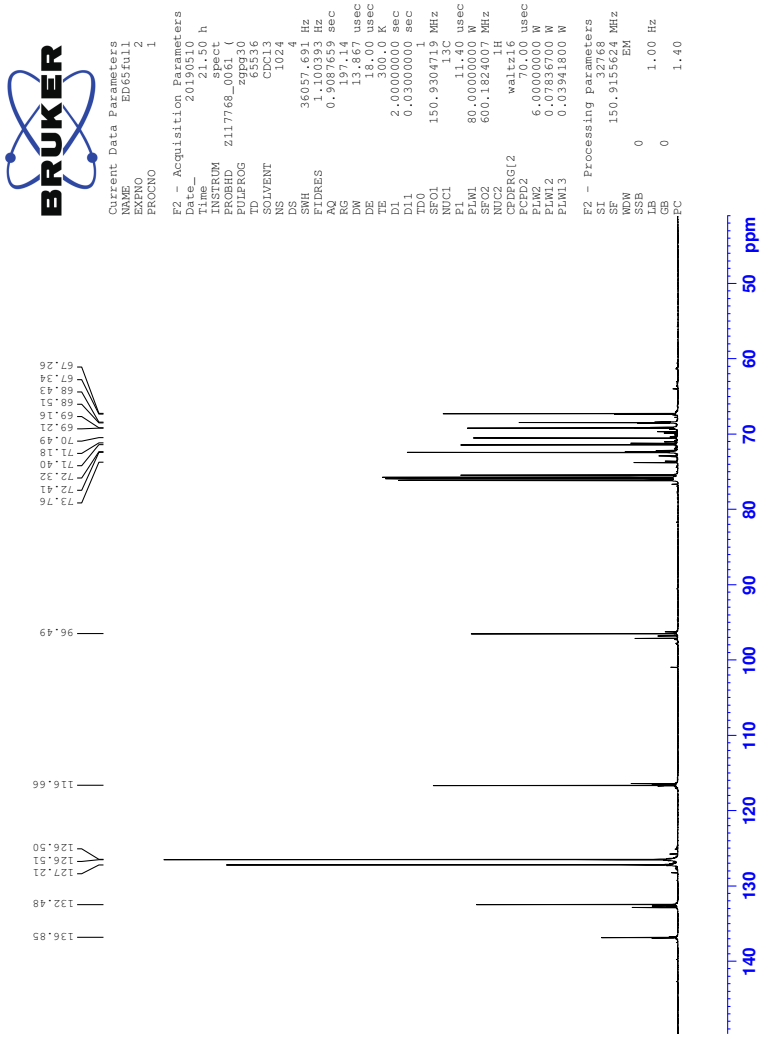

Figure 48: ^{13}C-NMR spectrum of compound **11**.

I Spectroscopic data for compound 12

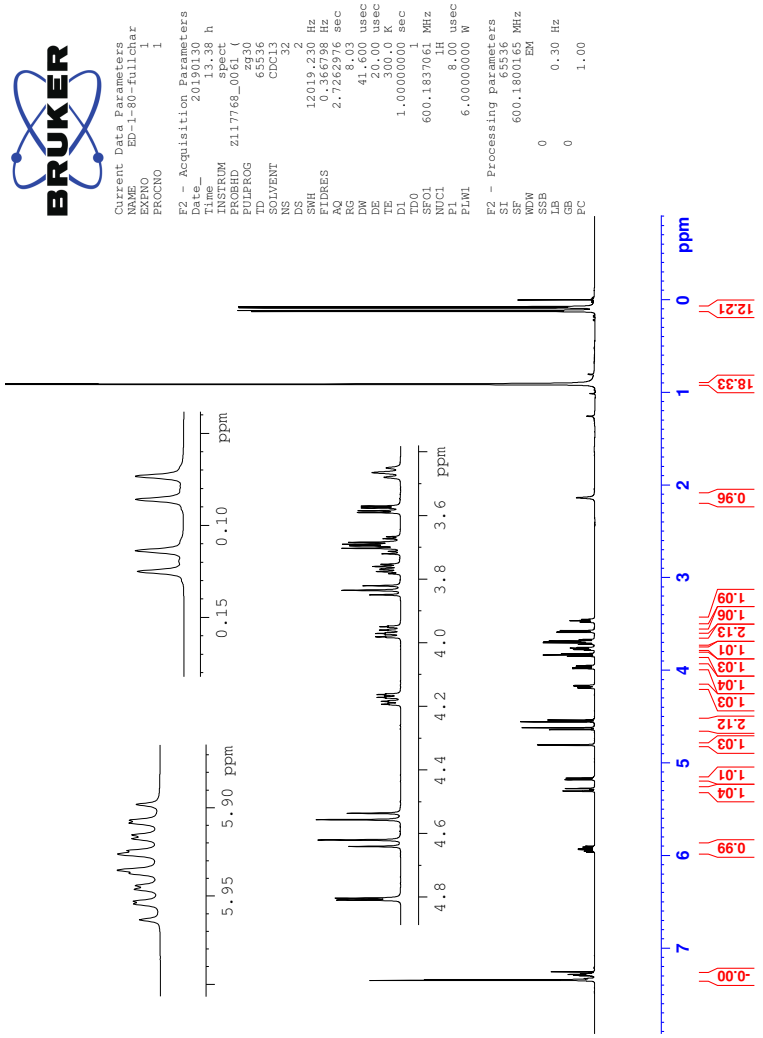

Figure 49: ^{1}H-NMR spectrum of compound **12**.

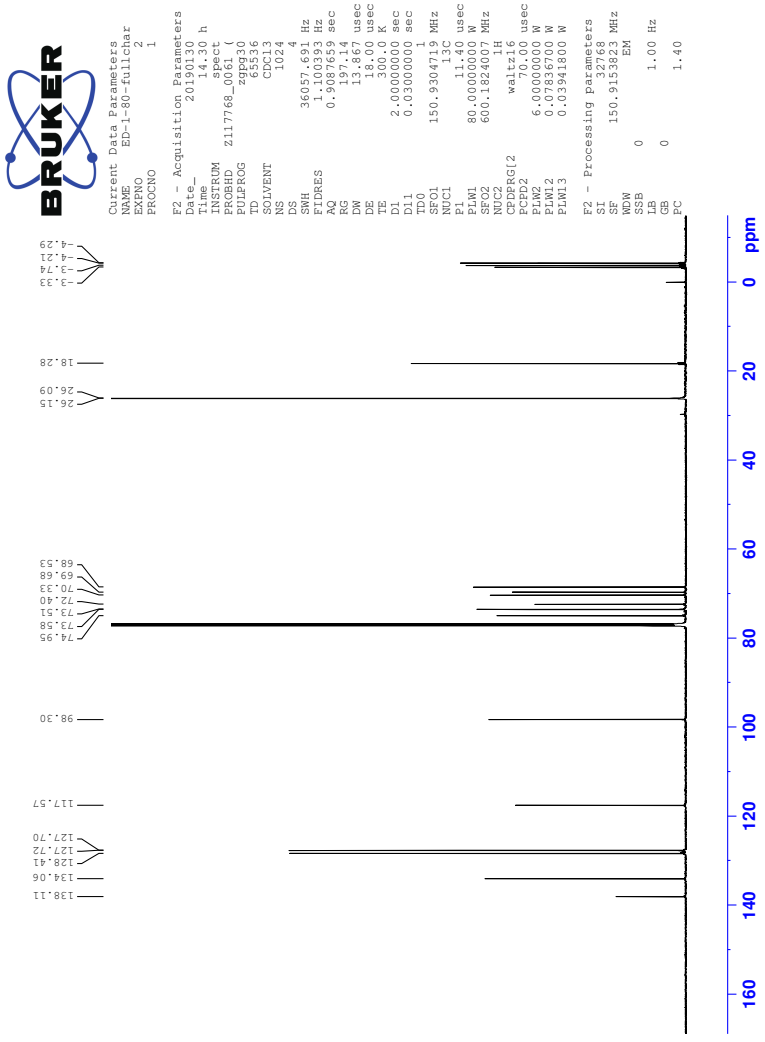

Figure 50: ^{13}C-NMR spectrum of compound **12**.

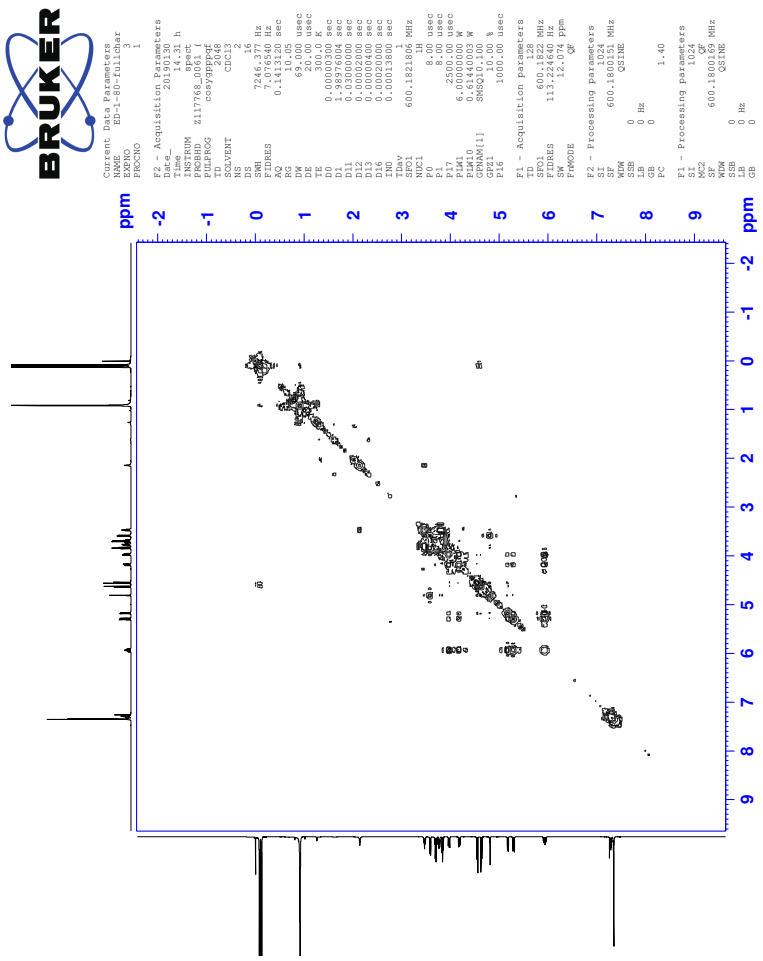

Figure 51: COSY spectrum of compound **12**.

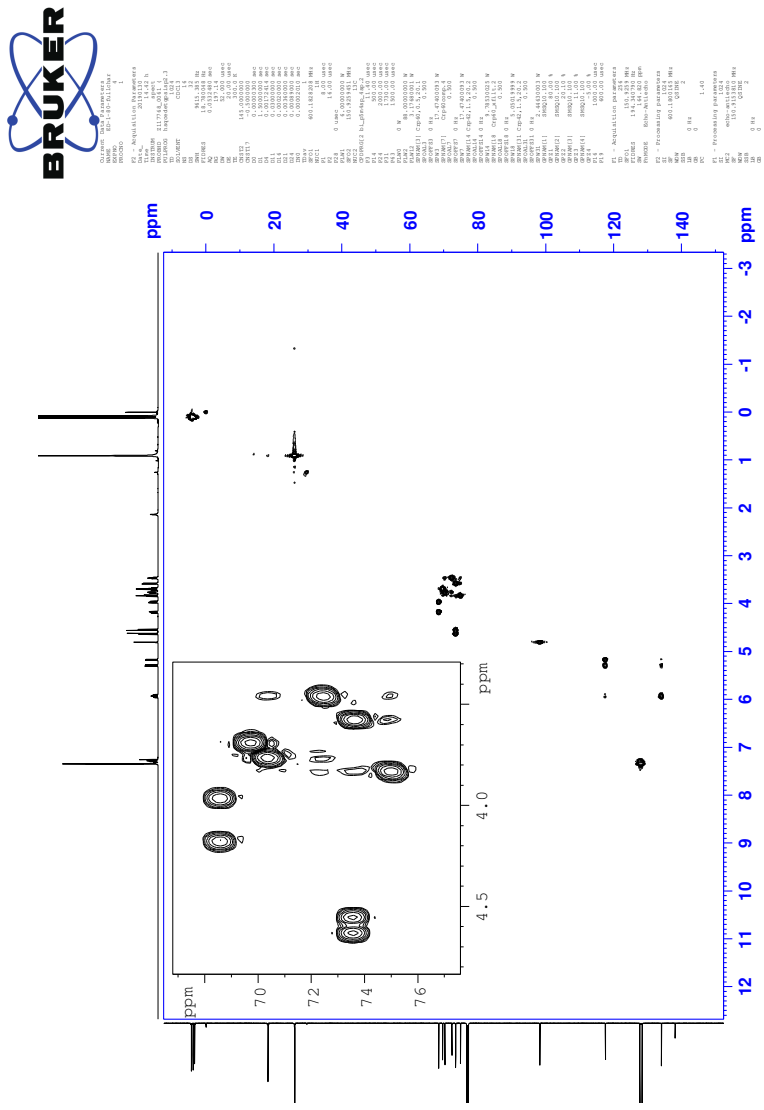

Figure 52: HSQC spectrum of compound **12**.

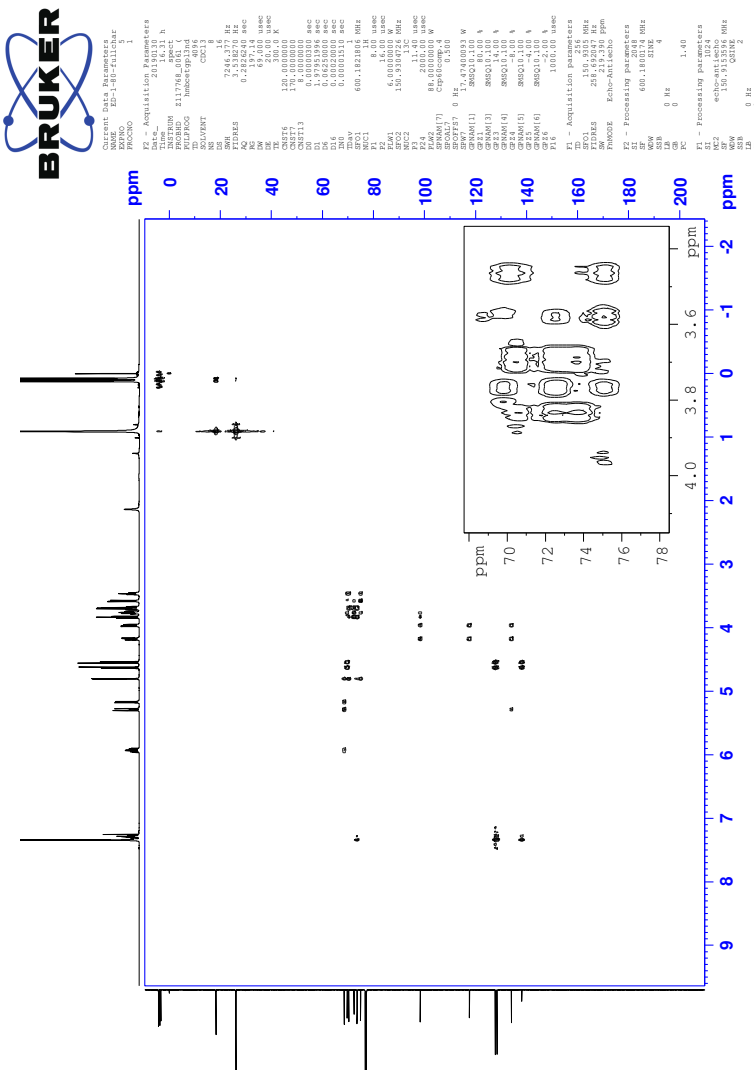

Figure 53: HMBC spectrum of compound **12**.

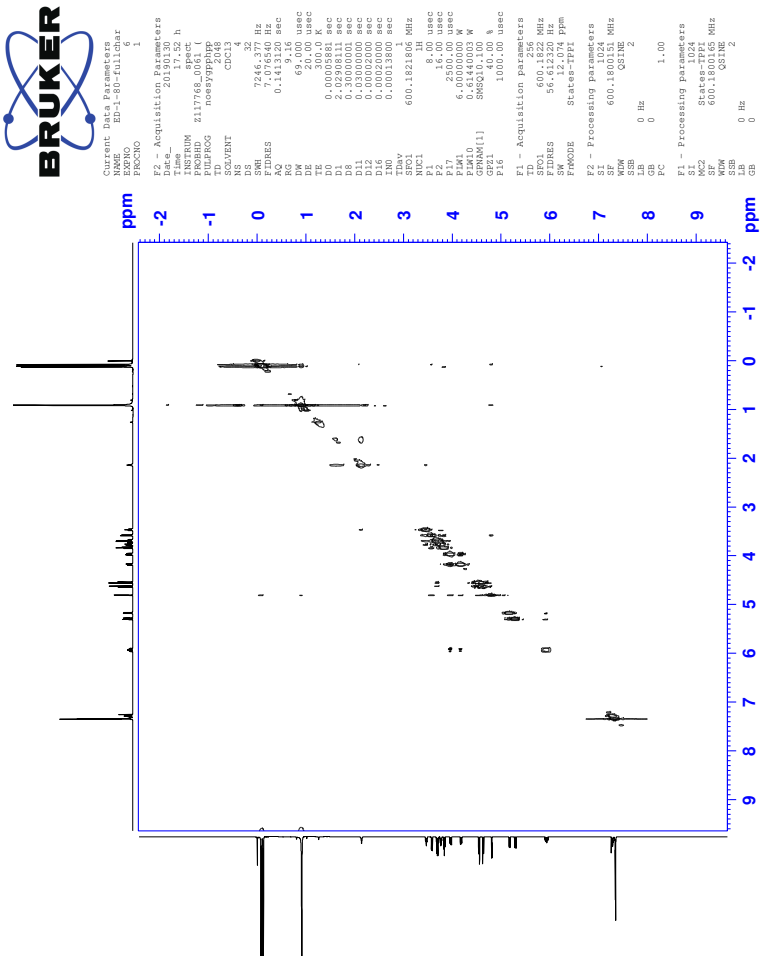

Figure 54: NOESY spectra of compound **12**.

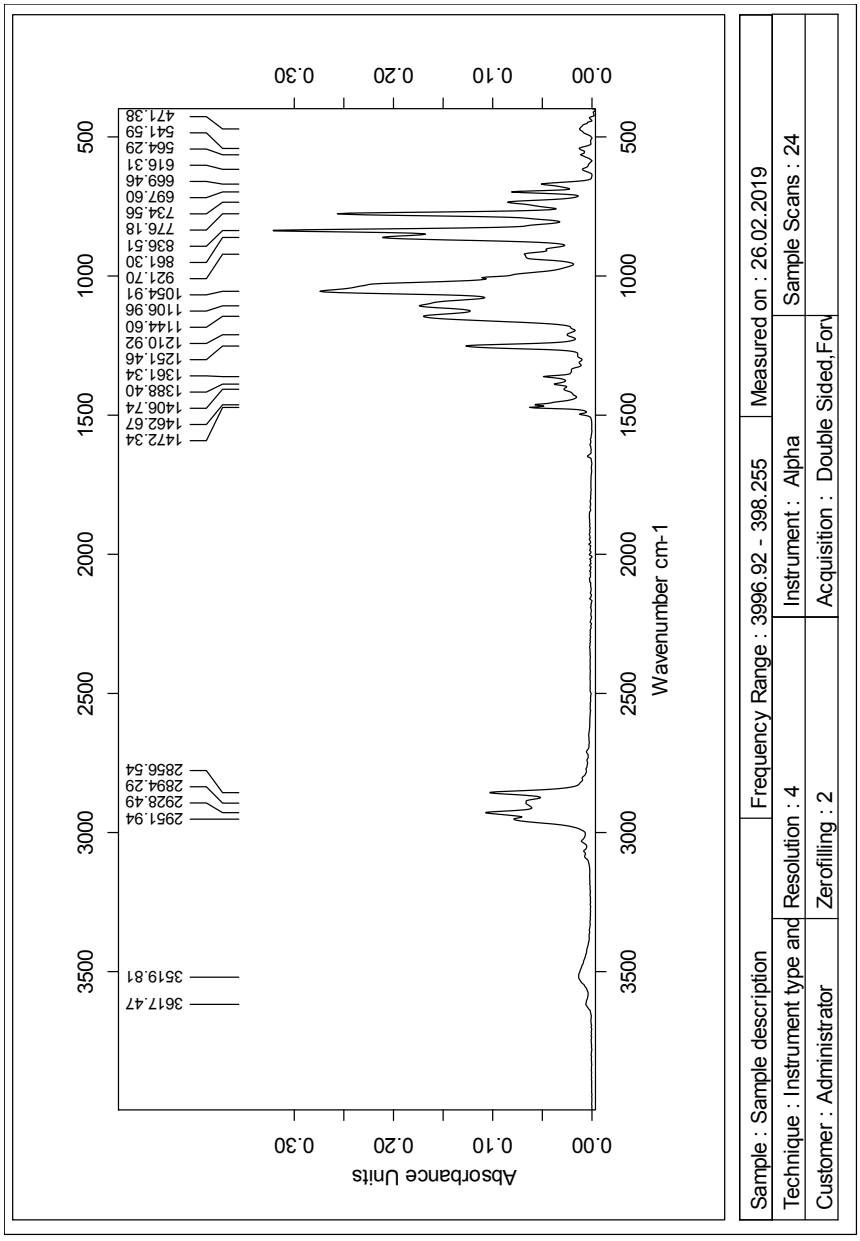

Figure 55: IR spectrum of compound **12**.

Elemental Composition Report **Page 1**

Single Mass Analysis
Tolerance = 4.0 PPM / DBE: min = -50.0, max = 50.0
Element prediction: Off
Number of isotope peaks used for i-FIT = 3

Monoisotopic Mass, Even Electron Ions
3337 formula(e) evaluated with 4 results within limits (all results (up to 1000) for each mass)
Elements Used:
C: 0-100 H: 0-150 N: 0-3 O: 0-10 Na: 0-1 Si: 0-2
svg_20190403_2019_267 18 (0.339) AM2 (Ar,35000.0,0.00,0.00); Cm (18)
1: TOF MS ES+

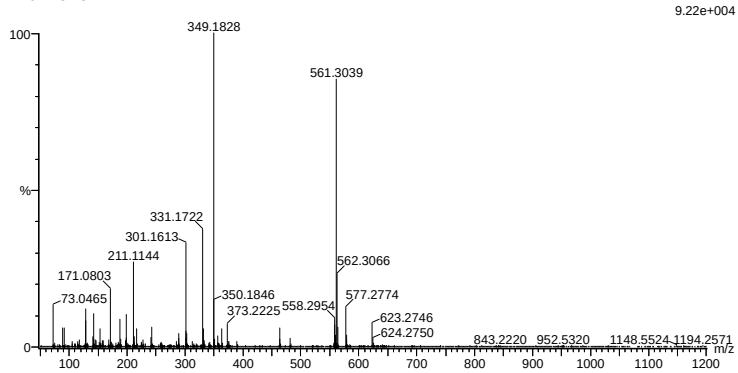

Minimum:				-50.0				
Maximum:		5.0	4.0	50.0				
Mass	Calc. Mass	mDa	PPM	DBE	i-FIT	Norm	Conf(%)	Formula
561.3039	561.3040	-0.1	-0.2	6.5	548.5	1.003	36.67	C29 H46 O9 Na
	561.3036	0.3	0.5	13.5	550.9	3.385	3.39	C34 H45 O5 Si
	561.3044	-0.5	-0.9	5.5	549.1	1.646	19.27	C28 H50 O6 Na Si2
	561.3027	1.2	2.1	4.5	548.4	0.900	40.66	C25 H49 N2 O8 Si2

Figure 56: MS results for compound **12**.

J Spectroscopic data for compound 13

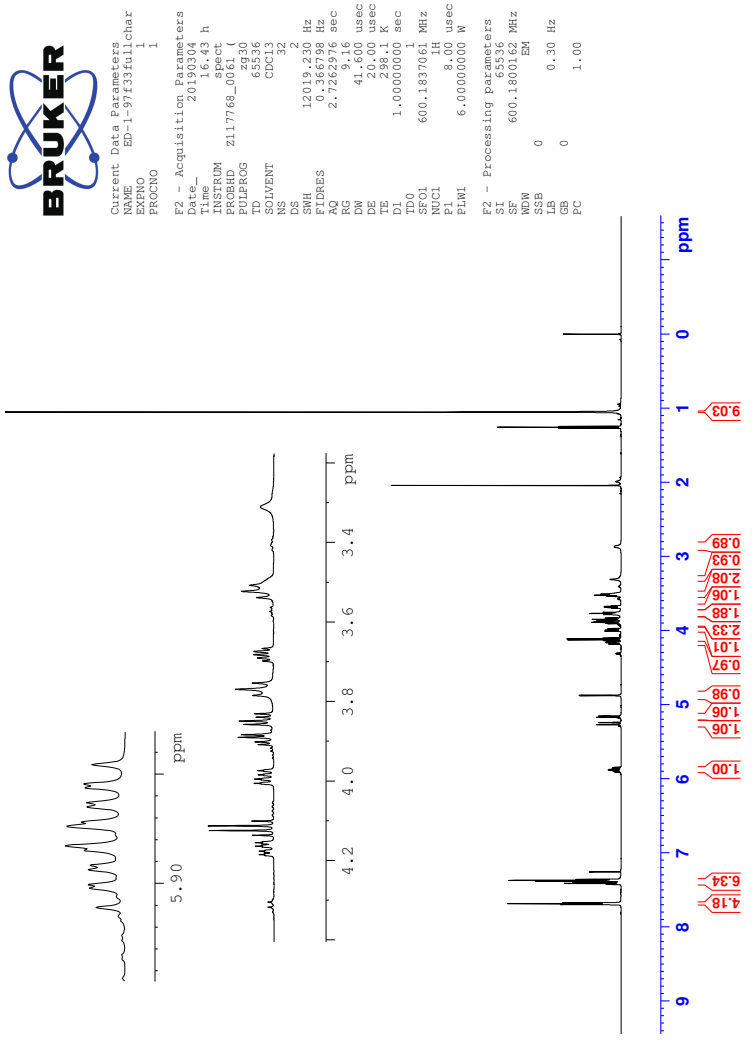

Figure 57: ^{1}H-NMR spectrum of compound **13**.

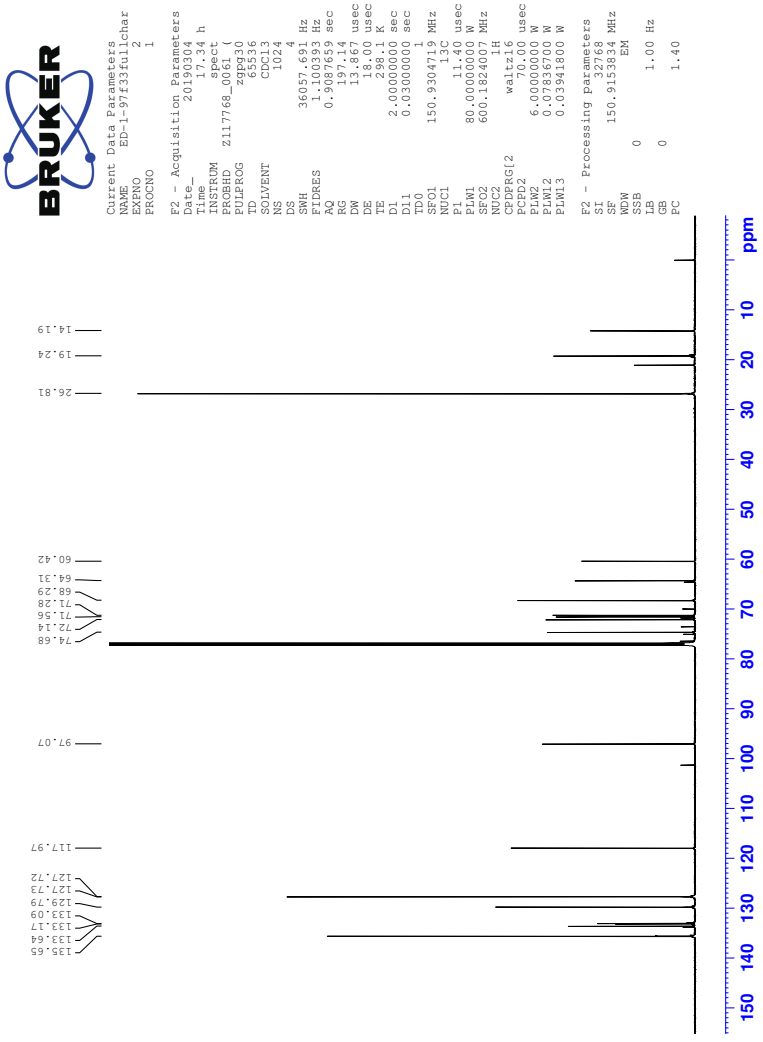

Figure 58: ^{13}C-NMR spectrum of compound **13**.

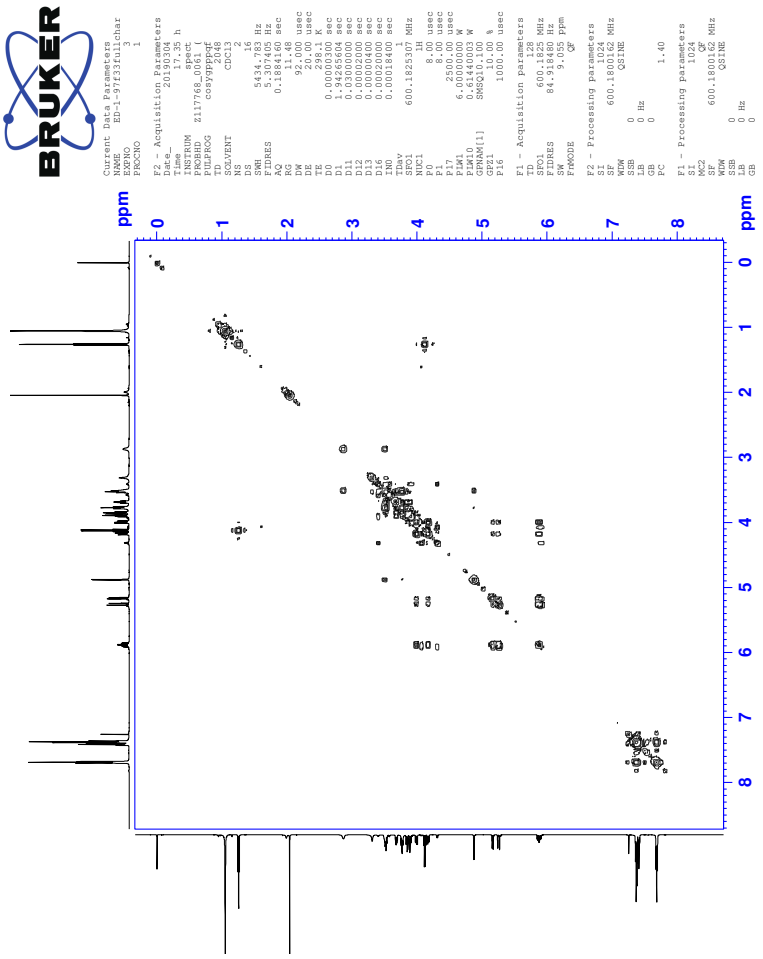

Figure 59: COSY spectrum of compound **13**.

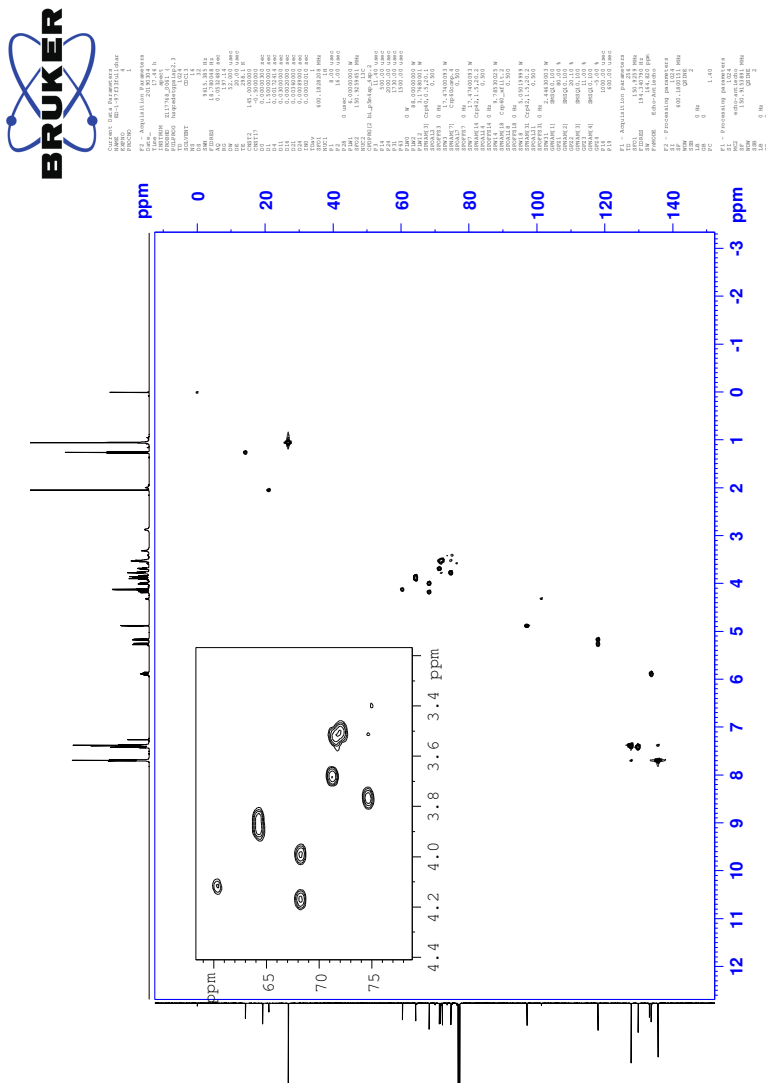

Figure 60: HSQC spectrum of compound **13**.

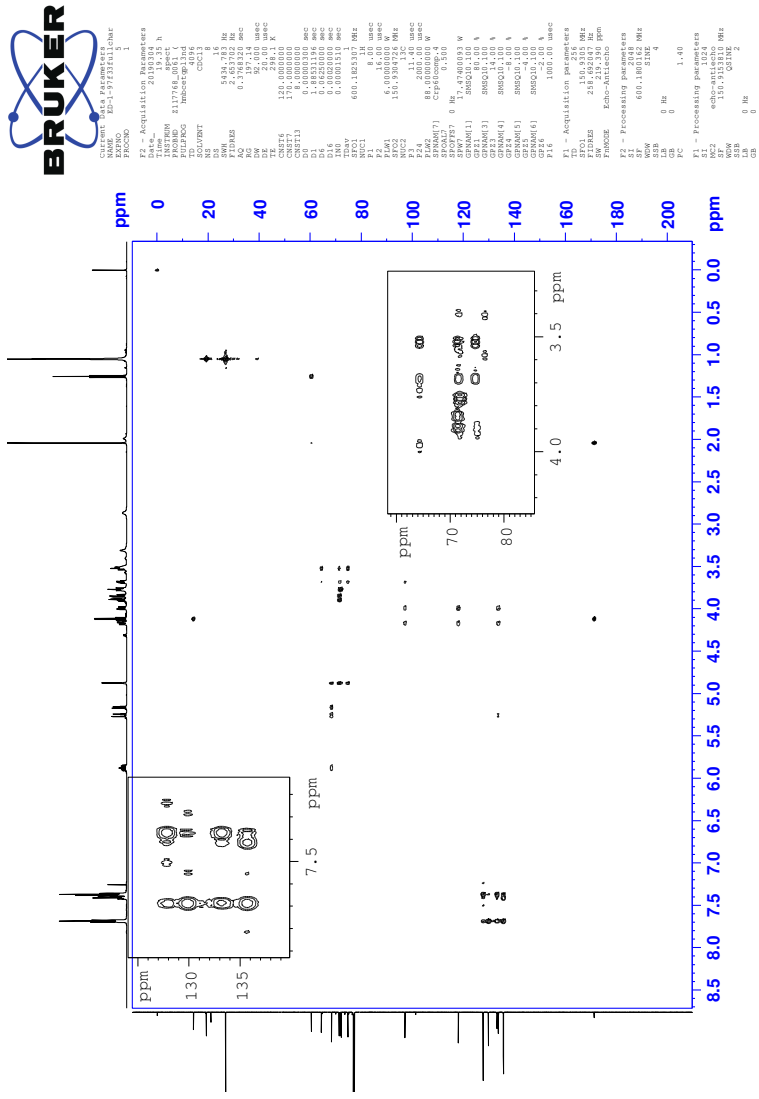

Figure 61: HMBC spectrum of compound **13**.

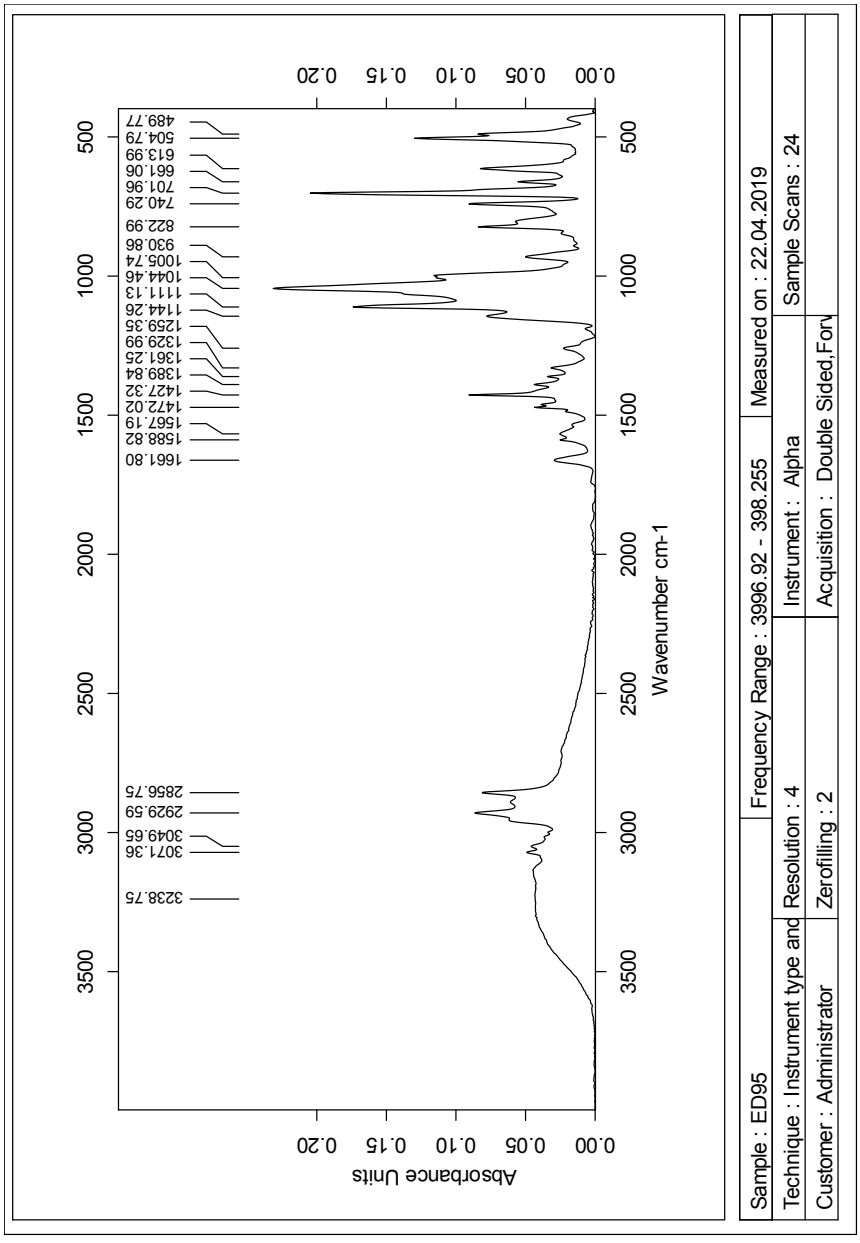

Figure 62: IR spectrum of compound **13**.

Elemental Composition Report **Page 1**

Single Mass Analysis
Tolerance = 2.0 PPM / DBE: min = -50.0, max = 50.0
Element prediction: Off
Number of isotope peaks used for i-FIT = 3

Monoisotopic Mass, Even Electron Ions
1064 formula(e) evaluated with 4 results within limits (all results (up to 1000) for each mass)
Elements Used:
C: 0-100 H: 0-150 O: 0-10 Si: 0-3 Na: 0-1

2019_321_fia 66 (0.743) AM2 (Ar,35000.0,0.00,0.00); Cm (56:70)
1: TOF MS ES+

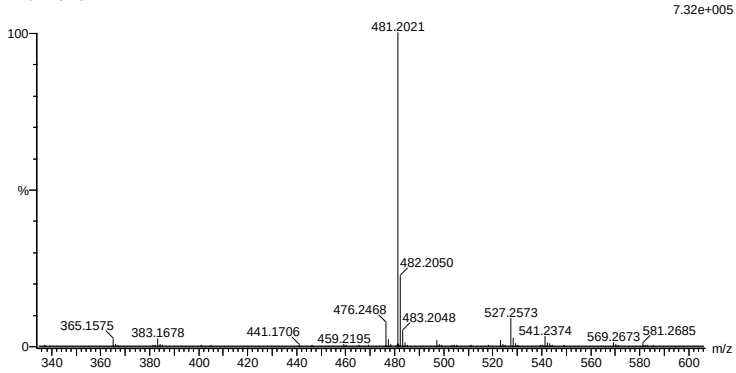

Minimum:				-50.0				
Maximum:		5.0	2.0	50.0				
Mass	Calc. Mass	mDa	PPM	DBE	i-FIT	Norm	Conf(%)	Formula
481.2021	481.2022	-0.1	-0.2	9.5	851.5	0.011	98.93	C25 H34 O6 Si Na
	481.2019	0.2	0.4	16.5	856.4	4.859	0.78	C30 H33 O2 Si2
	481.2026	-0.5	-1.0	8.5	859.2	7.718	0.04	C24 H38 O3 Si3 Na
	481.2015	0.6	1.2	17.5	857.5	5.979	0.25	C31 H29 O5

Figure 63: MS results for compound **13**.

K Spectroscopic data for compound 14

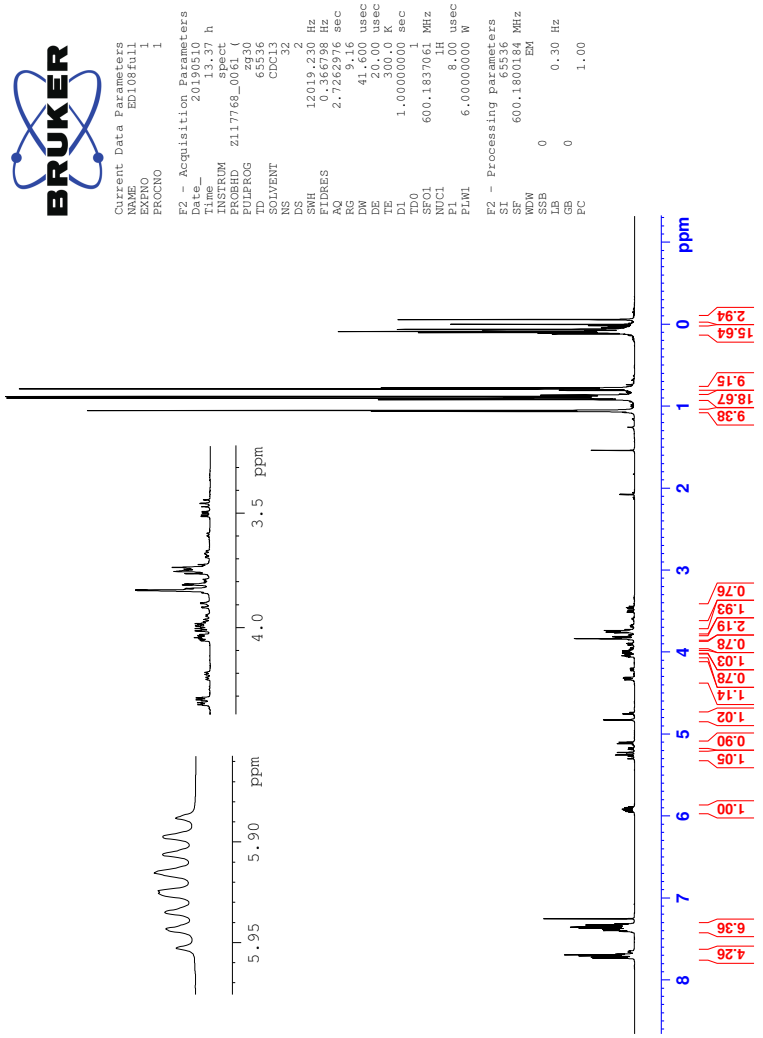

Figure 64: ^{1}H-NMR spectrum of compound **14**.

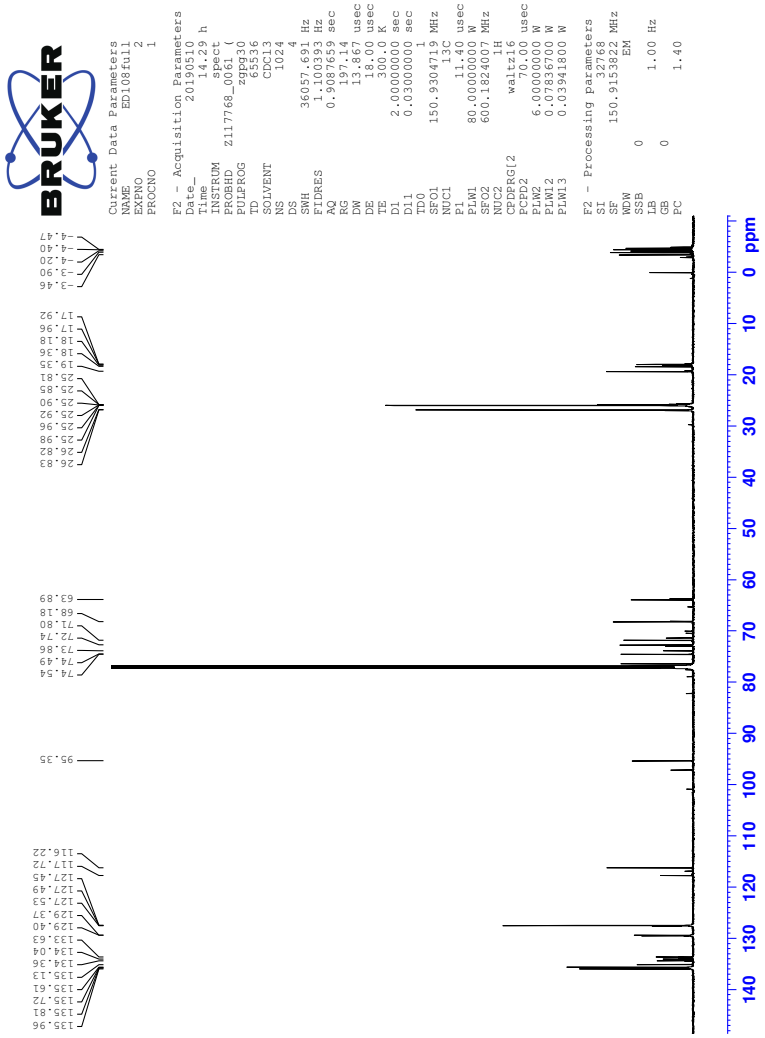

Figure 65: ^{13}C-NMR spectrum of compound **14**.

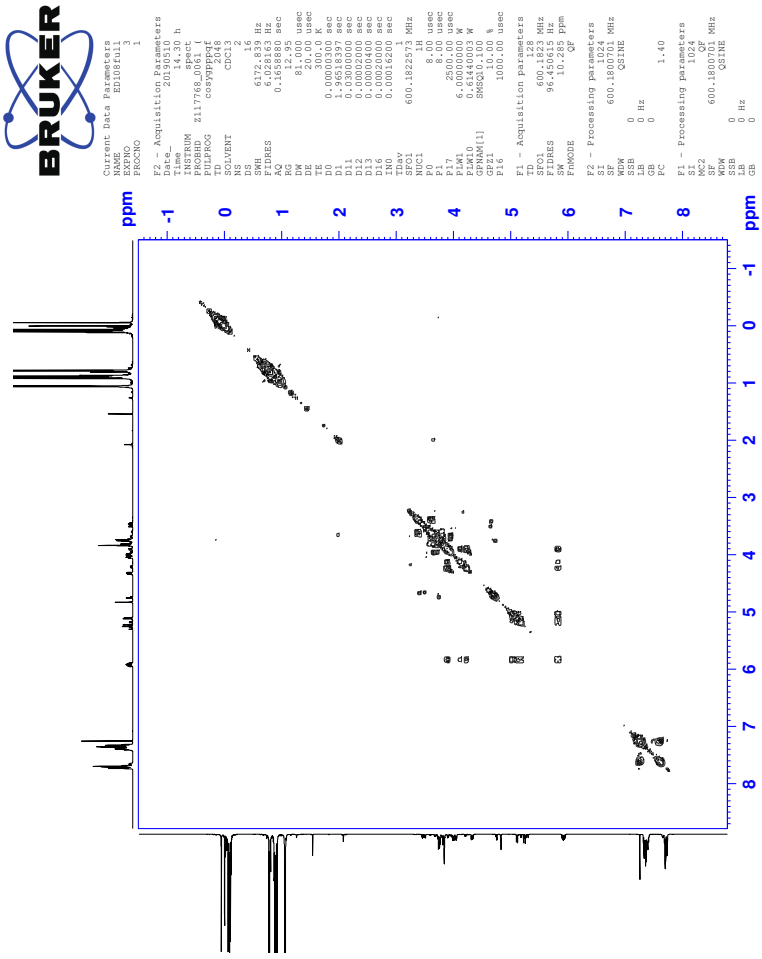

Figure 66: COSY spectrum of compound **14**.

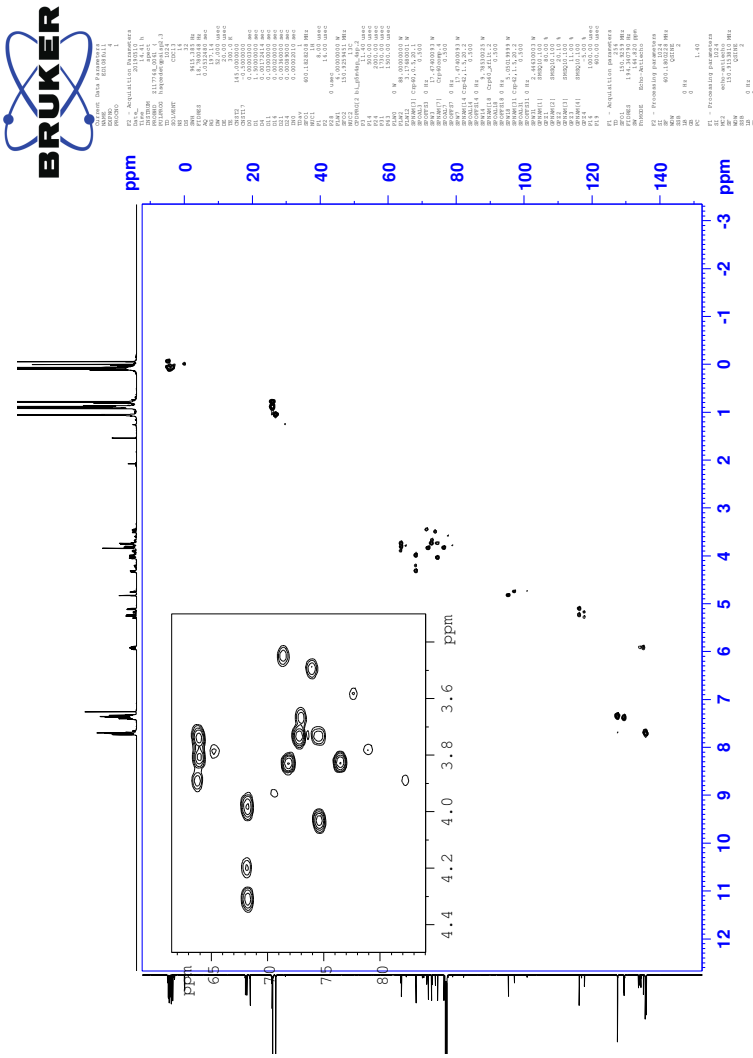

Figure 67: HSQC spectrum of compound **14**.

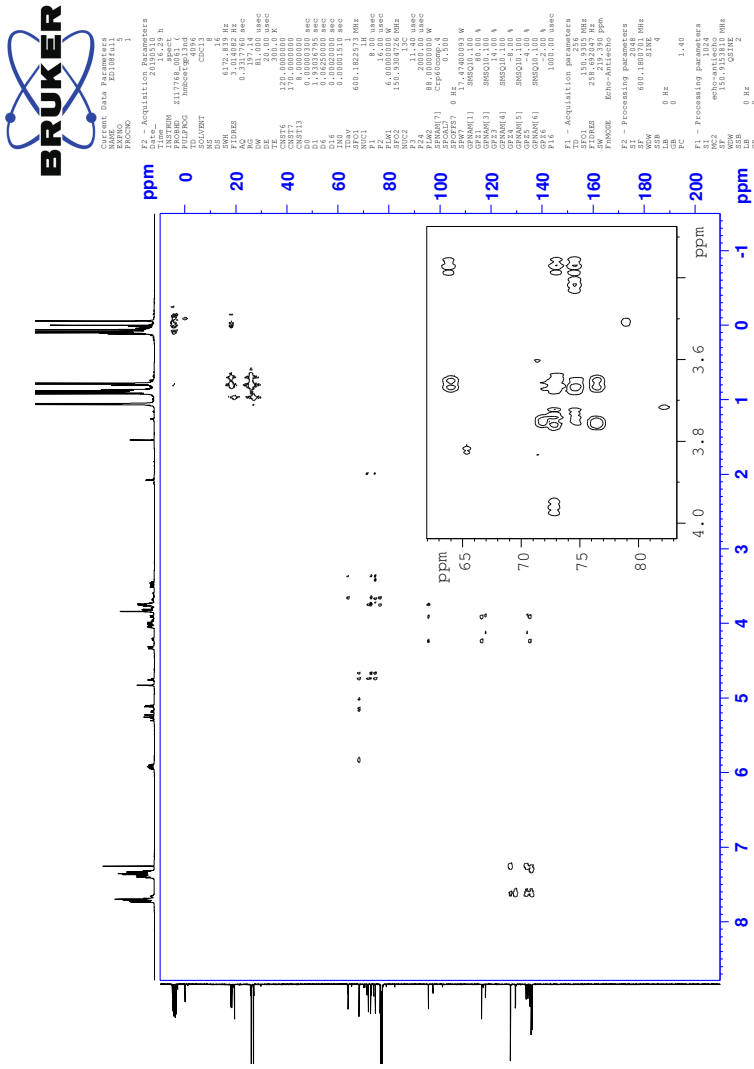

Figure 68: HMBC spectrum of compound **14**.

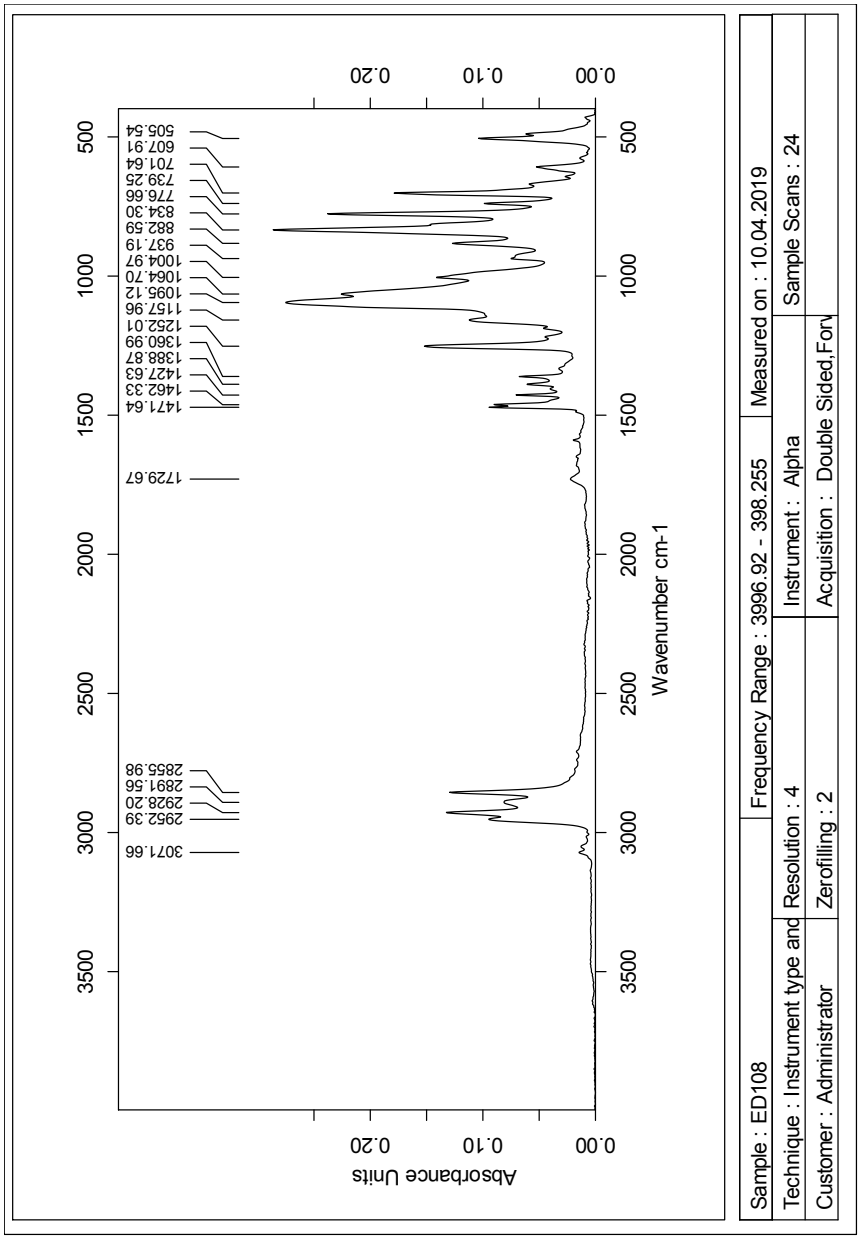

Figure 69: IR spectrum of compound **14**.

Elemental Composition Report **Page 1**

Single Mass Analysis
Tolerance = 2.0 PPM / DBE: min = -2.0, max = 50.0
Element prediction: Off
Number of isotope peaks used for i-FIT = 3

Monoisotopic Mass, Even Electron Ions
2071 formula(e) evaluated with 4 results within limits (up to 50 closest results for each mass)
Elements Used:
C: 0-500 H: 0-1000 N: 0-1 O: 0-10 Na: 0-1 Si: 0-4
2019_322_fia 52 (0.589) AM2 (Ar,35000.0,0.00,0.00); Cm (42:52)
1: TOF MS ES+

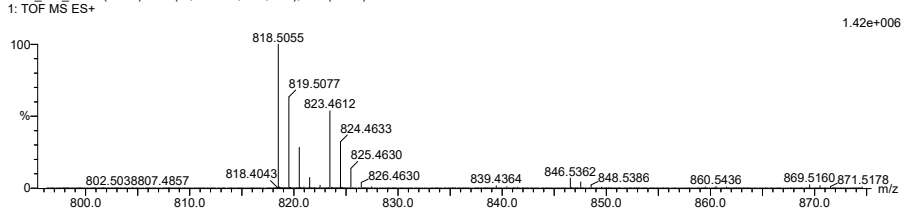

Minimum:			-2.0					
Maximum:		5.0	2.0	50.0				
Mass	Calc. Mass	mDa	PPM	DBE	i-FIT	Norm	Conf(%)	Formula
823.4612	823.4613	-0.1	-0.1	10.5	616.5	0.000	99.99	C44 H72 O9 Na Si2
	823.4609	0.3	0.4	17.5	627.3	10.744	0.00	C49 H71 O5 Si3
	823.4617	-0.5	-0.6	9.5	627.8	11.256	0.00	C43 H76 O6 Na Si4
	823.4605	0.7	0.9	18.5	625.8	9.246	0.01	C50 H67 O8 Si

Figure 70: MS results for compound **14**.

L Spectroscopic data for compound 15

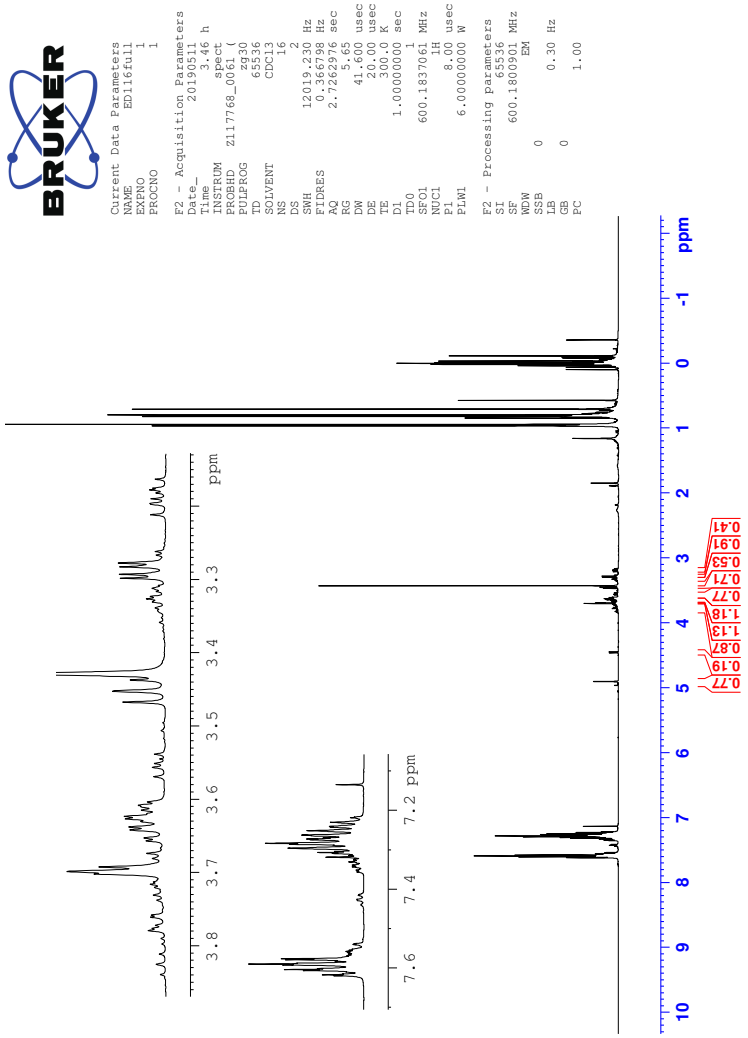

Figure 71: ^{1}H-NMR spectrum of compound **15**.

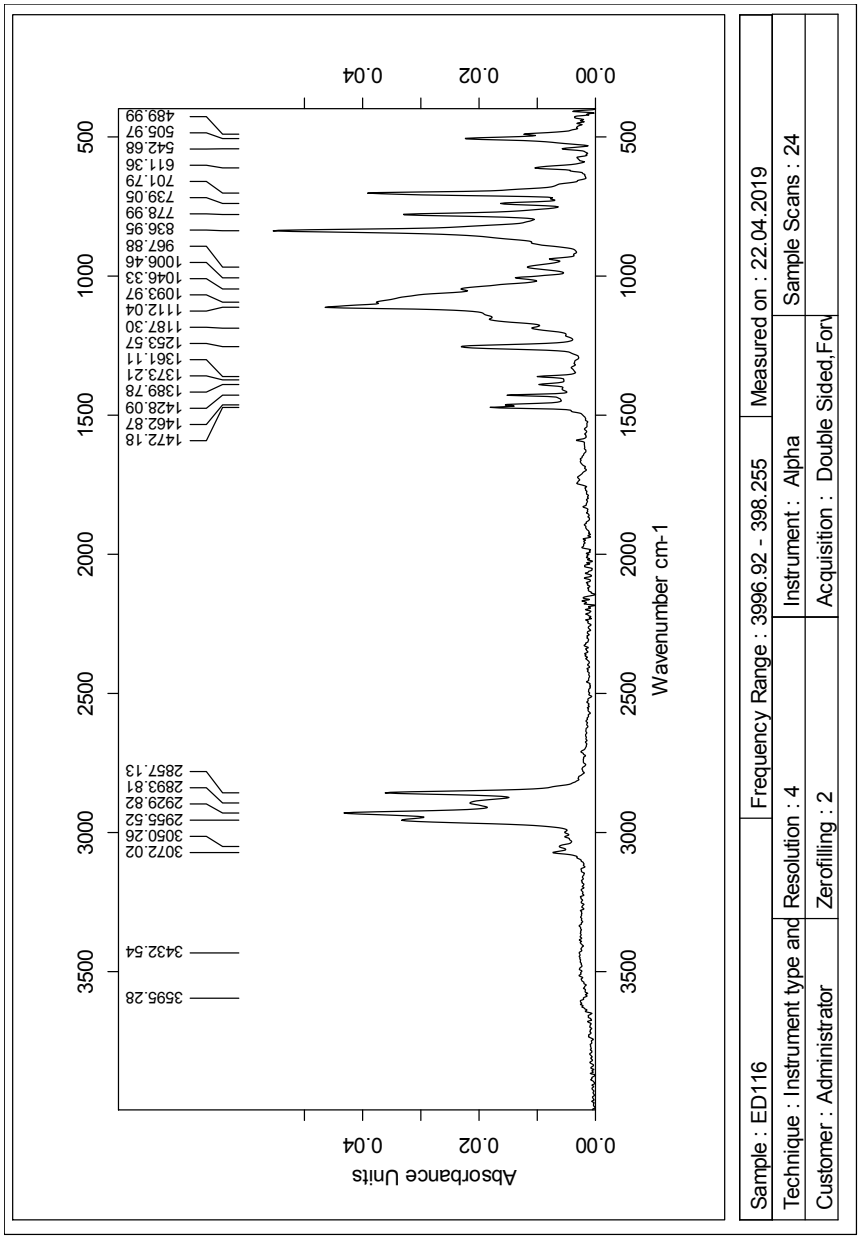

Figure 72: IR spectrum of compound **15**.

Elemental Composition Report **Page 1**

Single Mass Analysis
Tolerance = 2.0 PPM / DBE: min = -50.0, max = 50.0
Element prediction: Off
Number of isotope peaks used for i-FIT = 3

Monoisotopic Mass, Even Electron Ions
1694 formula(e) evaluated with 5 results within limits (all results (up to 1000) for each mass)
Elements Used:
C: 0-100 H: 0-150 O: 0-10 Na: 0-1 Si: 0-5

2019-372 33 (0.619) AM2 (Ar,35000.0,0.00,0.00); Cm (25:34)
1: TOF MS ES+

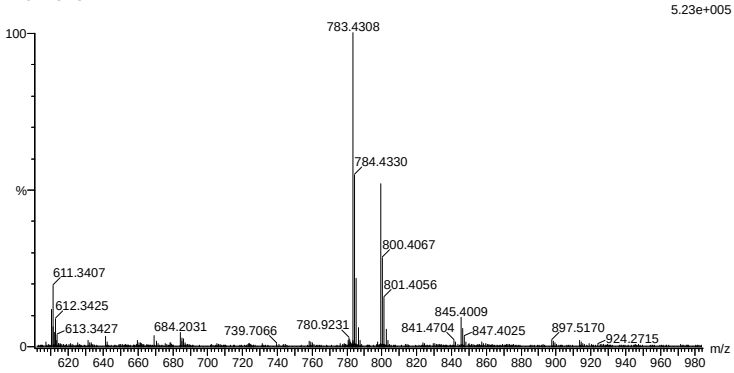

Mass	Calc. Mass	mDa	PPM	DBE	i-FIT	Norm	Conf(%)	Formula
Minimum:				-50.0				
Maximum:		5.0	2.0	50.0				
783.4308	783.4304	0.4	0.5	8.5	660.5	6.032	0.24	C40 H72 O6 Na Si4
	783.4300	0.8	1.0	15.5	662.7	8.264	0.03	C45 H71 O2 Si5
	783.4300	0.8	1.0	9.5	654.5	0.015	98.48	C41 H68 O9 Na Si2
	783.4296	1.2	1.5	16.5	660.7	6.223	0.20	C46 H67 O5 Si3
	783.4324	-1.6	-2.0	12.5	659.0	4.551	1.06	C43 H67 O9 Si2

Figure 73: MS results for compound **15**.

M Spectroscopic data for compound 16

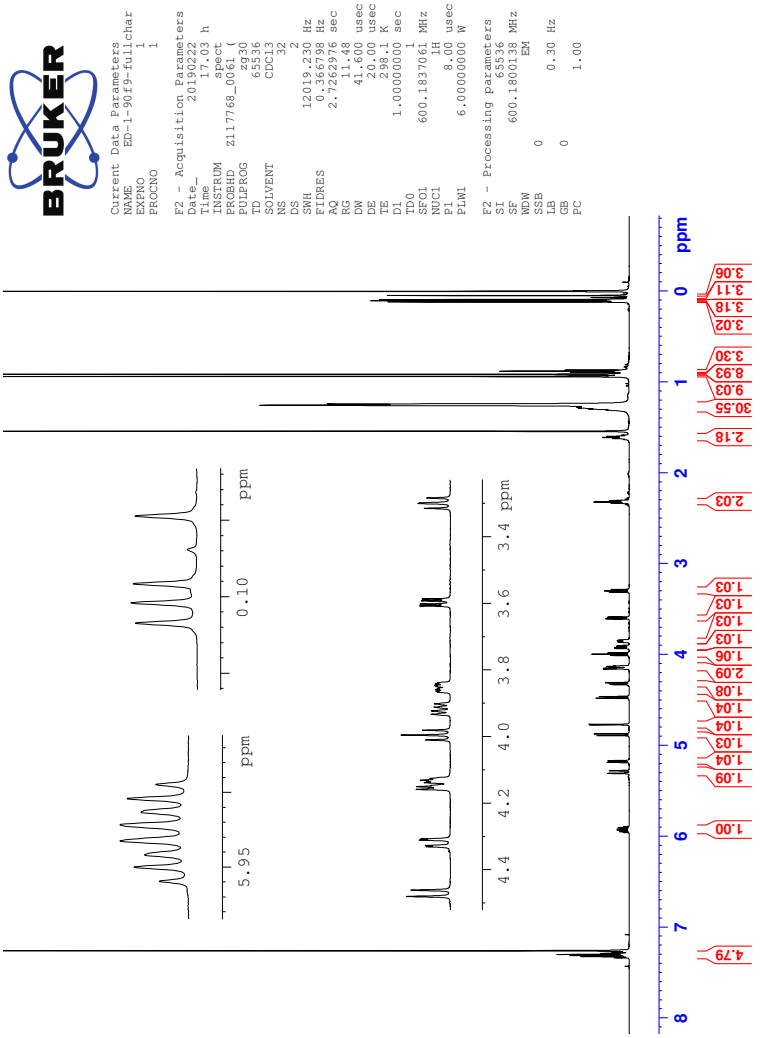

Figure 74: ^{1}H-NMR spectrum of compound **16**.

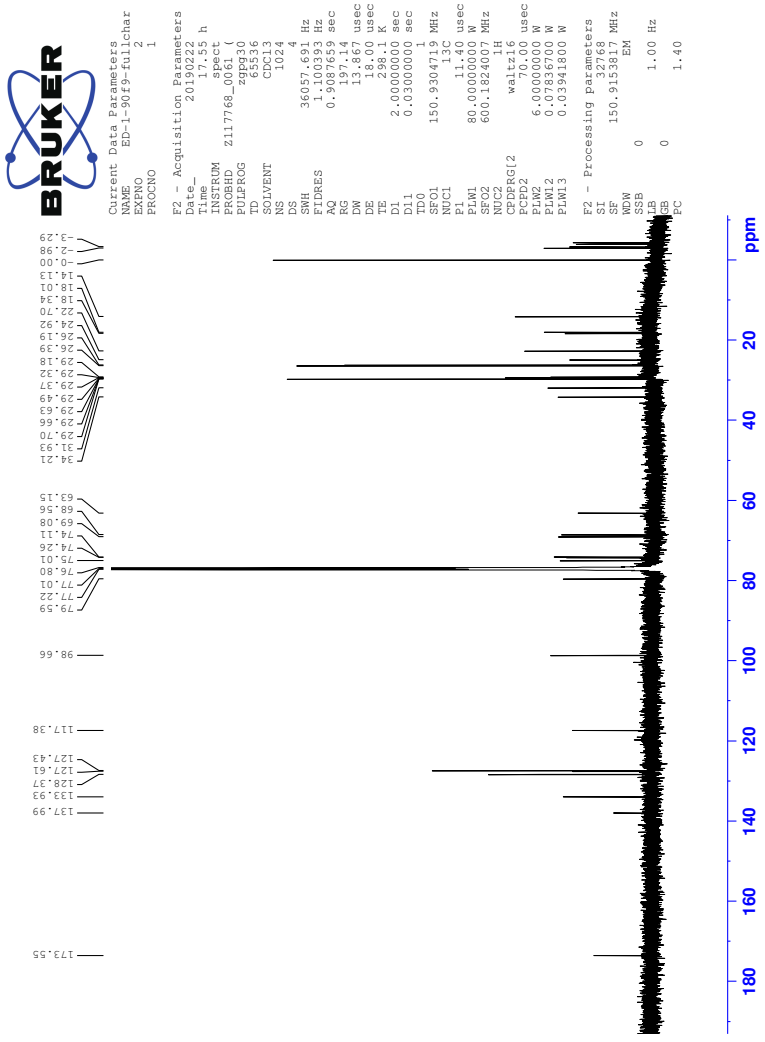

Figure 75: ^{13}C-NMR spectrum of compound **16**.

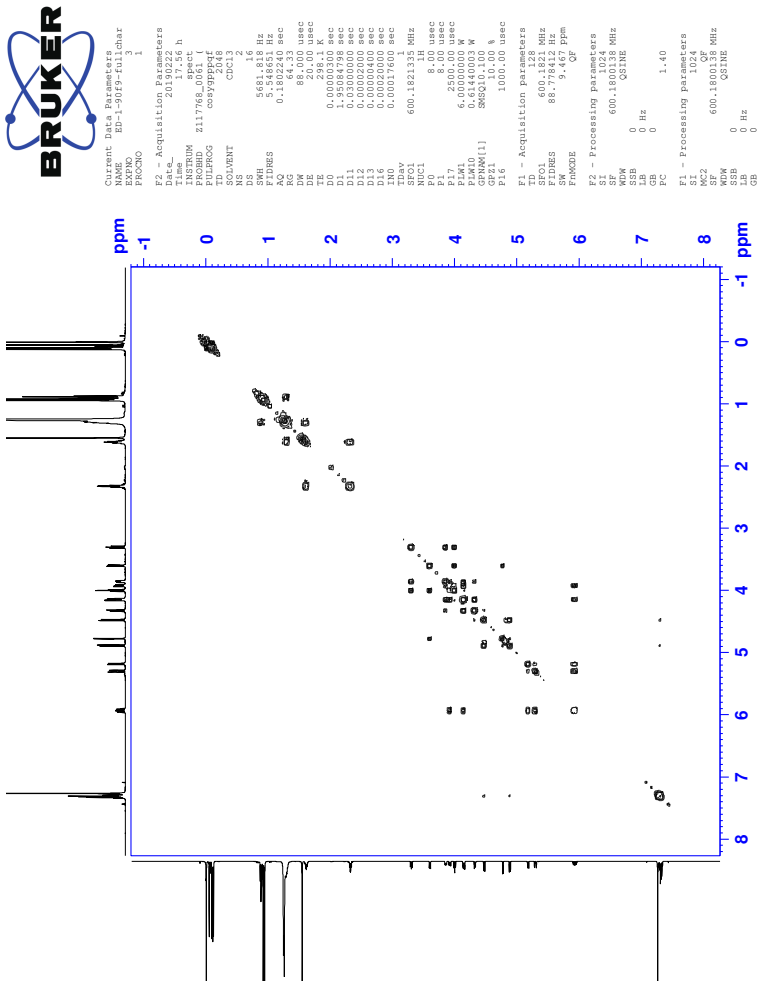

Figure 76: COSY spectrum of compound **16**.

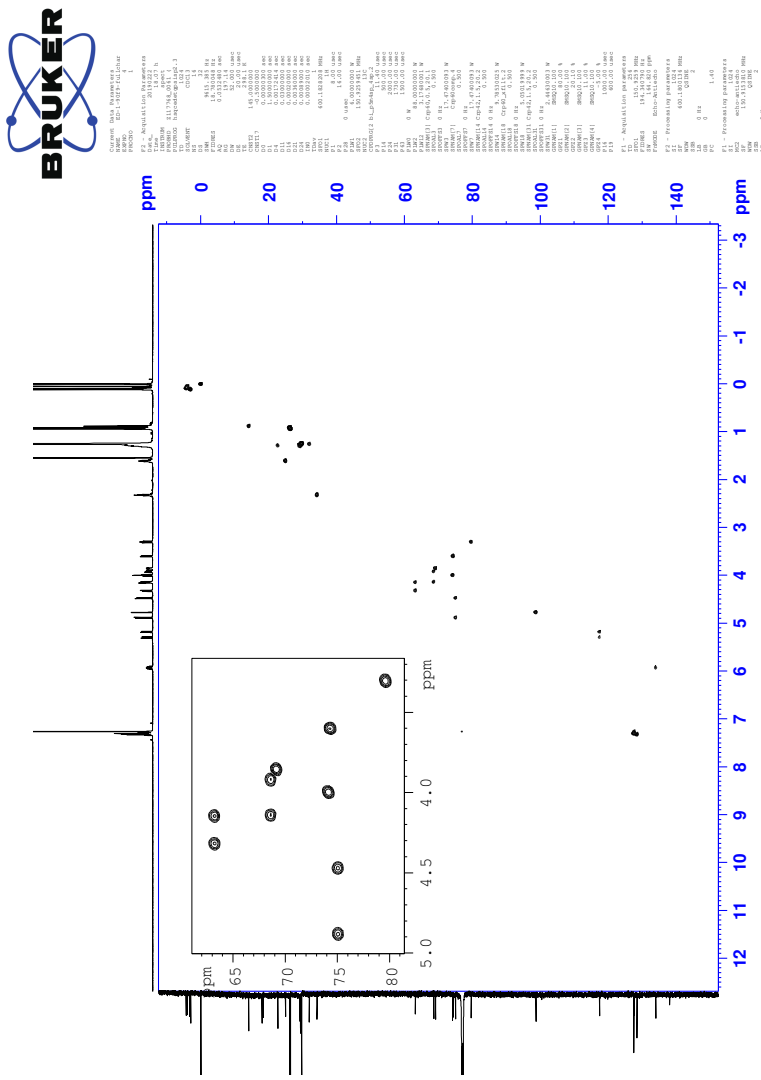

Figure 77: HSQC spectrum of compound **16**.

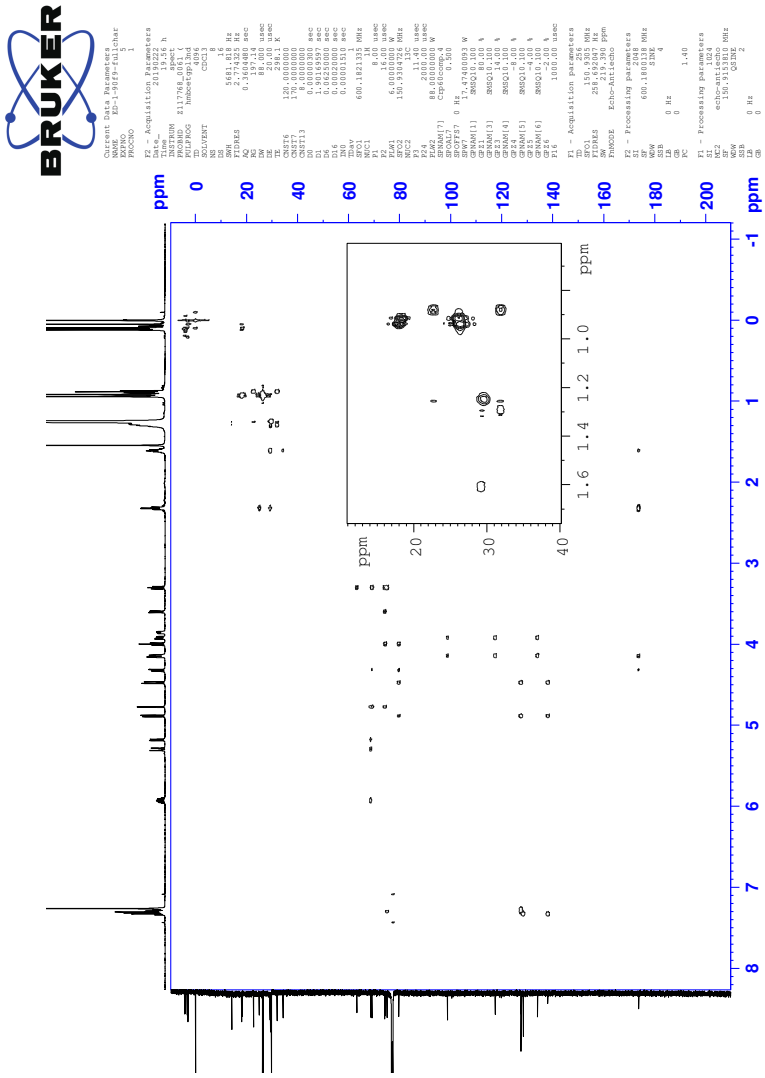

Figure 78: HMBC spectrum of compound **16**.

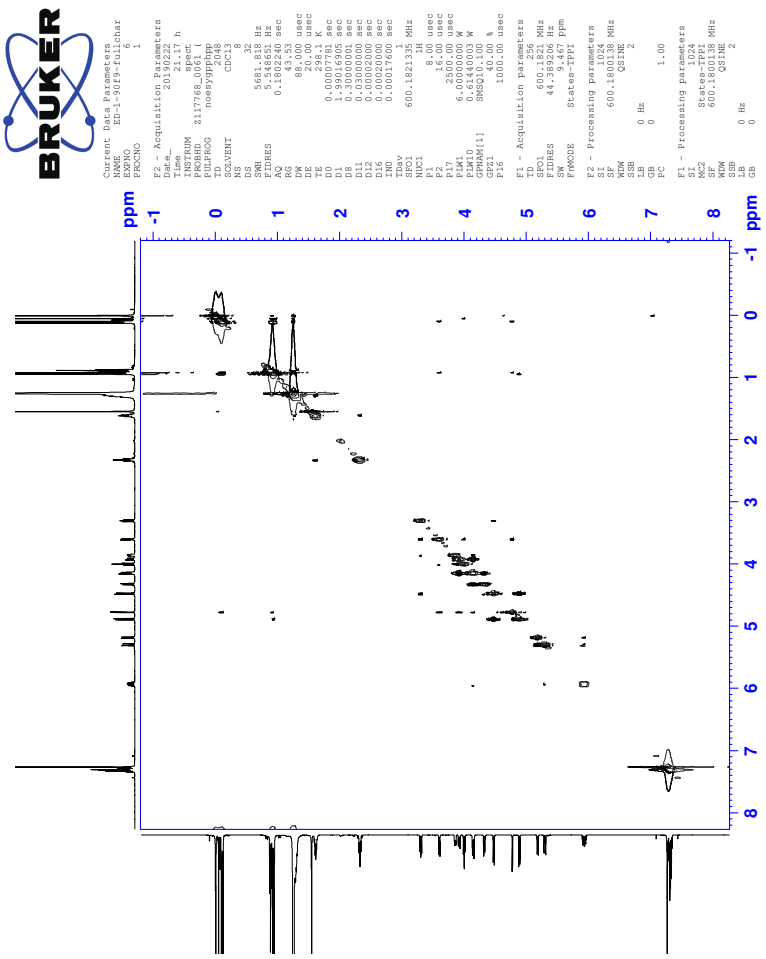

Figure 79: NOESY spectra of compound **16**.

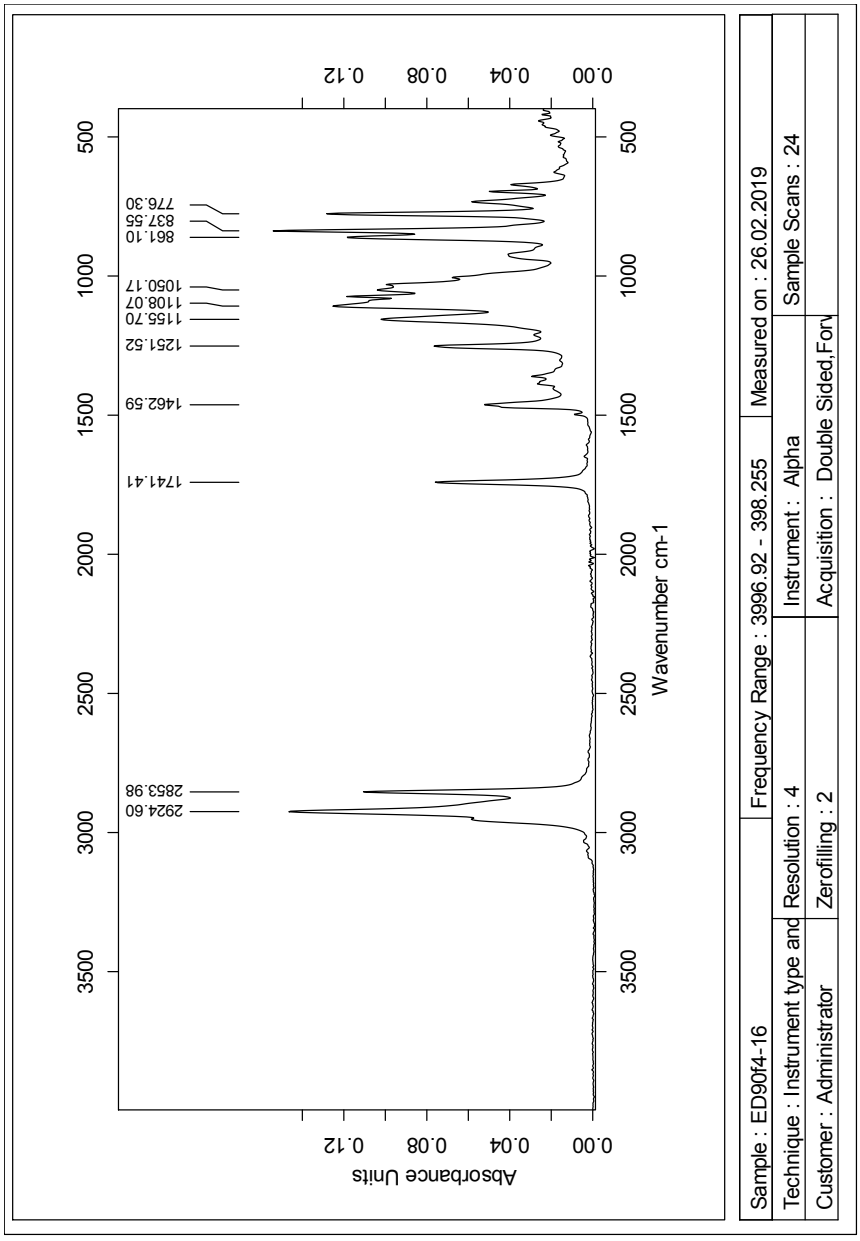

Figure 80: IR spectrum of compound **16**.

Elemental Composition Report **Page 1**

Single Mass Analysis
Tolerance = 2.0 PPM / DBE: min = -2.0, max = 50.0
Element prediction: Off
Number of isotope peaks used for i-FIT = 3

Monoisotopic Mass, Even Electron Ions
2082 formula(e) evaluated with 5 results within limits (up to 50 closest results for each mass)
Elements Used:
C: 0-500 H: 0-1000 N: 0-1 O: 0-10 Na: 0-1 Si: 0-4
2019_325_fia 57 (0.640) AM2 (Ar,35000.0,0.00,0.00); Cm (57:64)
1: TOF MS ES+

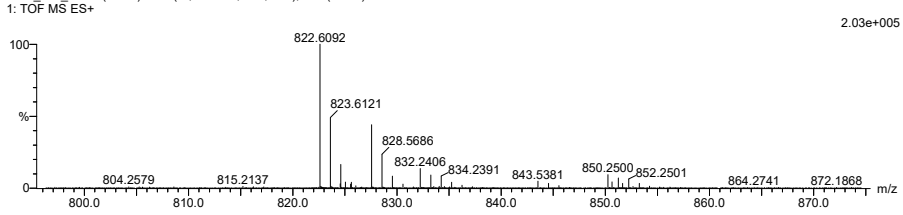

Minimum:				-2.0				
Maximum:		5.0	2.0	50.0				
Mass	Calc. Mass	mDa	PPM	DBE	i-FIT	Norm	Conf(%)	Formula
827.5652	827.5653	-0.1	-0.1	6.5	568.5	0.620	53.77	C46 H84 O7 Na Si2
	827.5650	0.2	0.2	13.5	571.3	3.486	3.06	C51 H83 O3 Si3
	827.5649	0.3	0.4	7.5	569.5	1.625	19.70	C47 H80 O10 Na
	827.5657	-0.5	-0.6	5.5	571.9	4.047	1.75	C45 H88 O4 Na Si4
	827.5646	0.6	0.7	14.5	569.4	1.527	21.72	C52 H79 O6 Si

Figure 81: MS results for compound **16**.

N Spectroscopic data for compound 17

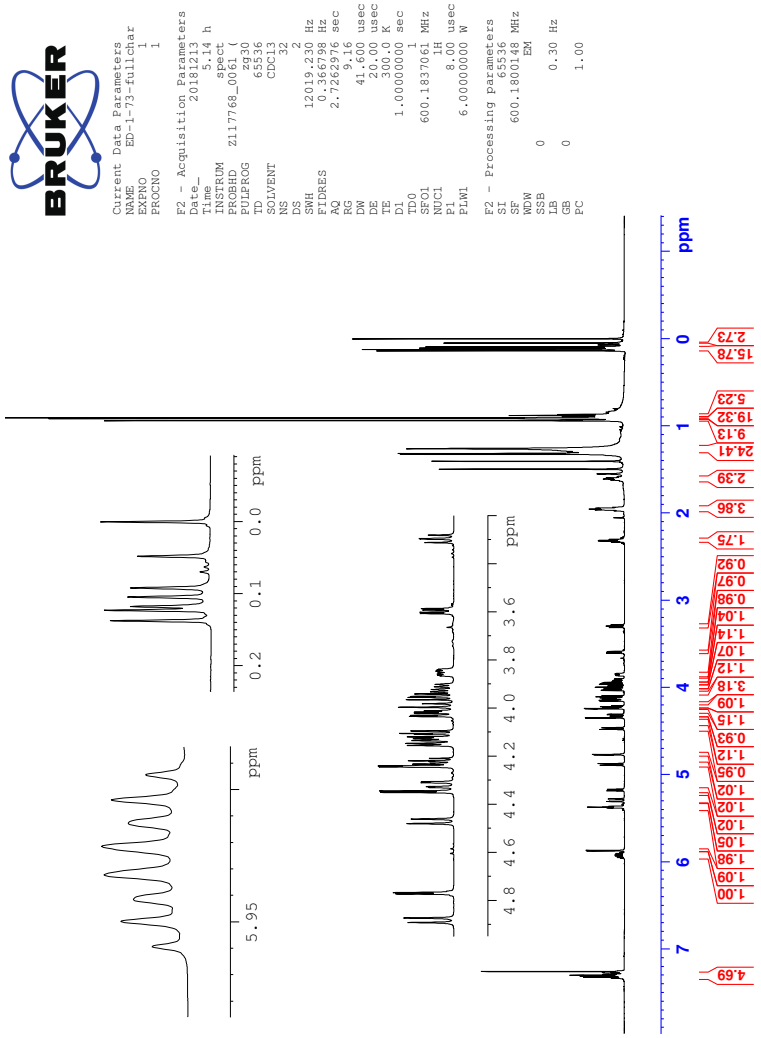

Figure 82: ^{1}H-NMR spectrum of compound **17**.

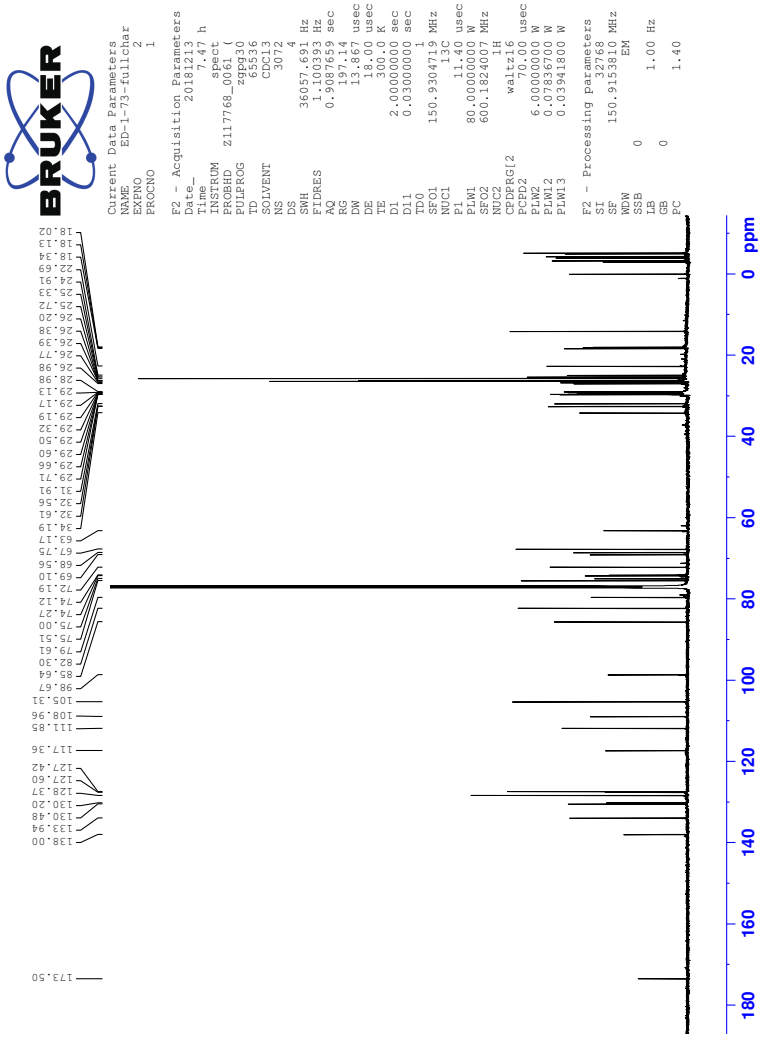

Figure 83: ^{13}C-NMR spectrum of compound **17**.

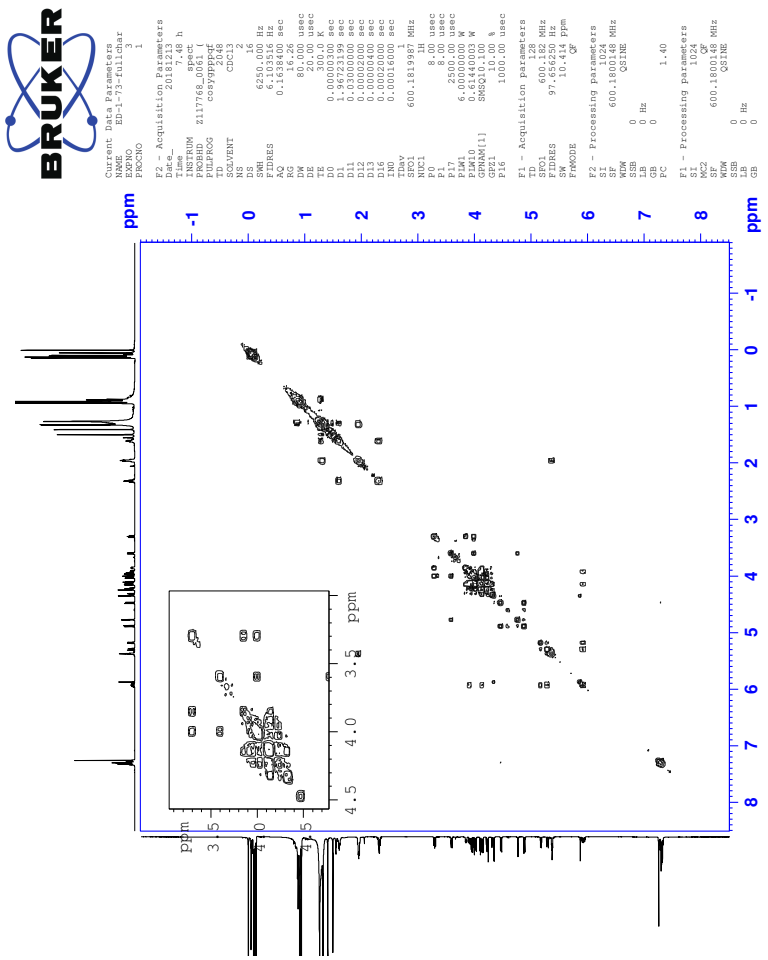

Figure 84: COSY spectrum of compound **17**.

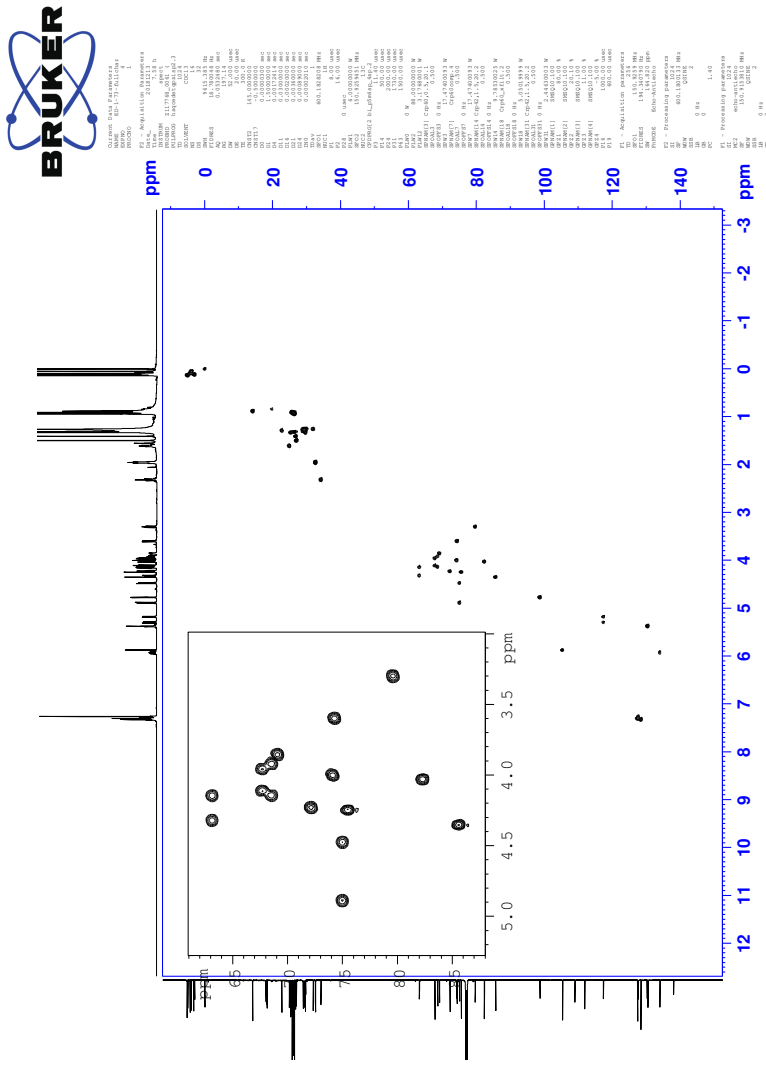

Figure 85: HSQC spectrum of compound **17**.

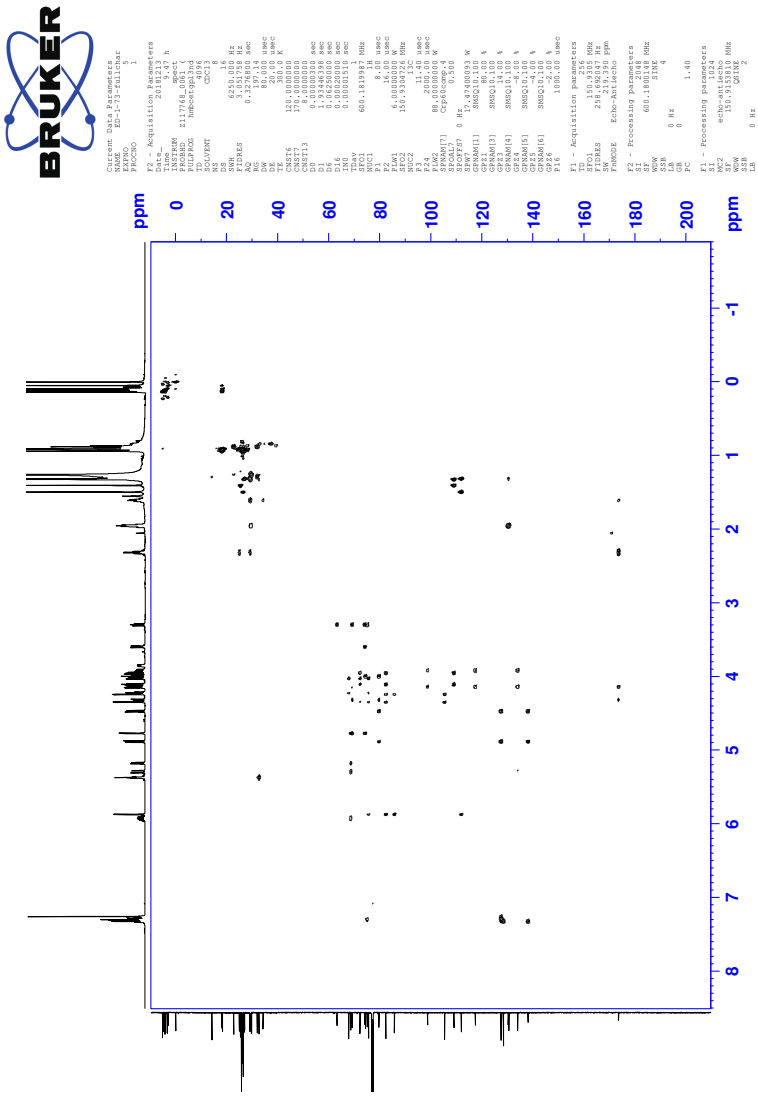

Figure 86: HMBC spectrum of compound **17**.

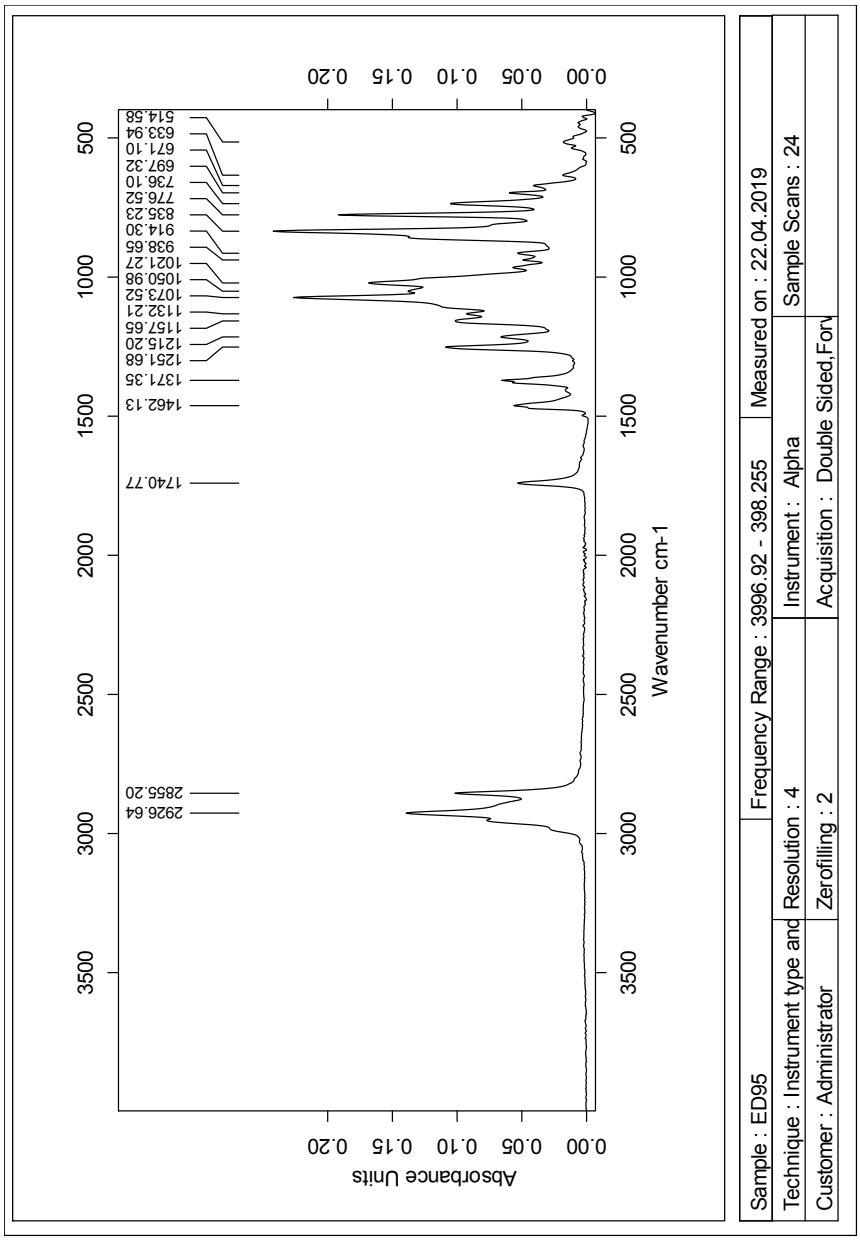

Figure 87: IR spectrum of compound **17**.

Elemental Composition Report **Page 1**

Single Mass Analysis
Tolerance = 2.0 PPM / DBE: min = -2.0, max = 50.0
Element prediction: Off
Number of isotope peaks used for i-FIT = 3

Monoisotopic Mass, Even Electron Ions
1048 formula(e) evaluated with 5 results within limits (up to 50 closest results for each mass)
Elements Used:
C: 0-500 H: 0-1000 O: 0-10 Na: 0-1 Si: 0-4
2019_323_fia 59 (0.662) AM2 (Ar,35000.0,0.00,0.00); Cm (59:66)
1: TOF MS ES+

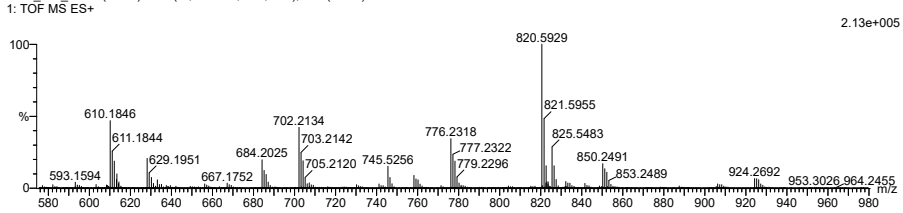

Minimum:				-2.0				
Maximum:		5.0	2.0	50.0				
Mass	Calc. Mass	mDa	PPM	DBE	i-FIT	Norm	Conf(%)	Formula
825.5483	825.5489	-0.6	-0.7	15.5	492.2	0.439	64.47	C52 H77 O6 Si
	825.5493	-1.0	-1.2	8.5	495.0	3.295	3.71	C47 H78 O10 Na
	825.5494	-1.1	-1.3	14.5	495.9	4.169	1.55	C51 H81 O3 Si3
	825.5469	1.4	1.7	11.5	495.5	3.723	2.42	C49 H82 O3 Na Si3
	825.5497	-1.4	-1.7	7.5	493.0	1.278	27.86	C46 H82 O7 Na Si2

Figure 88: MS results for compound **17**.

O Spectroscopic data for compound 18

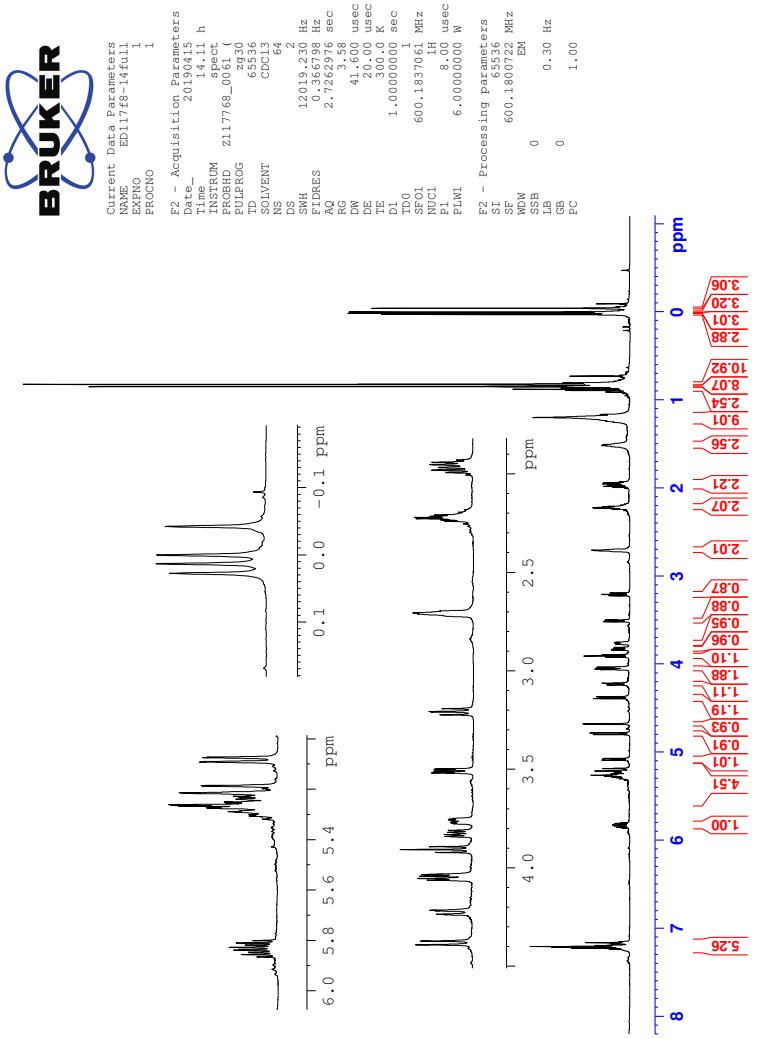

Figure 89: ^{1}H-NMR spectrum of compound **18**.

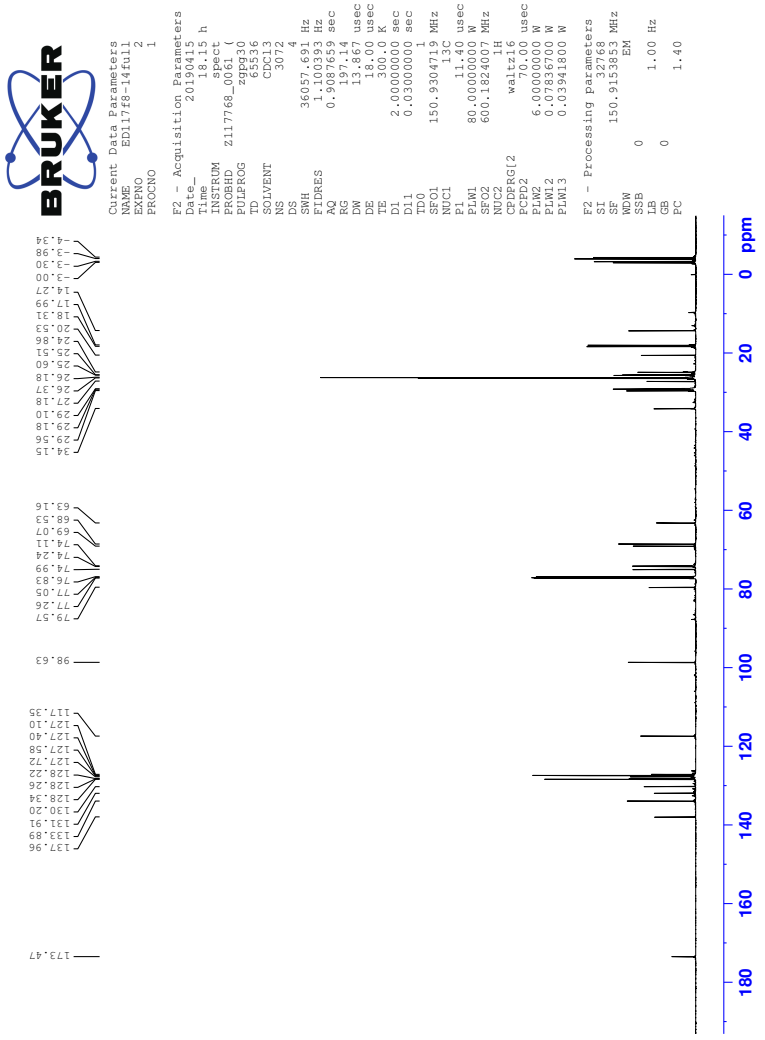

Figure 90: ^{13}C-NMR spectrum of compound **18**.

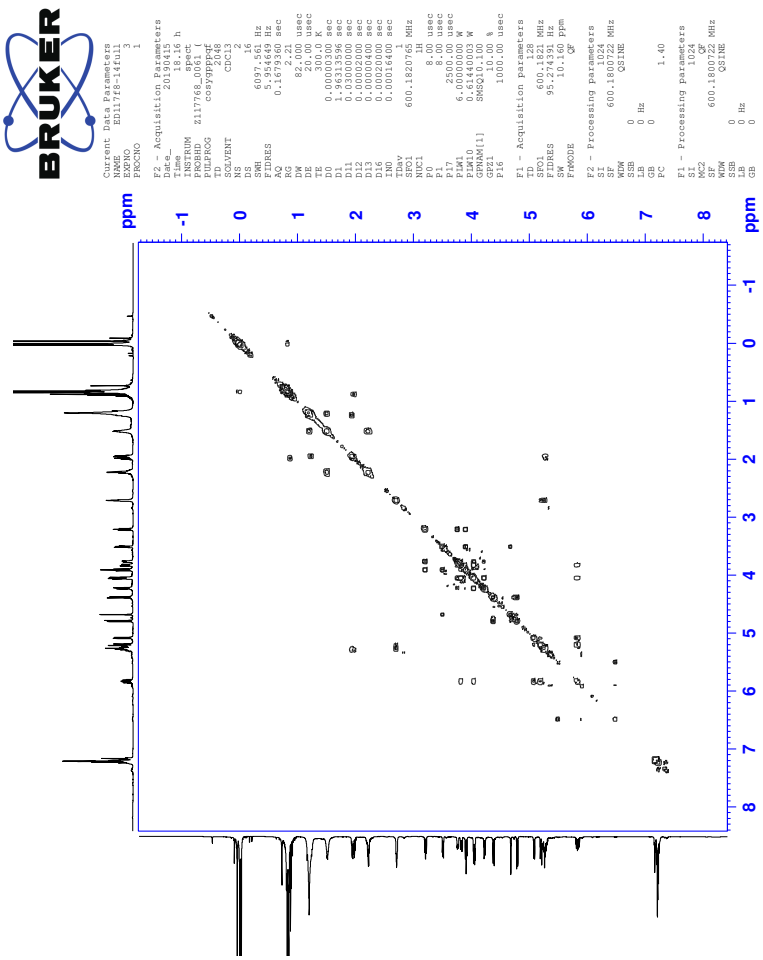

Figure 91: COSY spectrum of compound **18**.

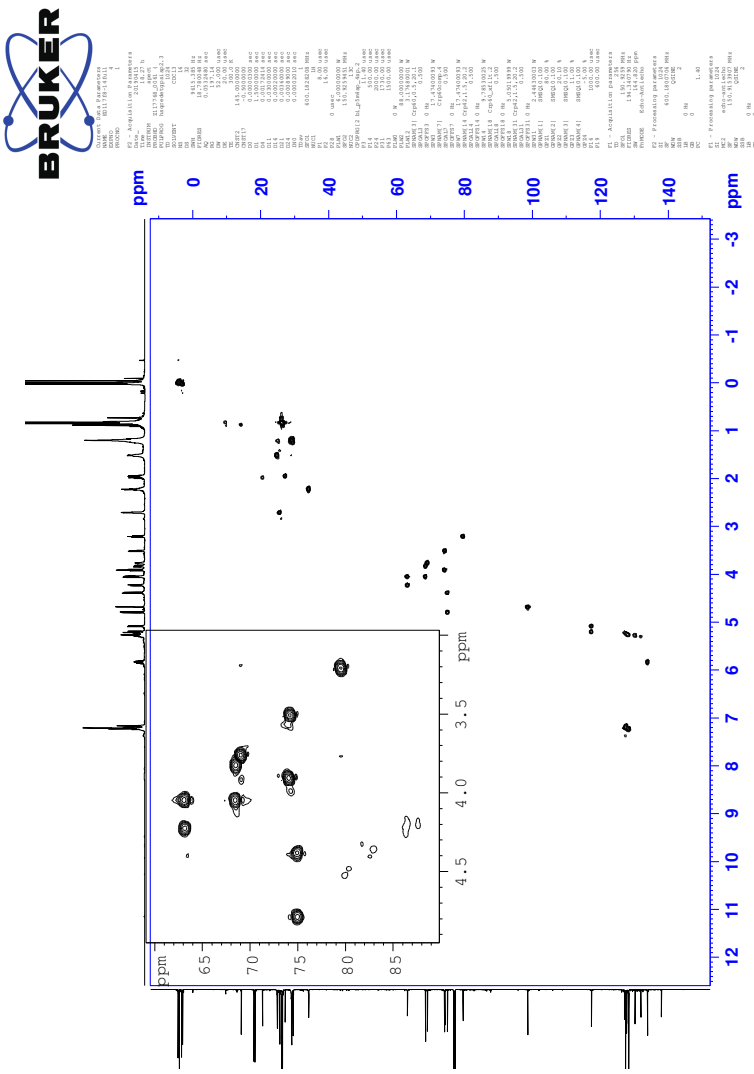

Figure 92: HSQC spectrum of compound **18**.

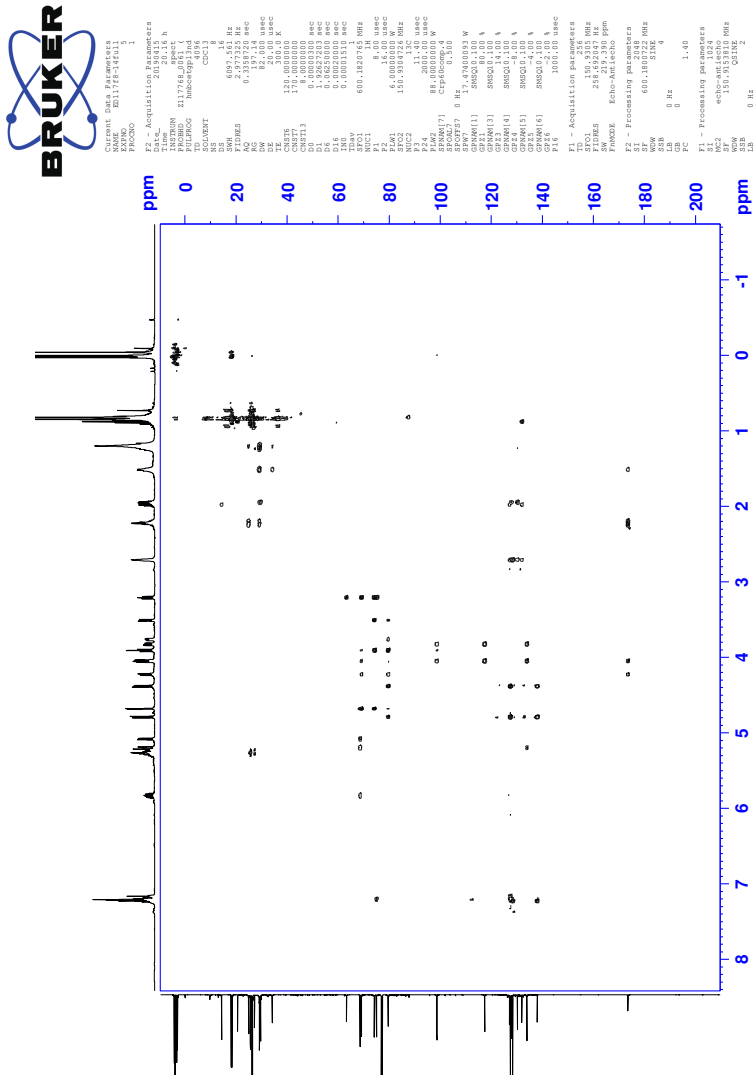

Figure 93: HMBC spectrum of compound **18**.

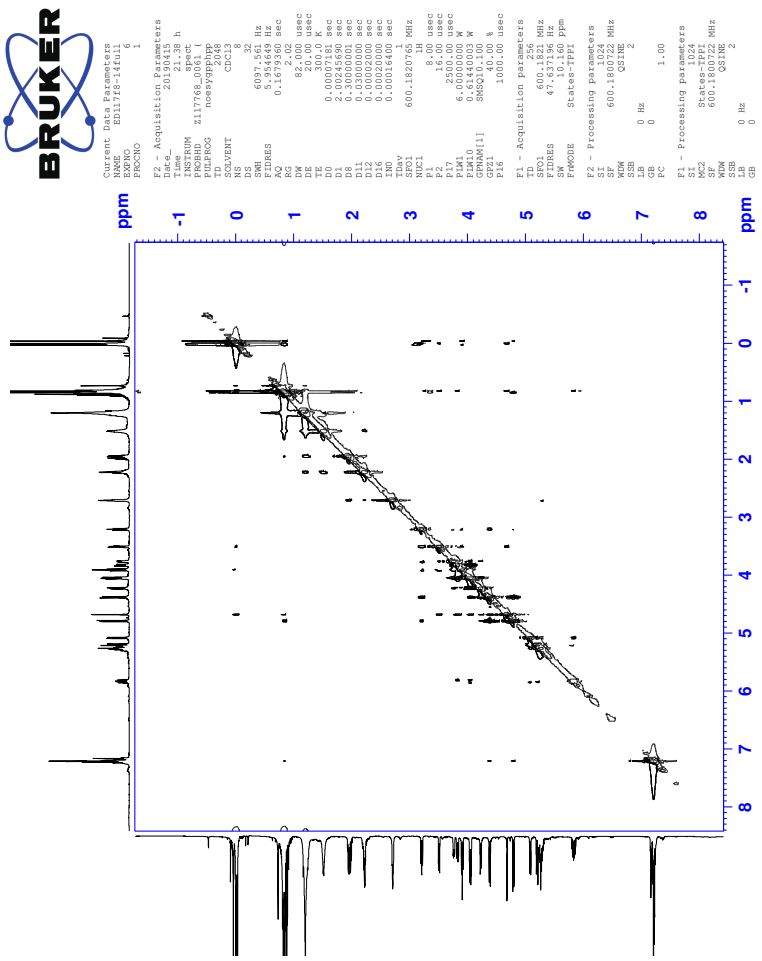

Figure 94: NOESY spectra of compound **18**.

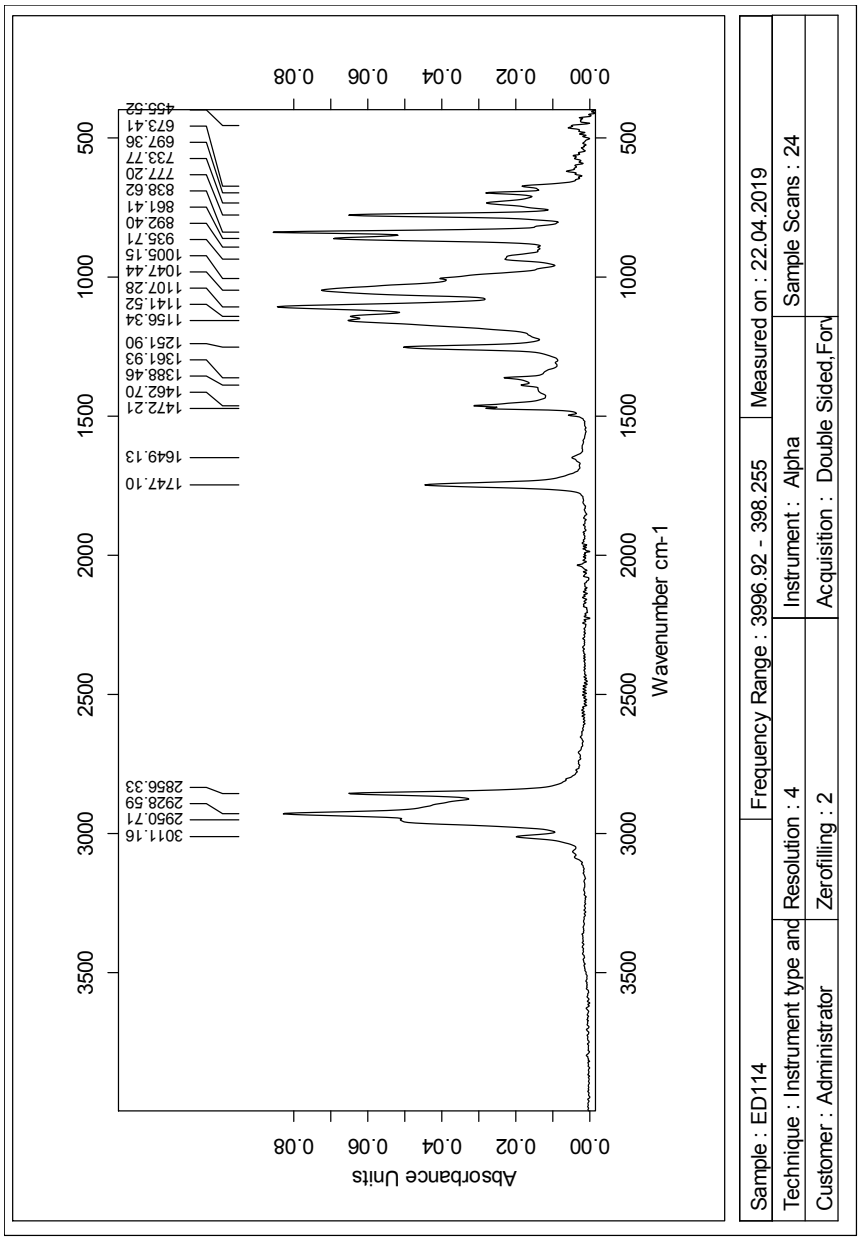

Figure 95: IR spectrum of compound **18**.

Elemental Composition Report **Page 1**

Single Mass Analysis
Tolerance = 2.0 PPM / DBE: min = -2.0, max = 50.0
Element prediction: Off
Number of isotope peaks used for i-FIT = 3

Monoisotopic Mass, Even Electron Ions
1042 formula(e) evaluated with 5 results within limits (up to 50 closest results for each mass)
Elements Used:
C: 0-500 H: 0-1000 O: 0-10 Na: 0-1 Si: 0-4
2019_330_fia 61 (0.690) AM2 (Ar,35000.0,0.00,0.00); Cm (57:67)
1: TOF MS ES+

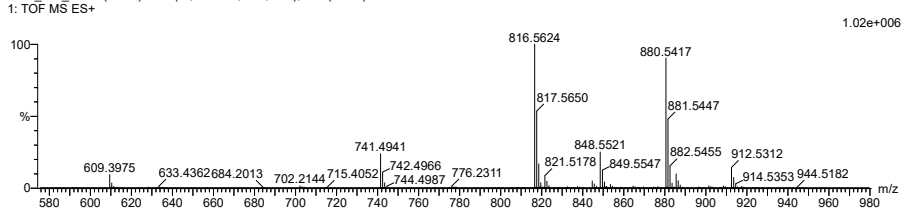

Minimum:				-2.0				
Maximum:		5.0	2.0	50.0				
Mass	Calc. Mass	mDa	PPM	DBE	i-FIT	Norm	Conf(%)	Formula
821.5178	821.5176	0.2	0.2	17.5	523.4	0.438	64.51	C52 H73 O6 Si
	821.5180	-0.2	-0.2	10.5	525.3	2.333	9.70	C47 H74 O10 Na
	821.5181	-0.3	-0.4	16.5	527.3	4.334	1.31	C51 H77 O3 Si3
	821.5184	-0.6	-0.7	9.5	524.4	1.417	24.24	C46 H78 O7 Na Si2
	821.5188	-1.0	-1.2	8.5	529.0	6.039	0.24	C45 H82 O4 Na Si4

Figure 96: MS results for compound **18**.

P Spectroscopic data for compound 19

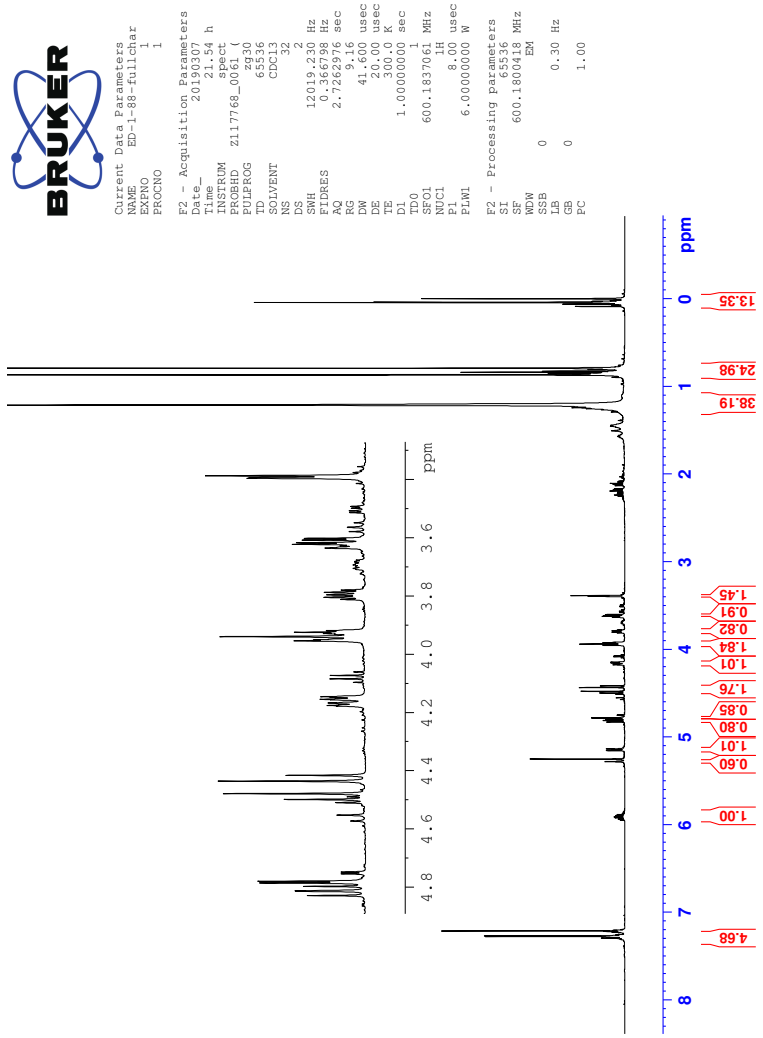

Figure 97: ^{1}H-NMR spectrum of compound **19**.

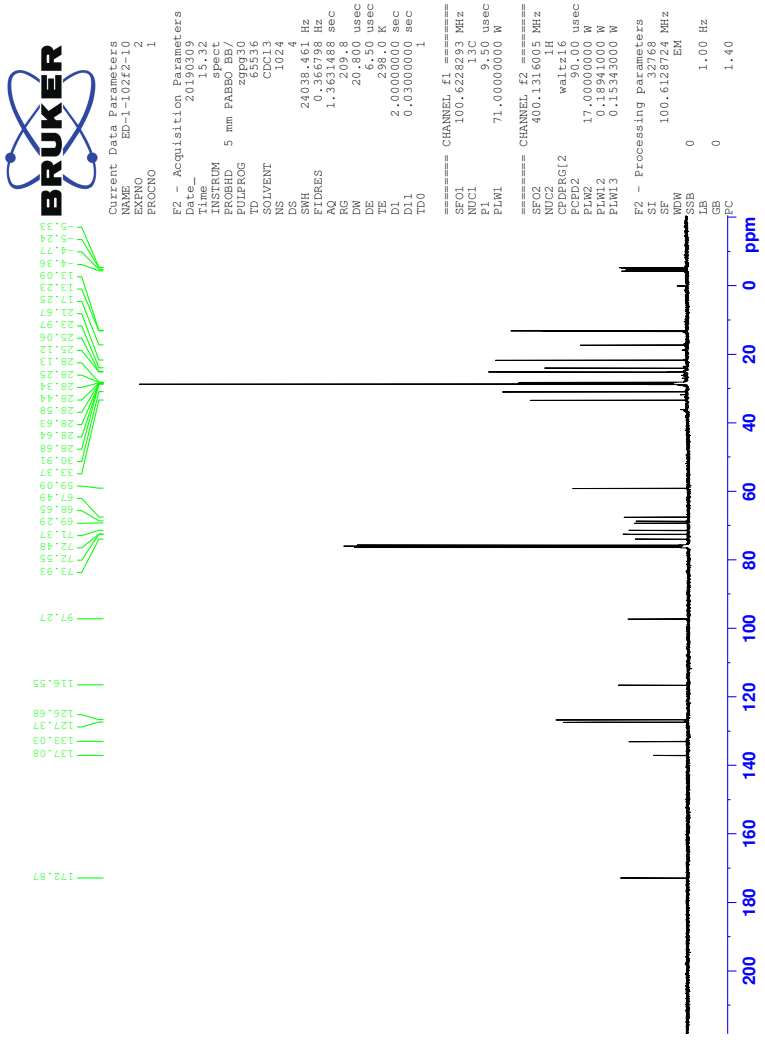

Figure 98: ^{13}C-NMR spectrum of compound **19**.

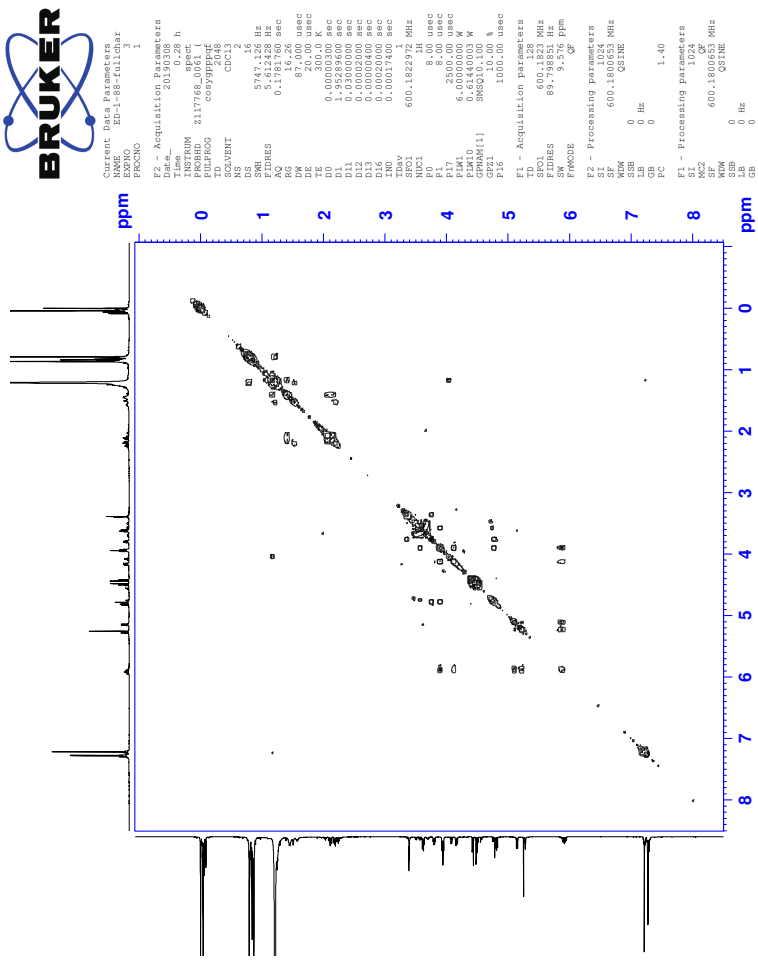

Figure 99: COSY spectrum of compound **19**.

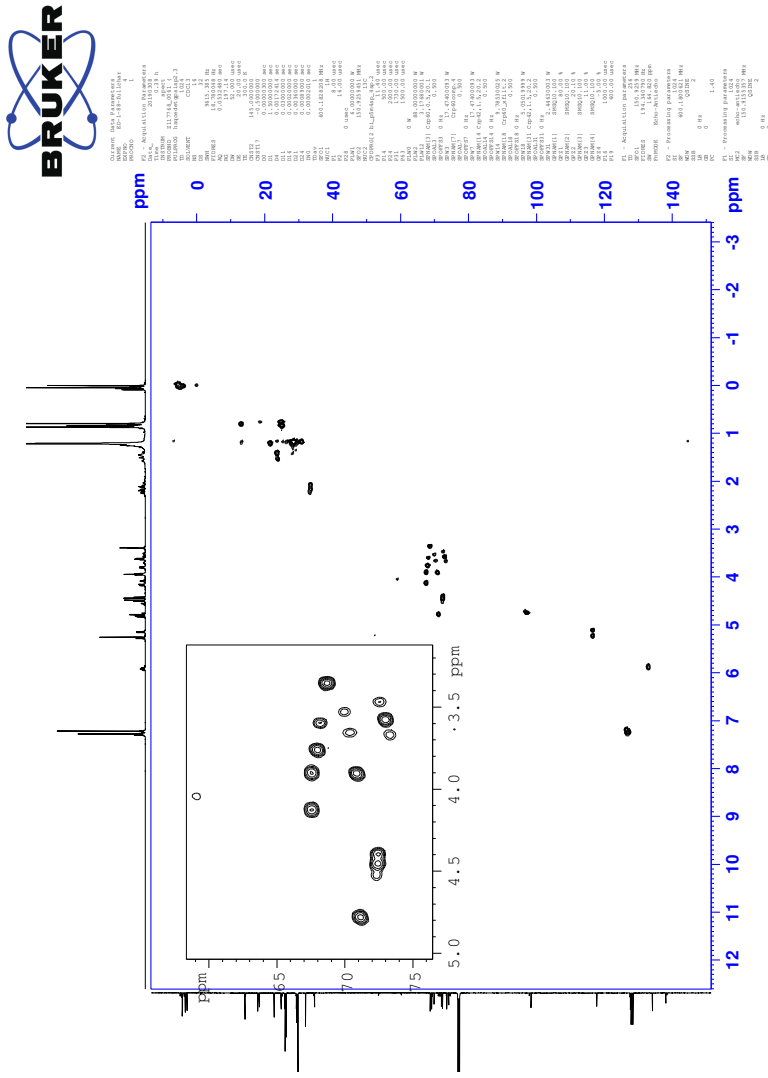

Figure 100: HSQC spectrum of compound **19**.

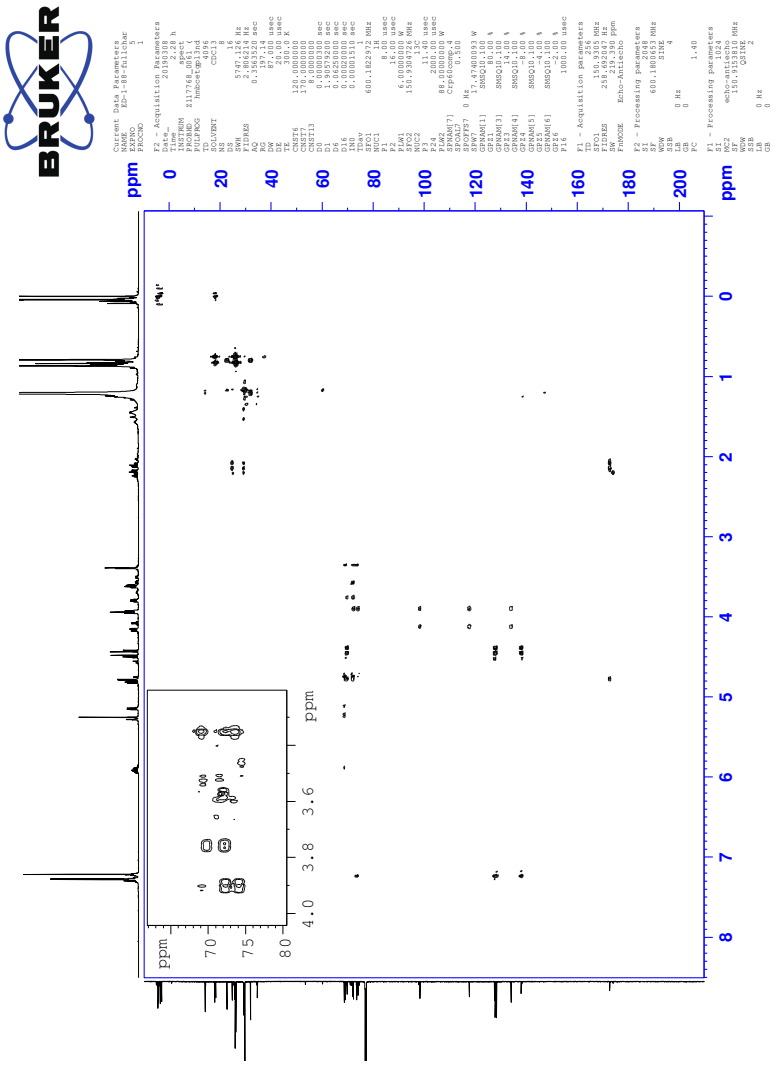

Figure 101: HMBC spectrum of compound **19**.

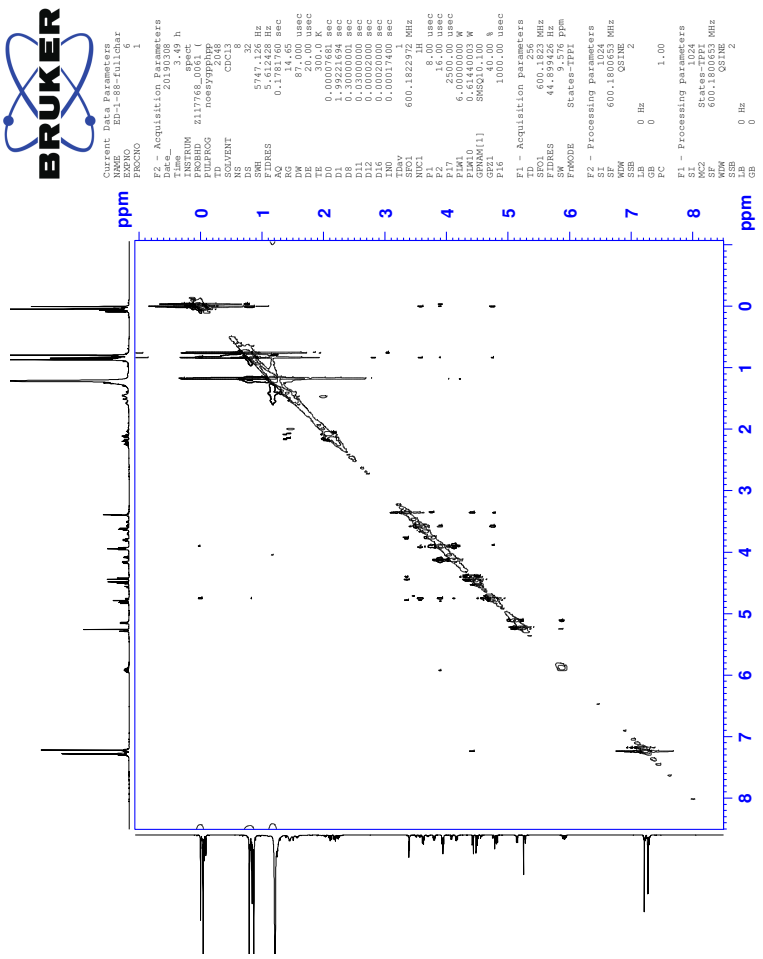

Figure 102: NOESY spectra of compound **19**.

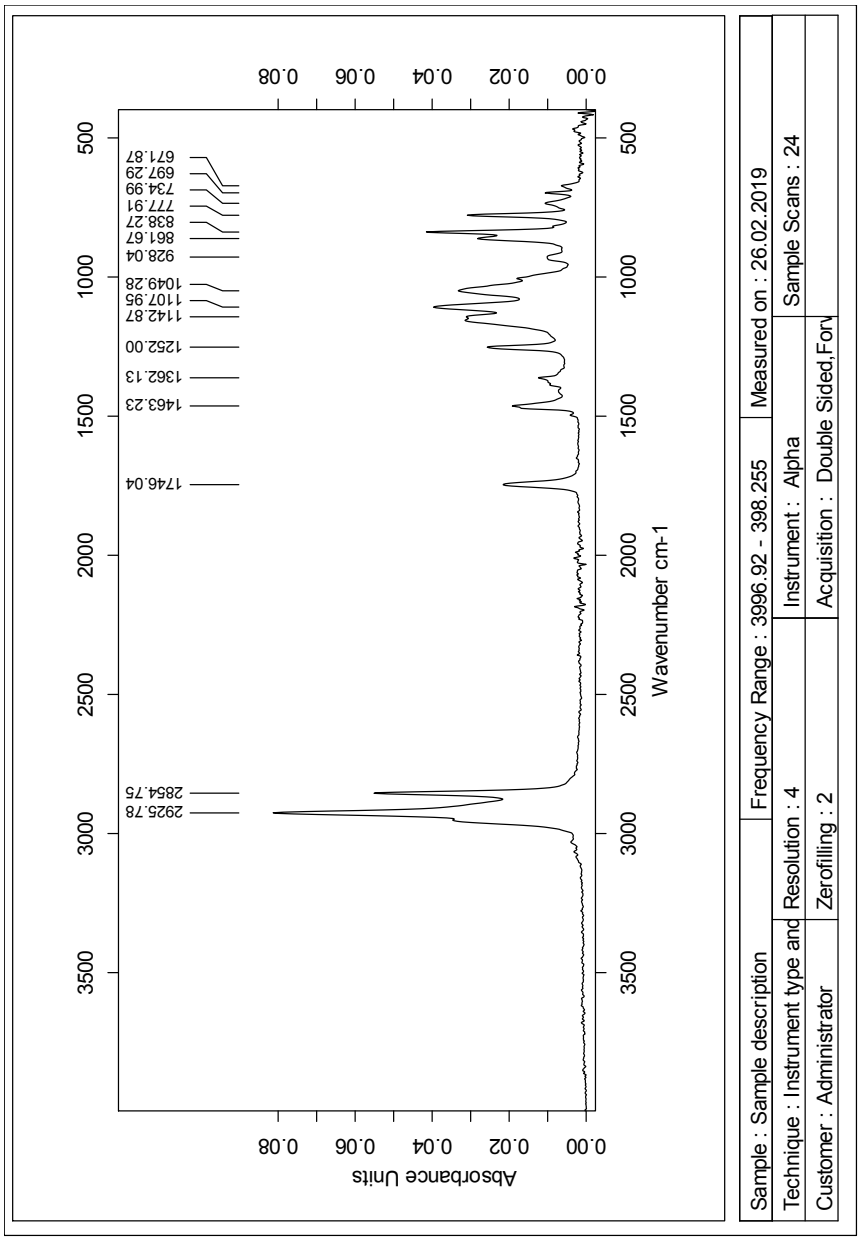

Figure 103: IR spectrum of compound **19**.

Elemental Composition Report **Page 1**

Single Mass Analysis
Tolerance = 2.0 PPM / DBE: min = -2.0, max = 50.0
Element prediction: Off
Number of isotope peaks used for i-FIT = 3

Monoisotopic Mass, Even Electron Ions
1050 formula(e) evaluated with 5 results within limits (up to 50 closest results for each mass)
Elements Used:
C: 0-500 H: 0-1000 O: 0-10 Na: 0-1 Si: 0-4
2019_326_fia 65 (0.732) AM2 (Ar,35000.0,0.00,0.00); Cm (65:80)
1: TOF MS ES+

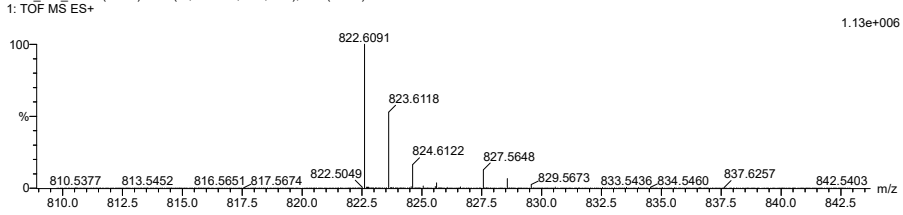

Minimum:				-2.0				
Maximum:		5.0	2.0	50.0				
Mass	Calc. Mass	mDa	PPM	DBE	i-FIT	Norm	Conf(%)	Formula
827.5648	827.5649	-0.1	-0.1	7.5	598.0	1.639	19.42	C47 H80 O10 Na
	827.5650	-0.2	-0.2	13.5	599.0	2.642	7.12	C51 H83 O3 Si3
	827.5646	0.2	0.2	14.5	597.7	1.281	27.78	C52 H79 O6 Si
	827.5653	-0.5	-0.6	6.5	597.2	0.839	43.19	C46 H84 O7 Na Si2
	827.5657	-0.9	-1.1	5.5	600.1	3.696	2.48	C45 H88 O4 Na Si4

Figure 104: MS results for compound **19**.

Q Spectroscopic data for compound 20

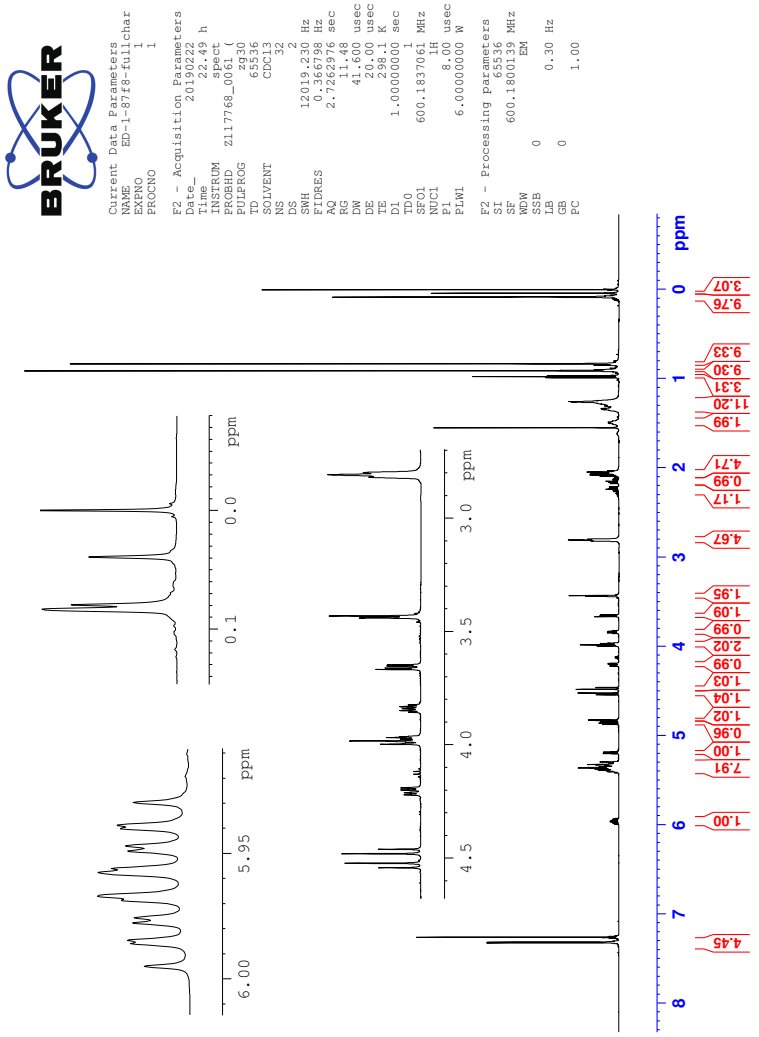

Figure 105: ^{1}H-NMR spectrum of compound **20**.

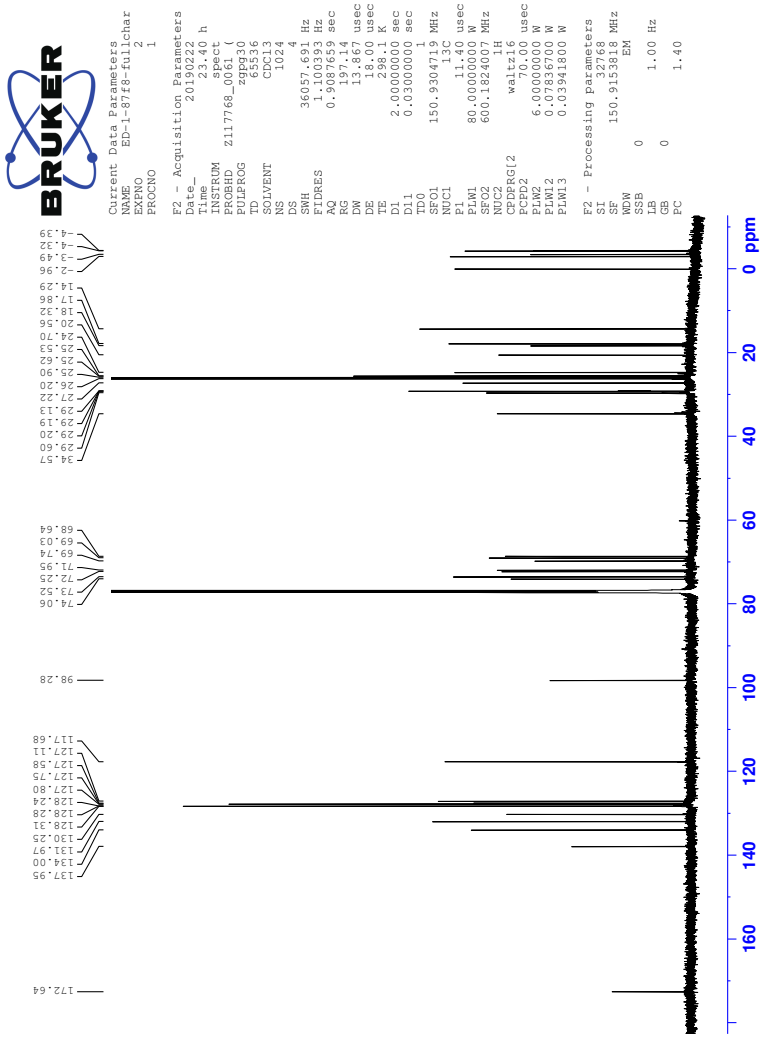

Figure 106: ^{13}C-NMR spectrum of compound **20**.

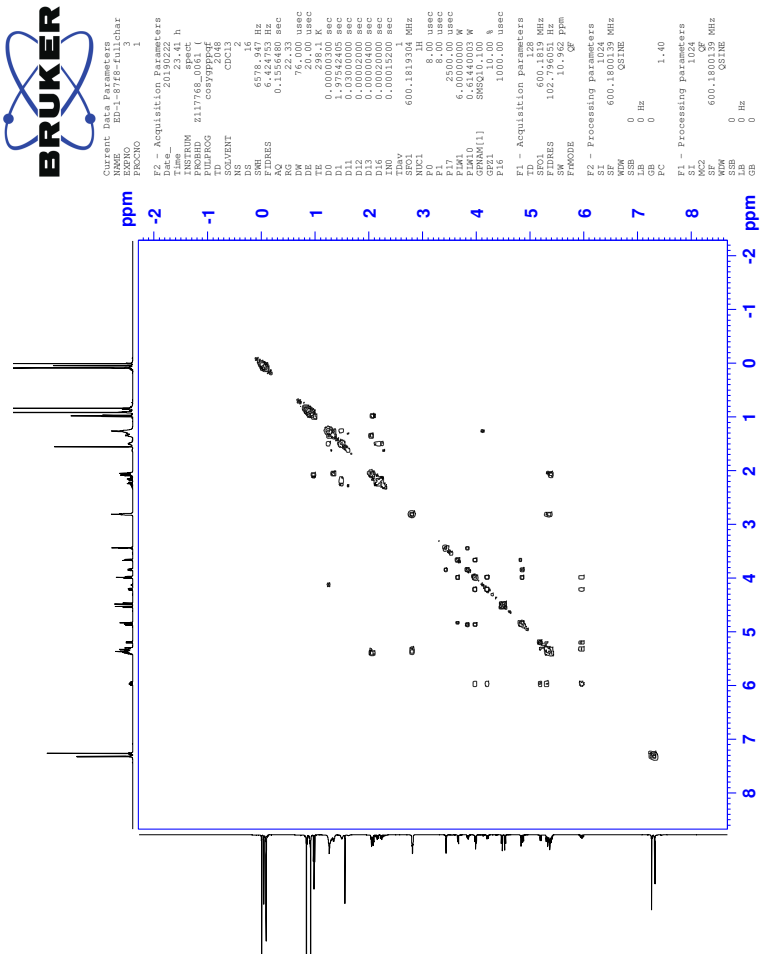

Figure 107: COSY spectrum of compound **20**.

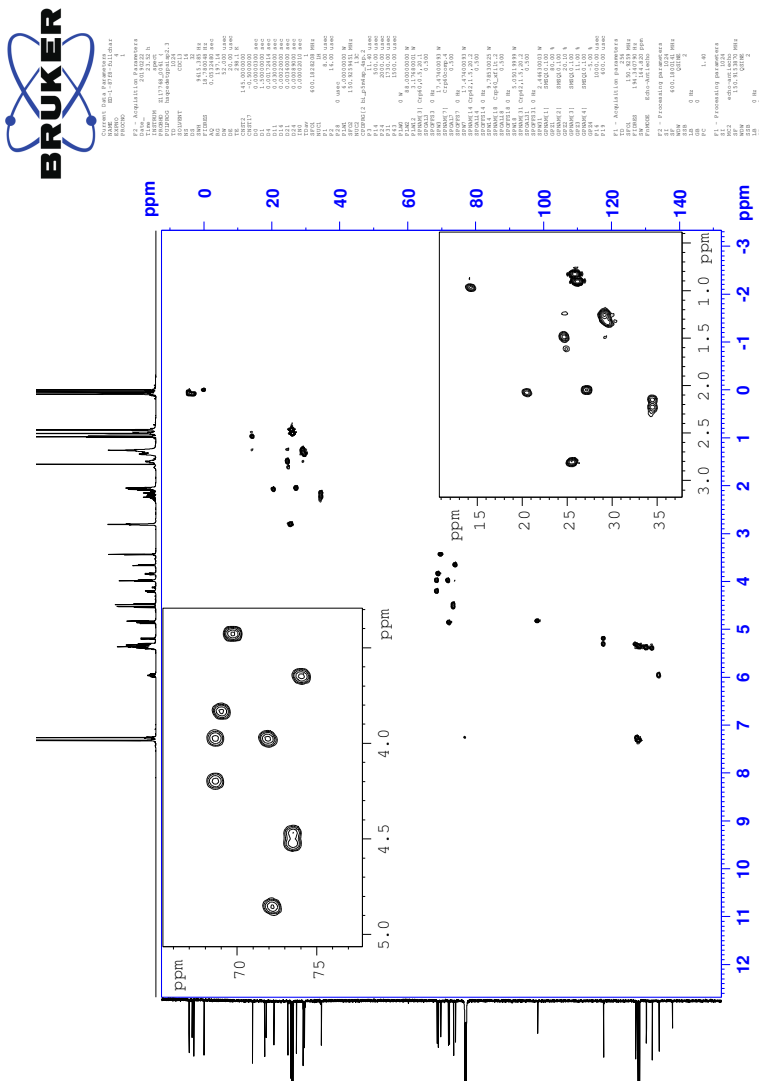

Figure 108: HSQC spectrum of compound **20**.

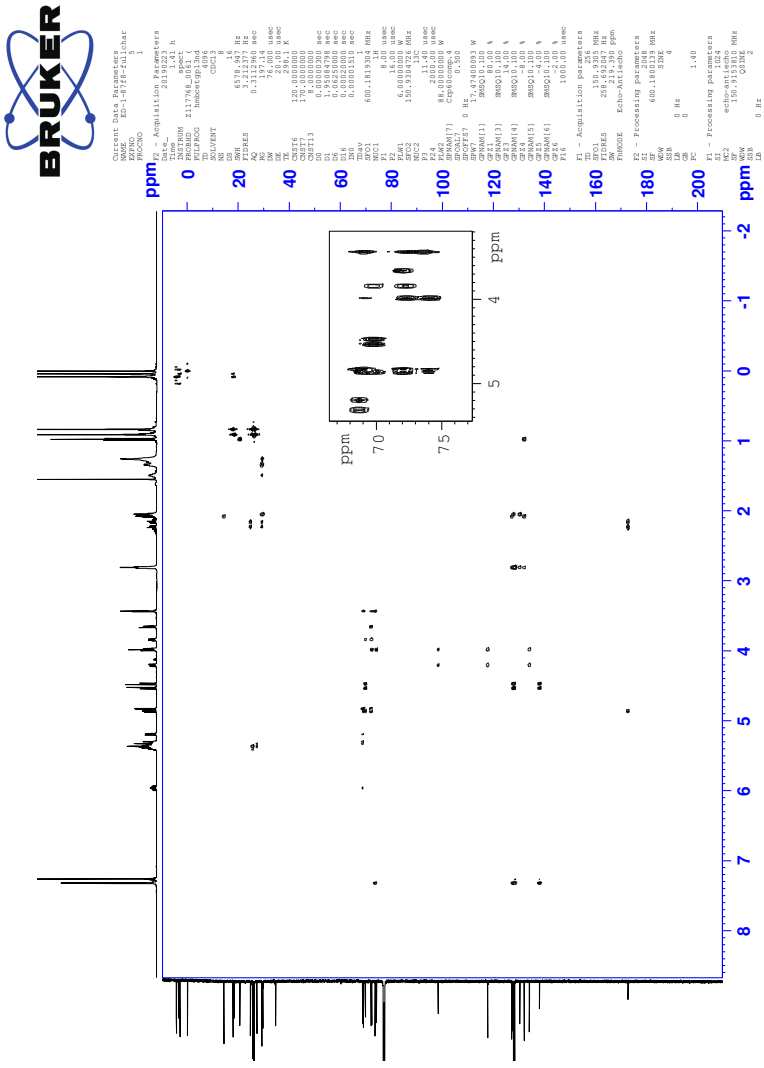

Figure 109: HMBC spectrum of compound **20**.

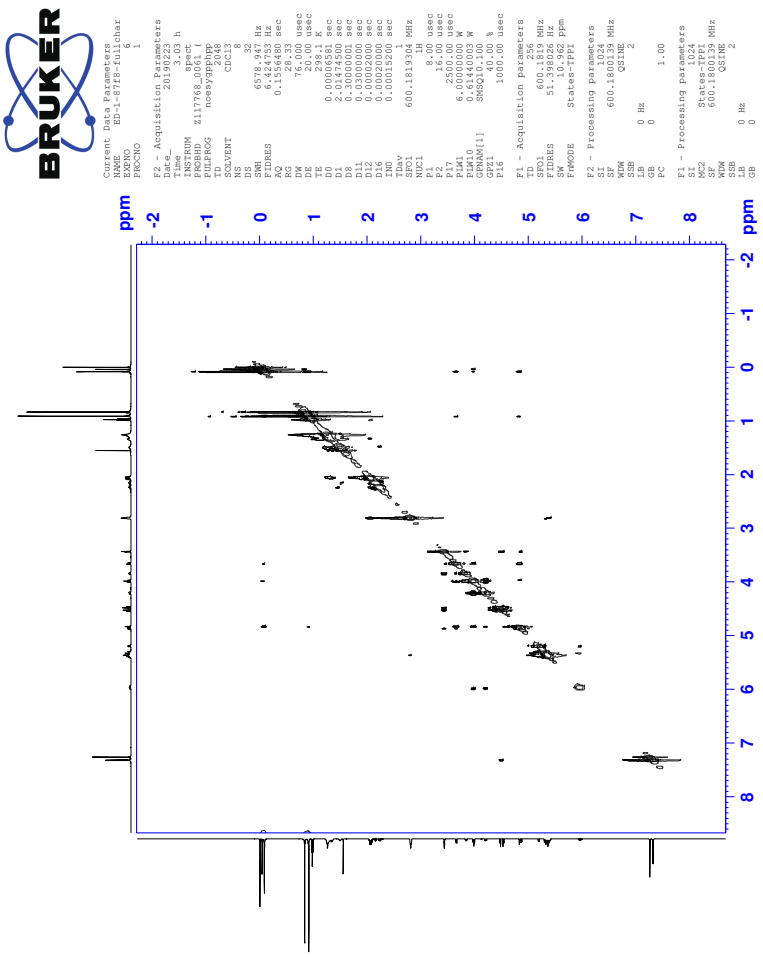

Figure 110: NOESY spectra of compound **20**.

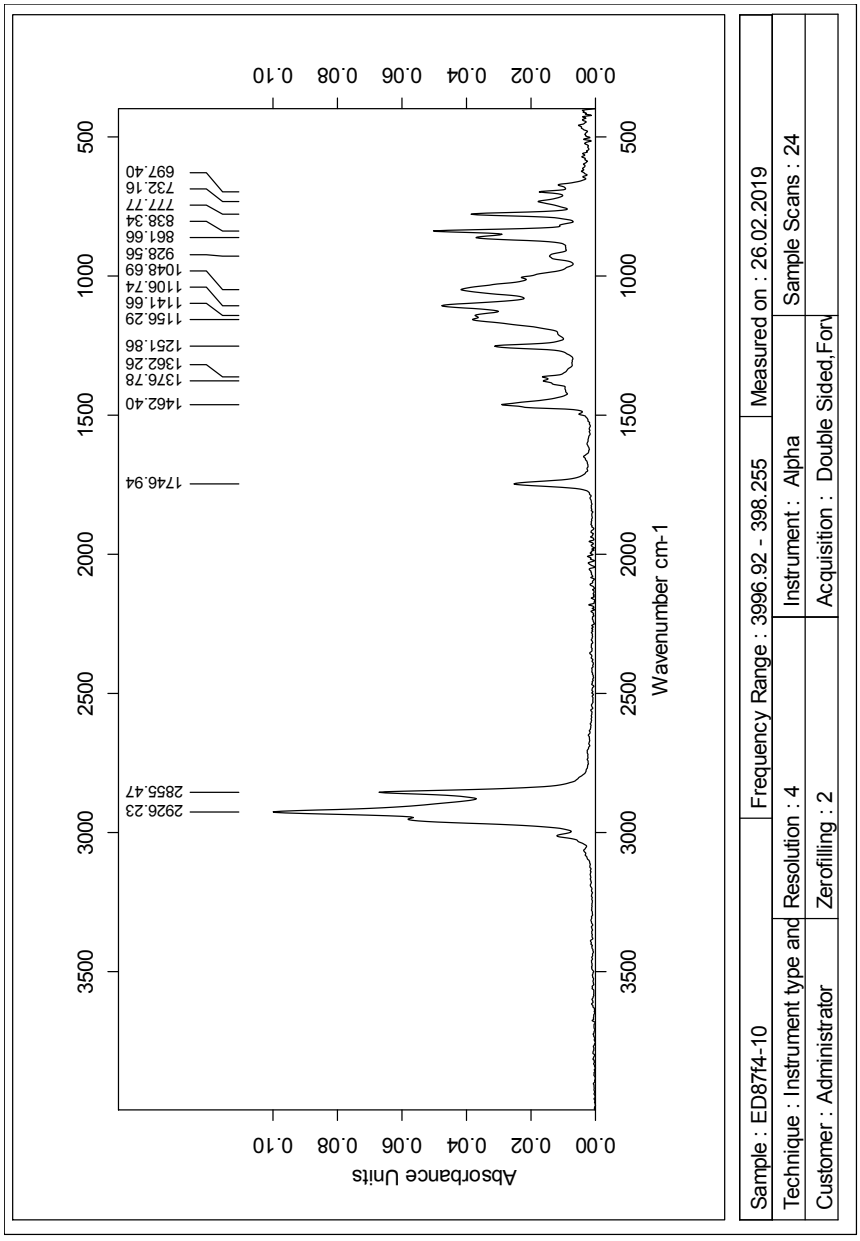

Figure 111: IR spectrum of compound **20**.

Elemental Composition Report **Page 1**

Single Mass Analysis
Tolerance = 2.0 PPM / DBE: min = -2.0, max = 50.0
Element prediction: Off
Number of isotope peaks used for i-FIT = 3

Monoisotopic Mass, Even Electron Ions
1042 formula(e) evaluated with 5 results within limits (up to 50 closest results for each mass)
Elements Used:
C: 0-500 H: 0-1000 O: 0-10 Na: 0-1 Si: 0-4
2019_329_fia 102 (1.137) AM2 (Ar,35000.0,0.00,0.00); Cm (87:102)
1: TOF MS ES+

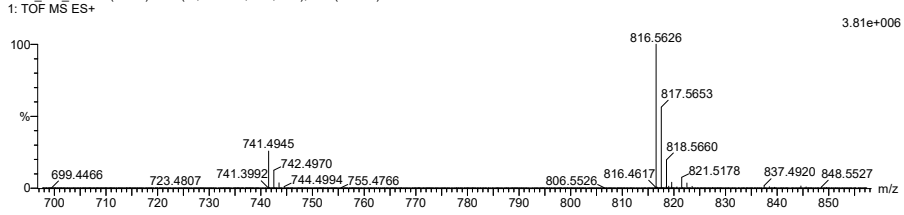

Minimum:				-2.0				
Maximum:		5.0	2.0	50.0				
Mass	Calc. Mass	mDa	PPM	DBE	i-FIT	Norm	Conf(%)	Formula
821.5178	821.5176	0.2	0.2	17.5	639.6	2.103	12.21	C52 H73 O6 Si
	821.5180	-0.2	-0.2	10.5	637.7	0.203	81.64	C47 H74 O10 Na
	821.5181	-0.3	-0.4	16.5	642.9	5.418	0.44	C51 H77 O3 Si3
	821.5184	-0.6	-0.7	9.5	640.4	2.879	5.62	C46 H78 O7 Na Si2
	821.5188	-1.0	-1.2	8.5	644.6	7.065	0.09	C45 H82 O4 Na Si4

Figure 112: MS results for compound **20**.

R Spectroscopic data for compound 21

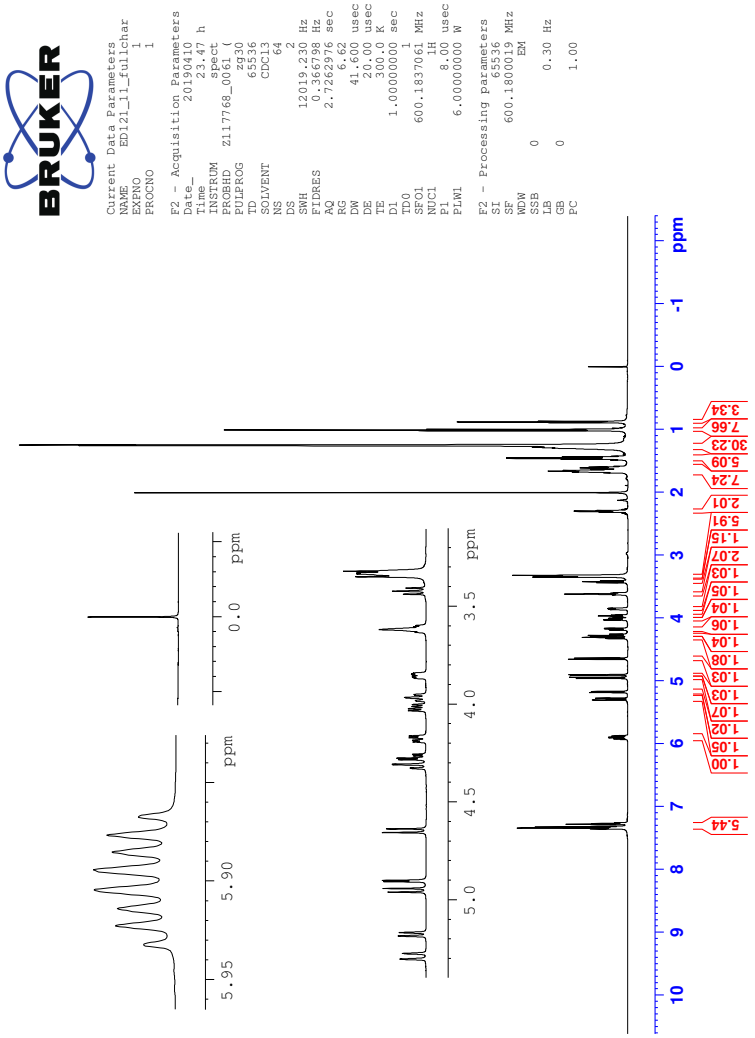

Figure 113: ^{1}H-NMR spectrum of compound **21**.

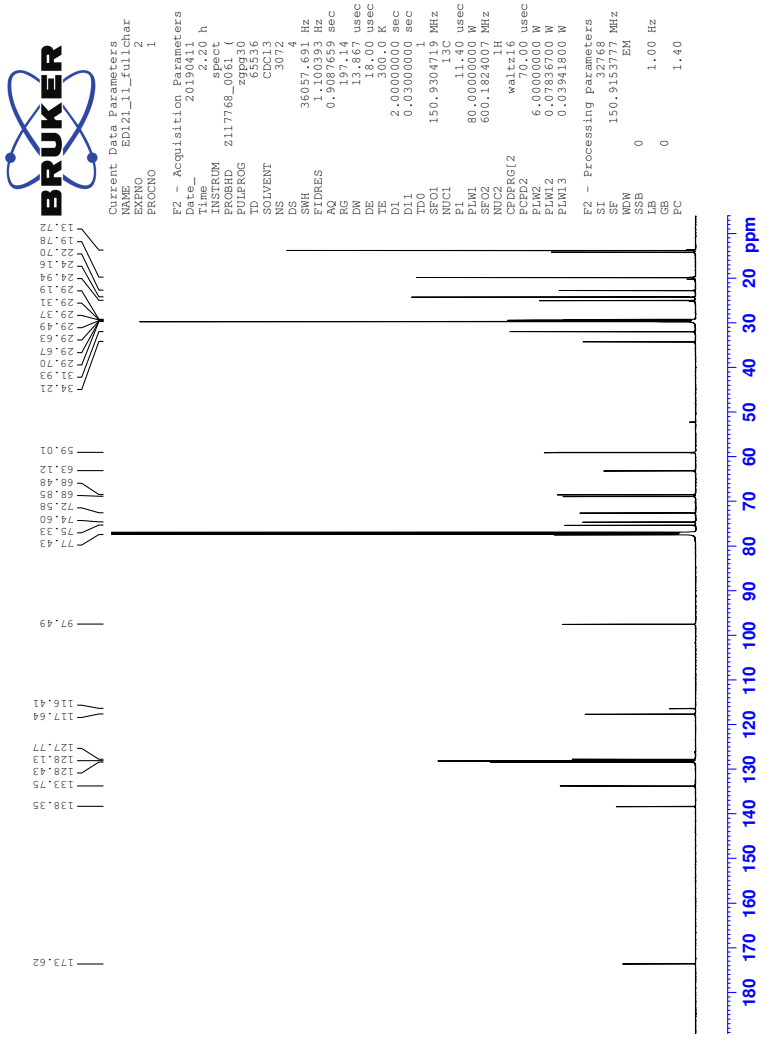

Figure 114: ^{13}C-NMR spectrum of compound **21**.

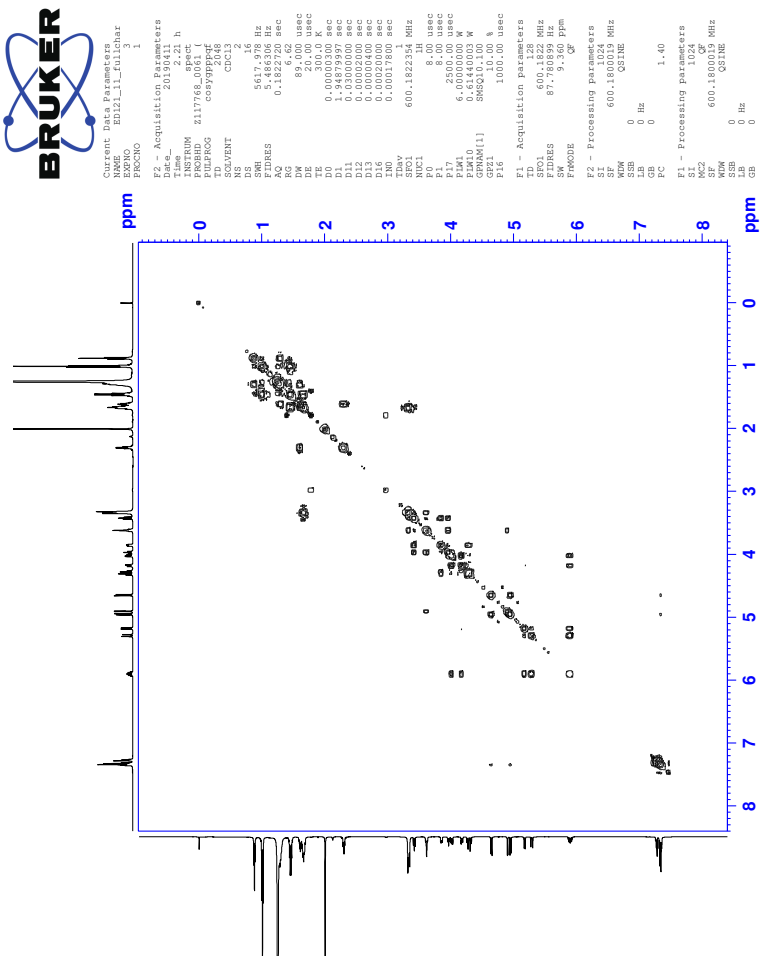

Figure 115: COSY spectrum of compound **21**.

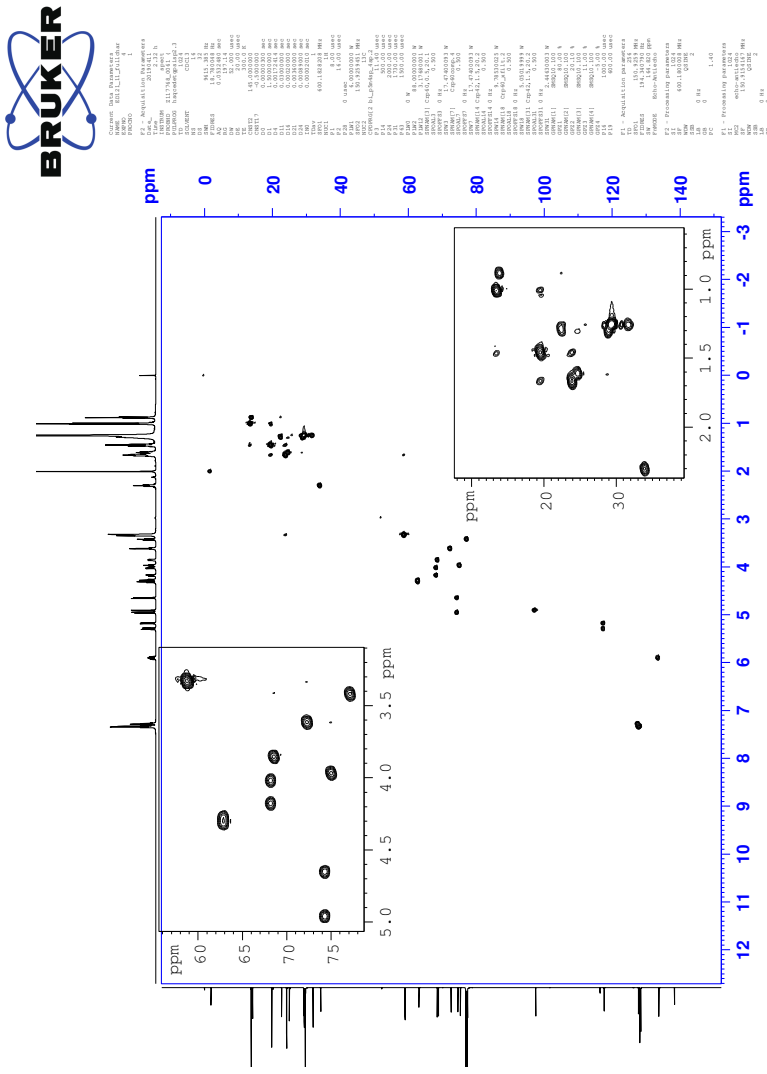

Figure 116: HSQC spectrum of compound **21**.

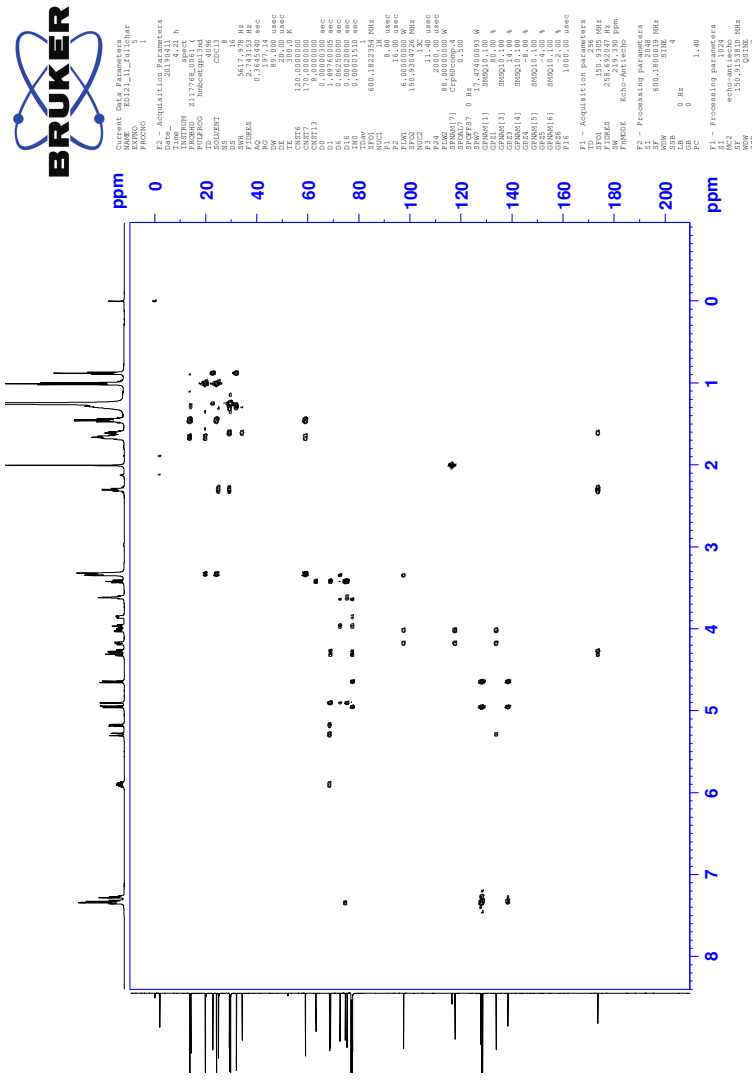

Figure 117: HMBC spectrum of compound **21**.

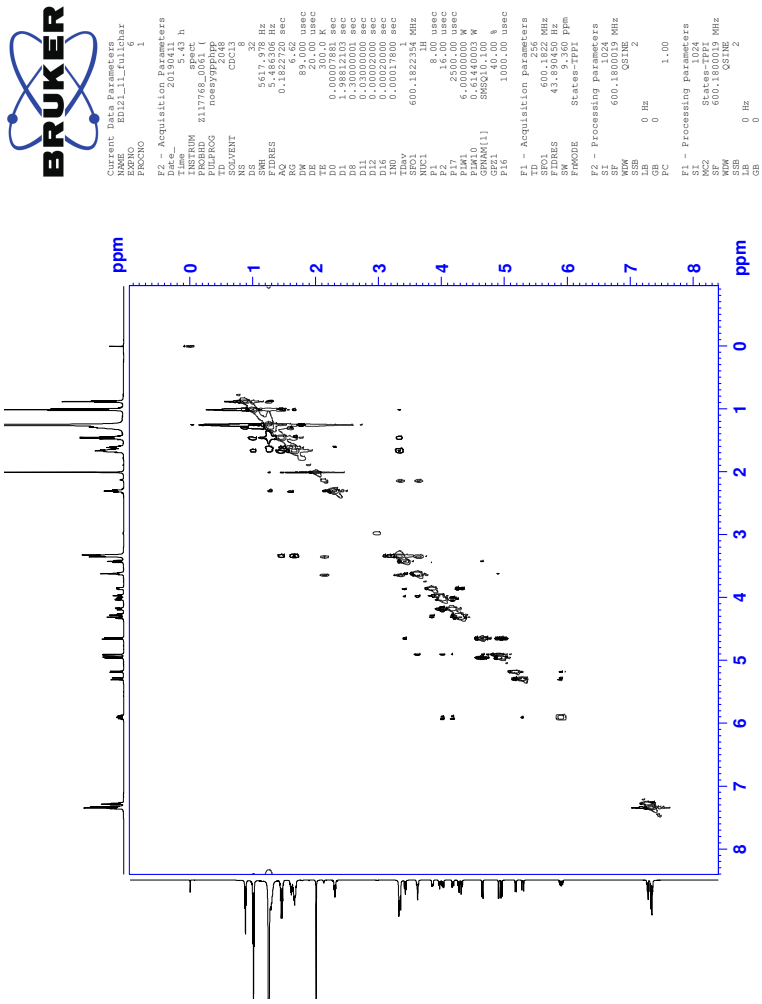

Figure 118: NOESY spectra of compound **21**.

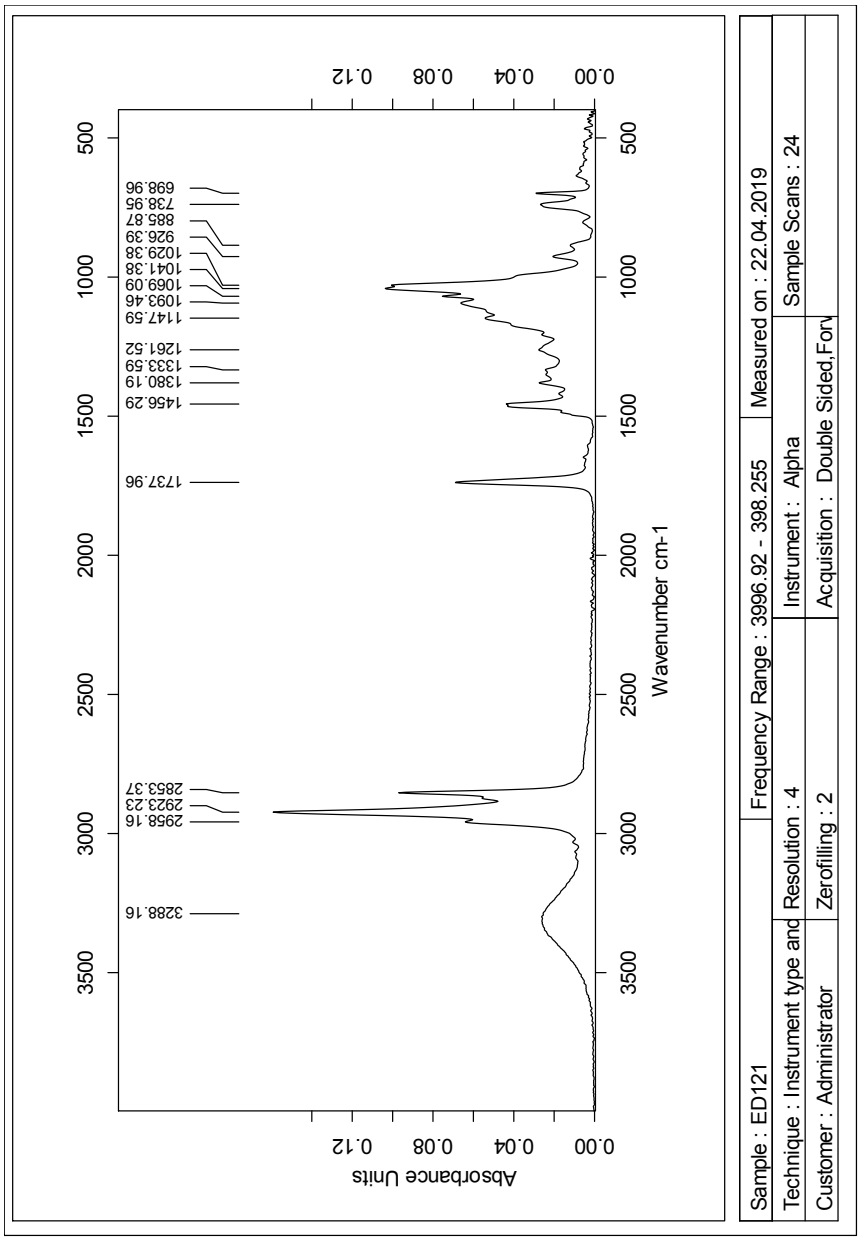

Figure 119: IR spectrum of compound **21**.

Elemental Composition Report **Page 1**

Single Mass Analysis
Tolerance = 2.0 PPM / DBE: min = -50.0, max = 50.0
Element prediction: Off
Number of isotope peaks used for i-FIT = 3

Monoisotopic Mass, Even Electron Ions
282 formula(e) evaluated with 1 results within limits (all results (up to 1000) for each mass)
Elements Used:
C: 0-100 H: 0-150 O: 0-10 Na: 0-1
2019_336_fia 46 (0.525) AM2 (Ar,35000.0,0.00,0.00); Cm (45:48)
1: TOF MS ES+

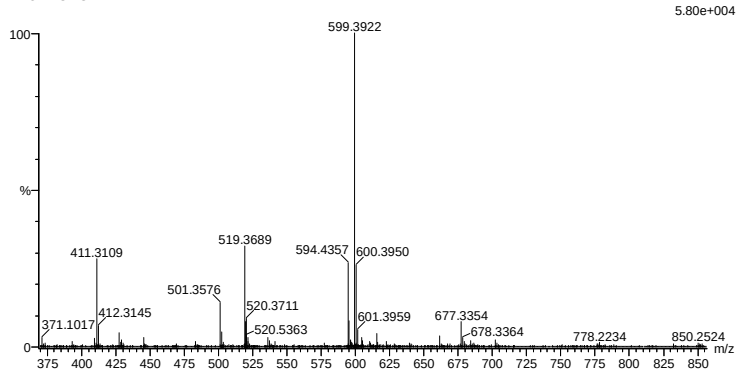

Minimum:				-50.0				
Maximum:		5.0	2.0	50.0				
Mass	Calc. Mass	mDa	PPM	DBE	i-FIT	Norm	Conf(%)	Formula
599.3922	599.3924	-0.2	-0.3	6.5	523.1	n/a	n/a	C34 H56 O7 Na

Figure 120: MS results for compound **21**.

S Spectroscopic data for compound 22

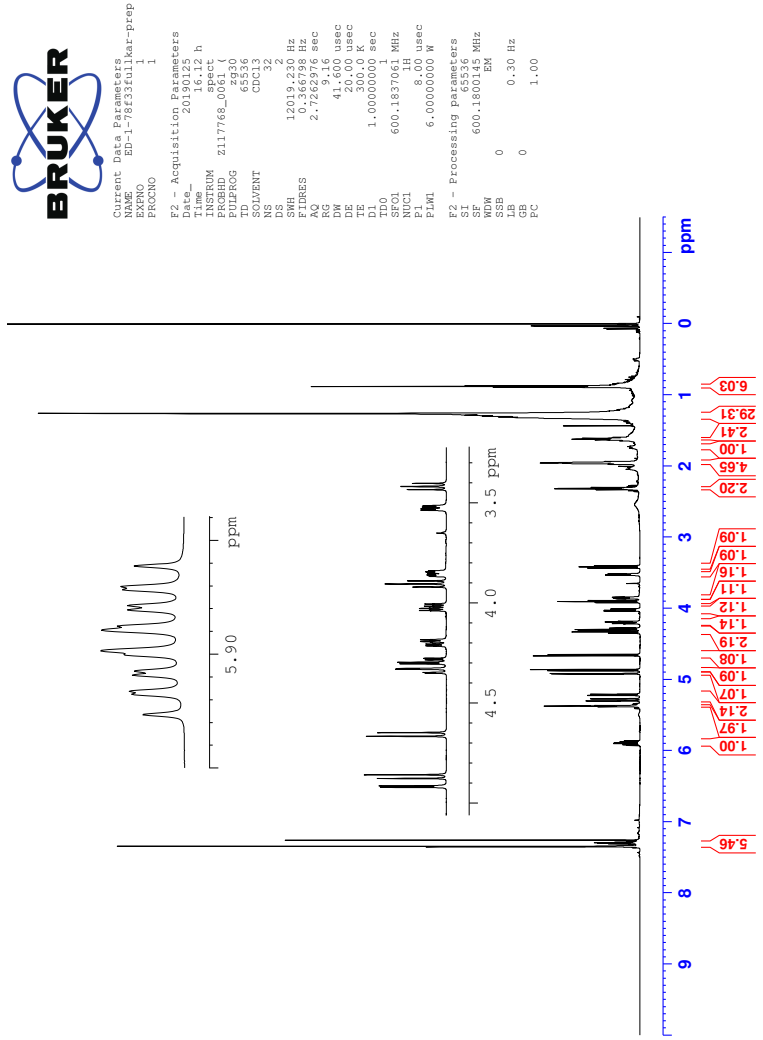

Figure 121: ^{1}H-NMR spectrum of compound **22**.

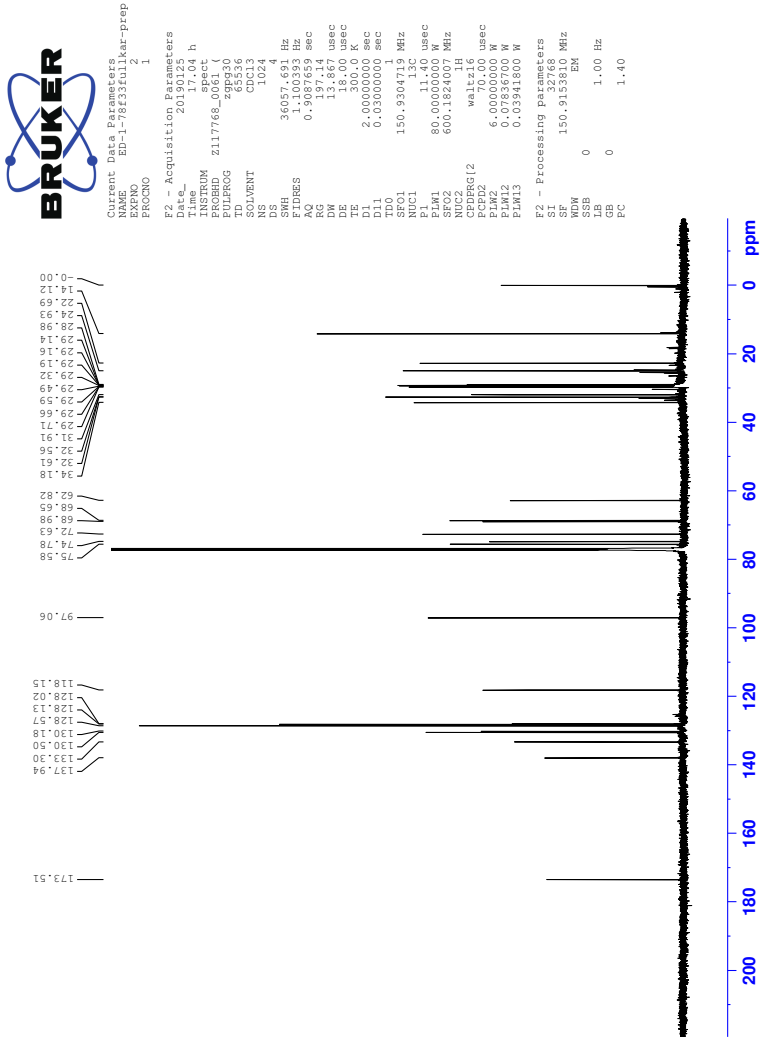

Figure 122: ^{13}C-NMR spectrum of compound **22**.

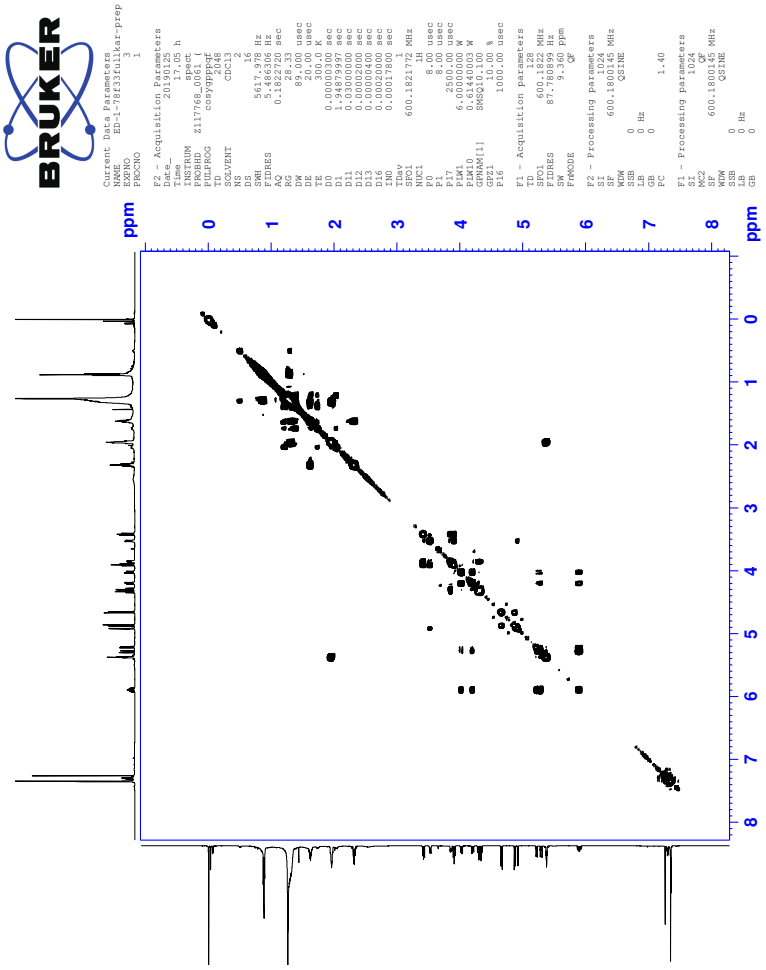

Figure 123: COSY spectrum of compound **22**.

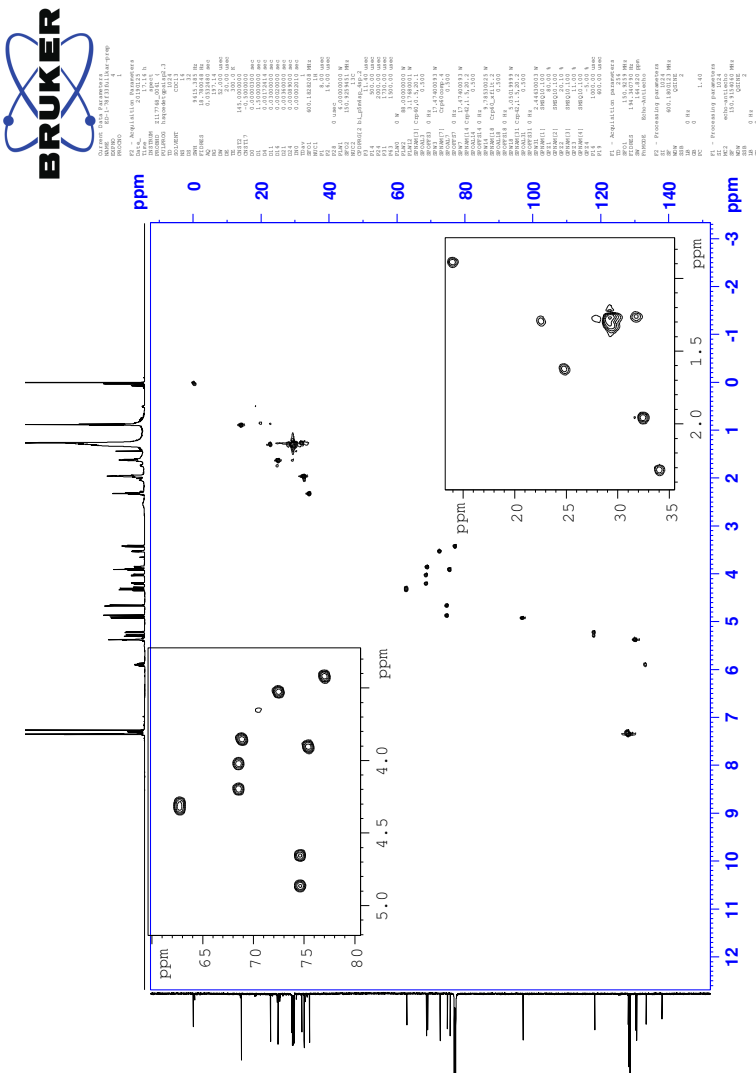

Figure 124: HSQC spectrum of compound **22**.

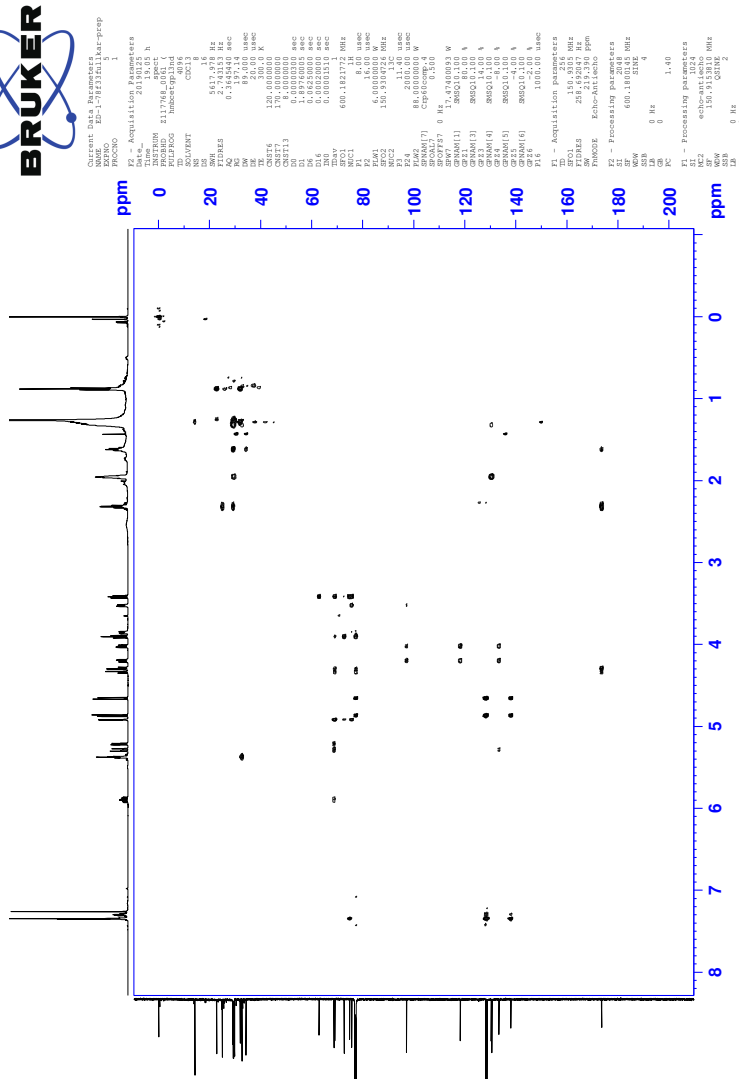

Figure 125: HMBC spectrum of compound **22**.

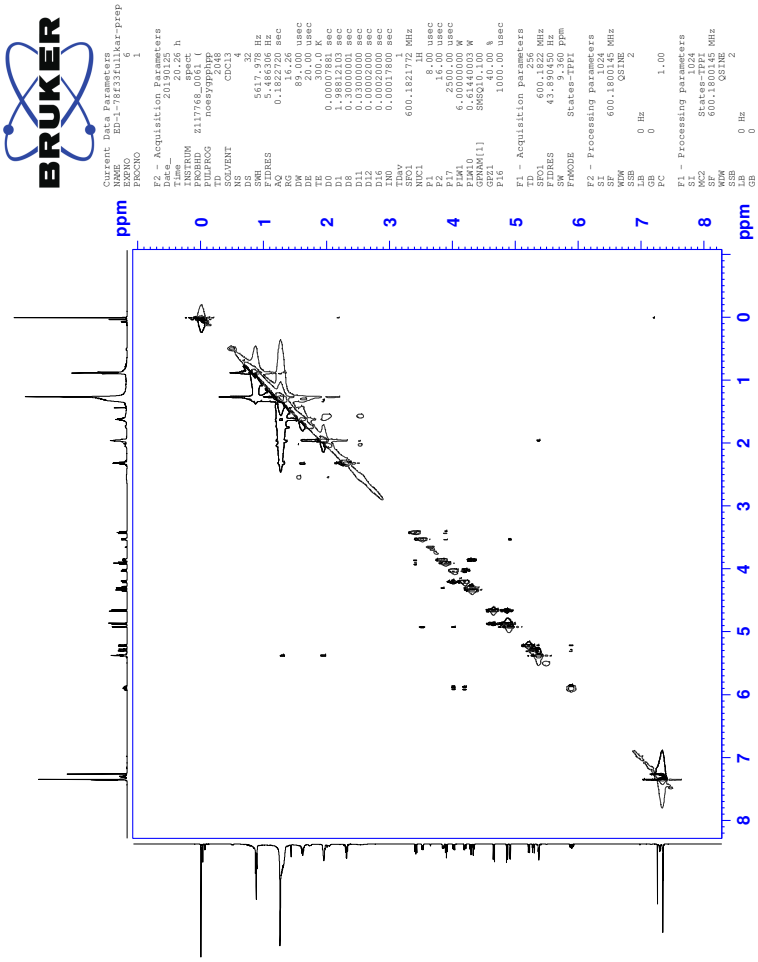

Figure 126: NOESY spectra of compound **22**.

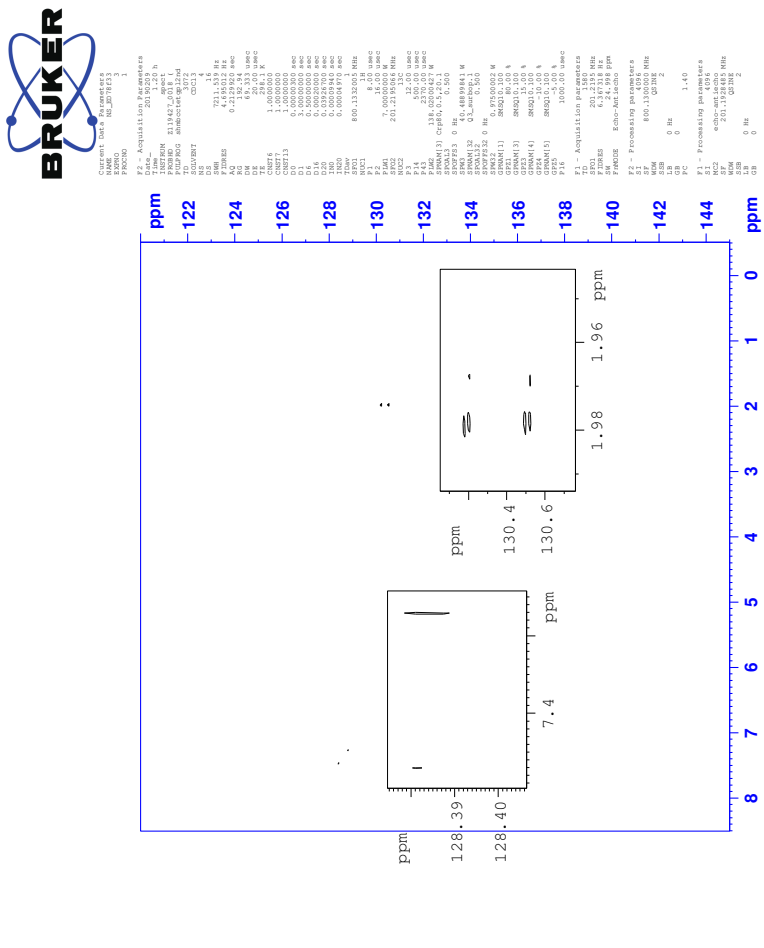

Figure 127: Slective HSQC spectrum of compound **22**, aromatic region.

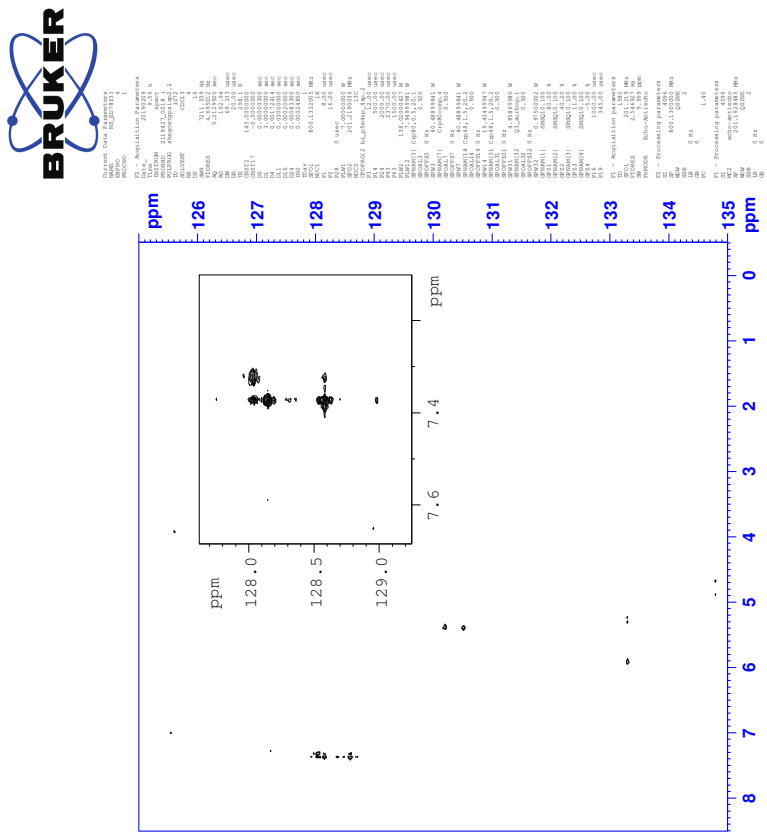

HSQC

Figure 128: Selective HSQC spectrum of compound **22**, aromatic region.

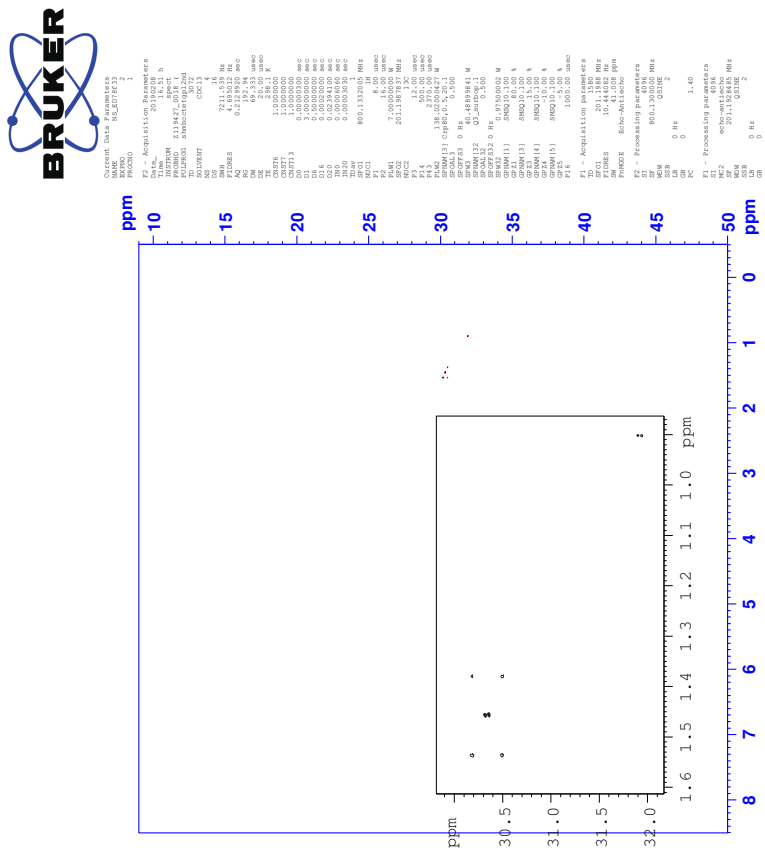

Figure 129: Selective HSQC spectrum of compound **22**, ester region.

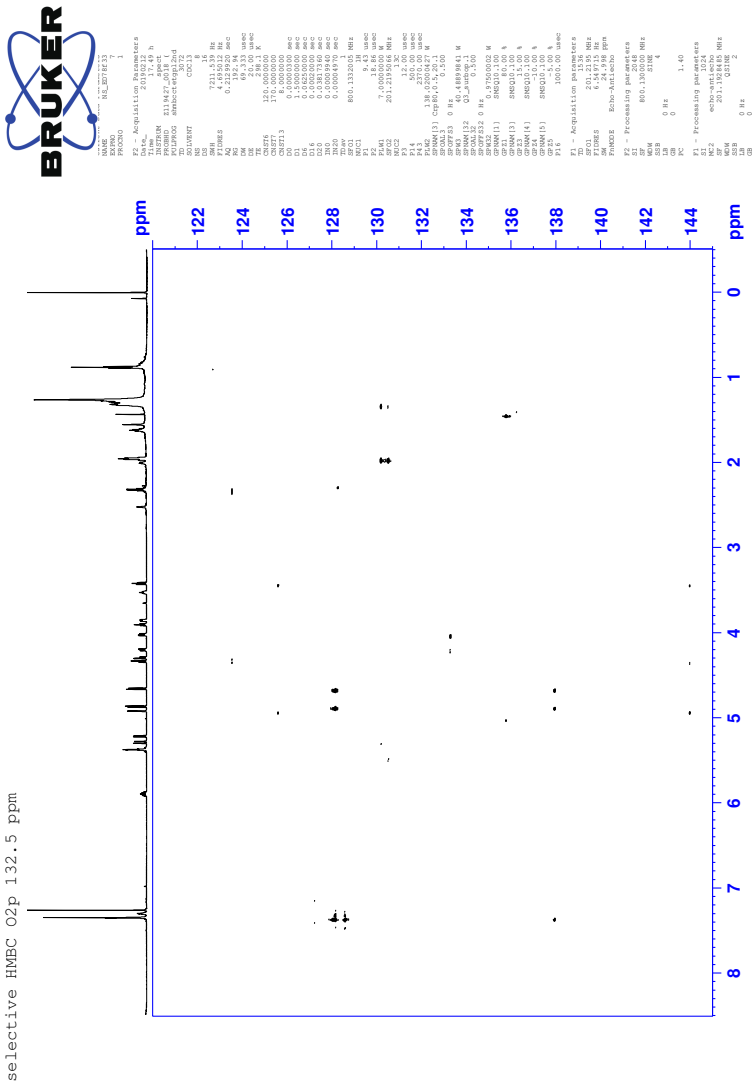

Figure 130: Selective HMBC spectrum of compound **22**, aromatic region.

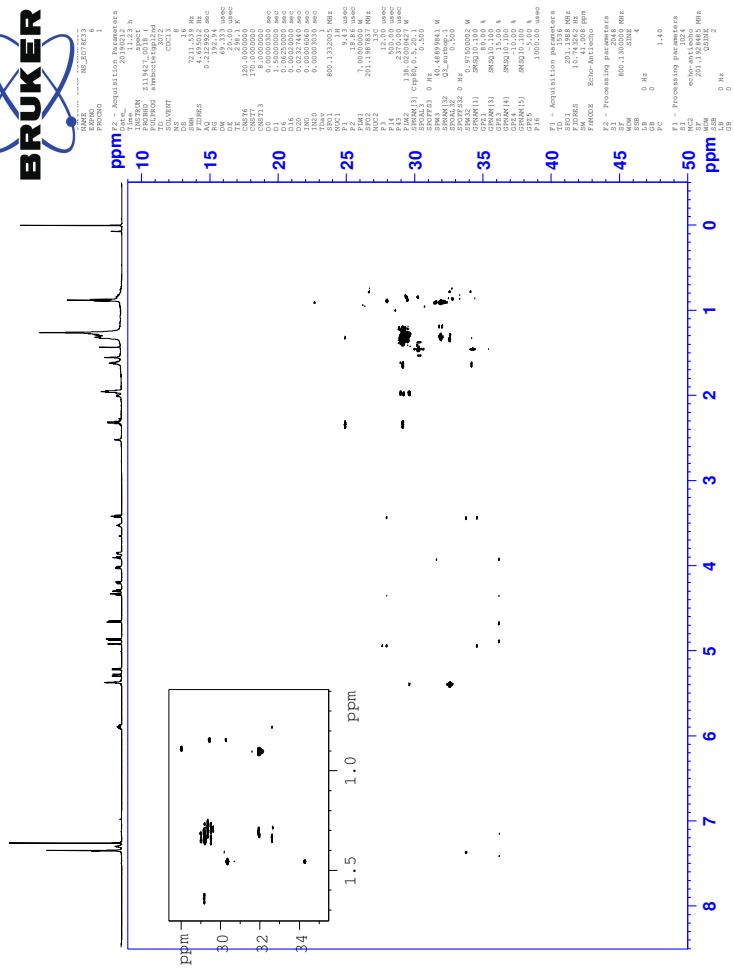

Figure 131: Selective HMBC spectrum of compound **22**, ester region.

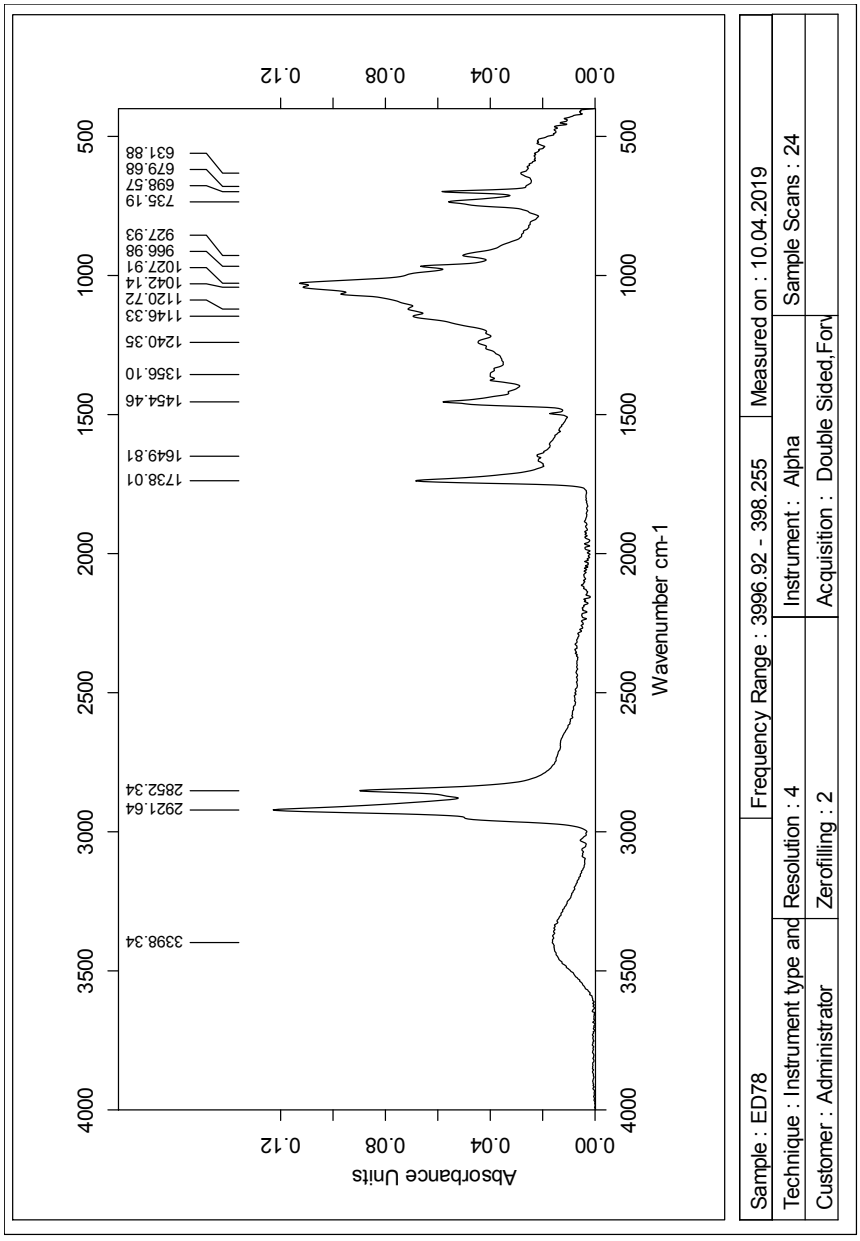

Figure 132: IR spectrum of compound **22**.

Elemental Composition Report **Page 1**

Single Mass Analysis
Tolerance = 2.0 PPM / DBE: min = -50.0, max = 50.0
Element prediction: Off
Number of isotope peaks used for i-FIT = 3

Monoisotopic Mass, Even Electron Ions
678 formula(e) evaluated with 1 results within limits (all results (up to 1000) for each mass)
Elements Used:
C: 0-100 H: 0-150 O: 0-8 Na: 0-1 Br: 0-2

2019-369 28 (0.533) AM2 (Ar,35000.0,0.00,0.00); Cm (28:35)
1: TOF MS ES+

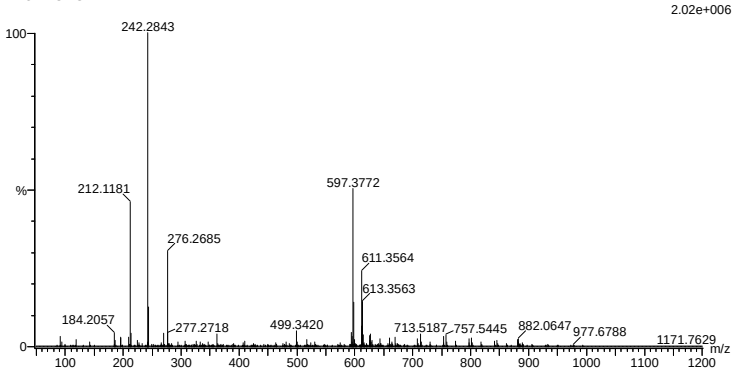

Minimum:				-50.0				
Maximum:		5.0	2.0	50.0				
Mass	Calc. Mass	mDa	PPM	DBE	i-FIT	Norm	Conf(%)	Formula
597.3772	597.3767	0.5	0.8	7.5	810.3	n/a	n/a	C34 H54 O7 Na

Figure 133: MS results for compound **22**.

T Spectroscopic data for compound 24

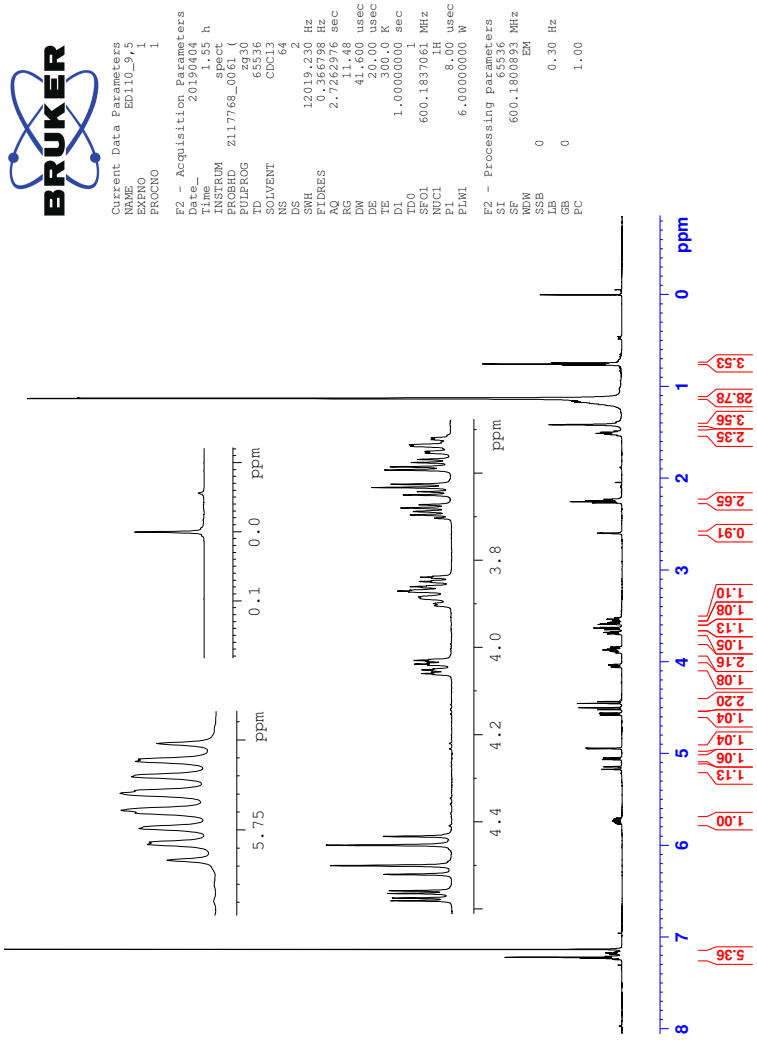

Figure 134: ^{1}H-NMR spectrum of compound **24**.

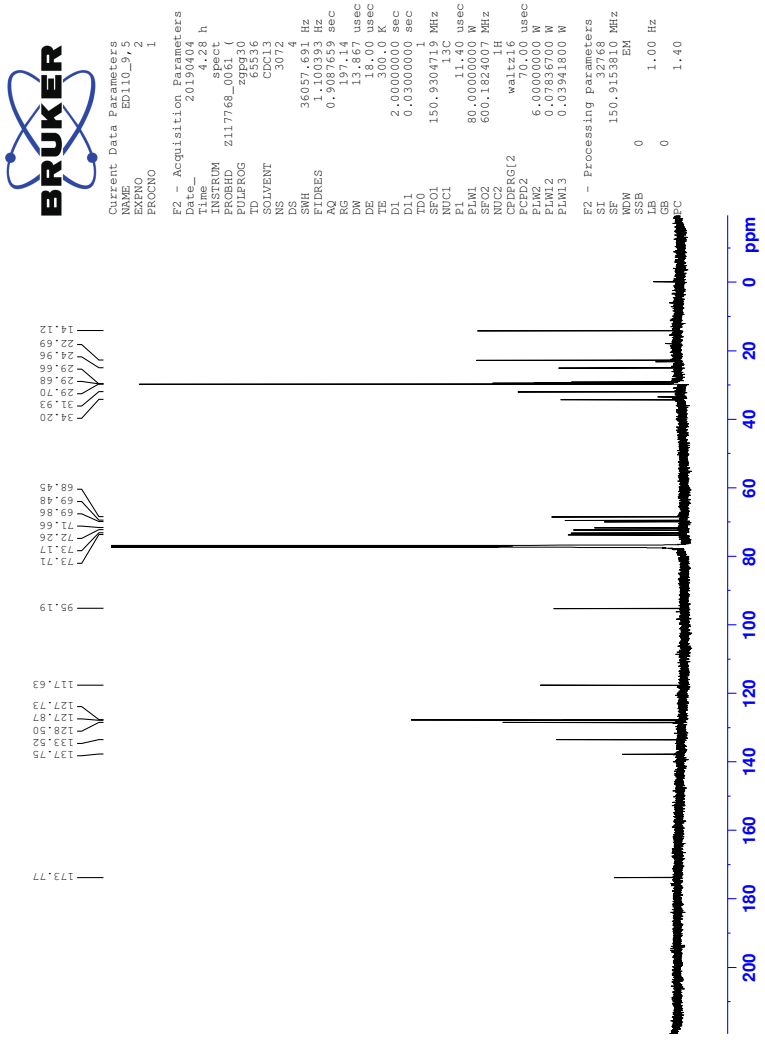

Figure 135: ^{13}C-NMR spectrum of compound **24**.

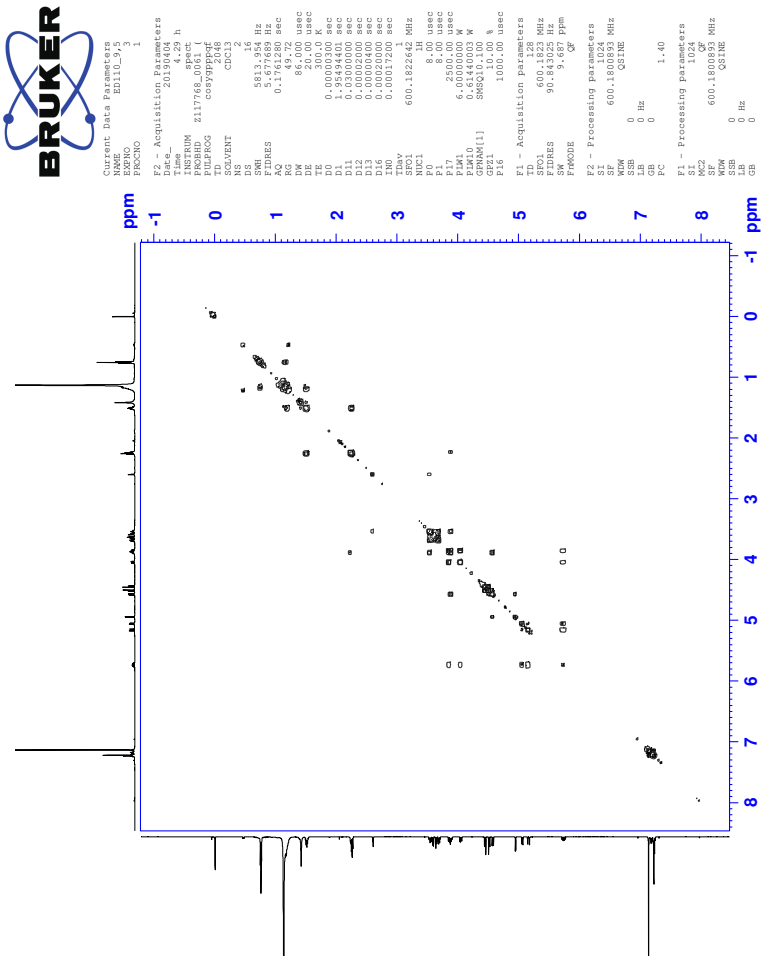

Figure 136: COSY spectrum of compound **24**.

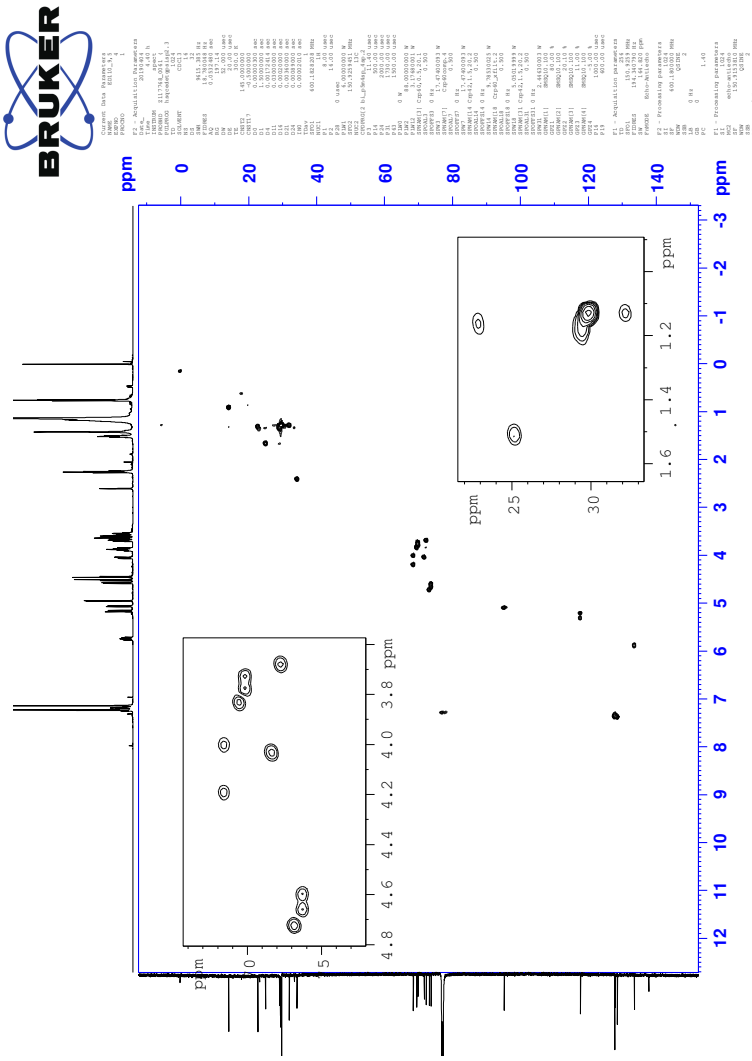

Figure 137: HSQC spectrum of compound **24**.

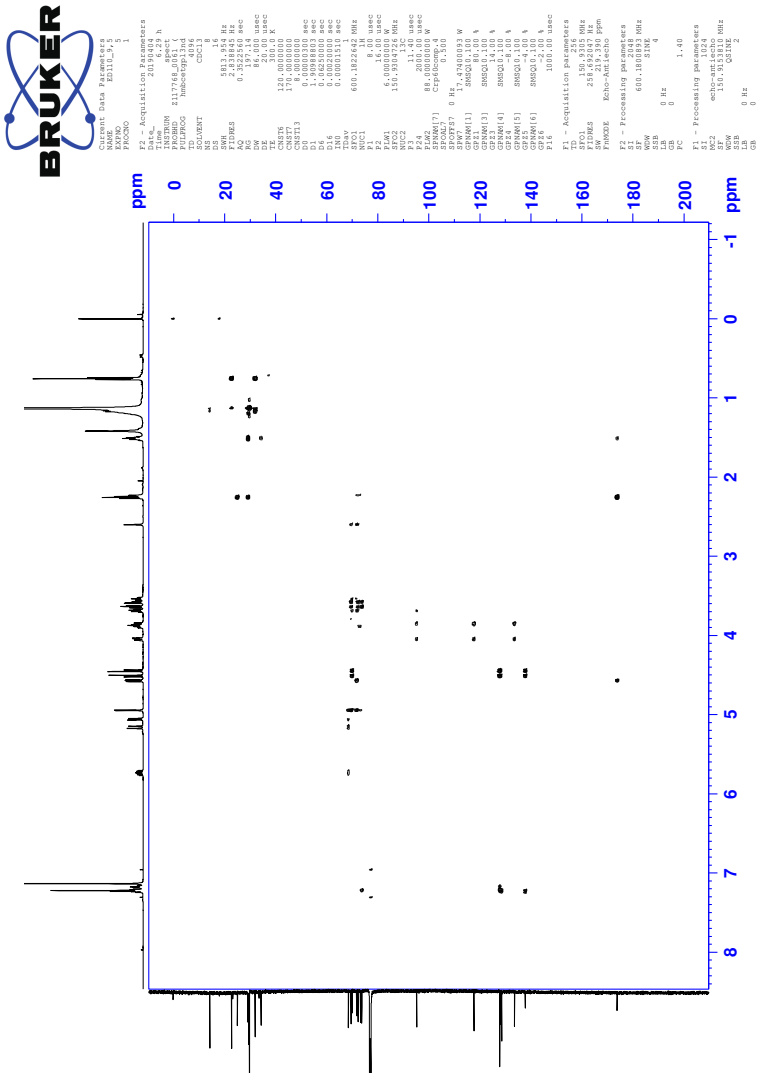

Figure 138: HMBC spectrum of compound **24**.

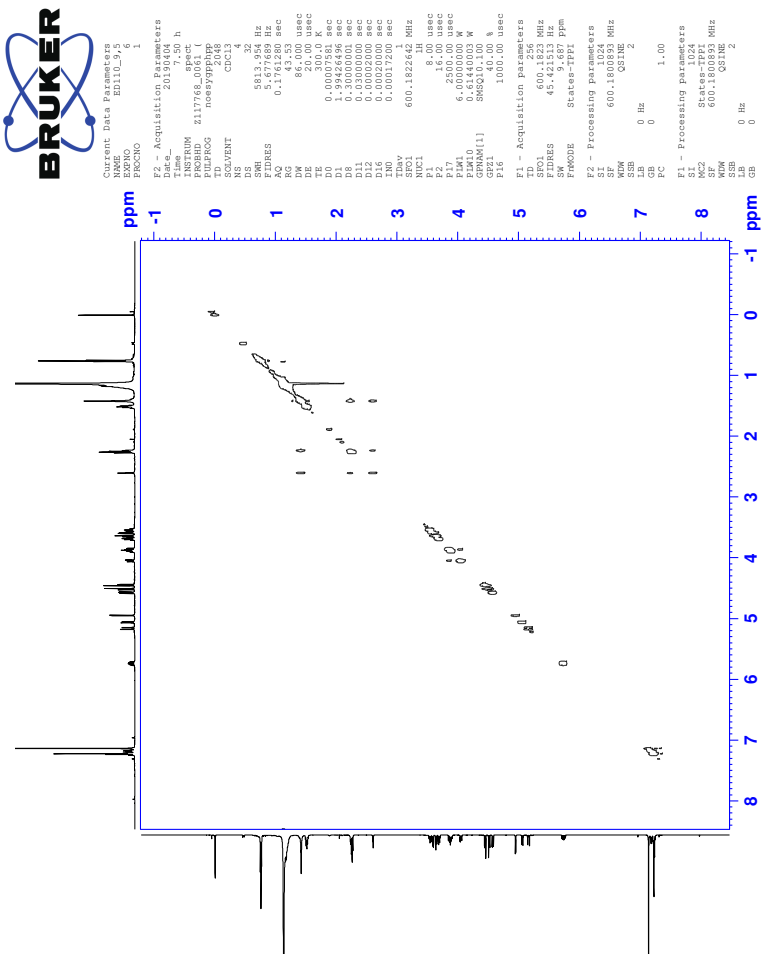

Figure 139: NOESY spectra of compound **24**.

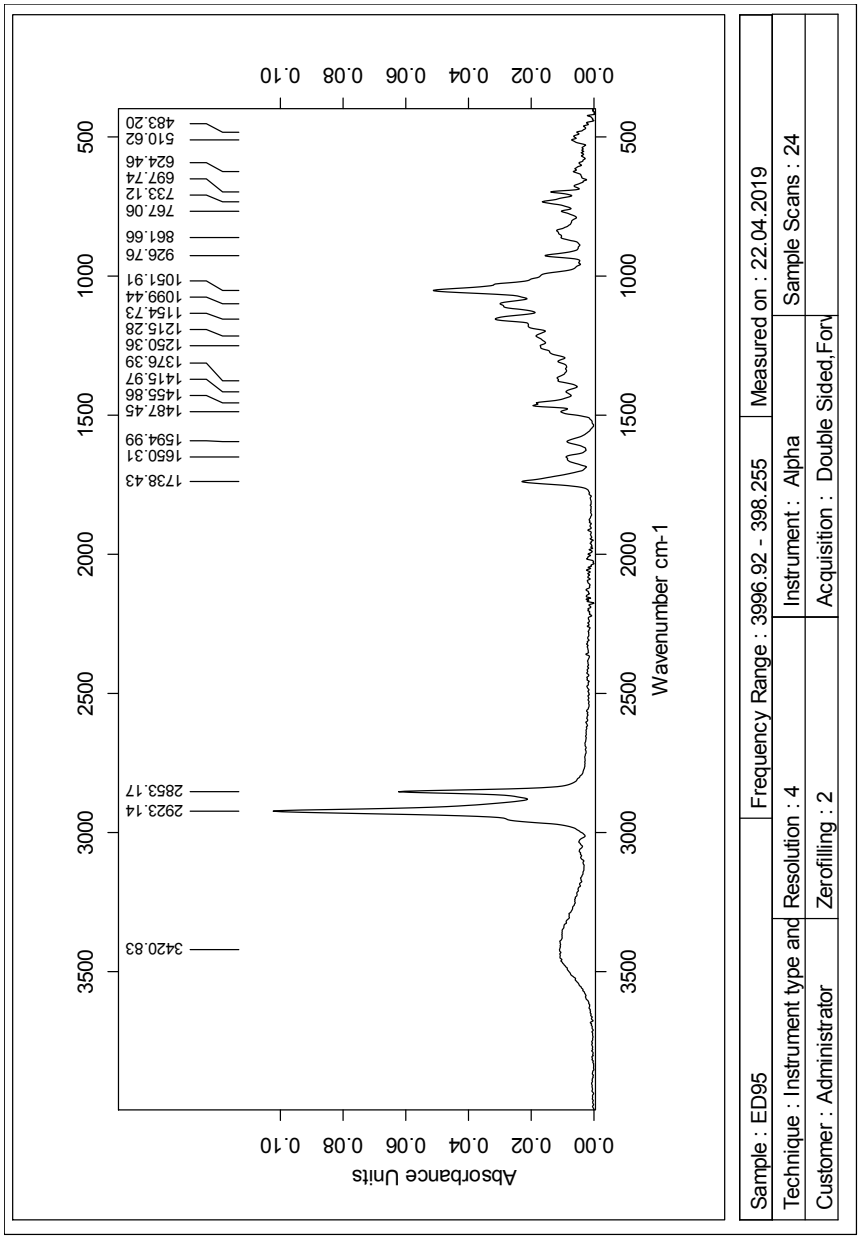

Figure 140: IR spectrum of compound **24**.

Elemental Composition Report **Page 1**

Single Mass Analysis
Tolerance = 2.0 PPM / DBE: min = -50.0, max = 50.0
Element prediction: Off
Number of isotope peaks used for i-FIT = 3

Monoisotopic Mass, Even Electron Ions
678 formula(e) evaluated with 1 results within limits (all results (up to 1000) for each mass)
Elements Used:
C: 0-100 H: 0-150 O: 0-8 Na: 0-1 Br: 0-2

2019-370 31 (0.585) AM2 (Ar,35000.0,0.00,0.00); Cm (31:37)
1: TOF MS ES+

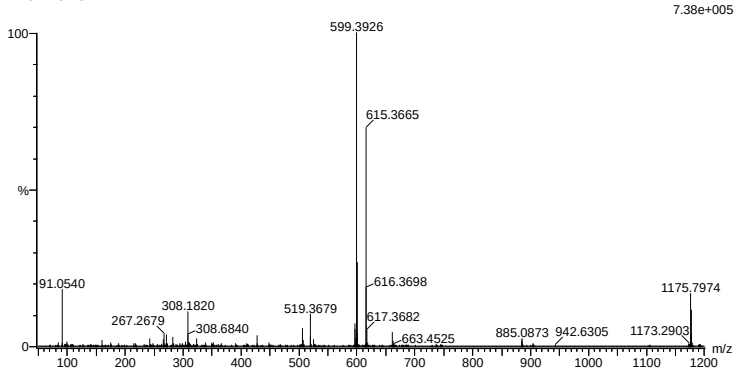

Minimum:				-50.0				
Maximum:		5.0	2.0	50.0				
Mass	Calc. Mass	mDa	PPM	DBE	i-FIT	Norm	Conf(%)	Formula
599.3926	599.3924	0.2	0.3	6.5	815.0	n/a	n/a	C34 H56 O7 Na

Figure 141: MS results for compound **24**.

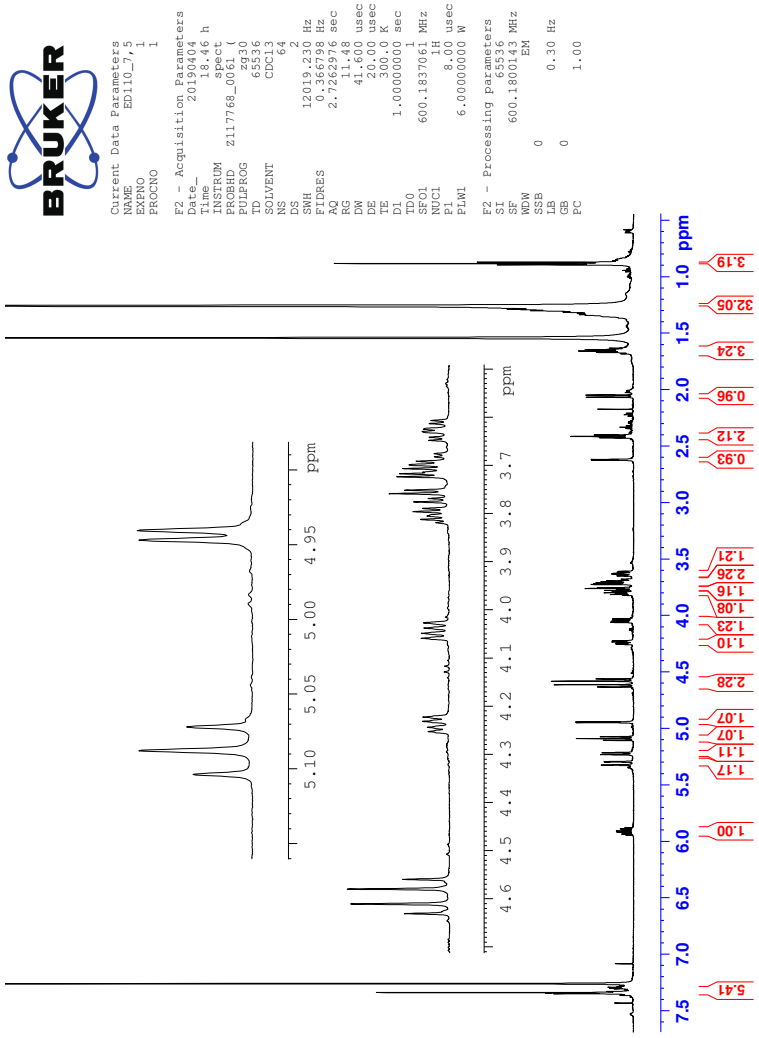

Figure 142: ^{1}H-NMR spectrum of compound **24**, 3-*O*-derivative.

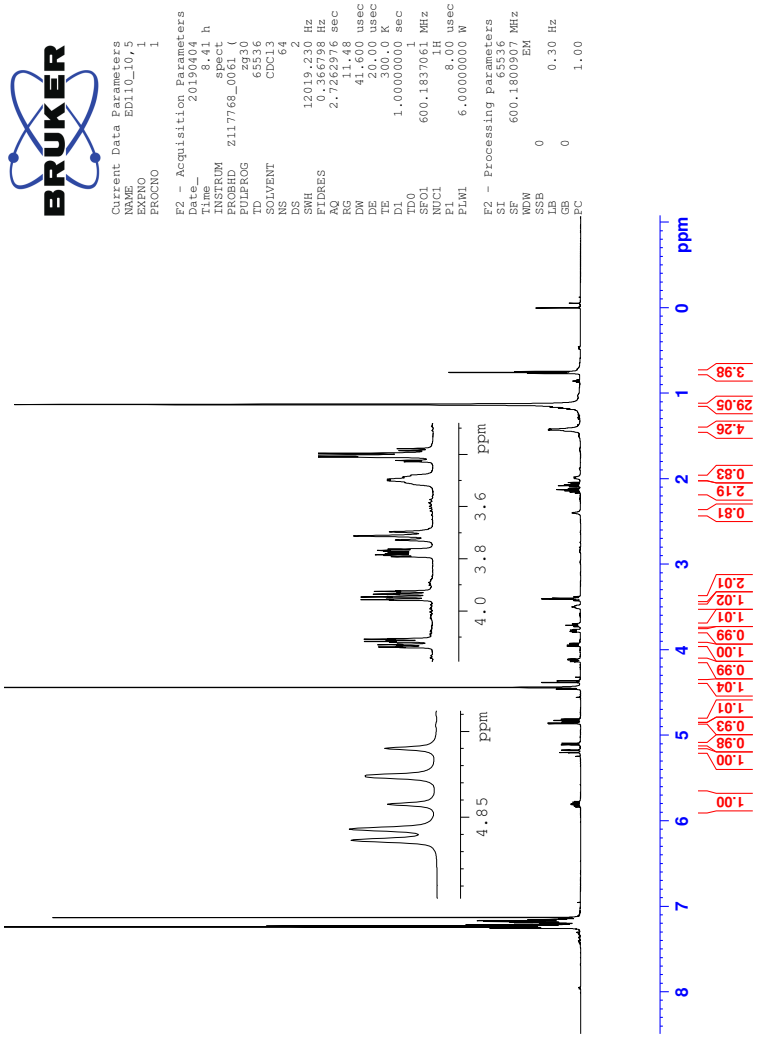

Figure 143: ^{1}H-NMR spectrum of compound **3**. 4-*O*-derivative.

U Spectroscopic data for compound 25

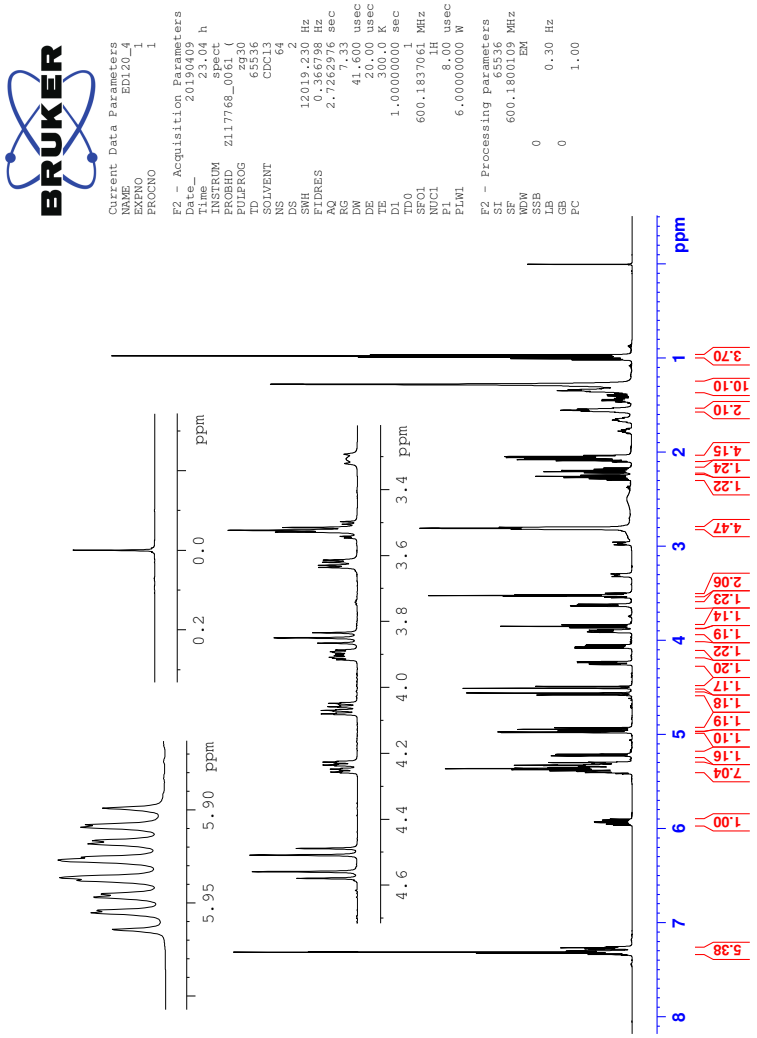

Figure 144: ^{1}H-NMR spectrum of compound **25**.

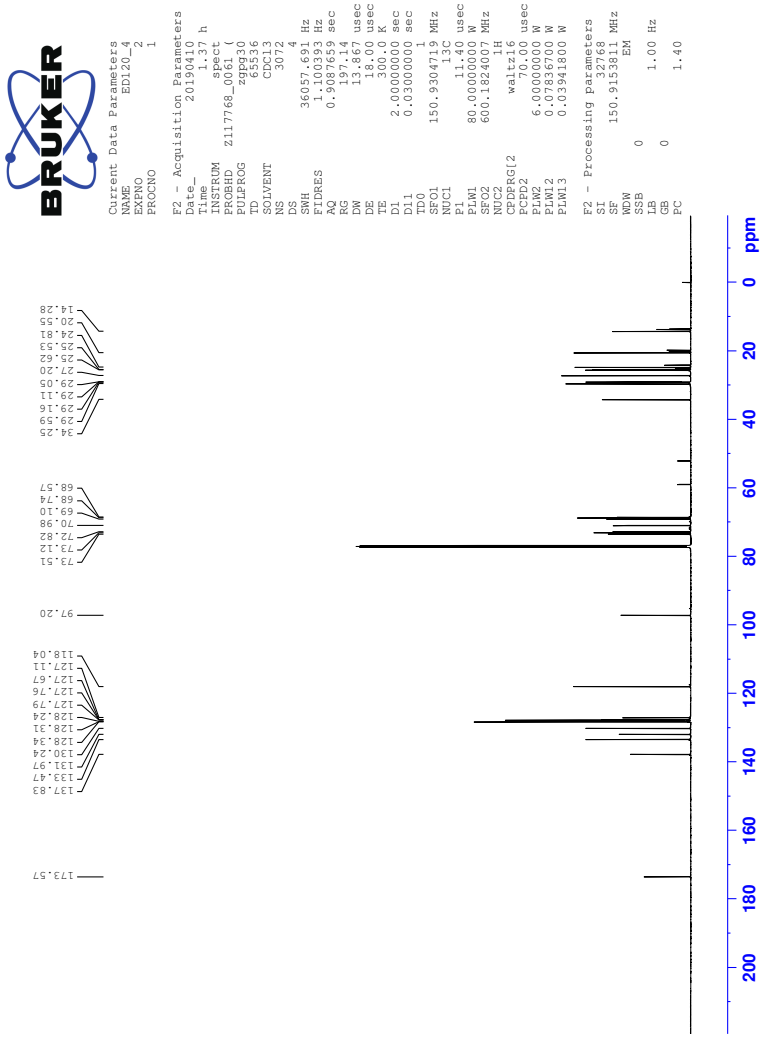

Figure 145: ^{13}C-NMR spectrum of compound **25**.

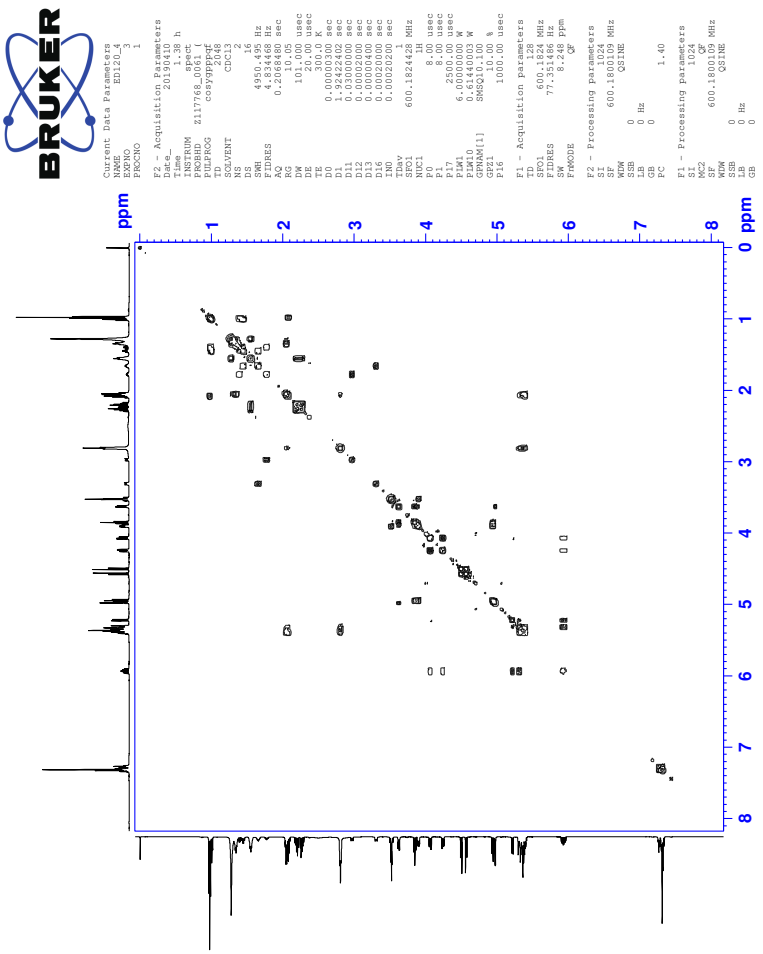

Figure 146: COSY spectrum of compound **3**.

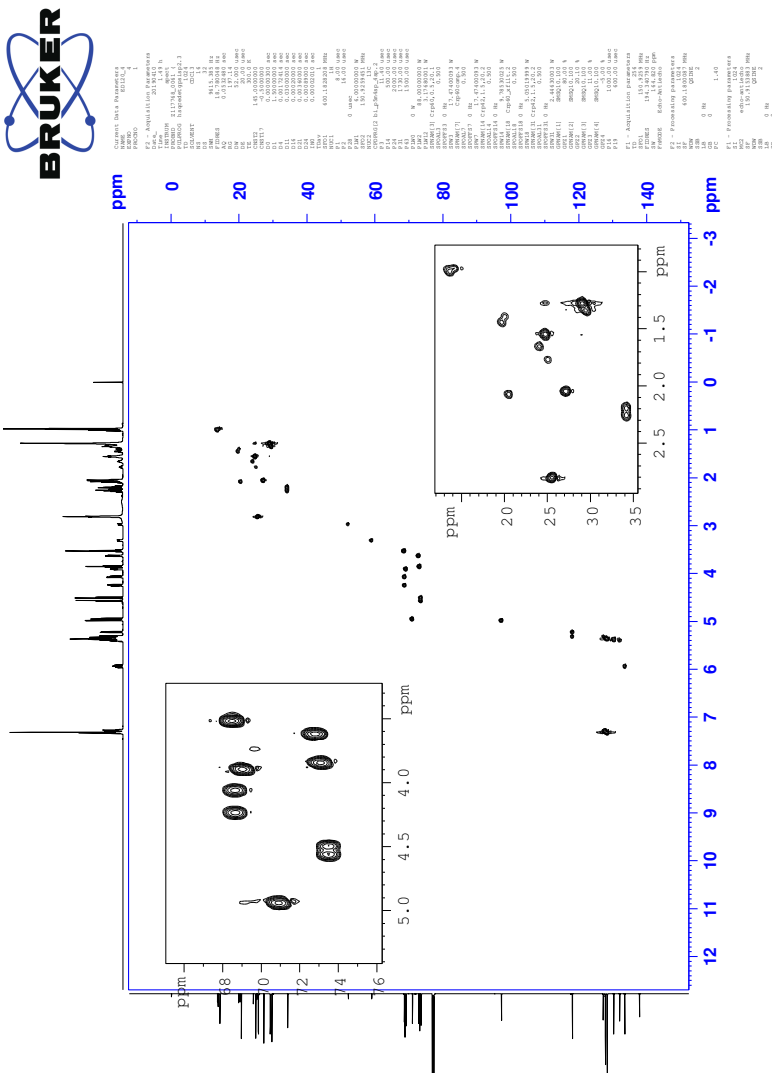

Figure 147: HSQC spectrum of compound **25**.

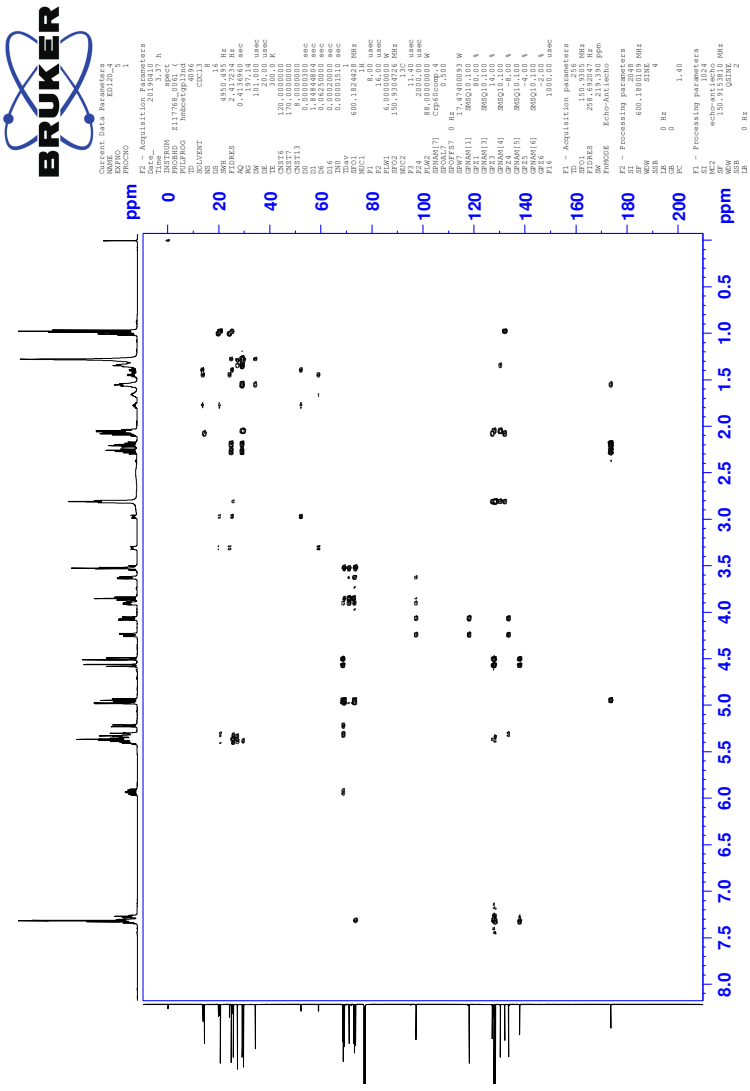

Figure 148: HMBC spectrum of compound **25**.

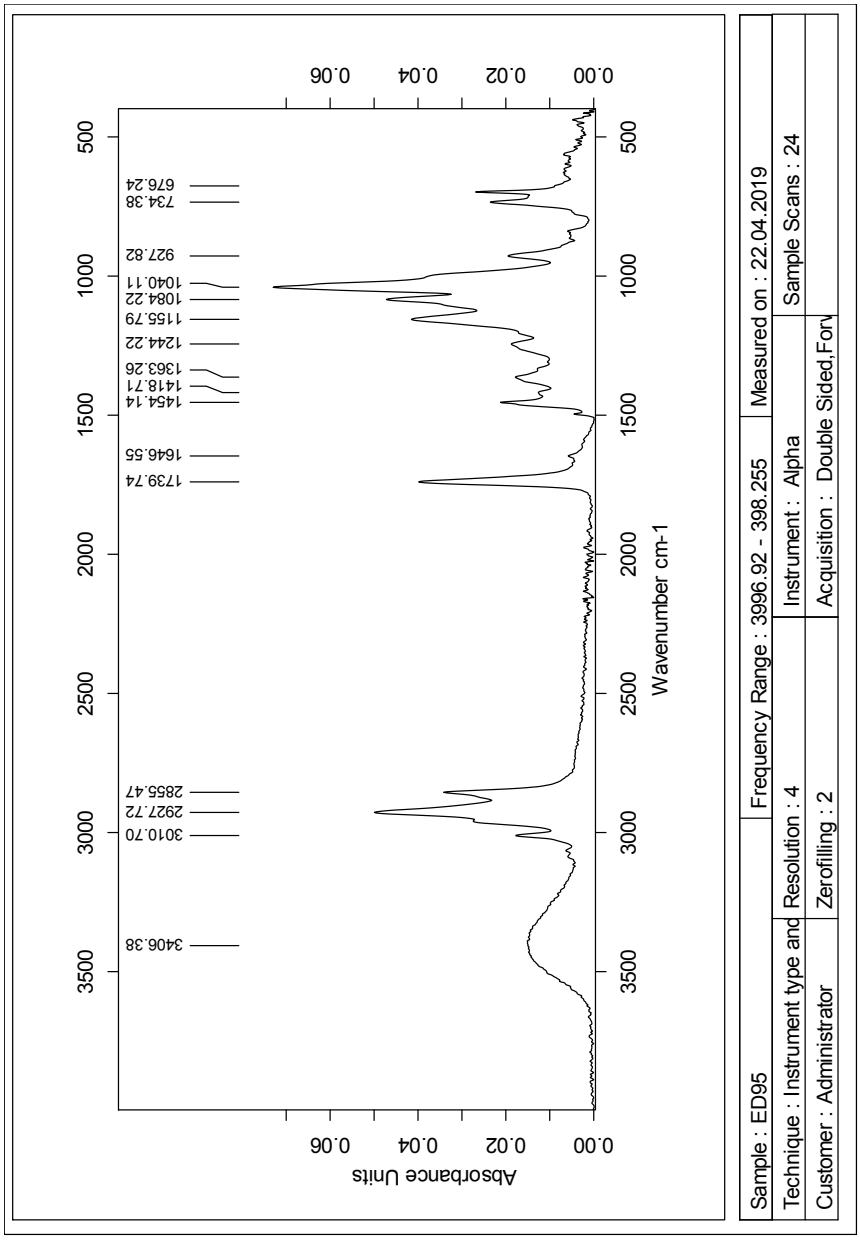

Figure 149: IR spectrum of compound **25**.

Elemental Composition Report **Page 1**

Single Mass Analysis
Tolerance = 2.0 PPM / DBE: min = -50.0, max = 50.0
Element prediction: Off
Number of isotope peaks used for i-FIT = 3

Monoisotopic Mass, Even Electron Ions
1681 formula(e) evaluated with 1 results within limits (all results (up to 1000) for each mass)
Elements Used:
C: 0-100 H: 0-150 N: 0-5 O: 0-10 Na: 0-1
2019-371 34 (0.636) AM2 (Ar,35000.0,0.00,0.00); Cm (34:42)
1: TOF MS ES+

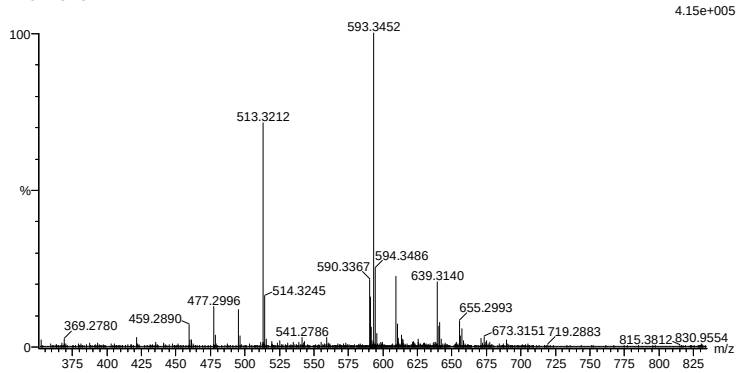

Minimum:				-50.0				
Maximum:		5.0	2.0	50.0				
Mass	Calc. Mass	mDa	PPM	DBE	i-FIT	Norm	Conf(%)	Formula
593.3452	593.3454	-0.2	-0.3	9.5	821.7	n/a	n/a	C34 H50 O7 Na

Figure 150: MS results for compound **25**.

cli

Edvard Solli Stenset

Selective functionalization of x-D-glucopyranosides in the synthesis towards sugar fatty acid esters

NTNU
Norwegian University of
Science and Technology